UNIVERSITÉ DE MONTRÉAL

BIODEGRADABLE BLENDS OF POLYCAPROLACTONE WITH THERMOPLASTIC STARCH

GANG LI
DÉPARTMENT DE GÉNIE CHIMIQUE
ÉCOLE POLYTECHNIQUE DE MONTRÉAL

THÈSE PRÉSENTÉE EN VUE DE L'OBTENTION
DU DIPLÔME DE PHILOSOPHIAE DOCTOR (Ph. D.)
(GÉNIE CHIMIQUE)
AVRIL 2010

UNIVERSITÉ DE MONTRÉAL

ÉCOLE POLYTECHNIQUE DE MONTRÉAL

Cette thèse intitulée:

BIODEGRADABLE BLENDS OF POLYCAPROLACTONE WITH THERMOPLASTIC STARCH

présentée par: LI Gang

en vue l'obtention du diplôme de: Philosophiae Doctor

a été dûment acceptée par le jury d'examen constitué de:

Mme DESCHÊNES Louise, Ph.D., présidente

M. FAVIS Basil, Ph.D., membre et directeur de recherche

M. GRMELA Miroslav, Ph.D., membre

M. VLACHOPOULOS John, D.Sc, membre

ACKNOWLEDGEMENTS

I would like to express my appreciation and thanks to my thesis director, Professor Basil D. Favis, for showing me how to be thorough and independent in research work, and for his knowledge, guidance, experience and financial support. I also would like to express my acknowledgement for his patience during the numerous discussions we had, which were very helpful for my scientific training.

I would like to give a special acknowledgement to Pierre Sarazin for his helpful discussions and suggestions during my research work. My special thanks to the staff of the Department of Chemical Engineering of ÉCOLE POLYTECHNIQUE DE MONTRÉAL for their understanding and cooperation during my study in the department. I would like to express my appreciation to Mr. Jacques Beausoleil for technical support. I also thank Zhenhua, Nick, Médina, Mihaela, Danut and all the group staff. I am indebted to my Chinese friends, Yunli, Zhijie, Jinkui, Zhenyu, Jing and Weiliang for their encouragement, useful suggestions and help.

I would like to express my sincerest appreciation to my parents and sisters for their love, support and encouragement. Finally, I wish to express my many thanks to my wife, Zhongmei Zhu, for her love, care, understanding and patience.

RÉSUMÉ

Ce travail présente une approche pour la préparation de mélanges polycaprolactone (PCL)/amidon thermoplastique (TPS) par extrusion en une seule étape. La mise en oeuvre en une étape à l'état fondu de mélanges polymères à base d'amidon thermoplastique est une opération complexe impliquant la plastification, la dévolatilisation, le mélange à l'état fondu et le contrôle de la morphologie. Tout ceci doit être complété en un temps de résidence total d'au plus deux minutes dans une extrudeuse. Afin de déterminer les limites de temps/température requises pour plastifier avec succès l'amidon dans un environnement de mise en oeuvre de polymères à l'état fondu, la calorimétrie par balayage différentiel (DSC), la microscopie optique et la diffraction de rayons X à grand angle (WAXS) ont été utilisées pour étudier les aspects clés de la gélification de l'amidon dans des mélanges glycérol/eau en excès. En même temps, ces résultats ont été liés à la morphologie de mélanges à l'état fondu d'amidon thermoplastique (TPS) et de polycaprolactone (PCL). Dans un deuxième temps, le développement de la morphologie et les interactions interfaciales dans les mélanges PCL/TPS ont été étudiés. Finalement, la biodégradation d'amidon natif, d'amidon thermoplastique (TPS) à haute teneur en glycérol, et de leurs mélanges avec du polyéthylène à basse densité (LDPE) et du poly(acide lactique) (PLA) a été démontrée sous des conditions de compostage.

ABSTRACT

This work presents an approach to preparing polycaprolactone (PCL)/thermoplastic starch (TPS) blends via a one-step extrusion approach. The one-step melt processing of polymer blends with thermoplastic starch is a complex operation involving plasticization, devolatilization, melt-melt mixing and morphology control. All this must be achieved within a maximum two minutes total residence time in an extruder. In addition, starch is a complex natural polymer and thus gelatinization is a delicate process. In order to determine the time/temperature boundaries ultimately required for the successful plasticization of starch in a polymer melt processing environment, differential scanning calorimetry (DSC), optical microscopy and wide angle X-ray diffraction (WAXD) were used to examine the critical aspects of starch gelatinization in glycerol/excess water mixtures. Simultaneously, these results were related to the morphology of melt-blended thermoplastic starch (TPS) in polycaprolactone (PCL). Secondly, the morphology development and interfacial interactions in PCL/TPS blends were studied. Finally, the biodegradation of native starch, thermoplastic starch (TPS) containing high concentration of glycerol, and its blends with low-density polyethylene (LDPE) and polylactic acid (PLA) were demonstrated under compost conditions.

In the first part of the work, starch gelatinization was examined in detail. The onset and conclusion temperatures for wheat starch gelatinization were obtained via differential scanning calorimetry (DSC), X-ray diffraction and polarized light microscopy. The results indicate that water and glycerol exhibit significantly different effects on the starch gelatinization temperature. With a constant concentration of glycerol related to dry starch, the onset, T_o, peak, T_p,and conclusion, $T_{c,}$ gelatinization temperatures all shift to low temperatures with increasing water concentration. Conversely, these gelatinization temperatures shift to high temperatures when the water concentration is held constant and the quantity of glycerol is increased. In both cases, the gelatinization endotherm becomes more pronounced with increasing plasticizer concentration in the system. These results are very useful to set up the extrusion temperatures since the gelatinization temperature can be changed by varying the ratio of water and glycerol in initial starch/water/glycerol mixtures.

Starch granules are semi-crystalline materials and are composed mainly of crystalline amylose and amorphous amylopectin. When observed via optical microscopy under polarized light, the starch granule shows birefringence. During starch gelatinization, starch crystallinity is destroyed gradually and is accompanied by a loss of birefringence. The ranges of gelatinization temperatures for starch/excess water and starch/excess glycerol mixture obtained were from 55.0°C to 64.5°C and 113.0°C to 126.5°C, respectively. However, a temperature range from 73.0°C to 82.7°C was obtained by using of water/glycerol mixture (50/50 w/w). These data give further support to the DSC results.

In order to determine the time/temperature boundaries, the dynamic of starch gelatinization was examined by tracking the diameter change of starch granules under isothermal conditions. Three kinds of starch mixtures, starch/water, starch/glycerol and starch/water/glycerol were chosen to study the dynamics of starch gelatinization. A number of interesting conclusions were obtained. Firstly, for all mixtures, no gelatinization whatsoever is observed below the onset temperature as derived from the DSC. Secondly, the gelatinization process is significantly slower (three minutes) for the starch/glycerol mixture even at high temperature. For starch/water and starch/water/glycerol mixtures, however, the gelatinization process is accomplished within one minute. The effect of water in the water/glycerol plasticization protocol evidently serves to improve ingress rates into the starch granules. In order to further examine the effect of temperature on degree of gelatinization, a water/starch sample was held at different temperatures for 20 minutes. After this treatment, a heating scan on the DSC was carried out to evaluate the degree of gelatinization. The results indicate that the peak gelatinization temperature (T_p) and the degree of starch gelatinization increase with increasing isothermal treatment temperature, and that complete gelatinization can only be achieved at temperatures higher than the conclusion temperature (about 80°C). Since starch gelatinization is accomplished in one minute, it is important to consider that, even if the kinetics are rapid, below the conclusion temperature (T_c) only a partial degree of gelatinization is achieved even after long times of treatment. It can be readily concluded that excess water is a necessary ingredient for glycerol to plasticize starch within the time constraints of a melt processing operation, and a sufficient residence time of water in contact with the starch is required prior to devolatilization.

Previous work from this laboratory has shown that the actual time to generate steady-state polymer blend morphologies for synthetic polymers in the twin-screw extruder can be quite low

(approximately 30 seconds) once the various components are in the melt state. The main challenge therefore in the one-step extrusion process is the efficiency of starch plasticization. Based on the above results, a series of one-step melt extrusion experiments for PCL/TPS blends was designed and the dispersed TPS morphology was examined. The TPS particle size (d_v) in a PCL matrix is 13.9 microns when only glycerol is used to plasticize native starch (contains only ambient water). This is very similar to the native starch granule size of 13.6 microns and clearly indicates the inability of glycerol alone to plasticize native starch within the time constraints of melt extrusion. When a glycerol-excess water mixture was used and the residence time was kept short before water removal, some of the plasticized starch was completely broken-down into order-of-magnitude smaller particles. A bimodal particle distribution was obtained with the large particles having a volume average diameter (d_v) of 10.2 μm and a d_n of 2.5 μm. However, the bimodal TPS phase size distribution clearly indicates that the starch plasticization process remains incomplete. By further increasing the residence time prior to water devolatilization, a completely plasticized starch is obtained. The efficacy of plasticization is demonstrated by a dramatic six-fold reduction in the dispersed TPS phase size and a unimodal TPS phase size distribution in the blend system. It is clear from the previous part of this paper that the approach of using excess water/glycerol mixtures to plasticize starch is a necessary requirement.

The second part of this work was carried out to investigate the morphology development and interfacial interactions in polycaprolactone/thermoplastic starch blends. This work closely examines the coalescence and continuity development in these systems. The rheological studies of TPS demonstrate a gel behaviour and a non-Newtonian plateau in viscosity. This implies strong interactions within the TPS due to the existence of hydrogen bonding between starch and plasticizer. The presence of physical crosslinking in the melt state leads to highly elastic properties and a high melt yield stress, which have a stabilizing effect on the elongated structure. Therefore, the morphology of PCL/TPS36 blends demonstrates remarkably low levels of coalescence. Elongated dispersed structures are observed and the fibre diameters of those elongated phases remain constant when TPS concentration increases. These results indicate the breakup of a TPS thread is significantly reduced and the thread remains stable.

A 25% (volume) TPS36 in PCL1 blend with droplet/matrix morphology was used to study the TPS coalescence at annealing temperatures of 110 and 150 ℃. The results clearly show that the TPS particle size in the blend does not change with either annealing time or temperature,

indicating no coalescence. In a second quiescent annealing experiment, high concentration TPS in PCL1 blend (50/50 by weight) was also observed even after long annealing times. As a comparison, a completely immiscible HDPE/TPS36 blend (50/50 by weight) was also subjected to quiescent annealing to study the coarsening of TPS. The results show strong coalescence effects for the TPS phase in HDPE/TPS36 blend. These results also suggest the presence of compatibilization effects between TPS and PCL.

DMTA studies show the T_α peak for 100% TPS36 is 28.0 ℃. However, PCL/TPS blends with 50 and 70 wt% TPS have a TPS T_α peak which only appears as a diffuse shoulder at -10 and -8 ℃. This is a peak shift in excess of 30 ℃. At TPS contents of 30 wt% and below, the TPS T_α peak disappears entirely. These results strongly imply interactions between PCL and the starch-rich phase of TPS. The interaction is likely to be caused by the hydrogen bonding interactions between the carbonyl groups of PCL and hydroxyl groups on starch. The T_β of PCL1/TPS36 blends decreases with increasing TPS36 concentration. This effect can be attributed to the further phase separation between starch and glycerol upon blending with PCL.

The FTIR spectra of PCL1, TPS36 and their blend at 50/50 wt% showed that PCL had a strong carbonyl stretching absorption at a wave number of 1720 cm^{-1}, which shifts to 1724 cm^{-1} after blending with TPS36. This shift in the stretching vibration frequency of carbonyl groups further suggests a hydrogen bonding interaction between the carbonyl groups of PCL and the hydroxyl groups of TPS.

Mechanical properties display an extremely high ductility even at very high TPS concentration and in the absence of any interfacial modifier. The samples with TPS36 content less than 50% could be broken during the tensile test and the elongations at break of the samples with 80% and 90% TPS36 are 450 and 550%, respectively. These values are significantly higher than those reported in the literature. All the results presented can be explained by a combination of two phenomena: a high elasticity of the thermoplastic starch phase and a strong compatibility between TPS and PCL. The high level of compatibility in this PCL/TPS system likely results from the high mobility of the TPS chains due to the high plasticizer content and a highly effective TPS plasticization protocol. This high chain mobility facilitates hydrogen bonding interactions between TPS and PCL. The images of cryogenic fracture surfaces of PCL/TPS36 blends show the characteristics of a system experiencing good adhesion with very little evidence of microvoiding or ejected particles.

In the third part of this study, the biodegradation of native starch, thermoplastic starch (TPS) containing a high concentration of glycerol, and its blends with low-density polyethylene (LDPE) and polylactic acid (PLA) were demonstrated under compost conditions. CO_2 evolution was measured to evaluate the biodegradation properties during the test. The mineralization rate for pure TPS is extremely high compared with native starch due to its amorphous structure. The degradation rate of TPS is twice that of the native starch after the first two weeks. The final mineralization percentages were 59% and 52% for TPS and native starch, respectively. These results are evidence that the biodegradation of starch occurs preferably in amorphous regions as compared to ordered semi-crystalline domains.

Comparing the biodegradability of TPS24 and TPS36, it can be concluded that glycerol content has very little effect on TPS degradation. The studies on the biodegradation of blends of LDPE/TPS36 and PLA/TPS36 indicated that neither LDPE nor PLA have any effect on TPS biodegradation. The only contribution to biodegradation in those blends comes from the TPS component, under these room temperature conditions, and 86% and 82% of the TPS component in LDPE/TPS36 and PLA/TPS36 respectively is accessible to biodegradation. The blending of TPS with LDPE and PLA in a co-continuous morphology at a 50/50 composition provides a significant increase in surface area for the TPS which increases the biodegradation rate for the blends as compared to pure TPS. The biodegradation of the TPS component in those blend systems was completed within 6 weeks. The biodegradation profile of the 30/70 TPS36/LDPE blend indicates that approximately 50% of the TPS biodegrades in that sample. As a whole, these results indicate a good relationship between morphology, phase continuity and biodegradation behaviour. Morphology control in the mixtures with thermoplastic starch can thus result, in efficacious pathways for moisture penetration and microbial invasion resulting in an increase in the biodegradation rate. Thus, the blending of TPS with other polymers can provide a potential route towards more economical and environmentally compatible materials.

CONDENSÉ EN FRANÇAIS

Ce travail présente une approche pour la préparation de mélanges polycaprolactone (PCL)/amidon thermoplastique (TPS) par extrusion en une seule étape. La mise en oeuvre en une étape à l'état fondu de mélanges polymères à base d'amidon thermoplastique est une opération complexe impliquant la plastification, la dévolatilisation, le mélange à l'état fondu et le contrôle de la morphologie. Tout ceci doit être complété en un temps de résidence total d'au plus deux minutes dans une extrudeuse. De plus, l'amidon est un polymère naturel complexe, ce qui complique sa gélification. Afin de déterminer les limites de temps/température requises pour plastifier avec succès l'amidon dans un environnement de mise en oeuvre de polymères à l'état fondu, la calorimétrie par balayage différentiel (DSC), la microscopie optique et la diffraction de rayons X à grand angle (WAXS) ont été utilisées pour étudier les aspects clés de la gélification de l'amidon dans des mélanges glycérol/eau en excès. En même temps, ces résultats ont été liés à la morphologie de mélanges à l'état fondu d'amidon thermoplastique (TPS) et de polycaprolactone (PCL). Dans un deuxième temps, le développement de la morphologie et les interactions interfaciales dans les mélanges PCL/TPS ont été étudiés. Finalement, la biodégradation d'amidon natif, d'amidon thermoplastique (TPS) à haute teneur en glycérol, et de leurs mélanges avec du polyéthylène à basse densité (LDPE) et du poly(acide lactique) (PLA) a été démontrée sous des conditions de compostage.

Tout d'abord, la gélification de l'amidon a été démontrée. Les températures de déclenchement et de terminaison de la gélification de l'amidon de blé ont été obtenues par calorimétrie par balayage différentiel (DSC). Les résultats indiquent que l'eau et le glycérol ont des effets passablement différents sur la température de gélification de l'amidon. À une fraction constante de glycérol par rapport à l'amidon sec, la température de déclenchement, T_o, de pic, T_p, et de terminaison, T_c, de la gélification montrent un décalage vers les températures plus froides lorsque la concentration d'eau augmente. Inversement, ces températures de gélification sont décalées vers le haut lorsqu'on maintient constante la teneur en eau mais qu'on augmente la concentration de glycérol. Dans les deux cas, l'endotherme de gélification devient plus marqué avec une augmentation de la concentration de plastifiant dans le système. Ces résultats s'avèrent très utiles pour déterminer la température d'extrusion, puisque la température de gélification peut être changée en variant les ratios d'eau et de glycérol dans les mélanges amidon/eau/glycérol

initiaux.

Les granules d'amidon sont des matériaux semi-cristallins et sont composées principalement d'amylose et d'amylopectine amorphe. Lorsqu'on l'observe sous microscope optique avec de la lumière polarisée, la granule d'amidon montre de la biréfringence. Lors de la gélification de l'amidon, la cristallinité est graduellement détruite et la biréfringence diminue. Les plages de températures de gélification obtenues avec des mélanges amidon/eau en excès et amidon/glycérol en excès sont respectivement de 55,0 °C à 64,5 °C et de 113,0 °C à 126,5 °C. Par contre, une plage de 73,0°C à 82,7°C a été obtenue avec un mélange 50/50 (massique) d'eau et de glycérol. Ces données appuient les données obtenues par DSC.

Afin de déterminer les limites temps/température, la dynamique de la gélification de l'amidon a été étudiée en suivant le changement de diamètre des granules d'amidon sous des conditions isothermiques. Trois types de mélange d'amidon, soit amidon/eau, amidon/glycérol et amidon/eau/glycérol, ont été choisis à cette fin. Cette étude a mené à plusiuers conclusions intéressantes. En premier lieu, pour tous les mélanges, même après un entreposage à long terme, aucune gélification n'a été observée sous la température de déclenchement telle que mesurée par DSC. Deuxièmement, le processus de gélification est significativement plus lent (trois minutes) pour le mélange amidon/glycérol, même à haute température. Pour les mélanges amidon/eau et amidon/eau/glycérol, cependant, le processus de gélification est complété en une minute tout au plus. L'effet de l'eau dans le protocol de gélification eau/glycérol est, de toute évidence, d'améliorer le taux de pénétration dans les granules d'amidon. Afin d'étudier davantage l'effet de la température sur la gélification, un échantillon eau/amidon a été maintenu à différentes températures pendant 20 minutes. Après ce traitement, un balayage en chauffage a été effectué par DSC pour évaluer le degré de gélification. Les résultats ont indiqué que la température du pic de gélification (T_p) et le degré de gélification de l'amidon augmentent avec l'augmentation de la température du traitement isothermique, et qu'une gélification complète ne peut être obtenue qu'à des températures plus élevées que la température de terminaison (environ 80 °C). Puisque la gélification de l'amidon s'accomplit en une minute, il est important de noter que, malgré une cinétique rapide, en deçà de la température de terminaison (T_c), la gélification n'est que partielle, même après de longs temps de traitement. On conclut donc aisément que l'eau est un ingrédient essentiel à la gélification de l'amidon par le glycérol dans les contraintes de temps imposées par un procédé à l'état fondu, et un temps de contact eau-amidon suffisant est requis avant la

dévolatilisation.

Des travaux antérieurs au sein de ce laboratoire ont démontré que le temps nécessaire à la génération de morphologies en régime permanent lors de l'extrusion bi-vis de polymères synthétiques peut être relativement court (environ 30 secondes) une fois que tous les composants du mélange sont à l'état fondu. Le défi principal dans le procédé d'extrusion en une étape est donc l'efficacité de la plastification de l'amidon. Suite aux résultats ci-dessus, un plan d'expériences d'extrusion en une étape à l'état fondu pour des mélanges PCL/TPS a été conçu et la morphologie de la phase dispersée (TPS) a été observée. La taille des particules de TPS (d_v) dans une matrice de PCL est de 13,9 microns quand le glycérol est utilisé seul comme plastifiant (l'amidon contient tout de même de l'eau provenant de l'humidité ambiante). Cette valeur est très proche de la taille des granules d'amidon natif (13,6 microns) et indique clairement l'inabilité du glycérol seul à plastifier l'amidon natif à l'intérieur des contraintes de temps imposées par l'extrusion à l'état fondu. Lorsqu'un mélange glycérol/eau en excès a été utilisé, et que le temps de résidence est demeuré court avant le retrait de l'eau, une partie de l'amidon gélifié a été complètement réduite en particules plus petites d'un ordre de grandeur. Une distribution bimodale de la taille des particules a été obtenue, et les grosses particules avaient une taille moyenne en volume (d_v) de 10,2 μm et un d_n de 2,5 μm. Cependant, la distribution bimodale de la taille des phases du TPS indique clairement que le processus de plastification de l'amidon est incomplet. En augmentant davantage le temps de résidence avant la dévolatilisation de l'eau, un amidon complètement plastifié est obtenu. L'efficacité de la plastification est démontrée par une réduction dramatique, d'un facteur six, de la taille de particules de la phase dispersée de TPS, et une distribution unimodale de la taille des phases dans le mélange. Il est clair que l'utilisation de mélanges glycérol/eau en excès est une condition *sine qua non* à la plastification de l'amidon.

La deuxième partie de ce travail consiste en l'étude du développement de la morphologie et des interactions interfaciales dans les mélanges polycaprolactone/amidon thermoplastique. Ce travail étudie particulièrement la coalescence et le développement de la continuité dans ces systèmes. Les études rhéologiques du TPS indiquent un comportement de gel et un plateau non newtonien en viscosité. Ceci implique la présence d'interactions fortes au sein du TPS causées par l'existence de ponts hydrogène entre l'amidon et le plastifiant. La réticulation physique à l'état fondu mène à des propriétés très élastiques et une contrainte à l'écoulement à l'état fondu élevée, avec pour résultat un effet stabilisateur sur les structures allongées. Ainsi, la morphologie

des mélanges PCL/TPS36 montre des niveaux de coalescence remarquablement faibles. Des structures allongées dans la phase dispersée sont observées et le diamètre des fibres qui constituent ces phases allongées demeure constant même en augmentant la concentration de TPS. Ces résultats indiquent que le bris des fils de TPS est considérablement réduit et que le fil demeure stable.

Un mélange de TPS36 (25% volumétrique)/PCL1 avec une morphologie matrice/gouttelettes a été utilisé pour étudier la coalescence du TPS à des températures de recuit de 110 et 150 °C. Les résultats indiquent clairement que la taille des particules de TPS dans le mélange ne change pas avec le recuit, ce qui implique l'absence de coalescence. Lors d'une deuxième expérience de recuit statique, en augmentant la concentration de TPS dans un mélange TPS/PCL1 à 50/50 massique, a aussi été observé même après de longs recuits. En comparaison, un mélange complètement immiscible HDPE/TPS36 à 50/50 massique a aussi été soumis à un recuit statique pour étudier l'augmentation de la taille des phases de TPS. Les résultats ont montré des effets de coalescence importants dans la phase de TPS. Ces résultats suggèrent des effets de compatibilisation entre le TPS et le PCL.

L'analyse dynamomécanique thermique (DMTA) montre que le pic T_α pour le TPS36 à 100% est à 28,0 °C. Cependant, le pic T_α du TPS pour les mélanges PCL/TPS à 50% et 70% de TPS en masse n'apparaît que sous la forme d'un épaulement diffus entre -10 et -8 °C. Ceci représente un décalage de plus de 30 °C dans la position du pic. À des concentrations de TPS de 30% et moins (massique), le pic disparaît complètement. Ces résultats suggèrent fortement la présence d'interactions entre le PCL et la phase riche en amidon du TPS. Ces interaction sont probablement dues à des ponts hydrogène entre les groupes carbonyle du PCL et les groupes hydroxyle de l'amidon. Le T_β des mélanges PCL1/TPS36 diminue avec l'augmentation de la concentration en TPS36. Cet effet peut être attribué à la progression de la séparation de phases entre l'amidon et le glycérol lors du mélange avec le PCL.

La spectroscopie infrarouge par transformée de Fourier (FTIR) effectuée sur le PCL1, le TPS36 et leur mélange à 50/50 massique, montre un fort pic d'absorption à un nombre d'onde de 1720 cm^{-1}, caractéristique de l'étirage d'un groupe carbonyle; ce pic est décalé à 1724 cm^{-1} dans un mélange avec le TPS36. Ce décalage dans la fréquence de vibration en étirage des groupes carbonyle suggère une interaction causée par des ponts hydrogène entre les groupes carbonyle du PCL et les groupes hydroxyle du TPS.

Mécaniquement, on observe une ductilité très élevée, même à de très hautes concentrations de TPS et en l'absence de tout agent interfacial. Les échantillons dont la concentration en TPS36 était inférieure à 50% ne brisent tout simplement pas lors du test de traction. Et les allongements à la rupture des échantillons à 80% et 90% de TPS36 sont respectivement de 450 et 550%. Cette valeur est plus élevée que celles rapportées dans la littérature. Tous les résultats présentés peuvent s'expliquer par une combinaison de deux phénomènes : l'élasticité élevée de la phase d'amidon thermoplastique, et une forte compatibilité entre le TPS et le PCL. Cette compatibilité est vraisemblablement causée par la mobilité élevée des chaînes de TPS, due à la haute concentration de plastifiant, et un protocole hautement efficace de plastification du TPS. La mobilité des chaînes facilite l'apparition de liens hydrogène entre le TPS et le PCL. Les images de surfaces de fracture cryogénique des mélanges PCL/TPS36 sont caractéristiques d'un système où l'adhérence est bonne; on y observe très peu de microvides ou de particules éjectées.

Dans la troisième partie de cette étude, la biodégradation de l'amidon natif, de l'amidon thermoplastique à forte teneur en glycérol, et de ses mélanges avec le polyéthylène basse densité (LDPE) et le poly(acide lactique) (PLA) a été démontrée dans des conditions de compostage. L'évolution du CO_2 a été mesurée afin d'évaluer la biodégradation durant le test. Le taux de minéralisation du TPS pur est beaucoup plus élevé que celui de l'amidon natif à cause de sa structure amorphe. Le taux de dégradation du TPS est deux fois plus élevé que celui de l'amidon natif après deux semaines. Les pourcentages finals de minéralisation pour le TPS et l'amidon natif étaient de 59% et 52%, respectivement. Ces résultats démontrent que la biodégradation de l'amidon se produit préférentiellement dans les régions amorphes; elle est inefficace dans les domaines semi-cristallins ordonnés.

En comparant la biodégradabilité du TPS24 et du TPS36, on peut conclure que le contenu en glycérol a moins d'effet sur la dégradation du TPS. Les études portant sur la biodégradation de mélanges LDPE/TPS36 et PLA/TPS36 ont montré que ni le LDPE, ni le PLA n'ont d'effet sur la biodégradation du TPS. La biodégradation des mélanges peut être obtenue par le TPS seulement. Cependant, le mélange du TPS avec le LDPE ou le PLA augmente la surface de TPS de manière significative, ce qui réduit le seuil de percolation du TPS. La valeur du seuil de percolation varie entre 20 et 30% (massique). Elle est inférieure à celle des granules d'amidon natif (environ 40%, selon la littérature). Ainsi, des chemins plus efficaces pour la pénétration de l'eau et l'invasion microbienne sont générés par rapport à l'amidon natif, ce qui mène à une biodégradation plus

rapide. Le mélange de TPS avec d'autres polymères constitue donc une avenue potentielle vers des matériaux plus économiques et plus avantageux d'un point de vue environnemental.

TABLE OF CONTENTS

LIST OF TABLES

LIST OF FIGURES

LIST OF APPENDICES

INTRODUCTION

Statement of the problem

The majority of plastic products are made from petroleum-based synthetic polymers that do not degrade in a landfill or in compost conditions. Therefore, the disposal of these products poses a serious environmental problem. An environmentally-conscious alternative is to develop biodegradable materials. Biodegradable materials include biodegradable polymers and biopolymers. Biodegradable polymers are synthetic polymers that have certain degrees of biodegradability such as polycaprolactone, polyhydroxybutyrate and poly(vinyl alcohol) (Brody and Marsh, 1997). Biopolymers are naturally occurring polymers such as cellulose, polysaccharides and proteins. Most biopolymers are biodegradable, and hence, they can be degraded by bacterial activity into natural metabolic products. Most commercially available biodegradable materials are based on natural materials, e.g. polysaccharides (starch). This is because starch is a renewable, abundant and inexpensive material. However, the conversion of agricultural-based raw materials into consumer products is not straightforward due to the lack of certain properties for agricultural products, which are critical for the manufacture of useful consumer products. For instance, they do not have thermal stability, nor good oxidative or water-resistant properties. Thus, successful conversion of agricultural-based materials into viable consumer products requires overcoming these shortcomings. To get over these problems, starch is often modified mechanically, physically or chemically, and/or combined with a plasticizer or polymeric additives.

Contrary to their biodegradation behaviour, the physical and mechanical properties of starch-based composite materials become quite poor with increasing starch content. This can be attributed to the incompatibility between the hydrophilic starch and hydrophobic polymer as well as to the poor interfacial adhesion between the components (Avella et al., 2000; St Lawrence et al., 2000; Averous et al., 2000). In order to overcome the problem of poor interfacial adhesion, modifications on both starches and matrix polymers have been studied by several authors (Avella et al., 2000; Wu, 2003). They concluded that acceptable mechanical properties could only be obtained in the presence of a compatibilizing agent or with lower starch content. More recently, the development of thermoplastic starch from granular starch and plasticizer allows for the

transformation of starch into a free-flowing fluid like other conventional thermoplastics. Further, the polymer blend strategy could be used to control the morphology of TPS-based blends. For this purpose, a one-step blending extrusion system combination of a twin-screw and a single-screw extruder has been setup by Favis and co-workers (Favis et al., 2003 and 2005). The systems had been successfully used in thermoplastic starch (TPS) based blends. It has been reported that the dispersed phase morphology control of thermoplastic starch in TPS/LDPE blends can result in materials with excellent mechanical properties (Rodriguez-Gonzalez et al., 2003 and 2004).

Starch can be converted into a thermoplastic material through the disruption of molecular interactions in the presence of plasticizer under specific conditions. Water and glycerol are the most widely used plasticizers in TPS materials. When starch granules are heated, starch undergoes an irreversible order-disorder transition. The swelling of the amorphous regions of the granules by absorption of plasticizer occurs, which disrupts the molecular structure of the starch granules. Simultaneously, some other phenomena are observed, such as: uptake of heat of starch granules, loss of crystallinity (Di Paola et al., 2003; Cagiao et al., 2004), increase in suspension viscosity (Sopade et al., 2004), change in electrical conductivity and plasticizer diffusivity (Gomi et al., 1998; Li et al., 2004). This process is known as gelatinization and the material is often referred to as thermoplastic starch (TPS). TPS can be processed using conventional plastic processing techniques, i.e. extrusion, injection molding and compression molding.

The one-step melt processing of polymer blends with thermoplastic starch is a complex operation involving plasticization, devolatilization, melt-melt mixing and morphology control. All these must be achieved within a maximum two minutes total residence time in an extruder. It is necessary to determine the time/temperature boundaries ultimately required for the successful plasticization of starch in a polymer melt processing environment.

As the final morphology has a controlling influence on the blend properties and on the application, knowledge of the mechanisms involved in the blending stage is required. As polymers are often immiscible, various morphologies, for instance, droplet/matrix, fibril, lamellar and co-continuous morphologies may occur during melt mixing. Each of them depends on several factors, such as composition, processing conditions (mixing time, temperature, shear and elongation rate) or nature of the polymers (interfacial tension, viscosity, elasticity). In order for the TPS phase to be sufficiently fluid to undergo the typical phase deformation/disintegration

phenomena required for morphology modification, very high plasticizer contents are required (Rodriguez-Gonzalez et al., 2004). The primary step is the conversion of native starch into complete thermoplastic starch. However, this conversion from native starch to highly plasticized TPS on melt processing equipment is much more difficult and problematic than what is often reported in the literature. Therefore, the ultimate objectives of the present work are stated in the following section.

Objectives of the project

Melt blending of starch with synthetic polymers is an excellent low-cost alternative. Mechanical properties of starch-based materials greatly depend on their morphology. For better control of the morphology of such immiscible blends, the objective of this work is below.

The first objective of this work is to understand the effect of excess water/glycerol mixtures on starch plasticization with a view to determining the time/temperature boundaries required for the successful plasticization of starch on an extruder, and ultimately to optimize the melt processed dispersed phase morphology of TPS-based blends. The study of the dynamics of gelatinization will be conducted under isothermal conditions by evaluating the starch granule swelling during starch gelatinization. Subsequently, the morphology of blends of polycaprolactone (PCL) and thermoplastic starch prepared via a one-step twin-screw extrusion process will be examined. The relationship between factors influencing the gelatinization and dispersed phase morphology will be discussed.

The second objective of this work is to understand the morphology development in PCL/TPS blends with high plasticizer content prepared using a one-step process. This work will closely examine the coalescence and continuity development in these systems. The resulting dynamic and static mechanical properties of the blends as well as the possible presence of specific interactions will also be considered.

The third objective of this work is to examine the biodegradability of starch granules, TPS with high concentration of glycerol, and its blends with biodegradable PLA and non-degradable LDPE. The effects of starch crystallinity, glycerol content in TPS, morphology of blends and continuity phase of TPS on biodegradation properties will also be studied.

CHAPTER 1

LITERATURE REVIEW

1.1 Overview

Over the last two decades, numerous papers have been published on polymer blends containing native granular starch. These studies have generally shown that the physical and mechanical properties of the composite material become quite poor with increasing starch content. This can be attributed to the incompatibility between the hydrophilic starch and hydrophobic polymer as well as to the poor interfacial adhesion between the components (Avella et al., 2000; St Lawrence et al., 2000; Averous et al., 2000). However, it has been reported that the dispersed phase morphology control of thermoplastic starch (TPS) in TPS/LDPE blends can result in materials with excellent mechanical properties (Rodriguez-Gonzalez et al., 2003).

Starch can be converted into thermoplastic material through the disruption of molecular interactions in the presence of plasticizer under specific conditions. Water and glycerol are the most widely used plasticizers. When starch granules are heated, starch undergoes an irreversible order-disorder transition. This process is known as gelatinization and the resulting material is often referred to as thermoplastic starch (TPS). It is interesting that TPS can be processed using standard plastics processing techniques, i.e. extrusion, injection and compression molding. Thermal and mechanical energy inputs associated with the addition of plasticizer are necessary to transform granular starch into a homogeneous matrix.

Polymer blends containing TPS have been demonstrated many times in the literature (Rodriguez-Gonzalez et al., 2003; Averous et al., 2000). In this chapter, detailed descriptions related to biodegradable plastics, starch, thermoplastic starch, polymer blends, and morphology control will be presented.

1.2 Degradable Plastics

1.2.1 Biodegradable Plastics

Plastics are the source of rising environmental problems since most of them are not used for long-lived materials but occur in waste [Steinbuchel, 1995]. The most desirable long-term solution to this problem is to use biodegradable plastics, which undergo biodegradation. ASTM (D6400-99) gives the following definition of degradable plastics/polymers: degradable plastic, a

plastic designed to undergo a significant change in its chemical structure under specific environmental conditions resulting in a loss of some properties that may vary, as measured by standard test methods appropriate to the plastic and the application in a period of time that determines its classification. Complete biodegradation will result in completely transforming plastics into microbial biomass, CO_2 and H_2O (Roper and Koch, 1990).

Polymers degrade by one of four primary degradation mechanisms: biodegradation, macroorganism degradation, photodegradation and chemical degradation. Of these forms, biodegradation is the most environmentally compatible and is the only pathway for the complete elimination of plastics and fragments from the environment (Swift, 1993). The degradation mechanism of biodegradable polymers in an aerobic composting environment is similar to that for organic matter. Biodegradable polymers are attacked and disintegrated by enzymes from naturally occurring microorganisms, such as bacteria and fungi, encountered under specific conditions in composts. Biodegradation occurs when microorganisms colonize the surface of the polymer and secrete enzymes that break down the macromolecules (Nayak, 1999). The biodegradation process depends on several factors such as microbial activity, the surface area of the polymer, temperature, pH, molecular weight and polymer crystallinity (Davis and Song, 2006).

1.2.2 Current Biodegradable Plastics

At present, there are three main classes of biodegradable plastics. The first class of materials are synthetic polymers, with carbonyl groups susceptible to hydrolysis attack by microbes, e.g. polycaprolactone (PCL) and poly(lactic acid) (PLA). The second class of materials is composed of naturally occurring processible bacterial polymers, polyhydroxybutyrate (PHB), polyhydroxyvalerate (PHV), and their copolymer, polyhydroxybutyrate-valerate (PHBV). These materials are truly biodegradable, being attacked by a wide variety of bacteria. The third class are natural biodegradable polymers and their blends, such as polysaccharides (e.g. starch), cellulose and polypeptides of natural origin (Averous, 2004).

The positive and negative attributes and potential applications of each of these biodegradable plastics are summarized in Table 1.1.

1.2.3 Biodegradable Polyester

Polyesters play a predominant role as biodegradable plastics due to their potentially hydrolysable ester bonds. As shown in Figure 1.1, the polyester family is made of two major

groups: aliphatic (linear) polyesters and aromatic (aromatic rings) polyesters (Nolan-ITU Pty Ltd, 2002).

Table 1.1 Biodegradable polymers and potential applications

Polymer (Class)	Positive Attributes	Negative Attributes	Potential Applications
(1) Starch & Starch blends	Low cost, rapid biodegradation	Hydrophilicity	Mulch film, compost bags, packing foams
(2) PVOH	Good oxygen barrier, rapid biodegradation	Solubility in water	Pesticide, fertiliser, detergent dispersal
(2) EVOH	Toughness, good oxygen barrier	Slow biodegradation	Food packaging
(2) PCL	Water stable, biodegradable, and hydrolysable, toughness	Low melting point	Compost bags, packaging for cold environments
(2) PLA	Tensile strength, clear films	Brittle, hydrolytically unstable	Injection Moulding, paper coating
(3) PHA	Rapid biodegradation, water stable	Cost	Paper Laminate

Reference: Mayer and Kaplan (1997)

1.2.4 Polycaprolactone (PCL)

Poly(ε-caprolactone) (PCL) has been thoroughly studied as a substrate for biodegradation (Potts, 1978a, 1984b; Fields et al., 1974; Benedict et al., 1983; Cook et al., 1981; Jarret et al., 1981) and as a matrix in controlled-release systems for drugs (Pitt et al., 1981). PCL is generally prepared from the ring-opening polymerization of ε-caprolactone. The chemical structure of polycaprolactone is shown in Figure 1.2. It is a linear, hydrophobic and partially crystalline polyester, and can be slowly utilized by microbes. Its degradation is much slower than that of poly (ε-hydroxyl acid). (Pitt et al., 1980). Thus, it is most suitable for controlled release devices with longer working lifetimes (1-2 years). Its physical properties and commercial availability make it very attractive, not only as a substitute of non-biodegradable polymers for commodity, but also for specific applications in the medical and agricultural fields (Dubois et al., 1991; Pott, 1978). PCL is suited for use as food-contact foam trays, loose and file bags. However, PCL is more expensive than conventional plastics. Therefore, blends of PCL with cheaper materials, such as starch (Wu, 2003; Singh et al., 2003), polystyrene (Biresaw et al., 2004), poly(lactic acid) (Broz et al., 2003; Tsuji et al., 2001), poly(vinyl alcohol) (Kesela et al., 1999) and poly(ethylene terephthalate) (Lim et al., 2003) were produced. The morphology, rheology, compatibility and

mechanical properties were widely investigated.

Typical properties and processing conditions of polycaprolactone are shown in Table 1.2.

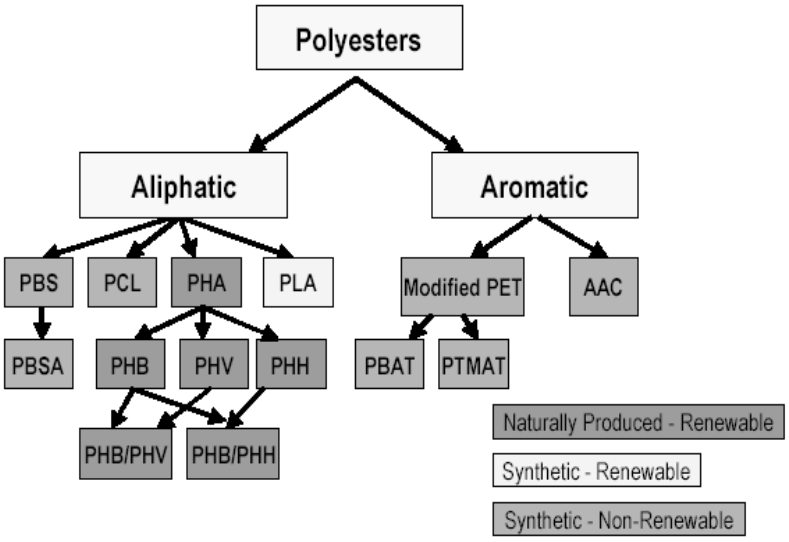

Figure 1.1 Biodegradable polyester family

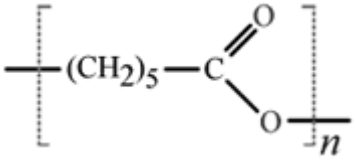

Figure 1.2. Chemical structure of polycaprolactone (PCL)

1.2.5 Poly(lactic acid) (PLA)

Polylactic acid (PLA) is a biodegradable polymer derived from lactic acid. It is a highly versatile material and is made from 100% renewable resources like corn, sugar beets, wheat and other starch-rich products. PLA is a thermoplastic, high strength, high modulus polymer that can be made from annually renewable resources to yield articles for use in either the industrial packaging field or the biocompatible/bioabsorbable medical device market (Donald, 2001). The chemical structure of PLA is shown in Figure 1.3. Some of the commercially available biodegradable PCL's are presented in Table 1.1.

Table 1.2 Typical properties and processing condition of polycaprolactone

	CAPA6800	CAPA6500
Melt index (g/10min)	3.0	7.0
Mn	69,000	47,000
Mw	120,000	85,000
Mw/Mn	1.74	1.78
Mean Mw.	80,000	50,000
Viscosity 70 ^{o}C 10 S^{-1}	12650	2890
(Pa.s) 100 ^{o}C 10 S^{-1}	5780	1350
150 ^{o}C 10 S^{-1}	1925	443
Melting point (^{o}C)	60	60
Crystallinity (%)	76.9	76.6
Crystallization Temp. (^{o}C)	25.2	27.4
Tg (^{o}C)	-60	-60
Yield stress (MPa)	17.5	16
Modules 1mm/min	470	440
(MPa) 10mm/min	430	500
Elongation at break (%)	700	920
Extrusion processing (^{o}C)		
Feed zone Temp.	50	50
Compression zone	70-90	130-165
Metering zone	75-105	140-150
Die zone	70-120	70-120

Poly(lactic acid) (PLA) has received much attention for two reasons: one is its excellent chemical and physical characteristics in appearance, shape formation and safety; the other is its recyclability characteristics, i.e., when PLA is abandoned to soil, it can be degraded by some microorganisms forming CO_2 and H_2O, which are then recycled to starch by photosynthesis

(Bastioli, 1998). The resulting starch can be used as a raw material to produce the lactic acid again by fermentation (figure 1.4). Carbon circulation from starch by fermentation takes less time than that of petroleum products. It may lead to a new environmentally friendly chemical industry.

Table 1.3 Polycaprolactone polymer (commercially available)

Trade name	Supplier	Origin
Tone	Union Carbide(UCC)	USA
CAPA	Solvay	Belgium
Placeel	Daicel Chemical Indus.	Japan

PLA resembles clear polystyrene. It can be processed like most thermoplastics into fibers and films, thermoformed, or injection molded (Drumright et al., 2000), and used for compost bags, plant pots, diapers and packaging. Unmodified PLA has several limitations such as brittleness, especially at low temperature, and low heat distortion temperatures. These can be improved by various means. For example, flexible film for compost bags can be produced by copolymerization with caprolactone or by some other modification. Slow crystallization rates (as for unmodified PET) can be accelerated through nucleation or post-annealing of molded or extruded products (Huneault and Li, 2007). High molecular weight PLA can produce thermoformed containers with living hinges that show higher flex-crack resistance than polystyrene. The typical properties of PLA are shown in Table 1.4. PLA is degraded by simple hydrolysis of the ester bond and does not require the presence of enzymes to catalyze this hydrolysis. The rate of degradation is dependent on the size and shape of particle, the isomer ratio, and the temperature of hydrolysis. PLA undergoes thermal degradation at a temperature of about 200℃ by hydrolysis, lactic reformation, oxidative main chain scission and transesterification reaction (Bastioli, 1998). Composting conditions are found only in industrial units with a high temperature (above 50 ^{o}C) and a high relative humidity (RH) to promote chain hydrolysis.

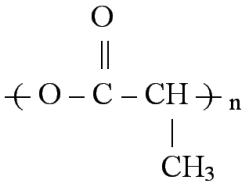

Figure 1.3 Chemical structure of PLA

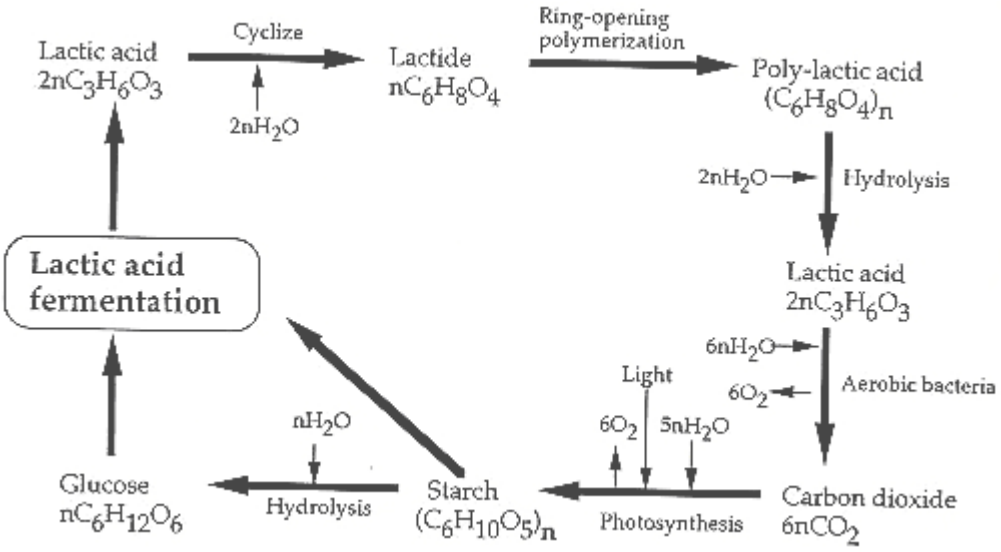

Figure 1.4 The characteristic of PLA recycle

Table 1.4 The physical properties of PLA

Properties	PLA
Molecular weight (Daltons) [2,3]	100,000 to 300,000
Glass transition temperature(^oC) [1,2]	50-70
Melting temperature(^oC) [1,2]	130-215
Crystallinity (%) [2]	10-40
Surface energy (dynes) [2]	38
Solubility parameter ($J^{0.5}$ $cm^{-1.5}$) [3]	19-20.5
Heat of melting (J g^{-1}) [2]	8.1-93.1
Specific gravity (g/cm^3) [1]	1.25
Melt-index range (g/10min)	2-30

1.2000 Cargill Dow u c, published 2000; *2*. Mobley, D.P. plastics from microbes, 1994; *3*.Hideto Tsuji, Kimika S. J. A P S, Vol 79 1582-1589, 2001.

1.3 Starch

1.3.1 Chemical structure: molecular and macromolecular constituents

Starch, a renewable degradable carbohydrate biopolymer, is one of the most common components of our food, and is especially high in staple foods such as rice and wheat. Starch can be isolated from plants. Main sources come from wheat, potato, rice, pea, cassava, corn, etc.

According to the resource, native starches have dimensions ranging from 0.5 to 175 mm and appear in variety of shapes (French et al., 1984). Chemically, starch is a polymer of glucose (Figure 1.5) groups linked by glucosidic linkages in the 1-4 carbon positions.

The length of the starch chains will vary with plant source but in general the average length is between 500 and 2000 glucose units (Zobel, 1988). Structurally, starch has two forms, amylose (which is a straight chain) and amylopectin (which is branched). α-1,4 linkages form the chains of glucose molecules and α-1,6 linkages occur at the branch points. The structures are shown in Figure 1.6 and Figure 1.7. Amylose is a linear polymer with a molecular weight of 10^5-10^6. Amylopectin is a highly multiple-branched polymer with a high molecular weight of 10^7-10^9 (Zobel, 1988). Starch properties are dependent upon the ratio of amylase and amylopectin and their structure. Very few reports are available concerning the conformation of amorphous amylose and amylopectin. However, the existence of starch strongly networked by hydrogen bonds was considered. The density of the starch granule is very high (about 1.5 g/cm^3 depending on the water content) (Bul éon et al., 1982). Native starch contains around 10% water at a relative humidity of 54% and a temperature of 20 ^{o}C.

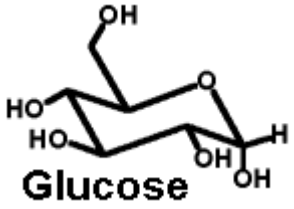

Figure 1.5 Chemical structure of glucose

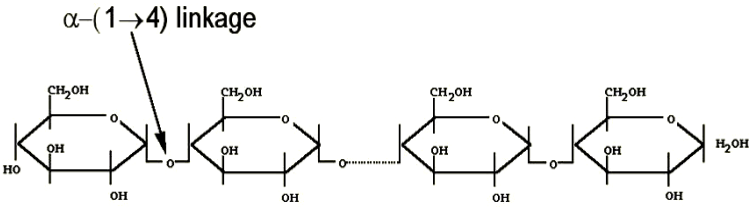

Figure 1.6 Structure of amylase

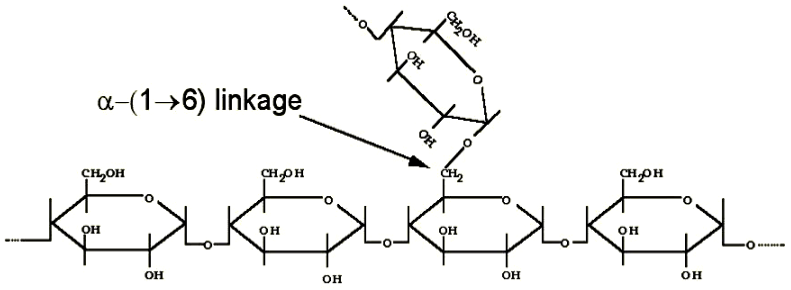

Figure 1.7 Structure of amylopectin

1.3.2 Molecular chain and the crystal

Starch molecular structure is complicated. However, several investigations have been carried out to establish the level of organization within the starch granules. Techniques such as X-ray diffraction experiments (Van Soest and Hulleman 1996), atomic force microscopy (AFM) (Tang and Copeland, 2007), and transmission electron microscopy (TEM) have been used. In the native form of starch, amylose and amylopectin molecules are organised in granules as alternating semi-crystalline and amorphous layers that form growth rings as illustrated in Figure 1.8. The semi-crystalline layer consists of ordered regions of double helices formed by short amylopectin branches. The amorphous regions of the semi-crystalline layers and the amorphous layers are composed of amylose and non-ordered amylopectin branches (Biliaderis, 1992 and Godet et al., 1995). The two forms cannot be evidenced by differential scanning calorimetry (DSC) since they yield very similar melting/decomplexing enthalpy and temperature values.

Native starch granules exhibit two main types of X-ray diffraction diagrams (Figure 1.9), the A type for cereal starches and the B type for tuber and amylose-rich starches (Zobel, 1988 and Colonna et al., 1982). Another type is the C-type diffraction diagram, which has been shown to be a mixture of A- and B-type diagrams (Biliaderis, 1992). The crystalline V-form characteristic of amylose complexed with fatty acids and monoglycerides, which was observed in starch after gelatinization, is rarely detected in native starches (Gernat et al., 1993). Native A- and B-type crystal lattices consist of double helical, six-fold structures. The difference between A- and B-type crystallinity is the packing density of the double helices in the unit cell (Imberty et al., 1991). In the A-structure (Imberty et al., 1991 and 1998), these double helices are packed in a monoclinic unit cell (a=1.24 nm, b=1.172 nm, c=1.069 nm) with eight water molecules per unit cell (Figure 1.10A). In the B-type structure (Imberty et al., 1991), double helices are packed in a hexagonal unit cell (a=b=1.85 nm, c=1.04 nm) with 36 water molecules per unit cell (Figure

1.10B). The B-type structure is described as a more loosely packed hexagonal assembly of the helices with a column of water molecules present in the centre of the hexagonal arrangement, whereas in the A-type structure, this column of water is replaced by a double helix. The B-type is converted into A-type by heat moisture treatment at about 100-120 ℃ (Kulp and Lorenz, 1981).

a)

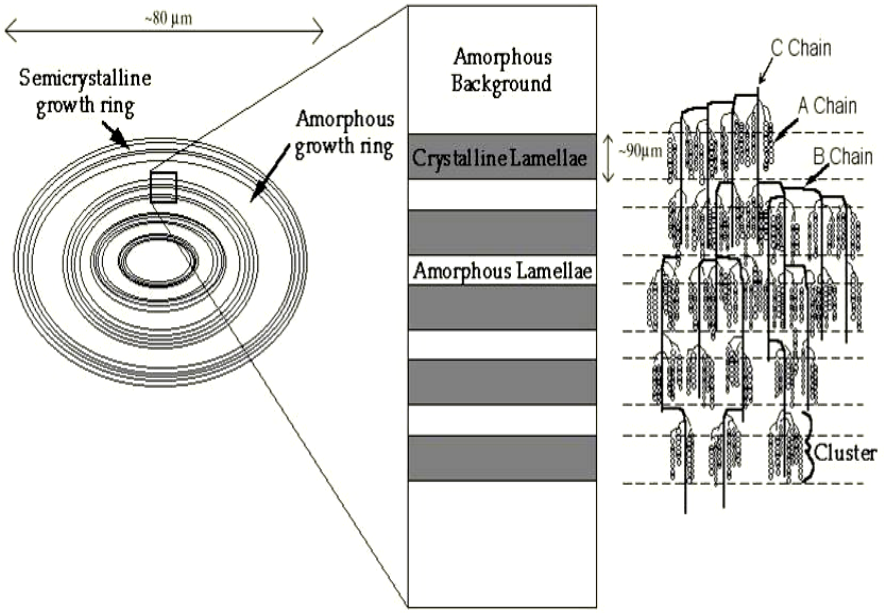

b)

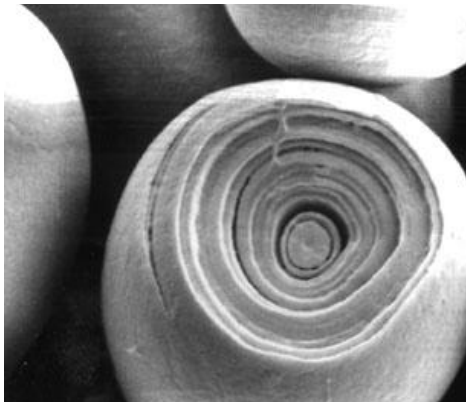

Figure 1.8 Schematic (a) and photography (b) view of the structure of a starch granule, with alternating amorphous and semi-crystalline zones constituting the growth rings

When the starch granules are observed under polarized light, a characteristic dark cross (centered at the hilum) is seen which has led to the granules being considered as distorted

spherocrystals (French, 1984). A variety of techniques has been used to determine the absolute crystallinity of native starch. The values vary from 15% to 45% depending not only on the origin and the hydration of starch but also on the technique used and moisture content (Zobel, 1988 and Bulέon et al., 1982). However, the melting temperature of native starch is difficult to measure because it is close to its decomposition temperature (Shogren, 1992).

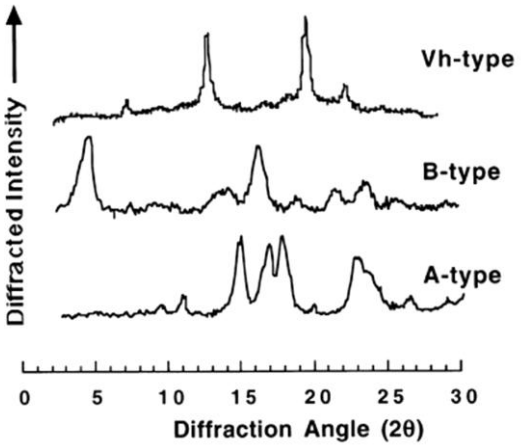

Figure 1.9 X-ray diffraction diagrams of A-, B- and Vh-type starch.

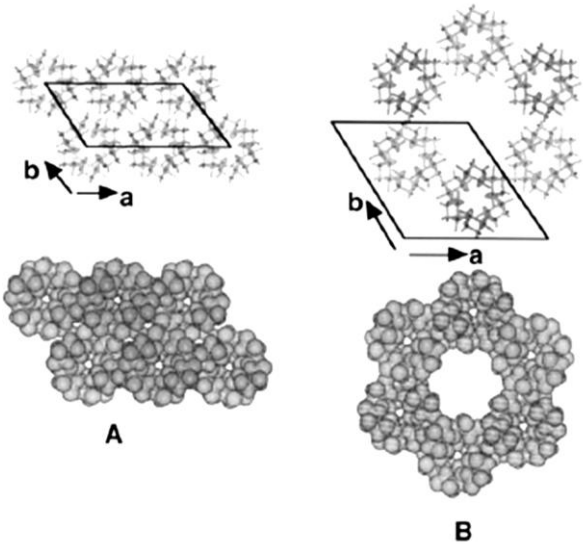

Figure 1.10 Crystalline packing of double helices in A-type (A) and B-type (B) amylose.

1.3.3 Starch lamellar assembly

Starch lamellar assembly is an important step during starch gelatinization. The dry, unsolvated starch granules are disordered, having no periodic lamellar structure and little defined crystallinity (Perry and Donald, 2000). The characteristic 9 nm spacing, seen in the small angle X-ray scattering curves of wet starch is absent when the starch is dry (unplasticized). The change in packing from the dry to hydrated state is shown in Figure 1.11. Upon heating or prolonged room-temperature storage, starch granules become solvated and plasticized. Glycerol and other non-aqueous solvents, with water, plasticize the amorphous lamellar regions, allowing the helices within the crystalline lamellae to take up enthalpically favorable crystalline arrangements. Assembly results in the formation of a periodic lamellar structure within a system that is immobile and a periodic at room temperature. The driving force for the assembly process is the enthalpy bonus derived from crystallization (Perry and Donald, 2000). The presence of low molecular weight plasticizer is necessary. In the absence of heating, it is sufficient alone to bring about lamellar assembly. Heating in the presence of moisture brings more rapid lamellar assembly. An effective solvent-temperature-time superposition governs lamellar assembly (Lillie and Gosline, 1990; Levine and Slade, 1986). High molecular weight plasticizer has less ability to penetrate the starch granule and a long time is required to initiate lamellar assembly. The lamellar assembly gives rise to the exothermic DSC transition (Perry and Donald, 2000).

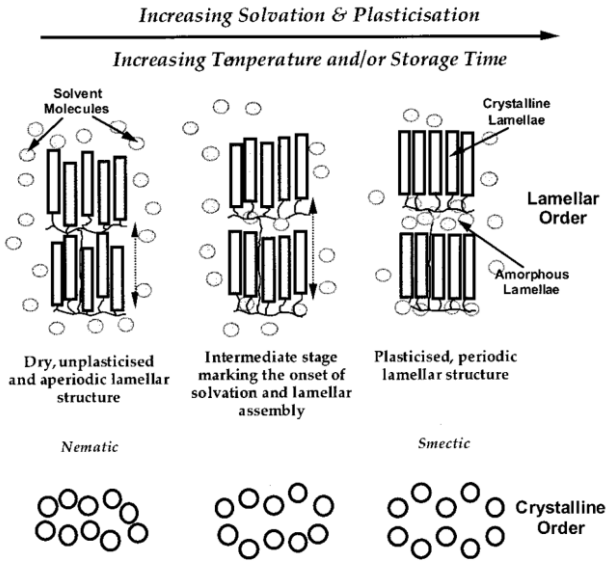

Fugure 1.11 Chematic representation of the proposed model of lamellar assembly in B-type starch.

1.4 Thermoplastic Starch

Dry starch is not a thermoplastic. However, in the presence of plasticizer, such as water, glycerol, etc., thermal processing starch can be achieved. Thermoplastic starch has several advantages. It is entirely comprised of annually renewable materials, is of low cost, requires low energy for its production and results in very low levels of green house gas emissions (Kurdikar et al., 2000; Patel et al., 2003). In addition, such TPS compounds can be processed on existing plastics fabrication equipment.

The applications of thermoplastic starch polymers are generally film, such as shopping bags, bread bags, bait bags, over-wrap, backing material. Foam loose fill packaging and injected molded products such as take-away containers are also potential applications. Furthermore, thermoplastic starch is a very attractive, low cost candidate for biomedical uses, expecially in soluble biodegradable poly applications in tissue scafford and controlled drug-delivery matrices (Takacs and Vlachopoulos, 2008). High starch content plastics are highly hydrophilic and readily disintegrate in contact with water. This can be overcome through blending, as the starch has free hydroxyl groups, which readily undergo a number of reactions, such as acetylation, esterification and etherification.

1.4.1 Starch gelatinization and retrogradatoion

Native starch granules swell when they absorb water through hydrogen bonding with their free hydroxyl groups, but they still retain their order and crystallinity at low temperature (Rodriguez-Gonzalez et al., 2003) even if lamellar assembly occurs (Perry and Donald, 2000). However, when these swollen starch granules are heated, hydrogen bonding between adjacent glucose units is disrupted and the crystallinity is progressively destroyed. This process is called gelatinization. The processing of starch and water in a heated extruder is an efficient way to obtain gelatinized starch (GS) since the high shear that can be generated in the extruder disrupts the starch granules. Once starch granules are disrupted, the gelatinized starch (GS) can be blended with a suitable plasticizer to reduce its melting temperature and improve its processability. This material is known as thermoplastic starch (TPS). Water has often been used as a plasticizer to destructure starch in its blending with various polymers to achieve a fine dispersion and, consequently, to obtain desirable product properties. Water is a convenient, economical, and effective plasticizer for starch and would likely affect the morphology and mechanical properties of the blend (Ke and Sun, 2000).

Figure 1.12 gives the different stages via extrusion processing (Avérous, 2004). Under temperature and shear, starch is destructured, plasticized, melted but also partially depolymerized. After the processing, a homogeneous molten phase was obtained.

Thermoplastics starch is unstable because of its retrogradation (recrystallization). During long-term storage, TPS forms a rigid structure. A good example of this retrogradation process is the aging of bread, which has been studied by following the retrogradation kinetics of gelatinized wheat starch (Roulet et al., 1987, Morikawa and Nishinari, 2000). Retrogradation or recrystallization can occur in TPS if the conditioning temperature is above the Tg of TPS (Parvinder et al., 2002). The X-ray diagrams of highly plasticized (30% glycerol) amylopectin film are demonstrated in Figure 11.3 (Myllärinen et al., 2002), which give the evolution of crystallinity upon storage at RH of 91%. The weak crystallinity is observed with time for a mixture of A and B crystalline types. The A /B ratio was evaluated to be about 40/60 and the crystallinity increased from 10% to 19% within one month; no additional changes occurred during the second month of storage at 20°C. If the plasticizer content was low or if stored at low RH, all the samples remained amorphous upon aging. This indicates that water is a necessary condition for TPS retrogradation (recrystallization). Water absorption of TPS increased with increasing ambient relative humidity and it was more pronounced when glycerol was used as plasticizer (Stading et al., 2001). Glycerol was shown to decrease the retrogradation rate of waxy maize starch in a gel. However, the overall re-crystallinity of TPS was lower than 10% even after long-term storage (Van Soest and Knooren, 1997). Mechanical properties testing indicated that the retrogradation increased the tensile stress, owing to the fact that the formed crystalline phases act as physical crosslinking (Van Soest and Knooren, 1997).

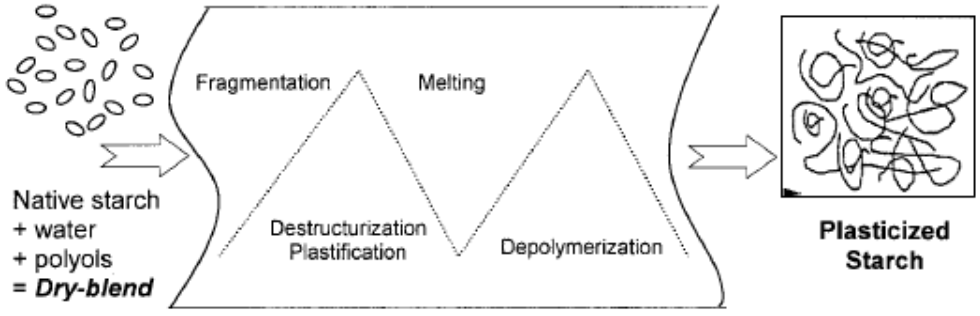

Figure 1.12 Schematic of starch process by extrusion.

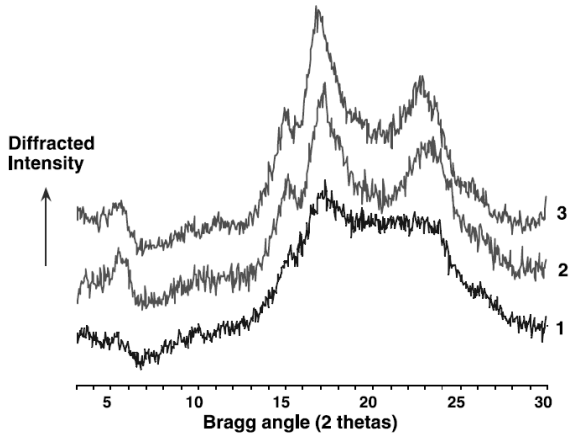

Figure 1.13 Evolution of the crystallinity upon storage of amylopectin film at RH 91%: 1) seven days; 2) one month; 3) two months.

1.4.2 Hydrogen bonding interaction between the plasticizers and starch

During the thermoplastic process, the plasticizers can form hydrogen bonds with starch, take the place of the strong interactions between hydroxyl groups of starch molecules, and allowing starch plasticization (Hulleman et al., 1998). Ma and Yu studied TPS plasticized using several plasticizers (Ma and Yu, 2004). The existence of hydrogen bonding between starch and plasticizer has been demonstrated via FTIR. The most likely types of hydrogen bonds in both acetamide-plasticized TPS and glycerol-plasticized TPS are illustrated in Figure 1.14. The hydrogen bonding energy between plasticizer and starch was also calculated. The calculated values of the hydrogen bonding energies for urea-starch, formamide-starch, acetamide-starch, and polyols-starch were 14.167, 13.795, 13.698 and 12.939 kacl/mol, respectively. The order of hydrogen bonding energies between plasticizer and starch was urea-starch > formamide-starch > acetamide-starch > polyols-starch.

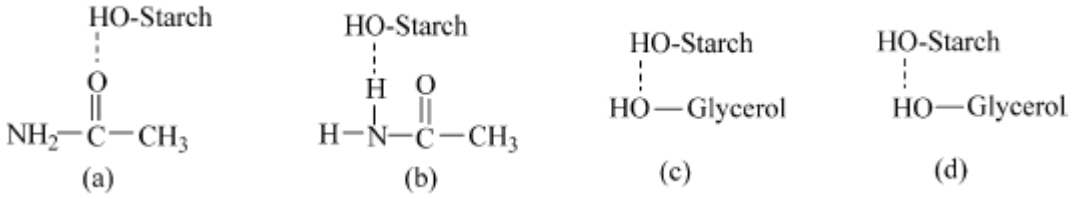

Figure 1.14 The styles of the most possible hydrogen bonds in both acetamide plasticized TPS (a,b) and glycerol plasticized TPS (c,d).

1.4.3 Study on the starch gelatinization

Many techniques, such as differential scanning calorimetry (DSC), wide angle X-ray diffraction (WAXD), light scattering, optical microscopy, thermo-mechanical analysis (TMA), NMR spectroscopy, rheometer analysis and ohmic heating have been used to study the gelatinization process of starch in food industries. (Palav and Seetharaman, 2006; Temsiripong et al., 2005; Liu et al., 2002; Fukuoka, et al., 2002). The gelatinization temperature is one of the most important parameters during starch gelatinization and has an effect on the properties of the TPS. When starch granules are heated in the presence of plasticizers, the temperature rises to a critical value, after which starch granules are gelatinized and plasticized. This critical value is referred to as the gelatinization temperature. The onset and conclusion temperatures of starch gelatinization, T_o and T_c, can be obtained. The properties of the plasticizer, such as diffusivity, viscosity, molecular size and hydrogen bonding capacity determine its effectiveness in gelatinizing starch. (Tan et al., 2004).

DSC is most commonly used to investigate the phase transitions of starch (Tananuwong and Reid, 2004; Mondragón et al., 2004, Tan et al., 2004). Typical DSC thermograms of botanical sources of starch are shown in Figure 1.15 (Jenkin and Donald, 1998). The onset (T_o), peak (T_p), and conclusion (T_c) temperatures, and the enthalpies (ΔH) for the gelatinization endotherm for different botanical sources of starch obtained from DSC are listed in Table 1.5. The enthalpies (ΔH) obtained from DSC can be applied to calculate the degree of starch gelatinization. The results clearly indicated that the botanical sources have a great effect on gelatinization. However, the use of DSC is limited in detecting the glass transition event during gelatinization and the glass transition is usually masked by the gelatinization endotherm.

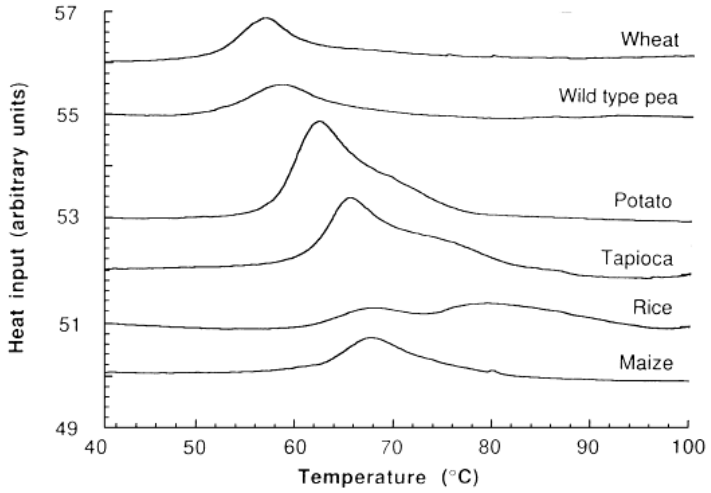

Figure 1.15 Effect of botanical source on DSC gelatinization characteristics. DSC traces for 40% (w/w) starch mixtures in water, heated at 5 ^{o}C/min.

DSC can also be used to investigate the gelatinization kinetics of starch under isothermal conditions (Zanoni et al., 1995; Spigno et al., 2004). Kinetic parameters (the activation energy (E_a), pre-exponential factor and model function) can be utilized for the optimization of some industrial scale processes, since almost all these processes occur under changing temperature. It has been reported that starch gelatinization is a first-order process (Zanoni et al., 1995). The rate constant varies with temperature according to the Arrhenius equation. However, Spigno et al. used a simple mathematical model proposed by Calzetta, Tesio and Suarez to evaluate the kinetic parameters of both rate constants and reaction orders under non-isothermal conditions:

$$\ln\frac{d\alpha}{dt} = \ln Z - n\ln(1-\alpha) - \frac{E_a}{R}\frac{1}{T} \qquad (1.4.3.1)$$

Here, α is the degree of gelatinization at any time t, Z is the pre-exponential factor, E_a is the activation energy and T is the temperature. The results show that rich starch gelatinization followed a *n*-order reaction model. The E_a and *n* decrease with increasing heating rate (Spigno et al., 2004). However, many aspects of the dynamics of starch gelatinization, for example time/temperature boundaries ultimately required for the successful plasticization of starch in a polymer melt processing environment, remain unclear.

Table 1.5 starch gelatinization parameter obtained from DSC

Starch sample	To (^{o}C)	Tp (^{o}C)	Tc (^{o}C)	ΔH (J/g)
Wheat	51.2 ±0.1	56.0 ±0.2	76 ±1	9 ±1
Potato	57.2 ±0.2	61.4 ±0.3	80.3 ±0.4	17.4 ±0.4
Maize	62.3 ±0.3	67.7 ±0.2	84 ±1	14 ±2
Rice	62.0 ±0.2	67.4 ±0.2	97.5 ±0.4	11 ±1
Tapioca	60.9 ±0.2	65.3 ±0.2	88 ±2	20 ±1
Wild pea	51.9 ±0.8	58.3 ±0.2	83 ±1	6.5 ±0.3

* 40% (w/w) starch mixtures in water

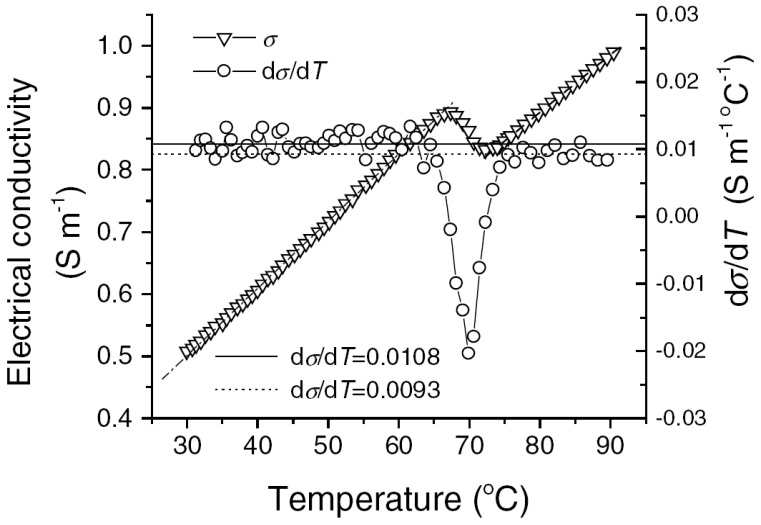

Figure 1.16 Electrical conductivity and dσ/dT curves for the cornstarch suspension with temperature.

Starch gelatinization also can be determined from the change in electrical conductivity (σ) during starch gelatinization. Figure 1.16 illustrated electrical conductivity and dσ/dT curves for the cornstarch suspension with temperature (Li et al., 2004). The results showed that electrical conductivity of native starch suspensions increased linearly with temperature except for the gelatinization range, however, it decreased with degree of starch gelatinization. It was seen that the shape and temperature range of dσ/dT versus temperature curve was essentially similar to the endothermic peak on a DSC thermogram. The decreasing could be explained by changes in structure and properties. Changes in water mobility due to gelatinization have been investigated

by Collsion et al. (Collsion and McDonald, 1960). The amount of mobile water in gelatinized sample was found to be much lower than in the raw materials. The decreasing unbound water results in the decrease of electrical conductivity.

1.4.4 Factors affect to starch gelatinization

The properties of the plasticizer, such as diffusivity, viscosity, molecular size and hydrogen bonding capacity determine its effectiveness to gelatinize starch (Tan et al., 2004). Onset temperature of starch gelatinization is found to be the only parameter that changes upon varying the solute or the concentration of the solution. The width of the gelatinization temperature range and the enthalpies of gelatinization are not significantly affected (Perry and Donald, 2002). Usually, the greater the molecular weight of the solute, and hence the less effective it is to plasticize starch granules, the greater the temperature elevation at a given concentration. The density of hydroxyl groups (number of -OH groups per carbon) also affect the starch gelatinization because hydrogen bonds are the crosslinks connecting starch and plasticizer (Perry and Donald, 2002). Water is found to decrease the gelatinization temperature of starch whereas glycerol increases it.

Maaruf et al. (Maaruf et al., 2001) have studied the effect of water content on sago starch gelatinization. Two endothermic transitions were observed for sago starch heated in the presence of a limited amount of water (starch/water=37-50% w/w). The first transition (G), occurring at about 63.6-78.5°C, remained constant with increasing water content over the range studied. The second transition (M), occurring at about 77.6°C, shifted to low temperature with increasing water content. G and M transitions have been assigned to a co-operative water-mediated melting of the starch crystalline phase and melting of remaining crystalline phases and/or melting of amylopectin crystalline phases (Shogren, 1992). For water contents greater than 50%, a single endotherm was observed at a peak temperature of 70.3°C and reached a maximum enthalpy of gelatinization (4.9 J/g) (Maaruf et al., 2001).

The effect of salt is one of great importance to the production and properties of a number of cereal-based products, as well as to the manufacture of modified starches. The presence of metal ions, such Ca^{2+}, Mn^{2+} and Fe^{2+} was found to inhibit the starch gelatinization (Koo et al. 2005; Chiotelli et al. 2002). Sodium chloride has been found to have a complex effect on the gelatinization of starch (Chiotelli et al. 2002). The addition of sodium chloride in a 60% water (w/w) wheat and potato starch slurry increased the gelatinization temperature and shifted the

swelling and rigidity increase during heating to higher temperatures. The reverse effect was observed when 7% of NaCl was used. The enthalpy (ΔH) for the gelatinization process decreased at high salt concentrations.

Chuang and Yeh applied a single extrusion cooking on processing rice flour (Chuang and Yeh, 2004). They found that starch gelatinization increased with residence time, as the degree of gelatinization is a function of cooking temperature and time. However, if the processing temperature is lower than the gelatinization temperature, starch cannot be completely gelatinized even if a long residence time is applied.

1.4.5 Properties of thermoplastic starch

Properties of thermoplastic starch, such as thermal, mechanical, dynamic mechanical and rheological properties have been investigated extensively. This section will show a summary of these studies.

Dynamic mechanical studies of TPS have been carried out by several authors (Curvelo et al., 2001; Mathew & Dufresne, 2002; Averous, 2004**).** Typical curves of the storage modulus (E) and tan δ with temperature are plotted in Figure 1.17 (Da Róz et al., 2006). The tan δ curves for all the TPS showed two relaxations, which appeared, respectively, between -77 and -40 ℃ and between 70 and 150 ℃. The high temperature relaxation was attributed to the glass transition temperature of the corresponding TPS, whereas the low temperature peak could have arisen from a plasticizer-rich phase, as already suggested by other authors (Curvelo et al., 2001; Mathew and Dufresne, 2002). The high temperature transition followed different trends, depending on the plasticizer used and on the amount added. For instance, the Tg is around room temperature when water content is 21%, but with the same concentration of glycerol Tg is high as 93 ℃. (Myllärinen et al., 2002). The classical softening effect was only clearly detected with the EG-based TPS up to 30% (Da Róz et al., 2006).

The melt viscosity of thermoplastic starch has been studied by Willett et al. (Willett et al., 1995). TPS exhibits power law behaviour over the range of shear rates from 1 to 1000 s^{-1}. Temperature has a greater effect on the power law index than moisture. The power law index increases with temperature. The viscosity of TPS decreases with increasing temperature and moisture content. Low molecular weight additives, such as lecithin, generally decrease the viscosity of TPS and this reduction is more effective than the addition of water. Rheology measurements were also used to study the thermal stability of TPS. Figure 1.18 illustrates the

time sweep test of TPS (41% water content) under controlled stress oscillatory shear condition (Della Valle et al., 1998). Both moduli increase markedly with time, which indicates poor stability of TPS. The main reason may be plasticizer evaporation during the experiment.

Shi et al. reported the ageing of thermoplastic starch with high glycerol content (Shi et al., 2007). The retrogradation was characterized by X-ray diffraction (XRD) and dynamic mechanical thermal analysis (DMTA). The XRD results indicated that high content of glycerol promotes the formation of V-type single helix structure, but inhibits B-type double helix structure. The glycerol content has less effect on the mechanical properties when it is high enough. Phase separation between starch and glycerol becomes more and more obvious during ageing.

The effect of orientation on microstructure and mechanical properties of thermoplastic starches with different amylase/amylopectin ratios was studied (Yu and Cristie, 2005). Orientation does not affect the crystallization rate of amylopectin due to the physical crosslinks by hydrogen bonds and a high molecular weight. On the other hand, orientation increased both modulus and yield stress but decreased the elongation at break and the effect of orientation on the modulus; yield stress was dependent on the amylase/amylopectin ratio.

The effect of the type and amount of plasticizer on the mechanical, thermal and water absorption properties have been well demonstrated in literature (Da Róz et al., 2006; Myllärinen et al., 2002).

Mechanical tests showed that tensile strength and Young's modulus of formamide-plasticized TPS were lower than glycerol-plasticized TPS, and elongation at break and energy at break were higher (Ma and Yu, 2004).

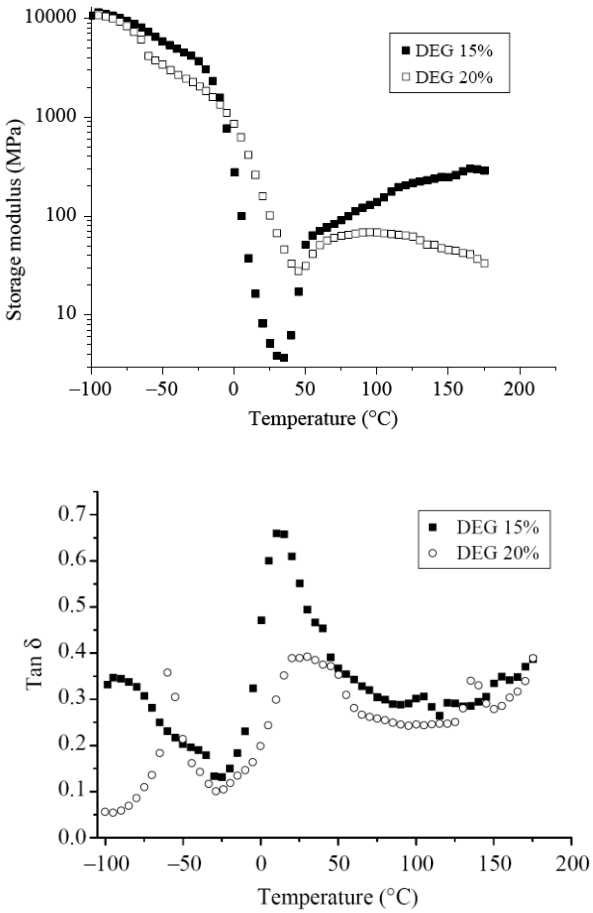

Figure 1.17 Storage modulus and tanδ versus temperature curves of TPS

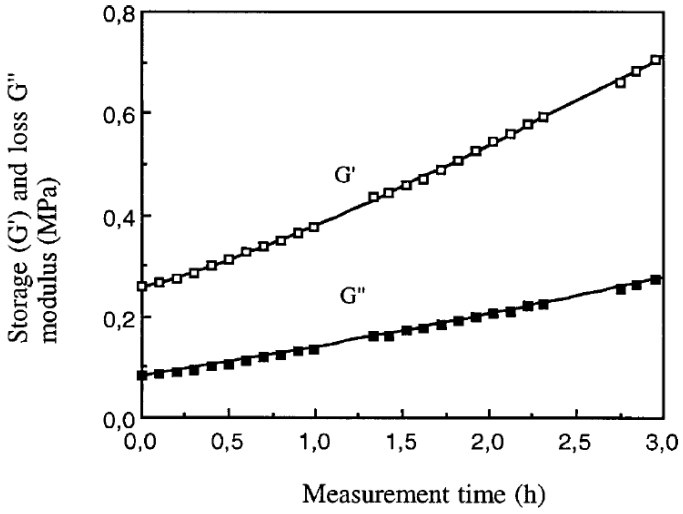

Figure 1.18 Variation of the storage modulus *G'* and loss modulus *G"* with time

1.5 Polymer Blends

1.5.1 Introduction of Polymer Blends

Multiphase and multicomponent polymers have become a very important research field in polymer science and engineering. New and comprehensive materials can be achieved through blending different polymers by physical or chemical blending techniques. At present, at least 80% of polymer materials occur in blend form in polymer applications. Many enterprises and research units show interest in this field. A polymer blend is a mixture of at least two polymers or two copolymers. Polymer blends are useful in designing tailor-made materials with good properties, processability and price/performance ratio. In order to develop polymer alloys and blends with desirable properties, an in-depth understanding of the following topics is needed:

- Miscibility - thermodynamics and phase behaviour
- Morphology - control via interfacial properties and processing conditions
- Homogenization - interchange reactions
- Blend compatibilization - use of compatibilizers.

In this chapter, we will introduce the theoretical and experimental studies of polymer blends, such as morphology control, rheology and mechanical properties.

1.5.2 Droplet Breakup and Coalescence

Properties of immiscible polymer blends depend not only upon the properties of their constituent components but strongly on their morphology as well. For instance, the impact strength of polymer blends can be drastically improved when the rubbery dispersed phase size is below a critical value (Wu, 1987). The final morphology of polymer blends mainly results from the deformation, relaxation, breakup, and coalescence of the dispersed phase induced by the flow field inside the processing equipment used to shape the polymer product. Thus, an improved understanding of the effects of these processes on blend morphology would obviously be valuable to better control the final properties of polymer blends.

The steady-state deformation and breakup of a Newtonian drop immersed in another Newtonian fluid were first studied by Taylor. For steady simple shearing flow in the small-deformation limit, Taylor pointed out that droplet deformation is controlled by two dimensionless parameters, the capillary number, *Ca*, and the viscosity ratio, η_r. *Ca* is defined as the ratio of viscous to interfacial tension forces. η_r is defined as the ratio between the viscosities

of the dispersed η_d and that of the matrix phase η_m.

In the case of small *Ca*, the droplet is gradually deformed and reaches a steady-state ellipsoidal shape in which the major axis of the ellipsoid orients at a certain angle θ in the flow direction. At steady state for small *Ca*, Taylor found that the orientation angle θ equal to 45 °, and a deformation parameter, *Def*, depending on *Ca* and η_r is given by:

$$Def = \frac{a-b}{a+b} = Ca\frac{19\eta_r + 16}{16\eta_r + 16} \qquad (1.5.2.1)$$

where *a* and *b* are the lengths of the major and minor axes of the deformed droplet respectively. When *Ca* increases, the droplet deformation increases until *Ca* reaches a critical value, Ca_{crit}, where the droplet cannot preserve a steady-state ellipsoidal shape. At Ca_{crit}, the ellipsoidal droplet transforms to a sigmoidal shape in which the central part of the sigmoid stretches and simultaneously becomes thinner under applied strain. After a critical strain is reached, the droplet breaks into smaller droplets. Taylor derived a simple expression to calculate the Ca_{crit} of Newtonian systems under simple shear flow:

$$Ca_{crit} = (1/2)((16\ \eta_r + 16)/(19\ \eta_r + 16)) \qquad (1.5.2.2)$$

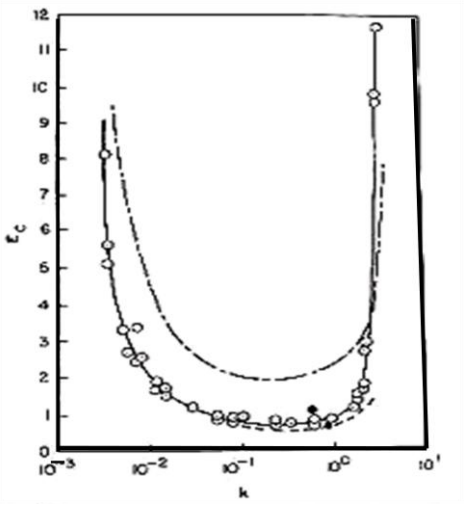

Figure 1.19 Critical value of droplet deformation versus viscosity ration for droplet breakup in uniform shearing flow.

Figure 1.19 gives plots of Ca_{crit} versus η_r, displaying the effect of viscosity ratio on the viscous to interfacial force ratio required for droplet breakup in uniform shearing flow. It is seen that, at a given value of $\eta_r = \eta_d / \eta_m$, if the droplet is exposed to a uniform shear flow field which produces a value of Ca greater than Ca_{crit}, the droplet will deform and break. It is interesting to note that limited boundaries exist at both ends of the U-shaped contour, below or above which breakup cannot be obtained. At $\eta_r < 0.1$ the droplet attains a sigmoidal shape and small drops are shed from the ends, at $0.1 < \eta_r < 2$, the droplets break up into daughter droplets. At $\eta_r > 4$ there is no further breakup and the droplets just undergo deformation.

The minimum obtainable droplet diameter in an immiscible blend system can also be estimated from the critical capillary number, Ca (Eq. 1.5.2.3).

$$Ca = \frac{\eta_m R \gamma}{\sigma} \tag{1.5.2.3}$$

η_m: Matrix viscosity (Pa.s)

R: Average radius of droplet (m)

γ: Shear rate (s^{-1})

σ: Interfacial tension (N/m)

From experiments, the final morphology of immiscible blends has been evaluated as a function of their viscosity ratio (Wu, 1987; Favis and Chalifoux, 1987). Based on the experimental data of PA/rubber blends with varying viscosity ratios and interfacial tensions, Wu has established an empirical equation fitting the capillary master curve:

$$2Ca = \frac{\eta_m \dot{\gamma} D_n}{\sigma_{12}} = 4\left(\frac{\eta_d}{\eta_m}\right)^{\pm 0.84} \tag{1.5.2.4}$$

In this equation, the exponent is positive for $\eta_r > 1$ and negative for $\eta_r < 1$; D_n represents the number average particle diameter. However, the blends investigated only contained 15% of the dispersed phase, leading to an overestimation of critical capillary number (Ca_{crit}).

1.5.3 Interfacial Tension

Several parameters can influence the final morphology of polymer blends, such as: viscosity ratio, composition, processing method, and types of flow. In addition to the above, the role of interfacial property is critical. The interface has a crucial role in controlling the morphology and final properties of an immiscible polymer blend. Interfacial tension between blend components is

the most basic parameter which characterizes the interface between polymers.

There are a variety of methods for determining the interfacial tension. The pendant drop (Kamal et al., 1994) and spinning drop (Elmendorp and De Vos, 1986) are the most widely used techniques. However, the above methods normally require long experimental times to equilibrate and involve complicated experimental procedures. A simpler and more expeditious technique is the breaking thread method based on an analysis developed by Tomotika (Tomotika,1935). The interfacial tension can be obtained by studying the breakup of a molten polymer fibre embedded into another polymer via a mechanism known as capillary instabilities. The analysis quantifies the disintegration of an elongated thread, which is subjected to a sinusoidal distortion. Once the thread and the matrix have melted totally and relaxed, distortions start to grow and the change in the amplitude is recorded with time.

Because TPS exhibits special rheological characteristics and PCL has a very low melting temperature, a TPS thread does not break in a PCL matrix. It is difficult to obtain the interfacial tension between PCL and TPS by the breaking thread method. However, if the surface energy is known, according to the fractional polarity theory, the interfacial tension between immiscible polymer melts is well approximated by the harmonic mean equation shown in Equation 1.5.3.1 (Wu, 1971).

$$\gamma_{12} = \gamma_1 + \gamma_2 - 4\gamma_{1d}\gamma_{2d} \Big/ (\gamma_{1d} + \gamma_{2d}) - 4\gamma_{1p}\gamma_{2p} \Big/ (\gamma_{1p} + \gamma_{2p}) \qquad (1.5.3.1)$$

Here, γ_{12} is the interfacial tension; γ_d and γ_p are the dispersive and polar components of the surface energy, respectively. Reported dispersive and polar surface energy parameters of PCL, starch and TPS30 (30% glycerol) obtained from the contact angle test under ambient temperature are summarized in Table 1.6.

Table 1.6 Surface energy parameters of starch, PCL and TPS30

Sample	γ	γ_d	γ_p	Ref.
PCL	44.0	37.0	7.0	Normand et al.,1995
starch	63.7	25.2	38.5	Carvalho et al., 2005
TPS30	43.6	29.4	14.2	Carvalho et al., 2005

1.5.4 Rheology and Morphology

Because the morphology of a blend of immiscible polymers has a controlling influence on the final properties of the materials, the development of morphologies during the blending process has been extensively studied in these past two decades. Many studies have reported on the influence of rheology on the morphology. The mechanical properties of polymer blends can be largely varied, even if the mean particle size and particle size distribution of the minor phase only slightly change. It is well known that the morphology of a polymer blend is determined by the shear rate, interfacial tension, blending composition, flow field and viscoelasticity of the components.

1.5.4 Rheology and Morphology

Because the morphology of the blend of immiscible polymers has a controlling influence on the final properties of the materials, the development of morphologies during the blending process has been extensively studied in these past two decades. There have been many studies, which have reported on the influence of rheology on the morphology. The mechanical properties of polymer blends can be largely varied, even if the mean particle size and particle size distribution of the minor phase only slightly change. It is well known that the morphology of a polymer blend is determined by the shear rate, interfacial tension, blending composition, flow field and viscoelasticity of the components.

1.5.4.1 Empirical mixing rules

The simplest viscosity mixing law for an incompatible mixture of two liquids is the linear relationship:

$$\eta = \eta_A \phi + \eta_B (1-\phi) \tag{1.5.4.1}$$

with η the blend viscosity, η_A and η_B those of components A and B, respectively, and ϕ the volume fraction of A. For polymer blends, where η_A and η_B can differ even by orders of magnitude, the log-linear mixing rule is often preferred

$$\log \eta = \phi \log \eta_A + (1-\phi) \log \eta_B \tag{1.5.4.2}$$

Equations (1.5.4.1) and (1.5.4.2) can be seen as special cases of a more general law, which is widely used to predict the physical properties of heterogeneous systems (Nielesen, 1974)

$$\eta^n = \eta_A^n \phi + \eta_B^n (1-\phi) \tag{1.5.4.3}$$

Equations (1.5.4.1) and (1.5.4.2) correspond to the cases of $n = 1$ and $n \rightarrow 0$, respectively.

When n = -1, Equation (1.5.4.3) becomes:

$$\frac{1}{\eta} = \frac{\phi}{\eta_A} + \frac{(1-\phi)}{\eta_B} \qquad (1.5.4.4)$$

This reciprocal mixing rule is more "physical" than the previous ones, as it represents the viscosity of an infinitely layered mixture of two Newtonian liquids.

Equation (1.5.4.3) contains one adjustable parameter. In general, when n＞1, a positive deviation from ideality is predicted; when n＜ 1, a negative deviation is obtained. Both deviations are observed experimentally (Han, 1981). Equation (1.5.4.3), however, is not able to predict the frequently observed change from a positive to a negative deviation behaviour when moving from low to high shear rates (Ablazova *et al.*1975).

1.5.4.2 Co-continuity and phase inversion prediction

Many rheological parameters of the blend constituents influence the position of phase inversion concentration and its width. Willemse et al. showed that the width of this interval is influenced by the interfacial tension (Willemse et al., 1999), In addition He et al. (He et al., 1997) found a narrowing of the co-continuity interval with increasing mixing time. In a publication Veenstra (Veenstra et al., 1999) revealed a direct correlation between the capillary number and the width of the continuity interval under shear flow. The factors influencing the position of the phase inversion range will be discussed below.

Experimental investigations of two-phase polymer blends have shown that for components of equal viscosity, phase inversion occurs around a volume fraction of 0.5. When the component viscosities differ significantly, the phase inversion point is shifted toward components richer in the high viscosity component (Miles and Zurek, 1988).

In order to predict the phase inversion point, i.e. the phase inversion concentration $\phi_{iI,}$ several authors have proposed semi-empirical equations based on viscosities η_i of the component (i=1,2). The following is a relationship describing the phase inversion composition in terms of volume fraction and zero shear viscosity.

$$\phi_1 / \phi_2 = \eta_1 / \eta_2$$

$$\phi_1 = 1 - \phi_2 \qquad (1.5.4.5)$$

where η_i is the zero shear viscosity and ϕ_i is the volume fraction at phase inversion of component *i.* This idea was first proposed by Avgeropoulos et al. (Avgeropoulos and Weissert, 1976) and was

generalized by Paul and Barlow (Paul and Barlow, 1980). The expression was extended by Miles and Zurek (Miles and Zurek, 1988).

Willemse et al. also developed a semi-empirical relation based on geometrical requirements for the formation of the co-continuous structures (Willemse et al., 1999):

$$\frac{1}{\phi_{dispI}} = 1.38 + 0.213\left(\frac{\eta_m \dot{\gamma}}{\sigma} R_0\right)^{4.2} \qquad (1.5.4.6)$$

This gives the lower and upper limits, respectively, of the range of volume fractions within which a co-continuous structure can exist, as a function of matrix viscosity η_m, interfacial tension, minimum radius of filaments R_0 and shear rate $\dot{\gamma}$ during blending for a capillary number value of one. This model cannot be used in a predictive manner because the filament radius has to be determined experimentally first. Willemse et al. checked their theory with five different blend systems lying in a very narrow range of values of $(\eta_m\gamma/\alpha)R_0$.

The models described up to now only account for the viscous properties of polymers. The more elastic phase tends to encapsulate the less elastic one, as found by Favis and Chalifoux (Favis and Chalifoux, 1998) for PP/PC blends with different elasticities of the PP phase. Consequently, Bourry and Favis (Bourry and Favis, 1998b) introduced elasticity as an important parameter for the understanding of phase inversion. They made an approach based on the elasticity ratio of blend components in which the storage moduli G'_i (i =1,2) represents the elasticity of phase i:

$$\frac{\phi_{1I}}{\phi_{2I}} = \frac{G'_2(\omega)}{G'_1(\omega)} \qquad (1.5.4.7)$$

These formulas account for the tendency of the more elastic phase to form the matrix at sufficiently high concentrations. Bourry and Favis achieved much better agreement with their experimental data particularly at high shear rates than with predictions based only on viscous effects. This approach is used to indicate the main tendencies that would be predicted from elastic effects.

Veenstra et al. investigated the morphology of blends of polystyrene and poly(ether-ester) thermoplastic elastomer (Veenstra et al., 1999). If the processing temperature was chosen below the block copolymer's order to discorder transition, the flow curves of poly(ether ester) did not show a Newtonian plateau in viscosity. Shear thinning behaviour over the entire range of measured shear rates was found. That was an indication of physical crosslinking of crystalline

structures in the melt. Melt yield stress was estimated in the range between 500 and 3800 Pa. The breakup and retraction behaviour of poly(ether-ester) threads was severely limited or even stopped, elongated structures were stable and co-continuous morphologies were observed at very low concentration. On the other hand, the viscosity ratio of blend components was shown to have less effect on the co-continuity composition range and only little effect on the microstructure of the blends.

1.5.5 Mechanical Properties of Polymer Blends

Materials when they were the application come in a variety of forms with a very wide range of properties. Material science is utilized to gain a fundamental understanding of materials behaviour, so that further improvements can be achieved. For two-material heterogeneous systems, one material being continuous and the other in the form of discrete inclusions, Hashin (1962) introduced the composite spheres model that is composed of a gradation of size of spherical particles embedded in a continuous matrix phase. The size distribution is not random, but rather has a very particular characteristic. Applicability of various composite models, such as the parallel model, the series model, the Takayanagi model, the Kerner model, and the Kunori model, were checked to predict the mechanical behaviour of the blends.

The parallel model (the highest upperbound model) is given by the following equation (Thomas and George, 1992):

$$M = M_1\phi_1 + M_2\phi_2 \qquad (1.5.5.1)$$

where M is the mechanical property of the blend, and M_1 and M_2 are the mechanical properties of the components 1 and 2, respectively, and ϕ_1 and ϕ_2 are the volume fractions of the components 1 and 2, respectively. In this model, the components are considered to be arranged parallel to one another so that the applied stress elongates each of the components by the same amount.

In the lowest lowerbound series model, the components are arranged in series with the applied stress. The equation is (Thomas and George, 1992):

$$1/M = \phi_1/M_1 + \phi_2/M_2 \qquad (1.5.5.2)$$

To predict the blend properties, the modulus for each phase and an estimate of the maximum packing fraction is needed. The modulus is much greater for the case of long rods. Aspect ratios greater than 100 are required to obtain a maximum modulus and, therefore, ribbons are especially effective. For very high aspect ratios, the longitudinal modulus can be expressed by the parallel

model:

$$E = E_1\phi_1 + E_2\phi_2 \qquad (1.5.5.3)$$

The parallel model can also be successfully used for the case of thin ribbons. The strength of fiber-filled composites is harder to predict due to the complex fracture phenomena. Only in the case of infinitely long aligned fibers is the strength given by the mixture rule, when testing is done in the direction of the fiber alignment. The composite strength does depend on the length of the fibers/ribbons. For continuous blends, the modulus can be represented by (Nielsen and Landel, 1994):

$$E^n = E_1^n\phi_1 + E_2^n\phi_2 \qquad (1.5.5.4)$$

where *n* is a constant between +1 and -1.

The fracture mechanisms of polymer blends have been widely investigated in the last two decades. A variety of deformation mechanisms of fracture surfaces were used to interpret the relationship between properties and material microstructure, such as stress whitening. In most of the literature, fracture mechanisms of immiscible blends were composed of three stages: debonding, void growth and failure. LDPE/TPS (Rodriguez-Gonzalez et al., 2003) blends could maintain excellent mechanical properties, especially ductility at high starch loading without having added any classical interfacial modifier or having chemically modified the starch surface. However, the fracture mechanism of blends containing TPS is not so clear. The aim of this work is try to get a better understanding on the role of TPS in the PCL/TPS blends system.

1.6 Polycaprolactone and Starch Blends

1.6.1 PCL/Starch Blends

During the last two decades, considerable effort has gone into the development of biodegradable polymers, polymer blends and composites using starch. Blends of PCL with both native starch and thermoplastic starch have been documented in the literature (Singh et al., 2003; Shin et al., 2004), but their commercial production is not very popular due to the high production cost and variation in mechanical properties.

Polymer blends containing various amounts of starch are being investigated as possible replacements for pure synthetic polymers. In the early stages of starch blends, the starch had been blended with polycaprolactone. These studies showed that the mechanical properties of native starch/PCL blends became poor with increasing starch content in the blend. This can be attributed

to the incompatibility between the hydrophilic starch and hydrophobic PCL and poor interfacial adhesion between the two components (Fig.1.20) (Blanshard, 1987; Dubois et al., 1999). Smooth and large starch particle sizes similar to native starch were obtained. However, physical or chemical modification of the starch molecule or granule is a viable alternative to solve some of these problems. Kweon (Kweon et al., 2004) prepared starch/PCL blends with high miscibility; the starch was chlorinated by using methanesulfonylchloride (CH_3SO_2Cl) in dimethylformamide and was blended with PCL in solution state under various conditions.

Polycaprolactone/high amylose starch blends were prepared by adding a proper compatibilizer, constituted by low molecular weight PCL modified on the terminal groups by pyromellitic anhydride (Avella et al., 2000). The starch granules were well distributed and covered by PCL material in the presence of compatibilizers (Fig. 1.21b), indicating a good interconnection between the two phases. On the other hand, the samples without compatibilizer showed poor interfacial adhesion (Fig. 1.21a). The resulting blends also showed better performances compared to the ones obtained without the use of the compatibilizers. More recently, the morphology of polycaprolactone/starch/pine-leaf composite with and without the silane coupling agent was studied and is shown in Figure 1.22 (Kim et al., 2007). The composites without coupling agent showed poor interfacial adhesion between PCL and the fillers. Many empty cavities were observed on the surface (Figure 1.22a). However, the composites with the coupling agent showed a good interfacial adhesion between the two phases due to the formation of hydrogen bonds between the hydroxyl groups of starch and the carbonyl groups of PCL (Figure 1.22b). As a result, tensile properties and water resistance of the composites were improved.

In recent years, many researchers have also focused on the modification of PCL in order to increase the compatibility between PCL and starch (Kim et al., 2001; Wu, 2003; Kim et al., 2004). A reactive functional group was grafted onto PCL to improve adhesion and dispersion of the two immiscible phases, offering good mechanical properties.

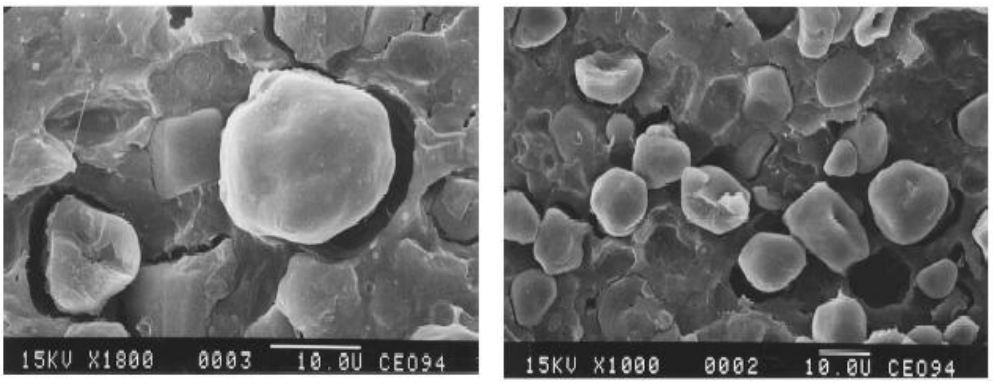

Figure 1.20 SEM images of a simple blend of native starch and PCL (50/50 wt.%)

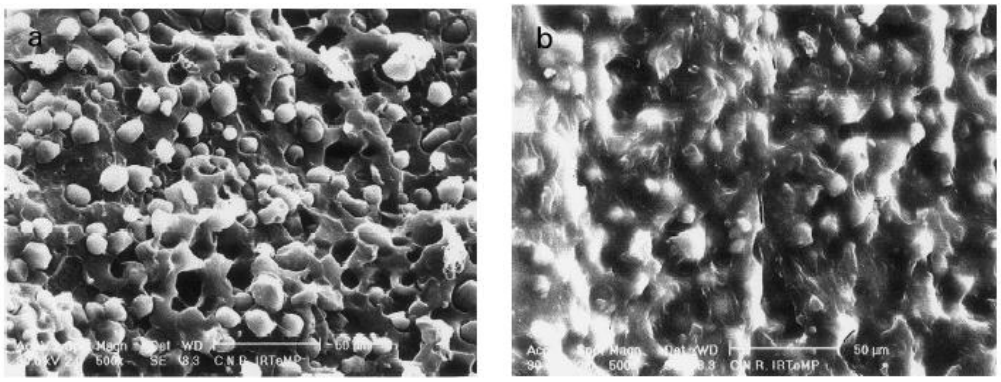

Figure 1.21 (a) SEM micrograph of fractured surface of PCL/starch. (b) SEM micrograph of fractured surface of PCL/starch with compatibilizers.

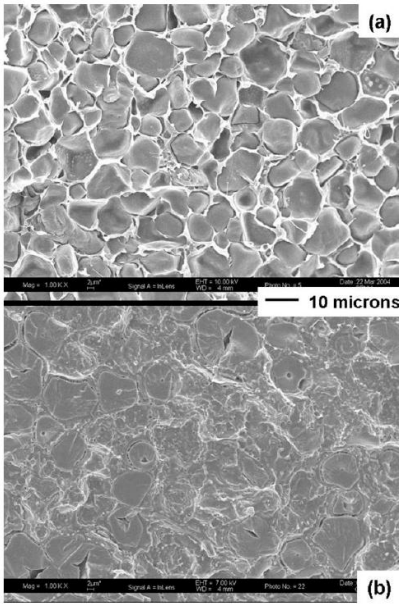

Figure 1.22 Morphology of polycaprolactone/starch/pine-leaf composite.

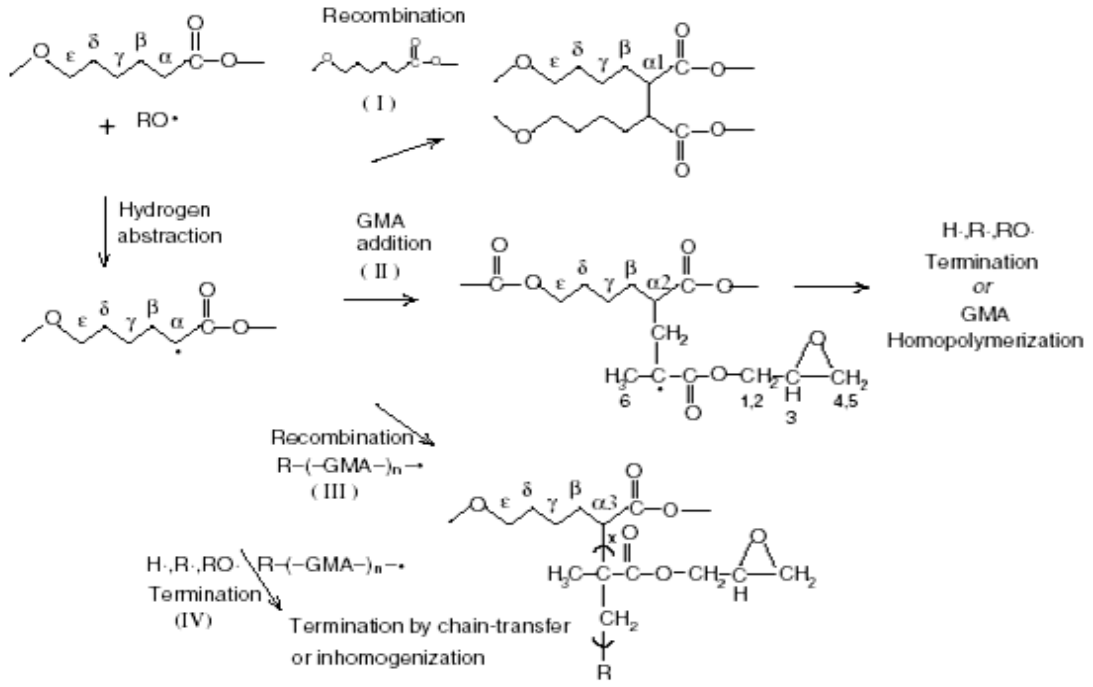

Figure 1.23 Reaction pathway for the grafting reaction of GMA on PCL

Modified polycaprolactone was synthesized by melt reaction of PCL and reactive monomers such as glycidyl methacrylate (GMA) and maleic anhydride (MAH) in the presence of benzoyl peroxide (BPO). The reaction mechanism is shown in Fig. 1.23. When modified PCL is blended with starch or gelatinized starch in a Brabender mixer, the torque is found to significantly increase after the initial melting of the blend. Such an increase in the torque is often observed in reactive blends, and is normally understood to be due to the reaction between the chemically reactive groups in the blend. The epoxide groups of the grafted GMA and the hydroxyl groups of either the starch or glycerol are expected to induce a chemical reaction, resulting in the formation of the ether linkage, as shown in Figure 1.24. When PCL-g-MAH was added, the size of the starch phase was much decreased compared with the ungrafted equivalent (Table 1.7). These results indicated a reduction in the interfacial tension between two polymers.

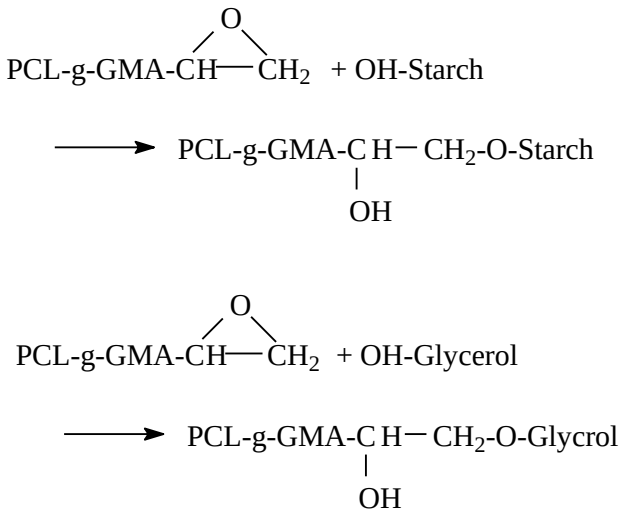

Figure 1.24 Reaction scheme between the epoxide group of PCL-g-GMA and the hydroxyl end group of starch or glycerol

Figure 1.25 shows the tensile properties of PCL/starch and PCL-g-MAH/starch blends (Wu, 2003). For PCL/starch blends, tensile strength and elongation at break decreased gradually as starch content increased. Although lower tensile strength and elongation at break was observed for PCL-g-MAH/starch blends compared with pure PCL, this decrease was smaller than that of the equivalent unmodified PCL. It is noticed that the resulting morphologies were affected by the amount of glycerol in PCL-g-GMA/starch blends (Fig. 1.26). The domain sizes of dispersed starch shown in Figure 1.26a and b are around 2-3 μm in diameter, while the domain size in Figure 1.26c and d is less than 1 μm in diameter. Thermal properties, water absorption and degradability were also studied in detail (Kim et al., 2001). It is noticed that elongation at break of PCL/starch (50/50) blends remained only 50% of that of pure PCL.

The biodegradability properties of poly(ε-caprolactone) (PCL) and modified adipate-starch blends were investigated in laboratory by burial tests (Mariani et al., 2007). The results indicated that the main mechanisms of PCL biodegradation is biological hydrolysis, whose reaction is catalyzed in general by enzymes. In the case of starch, the biodegradation occurs by chain cleavage. A significant increase in the blend crystallinity as a function of the time of incubation was observed, confirming the preferential attack of the microorganisms on the starch.

Table 1.7 The starch size of PCL-g-MAH/starch and PCL/starch blends

Starch (wt.%)	Phase size (μm)	
	PCL/starch	PCL-g-MAH/starch
10	6.5	1.5
20	12.0	2.1
30	15.5	3.3
40	18.0	3.8
50	21.0	4.1

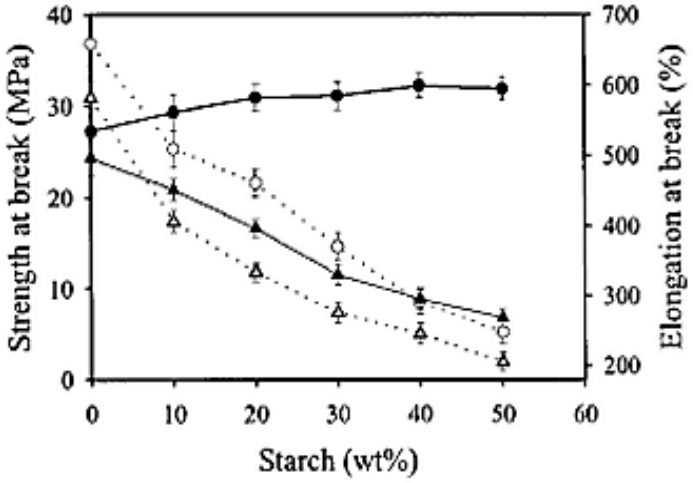

Figure 1.25 Tensile properties vs. starch content for PCL-g-MAH/starch blends.(solid lines) and PCL/starch blends (dotted lines)

1.6.2 PCL/Thermoplastic Starch Blends

In order to overcome the problem of poor interfacial adhesion, modified starches and modified matrix polymers have been studied by several authors. They concluded that acceptable mechanical properties could only be obtained in the presence of a compatibilizing agent or with lower starch content. More recently, the development of thermoplastic starch from granular starch and plasticizer allows for the transformation of starch into a free-flowing fluid like other conventional thermoplastics. Shin et al. have studied the rheological, mechanical, thermal and morphological properties of blends of polycaprolactone and thermoplastic starch (Shin et al., 2004). Averous et al. prepared blends of wheat thermoplastic starch (TPS) and polycaprolactone

(PCL) by extrusion and injection molding (Averous et al., 1999).

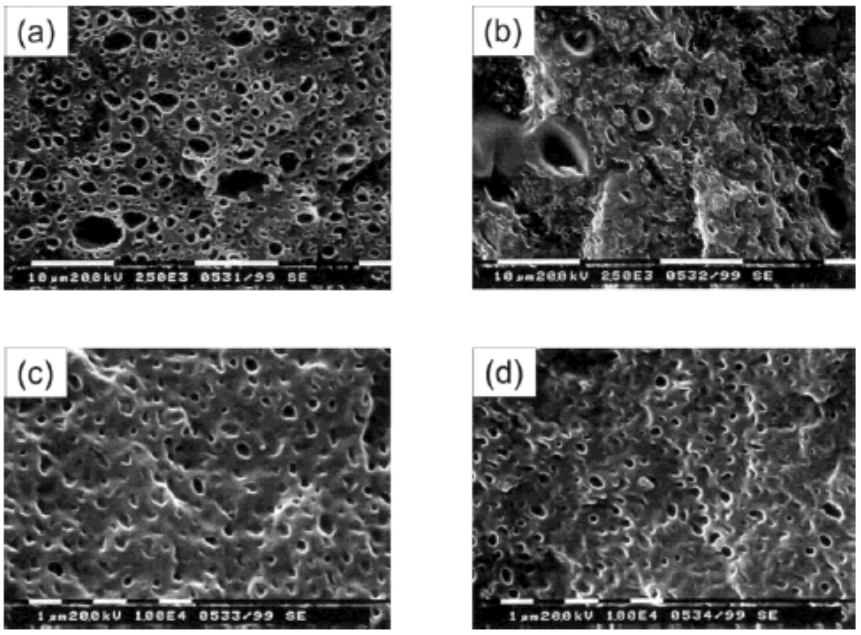

Figure 1.26 SEM of PCL-g-GMA/starch blend (50/50) containing different amounts of glycerol: (a) 30 wt.%, (b) 40 wt.%, (c) 50 wt.%, and (d) 60 wt.%

1.6.2 PCL/Thermoplastic Starch Blends

In order to overcome the problem of poor interfacial adhesion, modified starches and modified matrix polymers have been studied by several authors. They concluded that acceptable mechanical properties could only be obtained in the presence of a compatibilizing agent or with lower starch content. More recently, the development of thermoplastic starch from granular starch and plasticizer allows for the transformation of starch into a free-flowing fluid like other conventional thermoplastics. Shin et al. have studied the rheological, mechanical, thermal and morphological properties of blends of polycaprolactone and thermoplastic starch (Shin et al., 2004). Averous et al. prepared blends of wheat thermoplastic starch (TPS) and polycaprolactone (PCL) by extrusion and injection molding (Averous et al., 1999).

Blends of polycaprolactone and thermoplastic starch containing 20% glycerol were prepared by two-step extrusion (Shin et al., 2004). Here, PCL forms the continuous phase and TPS the dispersed phase. Thermal analysis results showed that PCL and TPS are thermodynamically immiscible. Rheological properties of PCL, TPS and their blends are shown in Figure 1.27. At

sufficiently low frequencies, the storage modulus of TPS is higher than that of PCL by about four orders of magnitude and the loss modulus is higher by two orders of magnitude. Storage moduli of blends increased with increasing TPS content up to 50 wt% TPS. The loss moduli of the blends also increased with increasing TPS content up to 30 wt% while blends with more than 40 wt% TPS showed higher moduli as compared to pure TPS.

In addition, blends containing TPS above 50% (wt%) showed a higher complex viscosity as compared to pure TPS. Tensile strength and elongation decreased with increasing TPS content (Table 1.8). This is expected since the starch component was simply diluted and does not possess desirable mechanical properties in itself. However, the modulus increased with increasing TPS content.

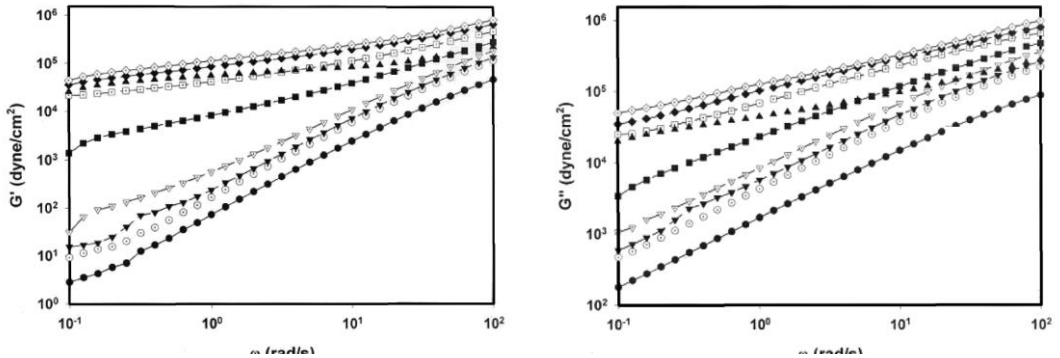

Figure 1.27 Rheological properties of PCL/TPS blends at 170°C

Thermoplastic starch with different plasticizer/starch ratios was blended with PCL by two-step extrusion (Averous et al., 1999). Thermoplastic starch forms the continuous phase and PCL the dispersed phase. The thermal, thermo-mechanical and mechanical characteristics of the blend clearly indicate a phase separation in the blend, as is generally found for non-miscible polymers. When the starch matrix has a glassy behaviour, blending with PCL results in a decrease of the material modulus but the impact resistance is improved. On the other hand, when the starch has a rubbery behaviour, PCL increases the modulus of the materials. The dimensional stability was improved significantly.

Table 1.8 Tensile properties of PCL/TPS blends

Sample	PCL (Wt %)	TPS (Wt %)	Strength (MPa)	Elongation (%)	Modulus (MPa)
PCL	100	0	29	1090	93
TP10	90	10	22	860	117
TP20	80	20	17	7060	125
TP30	70	30	12	560	136
TP40	60	40	10	150	144
TP50	50	50	10	18	176
TP60	40	60	5	15	180

1.7 Conclusion of literature review

The use of starch as a material is an alternative to develop biodegradation materials. Especially, blending with synthetic polymers is an important route towards an economical application. However, the physical and mechanical properties of starch-based composite materials become quite poor with increasing starch content due to the incompatibility between the hydrophilic starch and hydrophobic polymer as well as to the poor interfacial adhesion between the components. The conversion of native starch into free-flowing fluid thermoplastic starch (TPS) can overcome the above problems. The one-step extrusion system combining a twin screw and a single screw extruder is the most practical processing method. Starch plasticization, water volatilization, melt-melt mixing and morphology control can be achieved in one step. Even if LDPE/TPS blends prepared via a one-step extrusion system can result in materials with excellent mechanical properties without any addition of modifiers, a few fundamental problems are still not clear.

The one-step processing is a complex operation involving starch gelatinization, water devolatilization, and melt-melt mixing. All these must be achieved within two minutes maximum total residence time inside the extruder. According to literature reviews above, many issues related to the processing and morphology control should be investigated:

1. Starch gelatinization of starch/glycerol/excess water mixtures, in order to determine the time/temperature boundaries ultimately required for the successful plasticization of starch in a polymer melt processing environment;
2. The effect of water and glycerol on starch gelatinization parameters, such as gelatinization temperature and enthalpy;

3. Dynamic study on starch gelatinization when water, glycerol, as well as a combination of water and glycerol were used as plasticizer;
4. Optimize melt processing conditions that allow the preparation of fully plasticized thermoplastic starch, according to the findings of gelatinization studies;
5. Study the morphology and rheological properties of the blends. Clarify the influence of the rheological properties of TPS on the morphology of blends;
6. Study tensile properties of PCL/TPS blends over the entire concentration range of TPS;
7. Test and evaluate the biodegradation properties of thermoplastic starch-based materials according to ASTM. Clearly understand the effects of starch structure, dispersed phase structure and glycerol content on biodegradability;

CHAPTER 2

ORGANIZATION OF THE ARTICLES

Starch can be converted into a thermoplastic material through the disruption of molecular interactions in the presence of a plasticizer under specific conditions. It is interesting that thermoplastic starch (TPS) can be processed using standard plastic processing techniques, i.e. extrusion, injection and compression molding. It has been reported that the dispersed phase morphology control of TPS in TPS/LDPE blends can result in materials with excellent mechanical properties (Rodriguez-Gonzalez et al., 2003 and Favis et al., 2005). However, in order for the TPS phase to be sufficiently fluid to undergo the typical phase deformation/disintegration phenomena required for morphology modification, very high plasticizer contents are required (Rodriguez-Gonzalez et al., 2003). The one-step melt processing used for polymer blends with thermoplastic starch is a complicated process, which involves starch plasticization, water devolatilization, melt-melt mixing and morphology control. All these must be finished within two minutes total residence time in an extruder. In order to achieve morphology control of thermoplastic starch-based polymer blends, the conversion of native starch into completely plasticized starch must be achieved before it is mixed with other components. However, this conversion from native starch to highly plasticized TPS on melt processing equipment is much more difficult and problematic than what is often reported in the literature.

Three principal papers result from this thesis. Since it is essential that the thermoplastic starch be well plasticized, the first paper examines the critical aspects related to understanding the thermodynamic and kinetic aspects of the gelatinization of starch in the presence of an excess water/glycerol mixture. This understanding is then related to the design of the appropriate conditions on a twin-screw extruder. The second paper takes these optimized conditions for thermoplastic starch and examines the morphology/interface/property relationships in a polycaprolactone (PCL)/TPS blend over the entire composition range. Finally, the last paper relates the morphology and continuity of the thermoplastic starch phase to its biodegradation behaviour in polyethylene and poly(lactic acid).

The first paper, “The Relationship between Starch Gelatinization and Morphology Control in Melt-Processed Polymer Blends with Thermoplastic Starch”, presents the critical aspects of starch plasticization in glycerol/excess water mixtures in order to determine the time/temperature

boundaries ultimately required for the successful plasticization of starch in a polymer melt processing environment, and then relates these findings to the morphology of melt-blended thermoplastic starch (TPS) in polycaprolactone (PCL). The morphology of PCL/TPS blends varies with processing conditions and plasticizer used. Finally, when a glycerol-excess water mixture is used as a plasticizer and a sufficient residence time is allowed prior to water devolatilization, a completely plasticized starch is obtained. The efficacy of plasticization is demonstrated by a dramatic six-fold reduction in the dispersed TPS phase size and a unimodal TPS phase size distribution in the blend system.

Morphology control is considered as one of the key factors to achieve the desired final material properties. The morphology of polymer blends greatly depends on the rheology of the components used in the blends. The second paper, “Morphology Development and Interfacial Interactions in Polycaprolactone/Thermoplastic Starch Blends”, presents an approach to the investigation of the morphology, thermal and mechanical properties of blends of polycaprolactone (PCL) and thermoplastic starch (TPS) with high glycerol content. Dynamic rheological measurements were carried out on a dynamic stress rheometer with frequencies from 0.1 to 500 rad/s. The morphology of the extruded PCL/TPS strands was obtained using scanning electron microscopy and a semi-automatic method of image analysis was applied to quantify the average size of the dispersed phase. The morphology of PCL/TPS36 blends demonstrates the features of a highly interacting system, and the tensile mechanical properties demonstrate exceptional ductility at very high levels of thermoplastic starch without any added interfacial modifier. In addition, the effects of viscosity ratio of dispersed phase/matrix on morphology of PCL/TPS36 were discussed. Dynamic mechanical analysis confirms the region of dual-phase continuity and also strongly indicates a specific interaction between PCL and TPS. FTIR results show the presence of a hydrogen bonding interaction between the carbonyl groups of PCL and the hydroxyl groups on starch. It is likely that the high plasticizer concentrations used here increase the mobility of the starch chains and thus promote a high level of specific interactions between the PCL and starch. Mechanical properties display extremely high elongations at break, even at high TPS concentrations, typical of those observed for highly compatibilized immiscible polymer blends.

Biodegradation is an important property for thermoplastic starch and its blends. Therefore, the biodegradation of native starch, thermoplastic starch (TPS) containing high concentration of

glycerol and its blends are demonstrated in the third paper entitled “Biodegradation of thermoplastic starch and its blends with poly(lactic acid) and polyethylene: influence of morphology”. CO_2 evolution was measured to evaluate biodegradation properties during the test. The relationship between biodegradability and morphology is discussed and the effect of glycerol content on TPS biodegradation property is evaluated. The results indicate neither LDPE nor PLA have any effect on TPS biodegradation. The biodegradation of the blends can be determined by TPS only. The value of the percolation threshold obtained varies between 20% and 30% by weight. It is lower than that of starch granules. More pathways for moisture penetration and microbial invasion were generated compared with the case of native starch. Subsequently, an increase in biodegradation rate was achieved.

CHAPTER 3

THE RELATIONSHIP BETWEEN STARCH GELATINIZATION AND MORPHOLOGY CONTROL IN MELT-PROCESSED POLYMER BLENDS WITH THERMOPLASTIC STARCH

3.1 Presentation of the article the relationship between starch gelatinization and morphology control in melt-processed polymer blends with thermoplastic starch

3.2 Abstract

The one-step melt processing of polymer blends with thermoplastic starch is a complex operation involving plasticization, devolatilization, melt-melt mixing and morphology control. All this must be achieved within a maximum two minutes total residence time in an extruder. In this paper, we examine critical aspects of starch plasticization in glycerol/excess water mixtures in order to determine the time/temperature boundaries ultimately required for the successful plasticization of starch in a polymer melt processing environment and then relate these findings to the morphology of melt-blended thermoplastic starch (TPS) in polycaprolactone (PCL). The onset and conclusion temperatures for wheat starch gelatinization in the presence of excess water were obtained via differential scanning calorimetry (DSC), optical microscopy and wide angle X-ray diffraction (WAXS). Dynamic studies of wheat starch gelatinization show that if the temperature is sufficiently high, gelatinization takes place within 60 seconds for the excess water/glycerol/wheat starch mixture and within 3 minutes for the glycerol/wheat starch case. However, below the conclusion temperature only a partial degree of plasticization is achieved even after long times of treatment. Based on the above results, a series of one-step melt extrusion experiments for PCL/TPS blends were designed and the dispersed TPS morphology was examined. The TPS particle size (d_v) in a PCL matrix is 13.9 microns when only glycerol is used to plasticize native starch (contains only ambient water). This is very similar to the native starch granule size of 13.6 microns and clearly indicates the inability of glycerol alone to plasticize native starch within the time constraints of melt extrusion. When a glycerol-excess water mixture

is used and a sufficient residence time is allowed prior to water devolatilization, a completely plasticized starch, as demonstrated by WAXS, is obtained. The efficacy of plasticization is demonstrated by a dramatic six-fold reduction in the dispersed TPS phase size and a unimodal TPS phase size distribution in the blend system.

3.3 Introduction

Over the last two decades, numerous papers have been published on polymer mixtures containing native granular starch. These studies have generally shown that the physical and mechanical properties of the composite material become quite poor with increasing starch content. This can be attributed to the incompatibility between the hydrophilic starch and hydrophobic polymer as well as to the poor interfacial adhesion between the components (Avella et al., 2000; St Lawrence et al., 2000; Averous, 2000 and Averous, 2004).

Starch can be converted into a thermoplastic material through the disruption of molecular interactions in the presence of plasticizer under specific conditions. Water and glycerol are the most widely used plasticizers in TPS materials, however only a limited number of studies have examined the combined use of glycerol and added water (Rodriguez-Gonzalez et al., 2003). When starch granules are heated, starch undergoes an irreversible order-disorder transition. The swelling of the amorphous regions of the granules by absorption of plasticizer occurs which disrupts the molecular structure of the starch granules. Simultaneously, some other phenomena are observed, such as: uptake of heat of starch granules, loss of crystallinity (Di Paola et al., 2003 and Cagiao et al., 2004), increase in suspension viscosity (Sopade et al., 2004), change in electrical conductivity and plasticizer diffusivity (Gomi et al., 2004 and Li et al., 2004). This process is known as gelatinization and the material is often referred to as thermoplastic starch (TPS). TPS can be processed using standard plastic processing techniques, i.e. extrusion, injection molding and compression molding. The thermal and mechanical energy input associated with the addition of plasticizer are necessary to transform granular starch into a homogeneous matrix (Souza and Andrade, 2002). The gelatinization process is influenced by many factors, such as: starch composition, starch/plasticizer ratio, processing temperature, time and other processing conditions. Gelatinization is an order-disorder transition, which involves the diffusion of solvents into the granules to bring about a lamellar self-assembly process at room temperature (Perry and Donald, 2000). Subsequently, granular swelling and finally the structural breakdown occurs under heating conditions.

Many techniques, such as differential scanning calorimetry (DSC), wide angle X-ray diffraction (WAXD), light scattering, optical microscopy, thermo-mechanical analysis (TMA), NMR spectroscopy, rheometer analysis and ohmic heating have been used to study the gelatinization process of starch (Palav and Seetharaman, 2006; Temsiripong et al., 2005; Liu et al., 2002; Fukuoka et al., 2002; Ndife et al., 1998). The DSC is most commonly used to investigate the phase transitions of starch. Its use is limited in detecting the glass transition event during gelatinization and the glass transition is usually masked by the gelatinization endotherm. The DSC can also be used to investigate the gelatinization kinetics of starch under isothermal conditions (Zanoni et al., 1995 and Spigno et al., 2004). It has been reported that starch gelatinization is a first-order process (Spigno et al., 2004). However, many aspects of the dynamics of starch gelatinization remain unclear.

The gelatinization temperature is one of the most important parameters during starch gelatinization and has an effect on the properties of the TPS. When starch granules are heated in the presence of plasticizers, the temperature rises to a critical value, after which starch granules are gelatinized and plasticized. This critical value is referred to as the gelatinization temperature. The properties of the plasticizer, such as diffusivity, viscosity, molecular size and hydrogen bonding capacity determine its effectiveness to gelatinize starch. (Tan et al., 2004) Water is found to decrease the gelatinization temperature of starch whereas glycerol increases it, however the effect of controlled mixtures of excess water and glycerol on the plasticization process have not been studied extensively in the literature.

The development of thermoplastic starch (TPS) from granular starch and plasticizer allows for the transformation of native starch into a material with a flow behavior resembling that of conventional thermoplastics (Rodriguez-Gonzalez et al., 2004). It has been reported that the dispersed phase morphology control of TPS in TPS/LDPE blends can result in materials with excellent mechanical properties (Rodriguez-Gonzalez et al., 2003 and Favis et al., 2005). However, in order for the TPS phase to be sufficiently fluid to undergo the typical phase deformation/disintegration phenomena required for morphology modification, very high plasticizer contents are required (Rodriguez-Gonzalez et al., 2003). This conversion from native starch to highly plasticized TPS on melt processing equipment is much more difficult and problematic than what is often reported in the literature. Thermoplastic starch has several advantages: it is entirely comprised of annually renewable materials, is of low cost, requires low

energy for its production and results in very low levels of green house gas emissions (Kurdikar et al., 2000). However, when used alone, it generally lacks suitable mechanical property performance and is highly susceptible to picking up ambient moisture. The blending of TPS with other polymers is an important route towards circumventing these weaknesses.

From the viewpoint of droplet deformation/breakup mechanisms during polymer blend morphology formation, the morphological study of blended TPS is an excellent tool to observe starch plasticity. Since morphology modification in blends requires high levels of fluidity of the respective phases, high glycerol contents are required in order to control the TPS phase size (Rodriguez-Gonzalez et al., 2003). Generally, plasticizer levels in excess of 28% (based on the total weight of TPS) are required before the morphology of the TPS phase begins to undergo the standard deformation/disintegration mechanics typically associated with polymer blends (Rodriguez-Gonzalez et al., 2004).

The objective of this work is to carry out a detailed study on the effect of excess water/glycerol mixtures on starch plasticization with a view to determining the time/temperature boundaries required for the successful plasticization of starch on an extruder and ultimately optimize the melt processed dispersed phase morphology of TPS based blends. The gelatinization of wheat starch will be followed using differential scanning calorimetry (DSC), optical microscopy and wide angle X-ray diffraction (WAXD). The dynamics of gelatinization will be conducted under isothermal conditions by evaluating the starch granule swelling during starch gelatinization. Subsequently, the morphology of blends of polycaprolactone (PCL) and thermoplastic starch prepared via a one-step twin-screw extrusion process will be studied. The relationship between factors influencing the gelatinization and dispersed phase morphology will be discussed.

3.4 Experimental

3.4.1 Materials

The polycaprolactone used in this study was CAPA® thermoplastics from Solvay, CAPA6500. It has a molar mass of 50,000 $gmol^{-1}$, a molecular distribution of 1.78 and a melt index of 7.0 g/10min. Native wheat starch (Supergell 1203-C) obtained from ADM/Ogilvie was composed of 25% amylose and 75% amylopectin. TGA measurements showed that the water

content in the native starch granules was about 10%. The water content of Glycerol (SIMCO Chemical Products Ins.) was determined by its refractive index to be below 1.0%.

3.4.2 Sample preparation

In order to investigate wheat starch gelatinization, four groups of starch mixtures were prepared and the compositions of those mixtures are listed in Table 3.1. In all the gelatinization studies, a constant weight of starch, 97g, was used. The starch was mixed with the required amount of plasticizer (water and glycerol) under vigorous stirring via a blender and allowed to equilibrate at room temperature for 24 h. before the DSC test. The concentrations of the starch mixtures used for extrusion are listed in the last two groups.

Table 3.1 Weight compositions of starch-water-glycerol mixtures

Samples	**Composition (g)**		
	Starch (10%water)	Water	Glycerol
DSC 1	97	0-77	56.5
DSC 2	97	47	0-87.3
Extrusion 1	97	0	56.5
Extrusion 2,3,4	97	47	56.5

3.4.3 Differential Scanning Calorimeter

In order to obtain the onset, peak, conclusion temperatures and enthalpy of gelatinization, a Perkin Elmer Pyris DSC 1 was used at a heating rate of 5 ^{o}C min^{-1} from 50 ^{o}C to 130 ^{o}C with an empty sample pan as the reference. The temperature and enthalpy parameters were calibrated using the melting of indium (T_m=156.6 ^{o}C, ΔH = 28.45 J/g). Starch mixtures were weighed (10-15mg) and then hermetically sealed using a volatile sample sealer accessory. The onset (T_c), peak (T_p) and conclusion temperatures (T_c) associated with the gelatinization of wheat starch as well as enthalpies of gelatinization were determined using TA analysis^{TM} software. The analyses were carried out in triplicate.

For the dynamic study of gelatinization a TA DSC Q1000 was used. A starch/water sample was maintained at different target temperatures for 20 min under isothermal conditions, and then

the sample was cooled rapidly. In order to evaluate the degree of starch gelatinization, after this treatment, a heating scan was carried out from 30 to 130 °C at 5 °C/min. The enthalpy of the gelatinization was obtained and the degree of gelatinization (α) was calculated as follows:

$$\alpha = 1 - \Delta H_t / \Delta H_{max} \qquad (3.4.3.1)$$

Here, ΔH_t is the enthalpy after treatment and ΔH_{max} is the maximum enthalpy obtained from the sample without preheating treatment.

3.4.4 Polarized Light Microscopy

A Nikon OPTIPHO-2 polarized light microscope with a Linkan THM5600 hot stage was used to study the morphology of starch gelatinization through the examination of the birefringence of a thin slice of sample. The samples were heated from 40 ℃ to 130 ℃ at heating rates of 5 ℃ min^{-1}, which is the same as that used in the DSC test. The temperature at which the starch diameter started to increase and where the birefringence of the granules began to decrease was defined as the onset temperature, T_o, and the temperature at which the birefringence was lost completely was defined as the conclusion temperature, T_c.

For the dynamic study of gelatinization, in order to distinguish starch granules clearly, the sample with low starch concentration (starch/plasticizer: 5/95) was used and examined using the light microscope with hot stage. The diameter change of starch granules due to the swelling was monitored during starch gelatinization under normal light. Image analysis was carried out to evaluate the gelatinization degree at different temperatures. 50 to 80 starch granules were analyzed to calculate each average diameter.

3.4.5 Wide Angle X-ray Diffraction

Starch mixtures were isothermally preheated at different temperatures for 15 min. The samples were cut into a flat sheet (20mm×20mm×2mm) after cooling in order to be placed in the sample holder of the X-ray diffractometer. The native wheat starch powder was packed tightly in the sample holder. X-ray diffraction patterns were recorded with a Philips diffractometer (Philips Electronic Instrument Co., Houston, TX). The generator of the diffractometer was operated at 50kV and 40mA. Nickel-filtered Cu Kα radiation (λ=1.542Å) was used. The scanning regions of the diffraction angle 2θ were 5-35°, at scanning rates of 2°/min, which covers all the significant diffraction peaks of wheat starch crystallinity. It has been reported that gelatinized starch has a

tendency to retrogradation (Hsu and Heldman, 2005), therefore, the entire X-ray test was conducted within 24 h. after sample preparation.

3.4.6 Blend Extrusion

A one-step blending approach based on previous work by Favis and co-workers (Favis et al., 2005, Rodriguez-Gonzalez et al., 2003) was used for preparing PCL/TPS blends. The extrusion system was composed of a twin-screw extruder (TSE) with a single-screw extruder (SSE) connected midway onto the TSE. The starch suspension (starch/water/glycerol) was fed in the 1st zone of the TSE. Native starch was gelatinized and plasticized in zones 2 to 4 of the TSE. Water was then removed in the 4th zone by venting under vacuum conditions. Molten PCL was fed from the SSE to the 5th zone of the TSE using an adapter designed specially for that purpose. The mixing of PCL with TPS started in the same zone and continued to the 8th zone of the TSE. In another set of experiments, in order to increase the residence time of water, the TSE was modified to 12 zones. In that case the starch was gelatinized and plasticized from the 1st to 8th zone and the PCL/TPS blending was carried out in zones 9-12. In both cases, extruder temperature profiles were set from 70℃ to 110℃ for starch gelatinization and 100℃ to 110 ℃ for blending, respectively.

3.4.7 Scanning Electron Microscopy

The extruded PCL/TPS strands were cut to a flat surface using a microtome (Leica-Jung RM2165) equipped with a glass knife. After completely extracting the TPS using 6N HCl, the sample was coated with a gold-palladium alloy and the morphology of the sample was examined using a Jeol JSM 840 scanning electron microscope at 10 to 15 kV. Image analysis of the blend morphology was carried out using a semi-automatic approach and Sigma Scan Pro.5 software. SEM micrographs were analyzed for each sample to estimate the number average diameter, d_n, and volume average diameter, d_v. Since the microtome does not necessarily cut the dispersed phase at the equator and it is necessary to correct for the dispersity, a correction factor was applied to the diameter determined from the SEM micrographs. Over 300 starch granules were analyzed per sample to calculate dispersed phase average diameter.

3.5 Results and discussion

3.5.1 Gelatinization of starch with excess water/glycerol mixtures

In this part, DSC, optical birefringence and X-ray experiments were undertaken to investigate starch gelatinization in the presence of plasticizer mixtures containing both excess water and glycerol.

DSC

The DSC was used to examine two groups of various starch-glycerol-excess water mixtures that maintain either glycerol or water constant. The onset, peak and conclusion temperatures, T_o, T_p, and T_c of these mixtures are listed in Tables 3.2 and 3.3, respectively. It is clear that water and glycerol exhibit significantly different effects on the starch gelatinization temperature. With a constant concentration of glycerol related to dry starch, the onset, T_o, peak, T_p and conclusion, T_c gelatinization temperatures all shift to low temperature with increasing water concentration. Conversely, these gelatinization temperatures shift to high temperature when the water concentration is held constant and the quantity of glycerol is increased. In both cases, the gelatinization endotherm becomes more pronounced with increasing plasticizer concentration in the system. The enthalpy of gelatinization (ΔH) and hence the degree of starch gelatinization, increases when either water or glycerol is increased in the mixture. It has recently been reported that the addition of high molecular weight plasticizers such as sugars and polyols to a starch-water system increases the starch gelatinization temperature and that the gelatinization temperature of starch is related to the plasticizer concentration in the total solvent (Tan et al., 2004). The DSC results above support these observations. The molecular weight of the plasticizer, its viscosity and also the hydroxyl group density are important factors potentially influencing the starch gelatinization.

Optical Birefringence

Starch granules are semi-crystalline materials and are composed mainly of crystalline amylose and amorphous amylopectin. When observed via optical microscopy, under polarized light, the starch granule shows birefringence. During starch gelatinization, starch crystallinity is destroyed gradually and is accompanied by a loss of birefringence. Figures 3.1, 3.2 and 3.3 reveal some typical micrographs of starch gelatinization with increasing temperature when water, glycerol and their mixtures were used as plasticizer, respectively. It can be seen from Figures (3.1a, 3.2a and 3.3a), that when the temperature achieves $55.0\,^{o}C$ for water, $113.0\,^{o}C$ for

glycerol and 73.0°C for water-glycerol mixtures, starch granules still show a Maltese cross pattern, indicating radial order. It should be noted that starch demonstrates lost birefringence for each case starting at these temperatures. As the temperature increases, more and more starch granules lose their characteristic Maltese cross pattern (see b and c for Figures 3.1, 3.2 and 3.3). Finally, all starch granules lose their birefringence at temperatures of 64.5°C (Figure 3.1d) for the water-starch system, 126.5°C for the glycerol-starch system (Figure 3.2d) and 82.7°C for the water-glycerol-starch system (Figure 3.3d). This indicates that starch crystallinity is destroyed at that temperature. These results compare well with the DSC study. For example, when the glycerol content in the total solvent is about 50%, the conclusion temperature T_c is about 84.4 °C from the DSC test, which is in agreement with the value of 82.7 °C obtained from the optical microscopy observation.

X-Ray Diffraction

It is important to consider X-ray diffraction patterns of thermoplastic starch since some aspects of crystallinity, not observed on the DSC, can remain in the starch sample. It has been reported that the starch molecular chain in a solvent atmosphere "relaxes" due to the incorporation of solvent molecules that facilitate a chain rearrangement, resulting in the appearance of a certain crystalline order (Perry and Donald, 2000). This chain rearrangement is defined as the self-assembly of amylopectin lamellae during hydration. Solvent (water or glycerol) plasticizes the amorphous lamellae and allows the amylopectin helices to organize in a side by side fashion (Donald et al., 2001). Figure 3.4 displays the wide angle X-ray diffraction (WAXD) diffractograms of native wheat starch (Figure 3.4a) and starch-glycerol-water mixtures (Figure 3.4b) before gelatinization. Native starch displays a typical A-type crystal diffractogram with peaks (2θ) at 15.0°, 17.2º, 18.0º and 23.2º (Souza Rosa and Andrade, 2004). After addition of glycerol and water, this A-type crystalline structure is destroyed. The peak at 17.2º weakens and is replaced by a stronger peak at 20.1º. These structural changes are related to the self-assembly of the starch molecular chain.

Figure 3.5 presents the X-ray diffraction patterns of samples of various starch-glycerol-water mixtures after isothermal treatment at the target temperature. In a low water content environment, starch is barely gelatinized even at 110°C (Figure 3.5A) and the starch clearly maintains its original crystal structure. In an intermediate water content environment, the material becomes amorphous below 110°C (Figure 3.5B and C). In an ample water condition, starch is readily

gelatinized even below 70 °C (Figure 3.5D). These results are also in good agreement with the DSC and the optical microscopy observations above.

Table 3.2 DSC characteristics of starch/glycerol/water mixtures with various water contents

Water/dry starch [a] g/100g	T_o [b] °C	T_p [c] °C	T_c [d] °C	ΔH [e] J/g dry starch
10	94.5	99.5	108.4	0.34
20	82.1	90.5	99.4	1.03
30	77.9	87.0	96.2	2.04
40	72.3	83.7	91.4	2.84
50	70.2	81.9	89.8	3.73
100	68.4	75.2	87.1	8.20

a) Glycerol/dry starch: 65/100, b) T_o: Onset temperature, c) T_p: Peak temperature.
d) T_c: Conclusion temperature, e) ΔH: Enthalpy of gelatinization

Table 3.3 DSC characteristics of starch/glycerol/water mixtures with various glycerol contents

Glycerol/dry starch [a] g/100g	T_o [b] °C	T_p [c] °C	T_c [d] °C	ΔH [e] J/g dry starch
0	57.5	64.4	71.6	1.21
10	61.3	68.3	74.2	1.58
20	64.4	72.0	79.8	1.95
30	66.3	73.1	82.1	2.71
50	69.2	76.6	85.3	3.76
100	74.9	83.5	94.4	7.69

a) Water/dry starch: 65/100, b) T_c: Onset temperature, c) T_p: Peak temperature.
d) T_c: Conclusion temperature, e) ΔH: Enthalpy of gelatinization

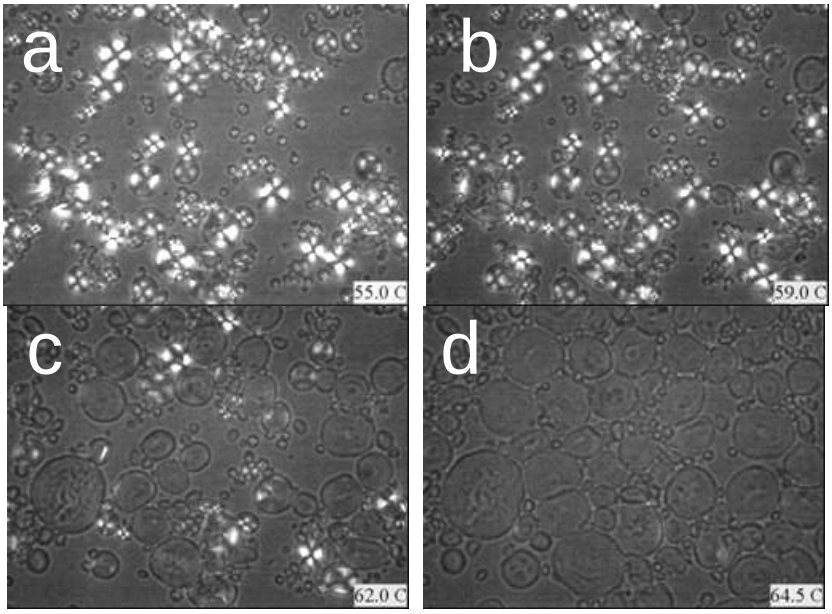

Figure 3.1 Optical microscope observation of starch gelatinization when plasticized by water (water/dry starch=300g/100g). a) 55.0 °C ; b) 59.0 °C ; c) 62.0 °C ; d) 64.5 °C .

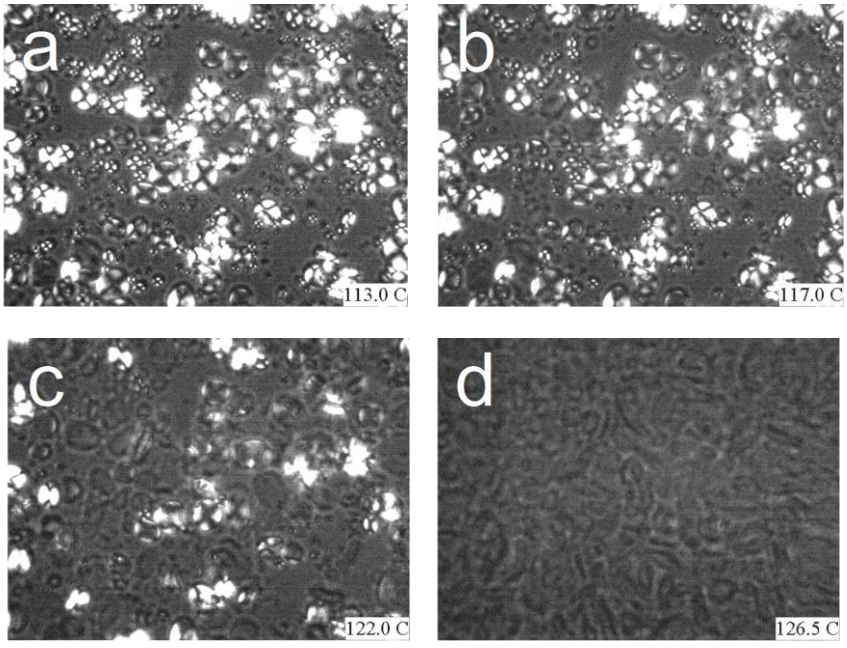

Figure 3.2 Optical microscope observation of starch gelatinization when plasticized by glycerol (glycerol/dry starch=300g/100g). a) 113.0 °C ; b) 117.0 °C ; c) 122.0 °C ; d) 126.5 °C .

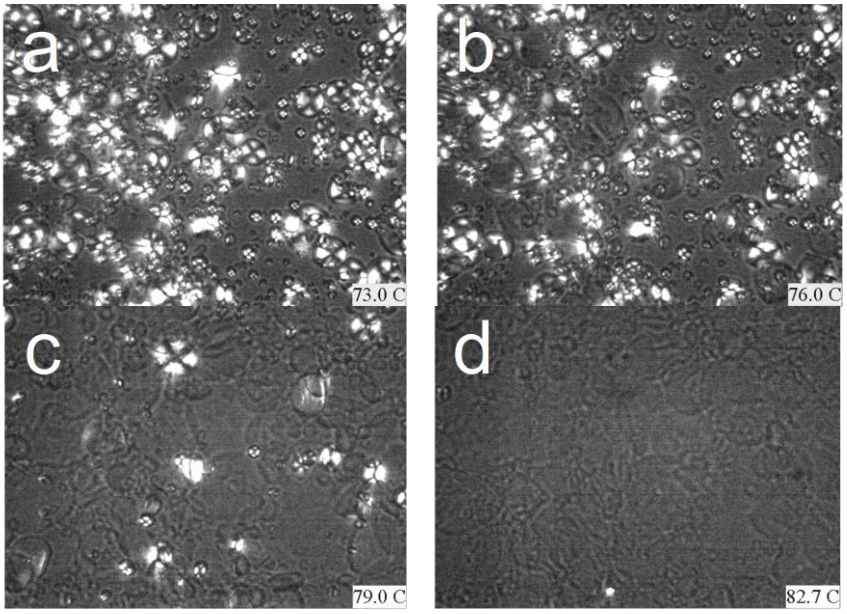

Figure 3.3 Optical microscope observation of starch gelatinization plasticized by mixtures of water and glycerol (water/glycerol/dry starch=150g/150g/100g). a) 73.0 °C ; b) 76.0 °C ; c) 79.0 °C ; d) 82.7 °C .

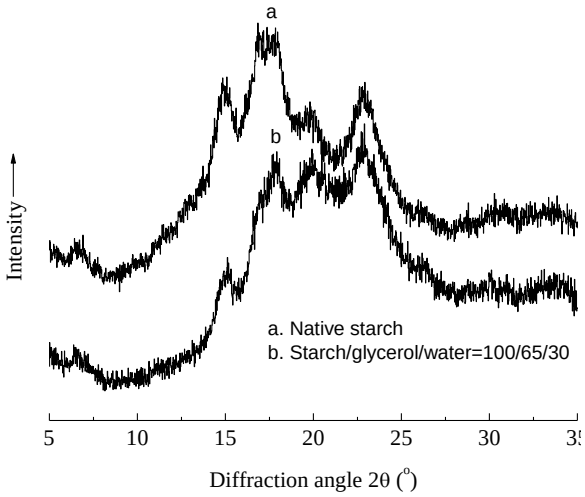

Figure 3.4 WAXS patterns of native starch (a) and its suspension (b) prior to gelatinization.

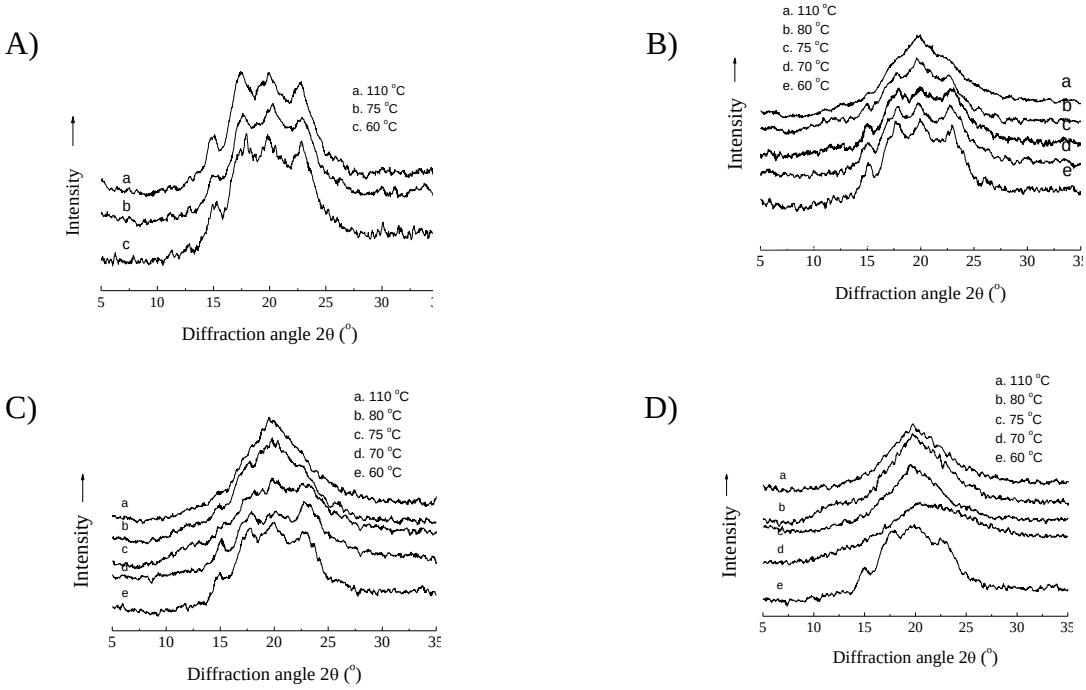

Figure 3.5 WAXS patterns of various starch/glycerol/excess water mixtures after treatment at various temperatures. A) 100/65/10; B) 100/65/30; C) 100/65/50; D) 100/65/100.

3.5.2 Dynamics of starch gelatinization with excess water/glycerol

During starch gelatinization, plasticizer penetrates into the amorphous regions and granules start to swell under heating conditions. Simultaneously, the degree of gelatinization can also be associated with the swelling. In this part, the dynamics of starch gelatinization was examined by tracking the diameter change of starch granules under isothermal conditions. Figures 3.6a, b, c shows the volume average diameter (d_v) and the number average diameter (d_n) change during gelatinization for water/starch, glycerol/starch and water/glycerol/starch mixture, respectively. Note also that the onset and conclusion temperatures for this particular mixture from the DSC test were 57.2 °C and 71.65 °C for water/starch; 120.4 °C and 139.2 °C for glycerol/starch; and 71.4 °C and 82.2 °C for the starch/water/glycerol mixture, respectively. A number of interesting features emerge. Firstly for all mixtures, even over long times, no gelatinization whatsoever is observed below the onset temperatures as derived from the DSC. Secondly, the gelatinization process is significantly slower for the glycerol/starch mixture where gelatinization, even well above the onset temperature, still requires approximately 3 minutes (Figure 3.6b). For the water/starch and water/glycerol/starch mixtures, the gelatinization process is accomplished within

a)

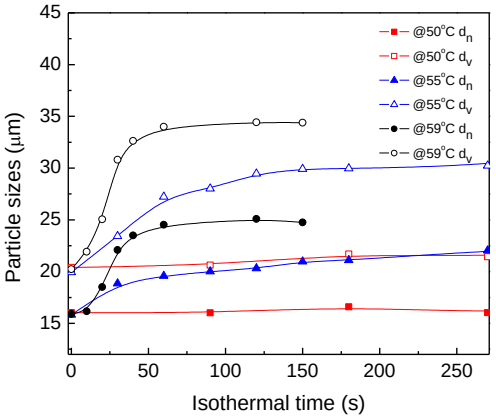

b)

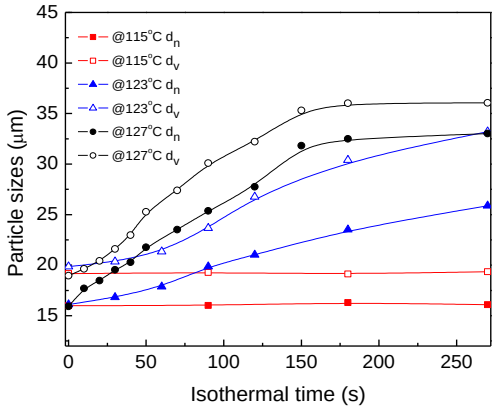

c)

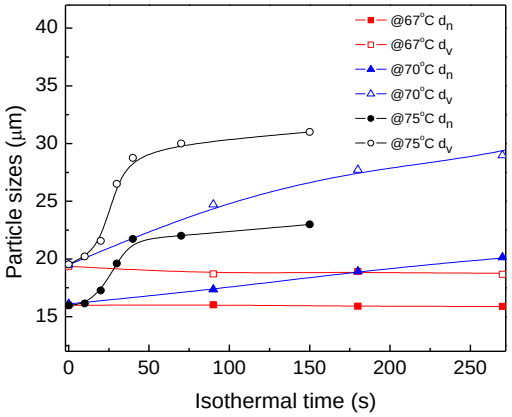

Figure 3.6 Dynamic study of starch gelatinization by evaluating the swelling of starch. a) starch/water (5/95), b) starch/glycerol (5/95), c) starch/water/glycerol (47.5/47.5/5).

60 seconds (Figure 3.6a, c). Note that these time differences would be considered to be very significant in a melt extrusion operation. Since the volume average diameter weights the large starch particles and the number average diameter weights the smaller ones within the same statistical group, a comparison of those two allows for an examination of the influence of starch

granule size on gelatinization kinetics. Clearly in figure 3.6, the starch size does not appear to have a significant influence on the kinetics and the d_v and d_n curves demonstrate virtually identical features. It is interesting to note that as the temperature increases the final plateau size achieved also increases and this is clearly associated with an increasing degree of plasticization with temperature. The effect of water in the excess water/glycerol plasticization protocol evidently serves to improve ingress rates into the starch granules.

In order to further examine the effect of temperature on degree of gelatinization, a water/starch sample was held at different temperatures for 20 minutes. After this treatment, a heating scan on the DSC was carried out to evaluate the degree of gelatinization. The result is shown in Figure 3.7. The peak gelatinization temperature (T_p) increases with increasing isothermal treatment temperature. The degree of starch gelatinization can be obtained from the DSC test. As shown in Figure 3.8, the degree of gelatinization also increases with the treatment temperature and complete gelatinization can only be achieved at high temperatures (about $80\,^{o}C$). Since starch gelatinization is accomplished in one minute, it is important to consider that, even if the kinetics is rapid, below the conclusion temperature (T_c) only a partial degree of gelatinization is achieved even after long times of treatment.

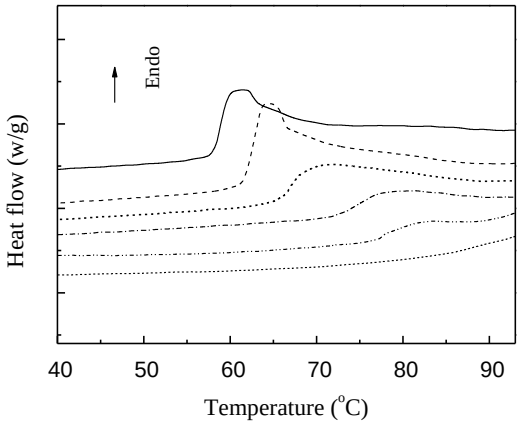

Figure 3.7 DSC traces of gelatinization for wheat starch/water systems after isothermal treatment at different temperatures for 20 min. Isothermal temperature: from top to bottom 48.5 ^{o}C, 53.5 ^{o}C, 57.5 ^{o}C, 65.0 ^{o}C, 70.0 ^{o}C and 80.0 ^{o}C. The scanning rate is 5 ^{o}C/min.

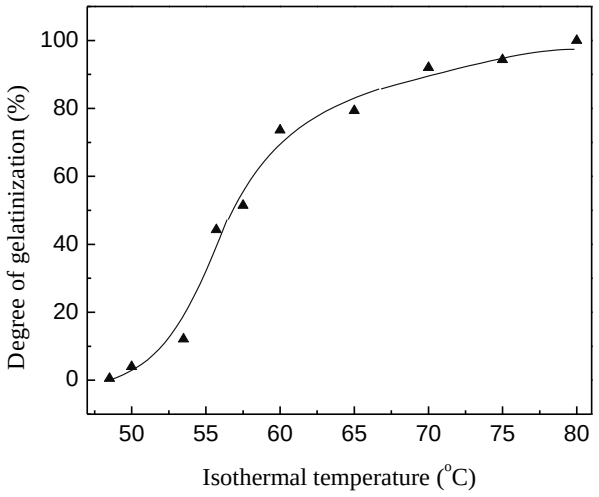

Figure 3.8 Degree of starch gelatinization for wheat starch/water systems after isothermal treatment at different temperatures for 20 min.

These results clearly support the notion that added excess water is a necessary ingredient for glycerol to plasticize starch within the time constraints of a melt processing operation, and a sufficient residence time of water in contact with the starch is required prior to devolatilization.

3.5.3 Effect of starch gelatinization on PCL/TPS blend morphology after extrusion

From the viewpoint of droplet deformation/breakup mechanisms during polymer blend morphology formation, the morphological study of blended TPS is an excellent tool to observe starch plasticity. Since morphology modification in blends requires high levels of fluidity of the respective phases, high glycerol contents are required in order to control the TPS phase size (Rodriguez-Gonzalez et al., 2003; Rodriguez-Gonzalez et al., 2004; Kurdikar et al., 2000). Generally, plasticization levels in excess of 28% (based on the total weight of TPS) are required before the morphology of the TPS phase begins to undergo the standard deformation/disintegration mechanics typically associated with morphology control in polymer blends.

One of the goals of this work is to carry out complete starch gelatinization, water devolatilization and polymer blending in one-step on a twin-screw extruder. Depending on the flow rate used, the residence time for the entire process can be as short as 1-2 minutes. This

approach therefore has to accommodate significant time constraints. From the blending point of view, previous work from this laboratory (Bourry and Favis, 1998) has shown that the actual time to generate steady state polymer blend morphologies for synthetic polymers in the twin-screw extruder can be quite low (approximately 30 seconds) once the various components are in the melt state. The main challenge therefore in the one-step extrusion process is the effective plasticization of starch. It is clear from the previous part of this paper that the approach of using excess water/glycerol mixtures to plasticize starch is a necessary requirement if TPS blends are to be twin-screw compounded in one-step in the limited time. Since about 28% glycerol in the thermoplastic starch is required to achieve sufficient fluidity for blend morphology control protocols (Rodriguez-Gonzalez et al., 2004) the morphology of the TPS in a given polymer blend is a good indicator of the effectiveness of plasticization.

In order to understand the effect of water and glycerol on starch gelatinization during extrusion, PCL/TPS blends were prepared under various conditions. In the first case, extrusion 1, a starch/glycerol mixture (97/56.5) was added at the hopper of an 8 zone twin-screw extruder. Note that the inherent ambient water content of the starch prior to extrusion was 10%, but no additional water was added to the mixture preparation. In addition, in that case no devolatilization was carried out during extrusion. In a second case, extrusion 2, a starch/glycerol/excess water slurry was prepared in the proportions of 97/56.5/47 respectively. Devolatilization of the water was carried out in zone 4 of the 8 zone extruder. The third case, extrusion 3, was exactly the same as the second one except that no devolatilization was carried out. This allowed us to evaluate the importance of residence time of the water in the system. In the fourth and last case, extrusion 4, 4 additional zones were added to the same twin-screw extruder (12 zones). In that last case, the starch/glycerol/excess water slurry was used and devolatilization was carried out in zone 8. Blending was carried out in zones 9-12. The temperature profiles are provided in the experimental.

A SEM study of the PCL/TPS36 (70/30) blends is shown for the four extrusion conditions as well as for native starch in Figure 3.9. Note that TPS36 indicates a level of 36% glycerol based on the total thermoplastic starch (starch + glycerol). In order to improve the contrast for microscopy purposes, the TPS phase was removed by selective extraction leaving cavities in the PCL matrix. The quantitative image analysis of these blends is shown in Figure 3.10a, b, c. Figure 3.9a and 3.10a show that when glycerol was added as a single plasticizer to plasticize

starch (extrusion 1 experiment), very large droplet-like particles dispersed in the PCL matrix are obtained with a volume average diameter (d_v) of 13.9 μm and a number average diameter (d_n) of 10.7 μm. These results are identical to that of the as-received native starch, which has a d_v of 13.6 μm (see Figure 3.9e). When starch is dispersed within a matrix carrier phase and is well plasticized at high enough contents of plasticizer, the classic deformation/disintegration phenomena normally associated with polymer blending come into play and large starch particles are transformed into much smaller ones (Rodriguez-Gonzalez et al., 2003). Clearly, in this case, the particle sizes from image analysis show that glycerol alone was unable to effectively plasticize the starch under these extrusion conditions.

In the extrusion 2 experiment, a excess water/glycerol/starch mixture was fed to the twin-screw and subsequently devolatilized (keeping all other component concentration and processing conditions unchanged). In this case, a much more effective gelatinization was achieved. The number of large starch particles decreased and a bimodal particle distribution was observed (Figure 3.9b and 3.10b). Some of the plasticized starch was completely broken-down into order of magnitude smaller particles. A bimodal particle distribution was obtained with the large particles having a volume average diameter (d_v) of 10.2 μm and a d_n of 2.5 μm. However, the bimodal TPS phase size distribution clearly indicates that the starch plasticization process remains incomplete.

In the extrusion 3 experiment, the excess water/glycerol/starch mixture was prepared under the same conditions as in the extrusion 2 case but without vacuum devolatilization of water, only the vent port was left open to the atmosphere. This results in a less efficient removal of water and has the effect of increasing the residence time of water in the twin-screw extrusion process. In this case the morphology of the TPS particles become unimodal with a d_v of 4.4 μm and a d_n of 3.0 μm (Figure 3.9c and 3.10c). These results support the conclusions of the previous section and underline the importance of not only adding excess water at the outset of the extrusion process, but also assuring a minimum residence time of water prior to removal and devolatilization. It is evident from figure 3.10c that the resulting effect on TPS morphology in the TPS/PCL blend is dramatic.

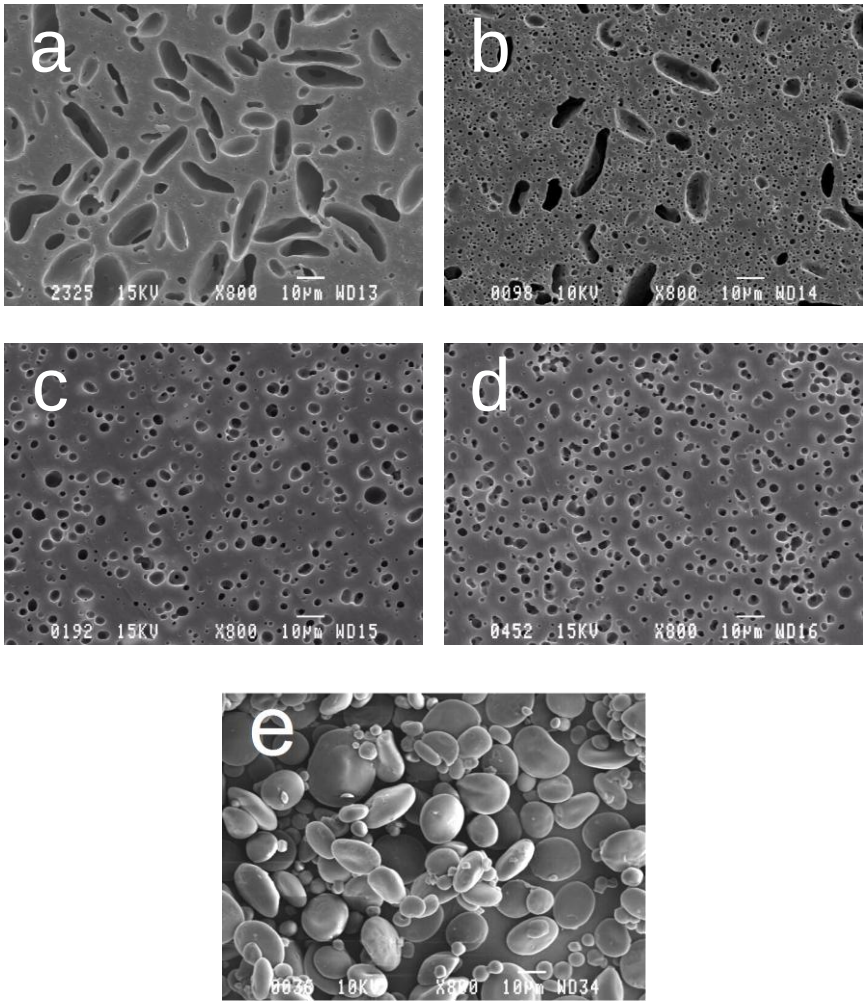

Figure 3.9 Morphology development of the PCL/TPS36 (70/30) blends. The sample was prepared under the following conditions: a) Extrusion 1 (starch/glycerol=97/56.5); b) Extrusion 2 (starch/glycerol/water=97/ 56.5/47); c) Extrusion 3 (starch/glycerol/water= 97/56.5/47); d) Extrusion 4 (starch/glycerol/ water =97/56.5/47); e) Native granular wheat starch.

It is well known that the presence of water in the extrudate can be detrimental to the final mechanical properties of TPS blend systems. In the extrusion 4 experiment, in order to maintain a sufficiently long residence time of water and still be able to ultimately devolatilize the system, the same twin-screw was extended from 8 zones to 12 zones. The same excess water/glycerol/starch mixture as in extrusion experiments 2 and 3 was used as well as the same basic temperature profiles for starch plasticization and blending with PCL. The final result of this experiment was an extrudate possessing water contents of less than 0.45% (from thermal

gravimetric analysis results not shown here) and a unimodal phase size distribution of dispersed TPS particles with a dv of 3.2 μm and a dn of 2.1 μm (Figure 3.9d and 3.10c).

Figure 3.11 shows the comparison of the X-ray diffraction patterns of native starch and TPS obtained at different extrusion conditions. If starch is not fully gelatinized, in the extrusion 2 experiment, there is still some crystallinity associated with the V_H-type ($2\theta = 19.5^o$) crystallinity as shown in Figure 3.11b. It is known that this crystal form develops in the case of starch containing lipid compounds that are comprised of the amylose component (Derycke et al., 2005). In Figure 3.11c this peak is absent and the X-ray profile clearly indicates a completely amorphous starch achieved in the extrusion 4 experiment.

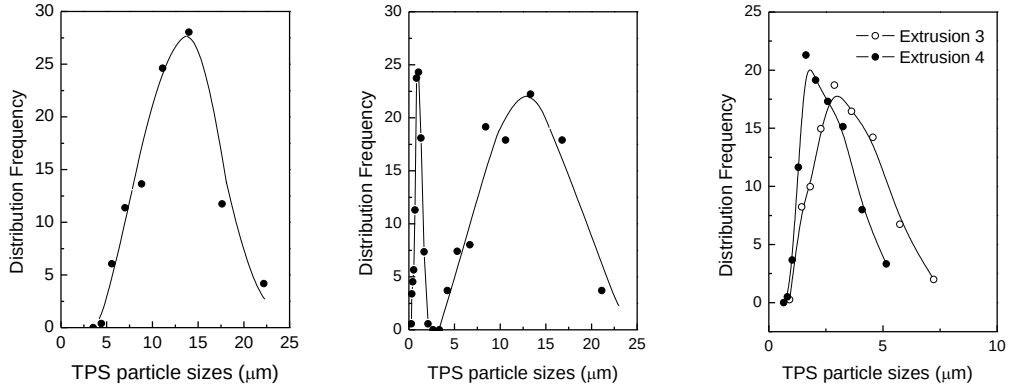

Figure 3.10 Morphological analysis of PCL/TPS36 (70/30) blends prepared under various processing conditions. a) Extrusion 1; b) Extrusion 2; c) Extrusion 3 and Extrusion 4.

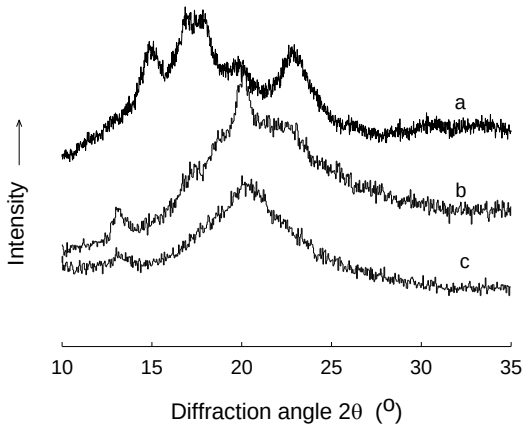

Figure 3.11 WAXS patterns of native starch and TPS36 prepared via different processing conditions. a) Native wheat starch; b) Partially gelatinized TPS36 prepared via extrusion 2; c) Completely gelatinized TPS36 prepared via extrusion 4.

3.6 Conclusion

In this paper, we examine critical aspects of starch plasticization in glycerol/excess water mixtures in order to determine the time/temperature boundaries ultimately required for the successful plasticization of starch in a polymer melt processing environment and then relate these findings to the morphology of melt-blended thermoplastic starch (TPS) in polycaprolactone (PCL). The onset and conclusion temperatures for wheat starch gelatinization in the presence of excess water were obtained via differential scanning calorimetry (DSC), optical microscopy and wide angle X-ray diffraction (WAXD). Dynamic studies indicate that the starch granule size has very little effect on gelatinization kinetics. If the temperature is sufficiently high, gelatinization takes place within 60 seconds for the excess water/glycerol/wheat starch mixture and within 3 minutes for the glycerol/wheat starch case. However, even if the kinetics is rapid, below the conclusion temperature only a partial degree of plasticization is achieved even after long times of treatment. Taking into account the above time/temperature constraints for starch plasticization, a series of one-step melt extrusion experiments for PCL/TPS blends were designed and the dispersed TPS morphology was examined. The TPS particle size (d_v) in a PCL matrix is 13.9 microns when only glycerol is used to plasticize native starch (contains only ambient water). This is very similar to the native starch granule size of 13.6 microns and clearly indicates the inability of glycerol alone to plasticize native starch within the time constraints of melt extrusion.

When a glycerol-excess water mixture is used and a sufficient residence time is allowed prior to water devolatilization, a completely plasticized starch is obtained. The efficacy of plasticization is demonstrated by a dramatic six-fold reduction in the dispersed TPS phase size, a unimodal TPS phase size distribution in the blend system and by a completely amorphous WAXS diffraction pattern.

3.7 Acknowledgements

The authors gratefully acknowledge the financial support received from the Natural Sciences and Engineering Research Council of Canada through a Strategic Grant.

3.8 Keywords

Differential scanning calorimetry (DSC); phase morphology; plasticization; polycaprolactone; polymer blends; thermoplastic starch; WAXS

3.9 References

M. Avella, H. E. Errico, P. Laurienzo, N. Manolova, M. Raimo, R. Rimedio, *Polymer,* **2000**, 41, 3875.

S. St. Lawrence, P. Walia, F. C. Felker, J. L. Willett, *J. Polym. Eng.Sci.,* **2000,** 44, 1839.

L. Averous, L. Moro, P. Dole, C. Fringant, *Polymer*, **2000**, 41,4157.

L. Averous, *J. Macromol. Sci., Part C: Polym. Rev.,* **2004,** 44, 231.

F. J. Rodriguez-Gonzalez, B. A. Ramsay, B. D. Favis, *Polymer*, **2003**, 44, 1517.

R. D. Di Paola, R. Asis, M. A. J. Aldao, *Starch/Stärke* 2003, 55, 403.

M. E. Cagiao, D. R. Rueda, R. K. Bayer, F. J. B. Calleja, *J. Appl. Polym. Sci.,* **2004**, 93, 301.

P. A. Sopade, P. J. Halley, L. L. Junming, *J. Food Eng.,* **2004**, 61, 439.

W. Wang, S. K. Sastry, *J. Food Eng.,* **1997**, 34, 225.

F. D. Li, L. T. Li, Z. Li, E. Tatsumi, *J. Food Eng.,* **2004**, 62, 113.

R. C. R. Souza, C. T. Andrade, *Adv. Polym. Technol.,* **2002,** 21, 17.

P. A. Perry, A. M. Donald, *Biomacromolecules*, **2000**, 1, 424.

T. Palav, K. Seetharaman, *Carbohydr. Polym.,* **2006,** 65, 364.

T. Temsiripong, R. Pongsawatmanit, S. Ikeda, K. Nishinarib, *Food Hydrocolloids,* **2005**, 19, 1054.

Q. Liu, L. G. Charlet, S. Yelle, *J. Arul, Food Res. Int.,* **2002**, 35, 397.

M. Fukuoka, K. I. Ohta, H. Watanabe, *J. Food Eng.,* **2002**, 53, 39.

M. Ndife, G. Sumnu, L. Bayndrli, *Lebensm.-Wiss. Technol.,* **1998**, 31, 484.

B. Zanoni, A. Schiraldi, R. Simonetta, *J. Food Eng.*, **1995**, 24, 25.

G. Spigno, M. Dante, D. Faveri, *J. Food Eng.*, **2004**, 62, 337.

I. Tan, C. C. Wee, P. A. Sopade, P. J. Halley, *Carbohydr. Polym.*, **2004**, 58, 191.

F. J. Rodriguez-Gonzalez, B. A. Ramsay, B. D. Favis, *Carbohydr. Polym.*, **2004,** 58, 139.

US 6605657 (2003) and 6844380 (2005), invs.: B. D. Favis, F. Rodriguez, B. A. Ramsay.

D. Kurdikar, L. Fournet, S. C. Slater, M. Paster, K. J. Gruys, T. U. Gerngross, R. Coulon, *J. Ind. Ecol.*, **2000**, 4, 107.

C. L. Hsu, D. R. Heldman, *J. Food Proc. Eng.*, **2005**, 28, 506.

A. M. Donald, K. Lisa Kato, P. A. Perry, T. A. Waigh, *Starch/Stärke*, **2001**, 53, 504.

R. C. R. Souza Rosa, C. T. Andrade, *J. Appl. Polym. Sci.*, **2004**, 92, 2706.

D. Bourry, B. D. Favis, *Polymer*, **1998**, 39, 1851.

V. Derycke, G. E. Vandeputte, R. Vermeylen, W. De Man, B. Goderis, M. H. J. Koch, J. A. Delcour, *J. Cereal. Sci.*, **2005**, 42, 3343.

CHAPTER 4

MORPHOLOGY DEVELOPMENT AND INTERFACIAL INTERACTIONS IN POLYCAPROLACTONE/THERMOPLASTIC-STARCH BLENDS

4.1 Presentation of the article of morphology development and interfacial interactions in polycaprolactone/thermoplastic-starch blends

4.2 Abstract

The coalescence, continuity development, dynamic and static mechanical properties and interfacial interactions are studied for polycaprolactone/thermoplastic starch blends. These blends, prepared by a one-step extrusion process, demonstrate the features of a highly interacting system and the tensile mechanical properties demonstrate exceptional ductility at very high levels of thermoplastic starch without any added interfacial modifier. Virtually all the results can be explained by two phenomena: a high elasticity of the thermoplastic starch phase and a strong compatibility between TPS and PCL due to hydrogen bonding. The high level of compatibility is facilitated by the high mobility of the TPS chains due to the high plasticizer content and a highly effective TPS plasticization protocol.

4.2 Introduction

Starch materials have attracted considerable attention in the bioplastics field due to their abundance, biodegradability and low cost. The development of thermoplastic starch (TPS) from starch granules and plasticizer allows for the transformation of native starch into a fluid similar to other conventional thermoplastics [Otey et al, 1980; Averous et al, 2000]. This is achieved through the application of heat and in the presence of water and/or another plasticizer for starch. The advantage of TPS is that it can be processed on typical melt-processing equipment. Thermoplastic starch, on its own however, has certain critical weaknesses namely poor mechanical strength and a susceptibility to pick up moisture. These failings can be overcome by blending thermoplastic starch with other polymers. The conversion of native starch into a fully plasticized thermoplastic starch using melt extrusion processing is a complex operation and an understanding of the time/temperature boundaries ultimately required for the successful plasticization of starch on melt processing equipment is critical [Li et al, 2008].

It is well known in polymer blends that the morphology control of the respective phases is a key factor to achieve desired material properties. Typically, the morphology of polymer blends is strongly dependant on the composition, the viscoelastic properties of the components, the interfacial tension and processing conditions. The phases in a polymer blend can be structured in droplet, fiber, laminated, and co-continuous form [Favis, 2000]. Recently even droplet-in-droplet and multiple percolated co-continuous systems have been developed [Reignier and Favis, 2000]. A co-continuous binary blend morphology is one in which neither of the blend phases can be defined as a matrix or the dispersed phase. It forms highly interconnected and intertwining structures and both the component phases remain fully continuous throughout the blend.

The mixing of conventional polymers with native unplasticized starch blends always leads to brittle materials [Willett, 1994; Evangelista etal, 1991; Sailaja and Chanda 2001]. In that case the starch component behaves as a solid filler. St Pierre *et al* [St-Pierre et al, 1997]. carried out an investigation on thermoplastic starch/polyethylene blends and demonstrated that dispersed phase/matrix morphology control protocols could be applied to this blend. In a later work, Rodriguez *et al*. [Rodriguez et al. 2003; Favis et al. 2003] developed an effective one-step melt processing technique and controlled the level of continuity of the TPS phase. This resulted in exceptional properties for the PE/TPS blends. This process was used to generate highly elongated morphological structures [Rodriguez 2002]. With this approach it was possible to achieve blends where the TPS morphology could be effectively controlled, yielding a wide range of sophisticated morphological states including co-continuous structures [Favis et al. 2003; Favis et al. 2006]. Rodriguez *et al*.[Rodriguez et al. 2003; Rodriguez 2002] succeeded in maintaining 96% of the elongation at break and 100% of the modulus of LDPE with a 71:29 HDPE/TPS blend that contained 36% of glycerol in the TPS phase. Moreover, this particular blend demonstrated very low levels of sensitivity to moisture and an absence of interfacial voiding.

Phase coalescence is an important phenomena affecting the final morphology of polymer blends and has been studied in some detail in recent years [Yuan and Favis 2005; Willemse et al. 1999; Venstra et al. 2000]. Typically, coalescence can be divided into two categories: dynamic and static processes [Yuan and Favis 2005]. The dynamic case is a flow-induced coalescence process during polymer blending with the final morphology being governed by a balance of particle breakup and coalescence. Static coalescence is a quiescent process whereby the phase or phases are coarsened over time at high temperature. Co-continuous systems, in particular can

demonstrate very elevated levels of coalescence during static annealing [Yuan and Favis 2005]. Willemse et al. reported that coarsening via coalescence is found only above the percolation threshold in a droplet/matrix morphology [Willemse et al. 1999]. Using a conceptual model of co-continuity based on the thin and thick rods, Yuan et al. have proposed that the driving force for coarsening process during static annealing is a capillary pressure effect [Yuan and Favis 2005]. The differences in capillary pressure throughout the co-continuous structure result in the continuous merging of thin parts toward the thick ones. Effective interfacial modification of a polymer blend has been shown to be capable of diminishing the dramatic effects of static coalesence coarsening discussed above to a small or even negligible effect [Pyun et al. 2007].

PCL is a synthetic polymer having unique properties that make it attractive for biomaterials applications. It has excellent biodegradability and biocompatibility properties. However, PCL is still more expensive than conventional plastics, and the degradation rate is not completely satisfactory in some instances [Pitt et al. 1980]. The blending of PCL with TPS could provide a potential route towards more economic fully biodegradable materials. A number of studies on PCL/TPS blends have been carried out [Shin et al. 2004; Matzinos et al. 2002; Averous et al. 2000; Sarazin et al. 2008; Shin et al. 2008]. Shin et al. reported large diameters of the TPS dispersed phase in blends of PCL and thermoplastic starch plasticized with 20% glycerol [Shin et al. 2004]. Matzinos et al. reported on the obtention of a completely plasticized thermoplastic starch and a morphology with a relatively fine and uniform dispersion of TPS phase within the PCL matrix after a three-times extrusion protocol [Matzinos et al. 2002]. The mechanical and thermal properties of PCL/TPS with various moisture and glycerol contents were investigated by Averous et al. [Averous et al. 2000]. Results indicated low compatibility between PCL and TPS according to DMA and DSC measurements. In the meantime, the elongation at break of PCL/TPS blends dramatically decreased as compared to pure PCL when the TPS concentration was increased up to 50%. Sarazin et al. [Sarazin et al. 2008;] showed that the addition of small amounts of polycaprolactone to a blend of poly(lactic acid) and thermoplastic starch significantly improved the ductility and impact strength of the blends. Recently Shin et al. [Shin et al. 2008] studied blends of polycaprolactone with thermoplastic starch and showed that the chemical modification of starch with maleic anhydride led to improvements in interfacial adhesion and processability. To date, very little work has been done on the detailed morphology development and morphology control in PCL/TPS blends.

The objective of this study is to carry out a detailed study on the morphology development in PCL/TPS blends with high plasticizer content prepared using a one-step process. This work will closely examine the coalescence and continuity development in these systems. The resulting dynamic and static mechanical properties of the blends as well as the possible presence of specific interations will also be considered.

4.3 Experimental

4.3.1 Materials

Two commercial grades of polycaprolactone from Solvay, CAPA6500 and CAPA6800, with different molecular weights were used in this work. The characteristics of polycaprolactone are summarized in Table 4.1. Throughout this paper CAPA6500 and CAPA6800 will be referred to as PCL1 and PCL2 respectively. Native starch was obtained from ADM/Ogilvie and is composed of 25% amylose and 75% amylopectin. TGA measurements showed that the water content in the native starch granules was around 10%. The plasticizers used were water and pure glycerol (SIMCO Chemical products Inc. 99.5%). In order to calculate the volume composition of blends, the densities of PCL1, PCL2, TPS36 and TPS 40 at the processing temperature were measured; the results are shown in Table 4.1.

For the composition study, the entire range of PCL/TPS36 blend composition from 100/0 to 0/100 in steps of 10 wt% were prepared. For the investigation of the effect of viscosity ratio on blend morphology, two kinds of PCL with different molecular weights and TPS with different glycerol contents were blended; the TPS content in the blend for the viscosity ratio study was held constant at 30% by weight.

Table 4.1 Materials Characteristics

Designation	Product	Mean Mw. [a)]	Melting point [a)] (℃)	Melt index[a)] (g/10min,160℃)	Density (g/cm^3)	
					110℃	150℃
PCL1	CAPA6500	50,000	58-60	7.0	1.03	1.03
PCL2	CAPA6800	80,000	58-60	3.0	1.05	1.05
TPS36					1.31	1.29
TPS40					1.31	1.29

a) obtained from suppliers

Note that the thermoplastic starch types used are designated as TPS 36 and TPS 40. The 36 in TPS 36 corresponds to the weight of glycerol divided by the weight of glycerol and starch (including ambient water in the as-received starch, but not including any added excess water). After plasticization of the starch, water was removed using a venting process. Under such conditions, virtually all of the water is removed (including native water within the as-received starch). As such, the actual final glycerol content of the TPS after extrusion is 38 wt% (based on the weight of thermoplastic starch) for TPS 36 and 42 wt% for TPS 40.

4.3.2 Processing

Starch granules were gelatinized, plasticized with glycerol and water, and blended with PCL in a one-step extrusion process. The processing of the polycaprolactone/thermoplastic starch blends was based on a process developed previously in this laboratory [Favis et al. 2003; Rodriguez et al. 2003; Favis et al. 2005]. The extrusion system was composed of a single-screw extruder (SSE) connected midway to a co-rotating twin-screw extruder (TSE). A starch/glycerol/water suspension was fed in the first zone of the TSE. The weight compositions of the starch suspensions are listed in Table 4.2. Native starch was gelatinized and plasticized and volatiles were extracted in the first part of the TSE. Molten PCL was fed from the SSE to midway on the TSE and the processing temperature was set at 110 ℃ and 130 ℃ for PCL1 and PCL2, respectively. TPS and PCL were then mixed in the latter part of the TSE. The TSE screw speed was 150 rpm for all blends. The draw ratio of the strands exiting the die was held at 1. Cylindrical extruded PCL/TPS strands were cooled and pelletized.

Standard tensile dumbbell specimens, ASTM D638 Type I, were prepared by injection molding (Sumitomo SE50S). The temperature profile was 110/115/120/120 ℃ and 130/135/140/140 ℃ for PCL1 and PCL2 blends, respectively. The nominal width and thickness of the tensile bars were 10mm and 3 mm, respectively.

Table 4.2 Weight compositions of starch-water-glycerol suspensions

Samples	**Composition (g)**			**Glycerol content in TPS (%)**
	Starch	Glycerol	Water	
TPS36	48.5	28.0	23.5	38
TPS40	48.5	32.5	19.0	42

4.3.3 Rheology Measurement

Dynamic rheological measurements were carried out on Rheometrics Scientific SR-5000 dynamic stress rheometer. Before rheological measurements, samples were conditioned at RH 50%, 23 ℃ for one week. These measurements were then carried out in a 25mm parallel plate geometry with a gap of about 1.0 mm under a nitrogen atmosphere at the same temperatures as extrusion processing. The sample outer edge was sealed by a thin layer of silicon grease to reduce the evaporation of plasticizer during the test. The dynamic viscoelastic properties were determined with frequencies from 500 to 0.1 rad/s. A stress sweep from 10 to 500 Pa was performed to define the region of linear viscoelasticity. The curves representing these rheological properties versus frequency are shown in Figure 4.1.

4.3.4 Scanning Electron Microscopy

The The extruded strands or injection molded bars were cut to a flat surface using a microtome equipped with a glass knife. Selective solvent extractions of TPS and PCL were performed at room temperature. 6N HCl and THF were utilized in order to extract the TPS and PCL phases respectively. After coating with a gold-palladium alloy, the morphologies of the samples were examined by a Jeol JSM 840 scanning electron microscopy at 10 to 15 kV. A semiautomatic method of image analysis was applied to quantify the average size of the dispersed phase. The number average diameter, *dn*, and volume average diameters, *dv*, were obtained from these measurements. Since the microtome does not necessarily cut the dispersed phase at the equator and since it is also necessary to correct for polydispersity effects on phase size, the Saltikov correction factor was applied to the diameter from the SEM micrographs [Saltikov 1967]. Over 300 dispersed particles were analyzed per sample to calculate the average phase diameter.

4.3.5 Continuity Analysis

A gravimetric method was used to calculate the extent of continuity of the phase. Three segments of extruded strands were cut into around 10mm length and immersed in the solvent at ambient temperature for 12 h. Weight loss measurements were carried out to calculate the percentage of continuity using the following equation:

$$\%continuity = \left(\frac{W_{init.} - W_{Fin.}}{W_{init.}} \right) \times 100\% \qquad (1)$$

Where, $W_{init.}$ corresponds to the weight in the blend before the solvent extraction step, and

W_{fin}. corresponds to weight remaining after extraction.

4.3.6 Quiescent annealing

Annealing tests were carried out in a compression molding machine. Samples were cut from injection molded tensile test bars which were then sandwiched between two aluminium foil sheets and subsequently transferred into the cavity of a frame. Both the frame and samples were placed between two metal plates on the compression molding machine at the target temperature. In order to minimize any deformation or flow of the samples, the compression plate just touches the metal plate without any pressure. Annealing temperatures were chosen as 110 ^{o}C and 150 ^{o}C. After annealing, the samples were quenched immediately in liquid nitrogen to freeze-in the morphology.

4.3.7 Thermal properties of blends

Experiments were carried out on a 2980 dynamic mechanical analyzer (DMA) from TA Instruments. The specimens were cut from tensile dumbbell specimens. The samples were tested in the dual cantilever bending mode at a frequency of 1 Hz with a target amplitude of 30μm. The scanning rate was set at 3 ^{o}C /min in the range of -80 to 50 ^{o}C. The thermal transitions were determined from the maximum of the Tan δ peaks.

4.3.8 FTIR

Fourier transform infrared spectroscopy (FTIR) was carried out on injection molded samples at a 2 cm^{-1} resolution with a BIO-RAD FTS3000 IR Spectrum Scanner combination with an attenuated total reflection (ATR) accessory. 128 scans were signal-averaged to reduce spectral noise.

4.3.9 Tensile mechanical properties

Tensile mechanical properties were measured at ambient temperature using an Instron testing system (Model 400R) with a 5kN cell, according to the ASTM D638. The specimens were preconditioned at 23 ^{o}C and 50% relative humility for one week before the test. The crosshead speed used was 50 mm/min. The stress at yield, elongation at break and Young's modulus were obtained from the test. Testing was stopped when the elongation reached 1000%.

4.4 Results and Discussion

4.4.1 Rheological properties of raw TPS and PCL

The rheological properties of the neat PCL and TPS as a function of frequency are shown in Figure 4.1 It can be clearly seen that this TPS with high glycerol concentration exhibits the rheological behavior of a typical gel and is characterized by a storage modulus (G') which is larger than the loss modulus (G") over the entire frequency sweep (Fig. 4.1a). This behavior has been observed by other authors and is generally explained by the presence of an elastic network embedded in a softer matrix, i.e. the existence of a protein network; remaining crystalline structure in the samples [Rodriguez et al. 2004; Della et al. 1998]; or strong hydrogen bonding [Wilhelm et al. 2005; Smits et al. 2003; Veenstra et al. 1999]. In the present case, no crystalline structure in this highly plasticized TPS was found as determined by X-ray diffraction (not shown here) and very little protein exists in the starch as well. The gel-like behavior is most likely the result of hydrogen bonding between the starch and plasticizer and could also be due to high levels of entanglement of starch molecules in the melt state creating a type of pseudo-crosslinking effect. Note that the elasticity is significantly higher than the complex viscosity over a wide range of shear rates. Also, the TPS is significantly more elastic than PCL. The G' for TPS at 300 rad/s from Figure 4.1a is about 3×10^5 while the G' for PCL1 and PCL2 is about 8×10^3 and 4×10^4 respectively (Fig. 4.1e). The gel-like properties of TPS and its elastic nature will tend to make it more difficult to deform/disintegrate as a dispersed phase in a polymer blend.

The complex viscosity (η^*) of TPS follows a power-law behavior and there is no Newtonian plateau for the viscosity curve within the measured region of frequency range (Fig.4.1b and 4.4.1.1c), another characteristic of gel-like behavior. Thus, the zero shear viscosity of TPS cannot be obtained. The extreme shear thinning behaviors have been associated with a melt yield stress [Veenstra et al. 1999]. The complex viscosities of both TPS36 and TPS40 decrease when the temperature increases from 110 to 130 ^oC as expected. Comparing Fig 4.1b and 1c clearly shows that η^* dramatically decreases with increasing glycerol concentration in TPS. It has been reported that the Cox-Merz rule used to predict the steady shear properties of a material from the dynamic rheological properties is not applicable to the TPS system due to the existence of strength gels [Tischer et al. 2006; Sopade et al. 2004; Dongryel and Byoungseung 2005]. The complex viscosity of TPS is greater than the apparent viscosity. However, the dynamic viscosity provides reasonable estimates of the apparent viscosity.

The complex viscosities of PCL1 and PCL2 were measured at temperatures of 110 and 130 ^{o}C, respectively. PCL1 and PCL2 demonstrate shear thinning behavior in the high frequency range from 0.5 to 500 rad/s (Figure 4.1d), and a Newtonian plateau with a zero-shear viscosity of 1450 and 7700 Pa.s were obtained, respectively.

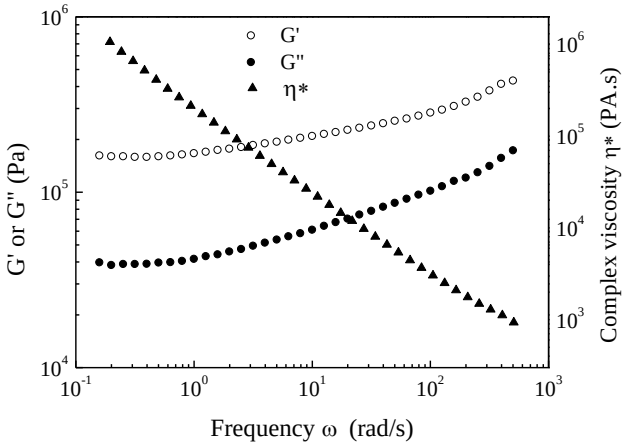

(a)

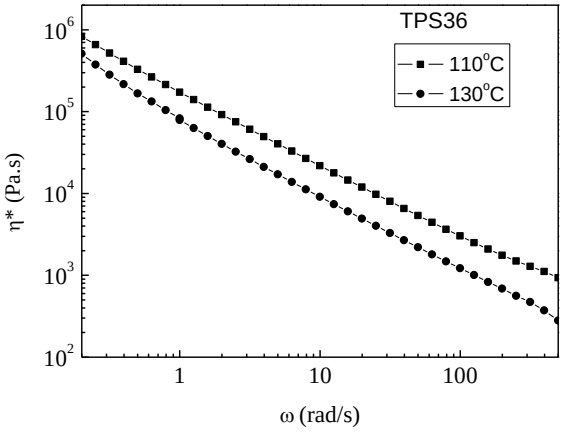

(b)

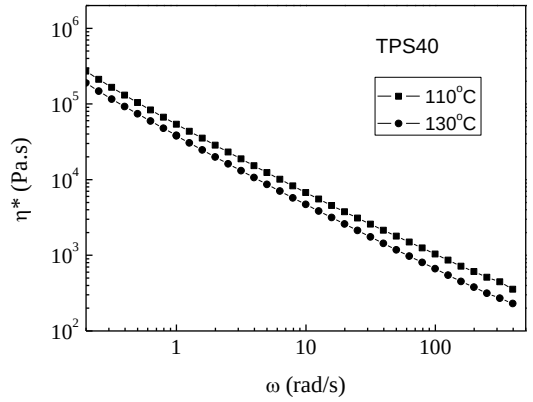

(c)

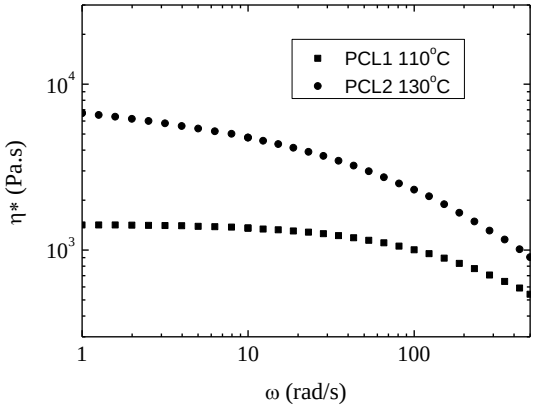

(d)

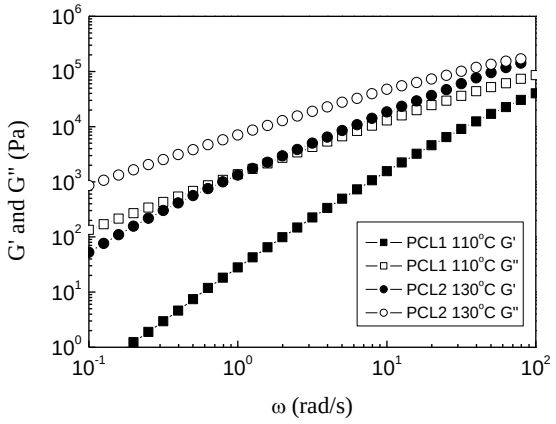

(e)

Figure 4.1 Rheological properties of a) TPS36 at 110°C; and complex viscosity at 110°C and 130 °C for b) TPS36, c) TPS40 and d), e) PCL.

4.4.2 Effect of viscosity ratio on TPS morphology

In the present work, two kinds of PCL with different molecular weights and two kinds of TPS with various glycerol concentrations were chosen to study the influence of viscosity ratio on the blend morphology of strands after twin-screw extrusion. Figure 4.1 shows that the viscosity of TPS is higher than that of PCL in the low frequency region. At high frequency and especially in the region of frequency corresponding to the estimated shear rate during extrusion, the viscosity of TPS is lower than that of PCL except for the case of 110 ^{o}C where the viscosity of TPS36 is higher than that of PCL1.

Figure 4.2 demonstrates the SEM image of PCL/TPS (70/30 weight %) blends at various viscosity ratios. Viscosity ratios of dispersed phase (TPS) to matrix (PCL) at different frequencies were calculated according to rheological results and the image analysis results are summarized in Table 4.3. The results show that the viscosity ratio, in the range studied, has virtually no influence on dispersed phase diameter. Although previous studies have clearly shown that the viscosity ratio has an important influence on phase size for immiscible blends [Favis and Chalfoux 1987], compatibilized blends often show significantly less dependence on viscosity ratio [Favis and Willis 1990]. Another potential explanation for the low dependence on viscosity ratio could be related to the presence of strong elongational flow fields present during twin-screw extrusion [Favis and Therrien 1991]. It is well known that elongation flow is much more effective in droplet breakup than shear flow [Taylor 1934].

Table 4.3 Viscosity ratio and dispersed phase diameters.

Samples	Frequency (rad/s)				d_n μm	d_v μm
	10	100	200	350		
TPS36/PCL1	16.09	3.01	2.21	1.85	1.4	1.8
TPS40/PCL1	4.97	1.04	0.76	0.69	2.0	2.6
TPS36/PCL2	1.90	0.55	0.45	0.41	1.6	2.2
TPS40/PCL2	0.96	0.29	0.25	0.22	1.3	1.8

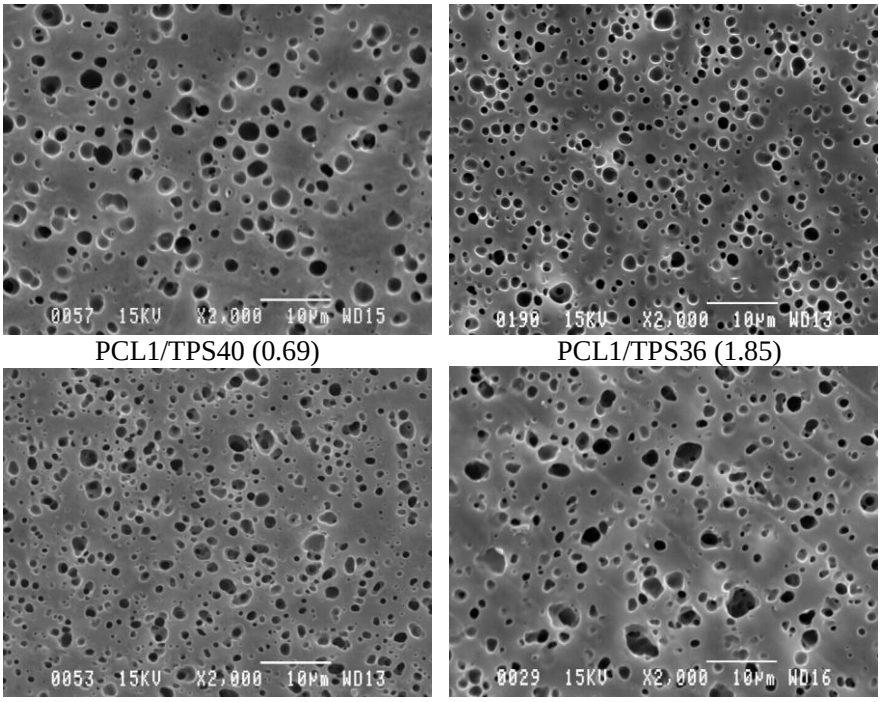

PCL1/TPS40 (0.69) PCL1/TPS36 (1.85)

PCL2/TPS40 (0.22) PCL2/TPS36 (0.41)

Figure 4.2 Effect of viscosity ratio on the morphology of PCL/TPS36 blends (70/30 weight %). The number in brackets indicates the viscosity ratio of dispersed phase to matrix.

4.4.3 Morphology/composition dependence

Figure 4.3 illustrates the SEM images of PCL1/TSP36 blends as a function of the weight fraction concentration of TPS. For the purpose of contrast enhancement, both phases were extracted by a selective solvent. It can be seen that TPS exists as dispersed droplets in a PCL matrix up to a TPS concentration of 30 wt% (Fig.4.3). Image analysis of these droplets indicate that the *dn* and *dv* are around 1.4 and 1.8 microns, respectively (Fig. 4.4). Figures 4.3 and 4.4 demonstrate that, upon further increasing the TPS concentration to 40 wt%, the co-existance of elongated structures (fiber-like) and droplets of TPS with a similar diameter are observed. The aspect ratio of fibrillar TPS is about 8. Finally, when the TPS content increases up to 50 wt%, a solely fibrillar TPS is attained and the aspect ratio increases to about 25 (Fig. 4.3). It is of particular interest in Figure 4.4 to note that the diameter of TPS droplets and fibers are independent of composition right up to 45 vol% TPS. Further increasing the TPS36 concentration above 54 vol%, results in dramatically increased TPS fiber diameters (Figure 4.4). The region of dual-phase continuity appears to exist in the concentration range of 54 to 65 vol% TPS. TPS appears to resist deformation/disintegration, but once deformed forms stable fibers. Note that the

concentrations shown in Figure 4.6 are given in vol% so that they can be more readily compared to the % continuity data which will be shown later in this paper.

Veenstra et al. investigated the morphology of blends of polystyrene and poly(ether-ester) thermoplastic elastomer [Veenstra et al. 1999]. When the processing temperature was chosen below the block copolymer order to disorder transition, the flow curves of poly(ether ester) did not show a Newtonian plateau in viscosity. Shear thinning behaviour over the entire range of measured shear rate was found. In that case, physical crosslinks of crystalline structures are present in the melt state and a melt yield stress was estimated in the range between 500 and 3800 Pa. These structures were found to limit and even stop the breakup and retraction behaviour of poly(ether ester) threads and formed stable elongated structures.

In the present work, the rheology of TPS demonstrates a gel behaviour and no Newtonian plateau in viscosity was obtained during melting processing (Fig. 4.1). It indicates the existence of strong interactions within the TPS that can be attributed to hydrogen bonding [Wilhelm et al. 2005; Smits et al. 2003]. The presence of physical crosslinks in the melt state leads to highly elastic properties and a melt yield stress, which also have a stabilizing effect on elongated structure. Thus, this highly elastic state in the TPS typically resists deformation, but once deformed forms stable fibers. It is possible that the elongated structure can also be attributed to twin-screw extrusion processing which provides a significant elongational flow component. It is well known that the deformation of a droplet to produce a fibril is more easily obtained by subjecting the fluid to an extensional flow [Taylor 1934]. Similar elongated phase structures were also observed in blends of LDPE/TPS and PHEE/TPS [Rodriguez et al. 2003; Ma et al.2002].

As a comparison, PCL2/TPS36 blends were prepared and the morphologies are presented in Figure 4.5. As observed for the PCL1/TPS36 blends, the dispersed TPS droplet/fiber diameters are independent of concentration.

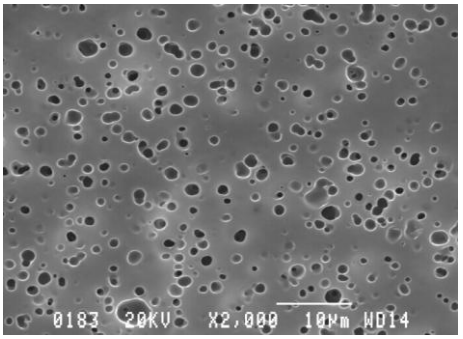

80PCL/20TPS

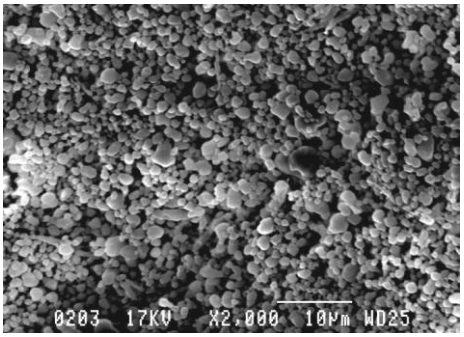

80PCL/20TPS

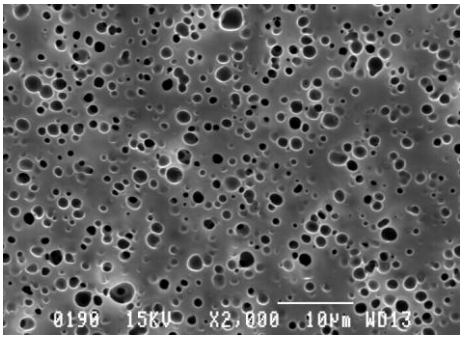

70PCL/30TPS

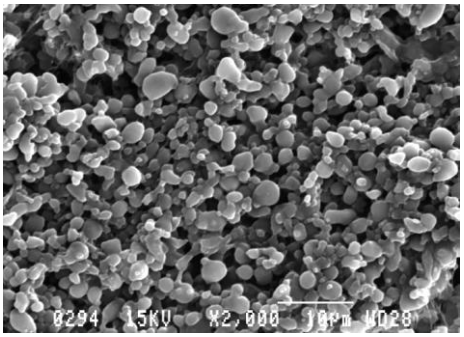

70PCL/30TPS

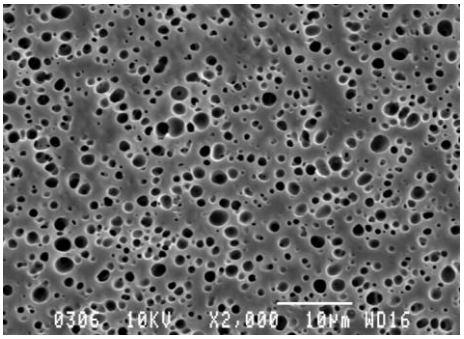

60PCL/40TPS

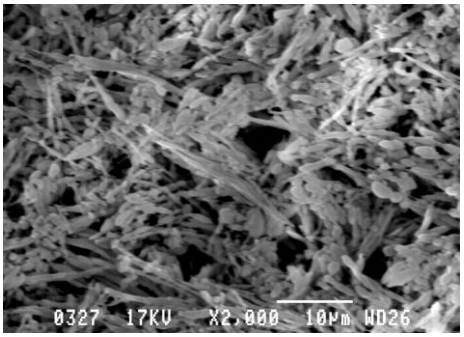

60PCL/40TPS

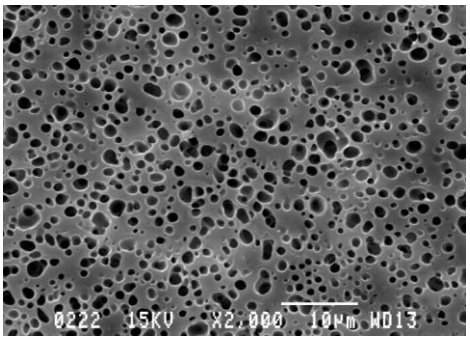

50PCL/50TPS

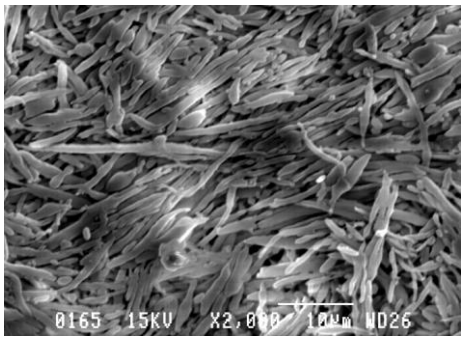

50PCL/50TPS

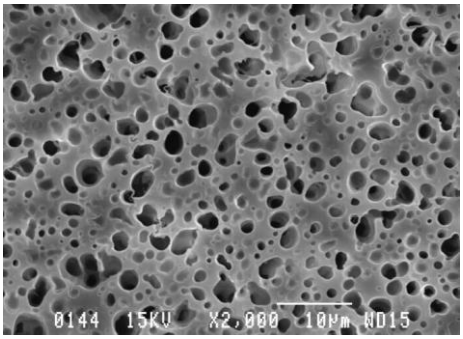

40PCL/60TPS

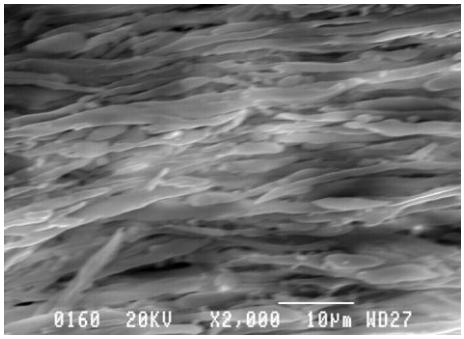

40PCL/60TPS

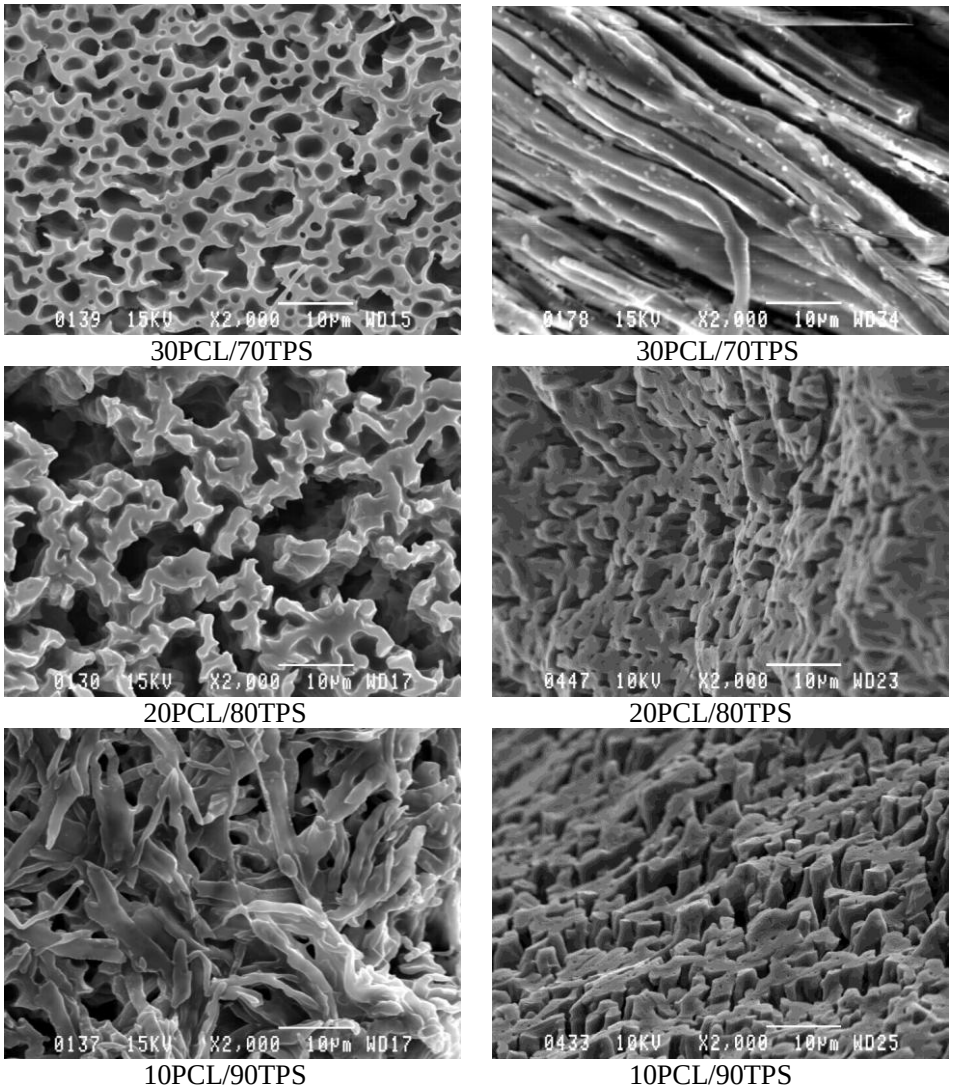

Figure 4.3 The effect of TPS36 concentration on the morphology of extruded strands of PCL1/TPS36 blends. On the left side TPS is extracted with HCl. On the right side PCL is extracted with THF. Concentrations shown are weight %.

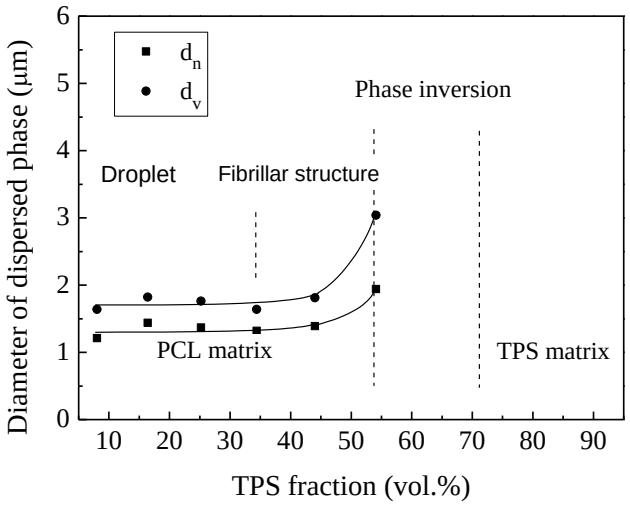

Figure 4.4 Diameter of phases as a function of TPS concentration obtained from the image analysis of PCL1/TPS36 extruded strands.

Figure 4.6 presents the results of percent continuity versus TPS36 concentration via gravimetric solvent extraction. The TPS phase continuity increases dramatically in PCL1/TPS36 blends when the TPS36 volume fraction increases from 25 to 43 vol%. This correlates well with the morphology/composition study in Fig. 4.4 where the onset of TPS fiber formation is observed in the same range. The preferential encapsulation of PCL about TPS is especially evident in the continuity development region at high TPS concentration where 13 vol % of PCL1 (the lower viscosity PCL) displays 40% continuity and 25 vol % PCL1 displays 80% continuity, a remarkable result. These latter data also correspond very well with the morphology study. The region of TPS/PCL co-continuity is from 55 to 67 vol%, which is in agreement with the morphology observation. This is an asymmetric phase inversion region and these results indicate a strong tendency of the polycaprolactone to preferentially encapsulate the thermoplastic starch.

The continuity of TPS/PCL2 via gravimetric solvent extraction is also shown in Figure 4.6 in order to examine the influence of a more viscous PCL on continuity development. In that case it can be seen that the percolation thresholds of both dispersed PCL2 and dispersed TPS36 are shifted to higher concentration. This is an unexpected shift since in typical thermoplastic blends, a lower viscosity ratio blend typically results in a more readily deformed dispersed phase and thus typically displays a lower percolation threshold. The opposite is observed here. This result is

likely a reflection of the fact that both the elastic nature and internal hydrogen bonding in TPS give it the character of a pseudo-partially-crosslinked material. In this case the dispersed TPS is quite difficult to breakup, but once deformed forms stable fibers with less of a tendancy to breakup than typical thermoplastics. Crosslinked materials classically demonstrate asymmetric continuity diagrams [Ma et al. 2002]. In the case of TPS 36/PCL2, since the more viscous PCL2 has virtually no additional effect on the deformation of dispersed TPS, the only effect is that the more viscous PCL2 actually

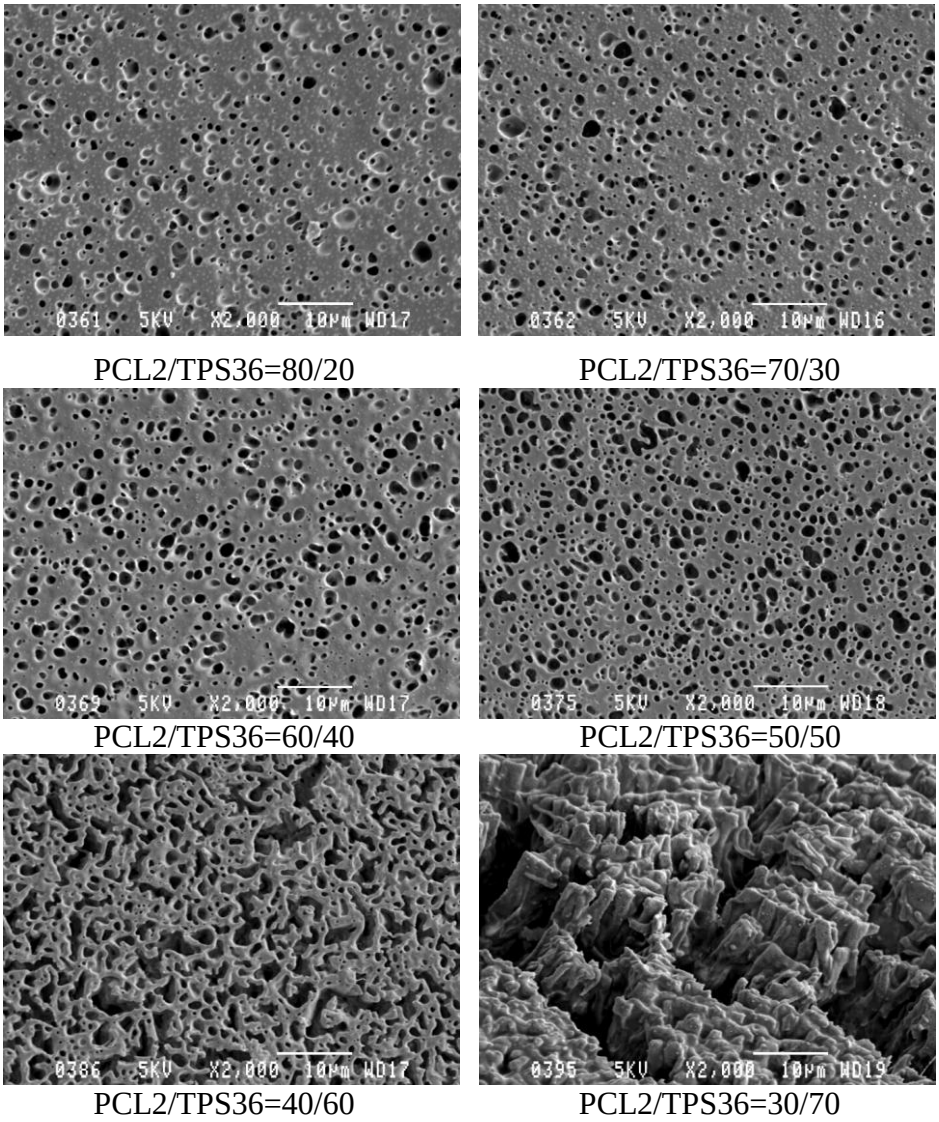

Figure 4.5 Morphology of extruded strands of PCL2/TPS36 as a function of TPS36 concentration. Extraction of TPS36 with HCl. Concentrations shown are weight %.

retards the coalescence required for TPS droplets to transit to stable TPS fibers. Previous work has shown that the breakup of these fibers can occur with dramatic changes in the flow field [Favis et al.2006]. Despite the differences in continuity development observed with PCL1/TPS and PCL2/TPS, Figure 4.6 shows that the region of co-continuity is virtually identical for both blend systems. Clearly these TPS/PCL blends do not respect the classical empirical description of the relationship of viscosity ratio and co-continuity composition [Jordhamo et al. 1986].

The results above were all obtained on extruded strands after twin-screw compounding. In order to examine the influence of processing technique, the morphologies of injection moulded samples were obtained and the results are presented in Figures 4.7 and 4.8. It can be seen that the TPS particle size is quite constant with composition in the composition range of 0-40 wt% TPS and confirms the small effect of concentration based coalescence. Note however in comparing these data to those in Figure 4.4 for the extruded strands, that the change in processing condition did lead to significantly different particle sizes. This indicates that changes in processing techniques, with their different balances of shear and elongation flow fields, can have an effect on TPS coalescence.

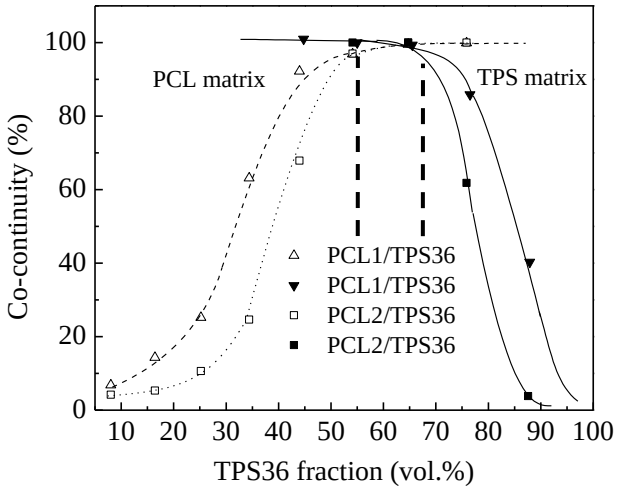

Figure 4.6 Phase continuity development of PCL/TPS36 blends using the gravimetric solvent extraction technique.

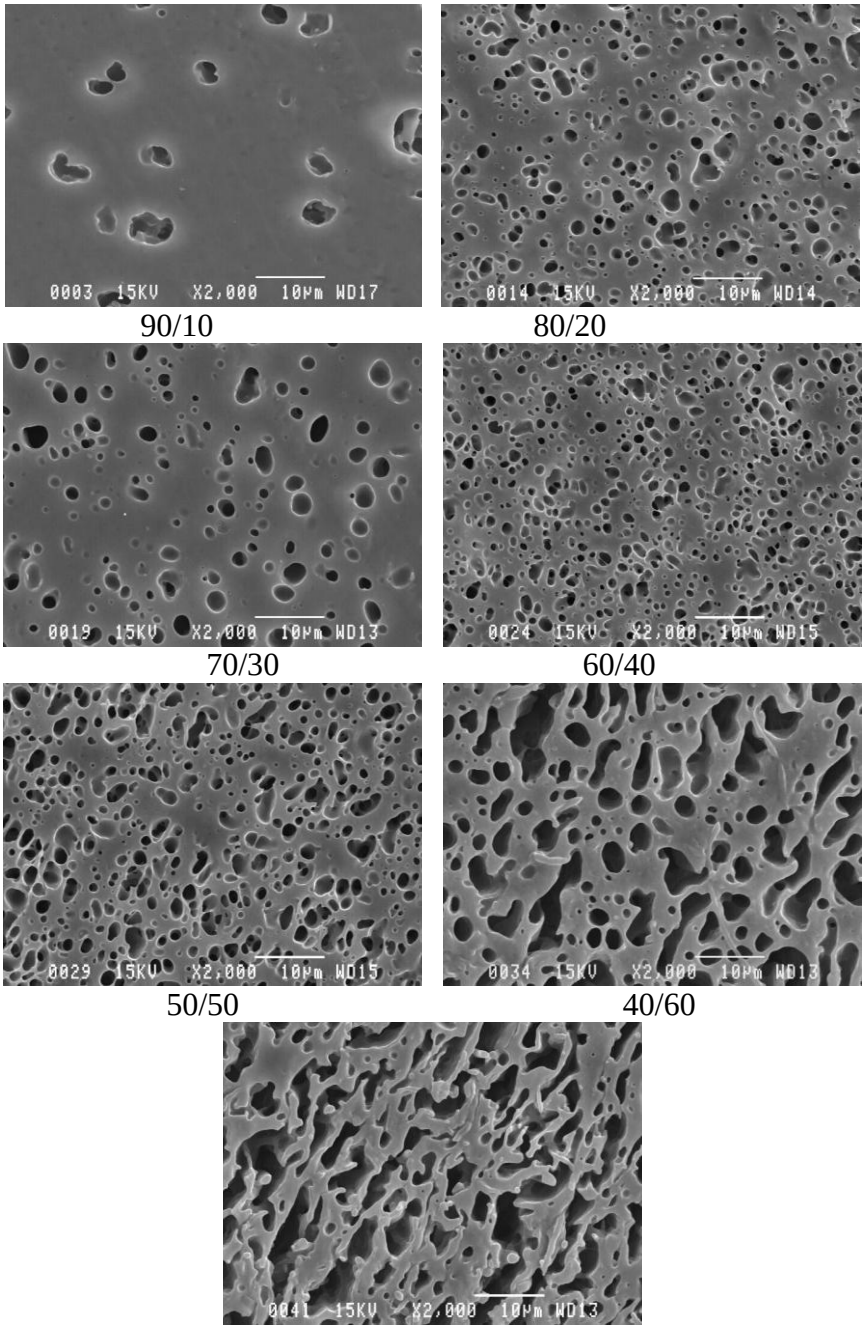

Figure 4.7 Morphology of PCL1/TPS36 blends (TPS36 extracted) after injection molding. Concentrations shown are weight %.

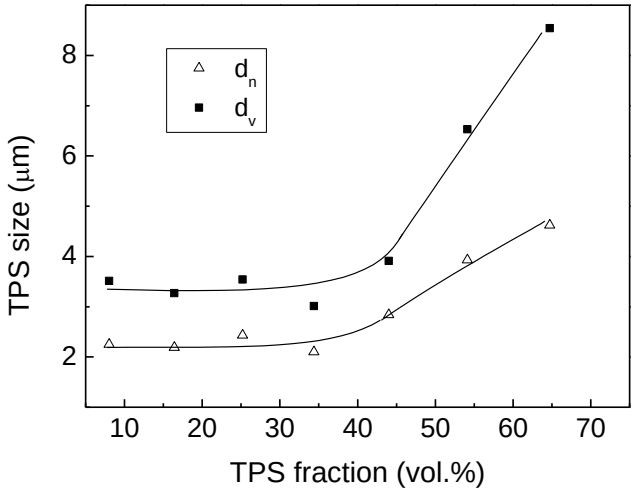

Figure 4.8 Diameter of phases as a function of TPS concentration obtained from the image analysis of PCL1/TPS36 blends after injection molding.

4.4.4 Quiescent annealing

As an immiscible blend is annealed in the melt state, the phase size grows as a function of annealing time and temperature indicating that significant coarsening effects are taking place. This coarsening is strongly affected by the state of the interface with compatibilized blends showing significantly less coalescence and more stable morphologies [Pyun et al. 2007; Yuan et al.2006]. A 25 vol% TPS36 in PCL1 blend with droplet/matrix morphology was used to study the TPS coalescence at annealing temperatures of 110 and 150 ^{o}C. The corresponding images and image analysis are shown in Figure 4.9and Table 4.4. The results clearly show that the TPS particle size in the blend does not change with annealing time and temperature indicating no coalescence whatsoever. In a second quiescent annealing experiment, a 43 vol% TPS in PCL1 blend (50/50 by weight), was also studied. Typically, highly continuous immiscible polymer blends demonstrate much more coalescence during quiescent annealing. However even at this concentration no further coarsening was observed even after long times of annealing. The morphologies after annealing are demonstrated in Figure 4.10 and it is evident that there is virtually no change in TPS phase size with annealing time for PCL1/TPS36 blends even at this high concentration of TPS. As a comparison, a completely immiscible HDPE/TPS36 blend (50/50 by weight) was also subjected to quiescent annealing to study the coarsening of TPS. The results are shown in Figure 4.11 In this case strong coalescence effects are observed for the TPS

phase with the average TPS36 phase diameter increasing from 6.0 to 14.9 μm when annealing time was increased from 0 min to 60 min. These results strongly suggest the presence of compatibilization effects between TPS and PCL.

Table 4.4 TPS particle size after annealing at different times and temperatures*

TIME (MIN)	110 °C		150 °C	
	D_N μM	D_V μM	D_N μM	D_V μM
10	2.2	2.9	2.5	3.2
30	2.0	2.7	2.4	3.1
60	2.1	2.8	2.5	3.2

*Injection molded sample of PCL1/TPS36 (70/30)

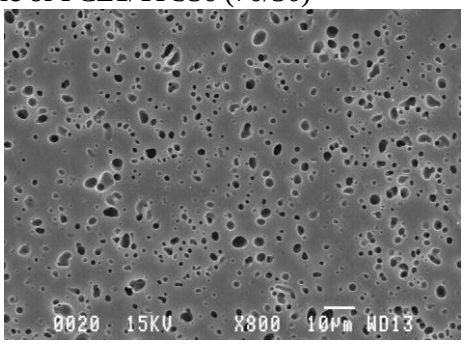

0 min

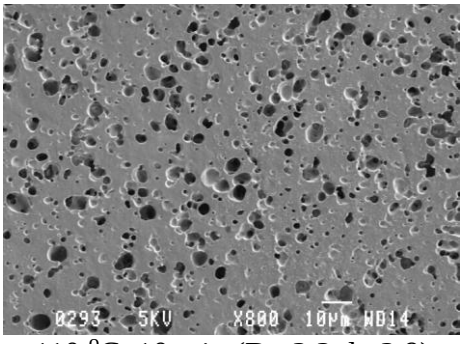

110 °C, 10 min (Dn 2.2 dv 2.9)

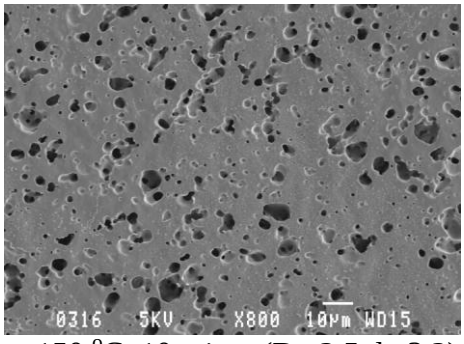

150 °C, 10 min (Dn 2.5 dv 3.2)

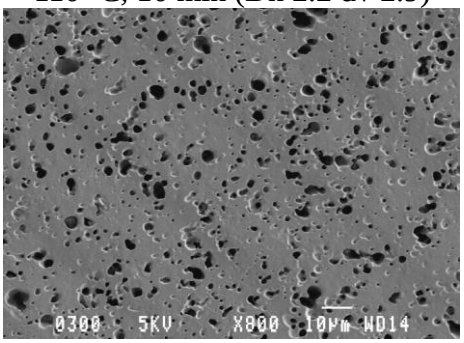

110 °C, 30 min (Dn 2.0 dv 2.7)

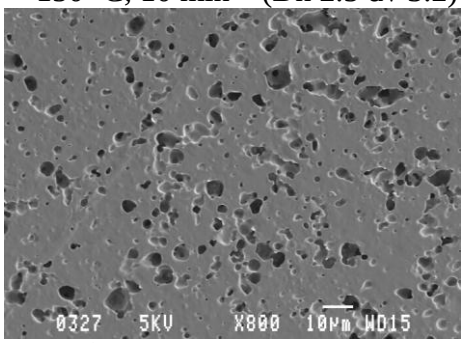

150 °C, 30 min (Dn 2.4 dv 3.1)

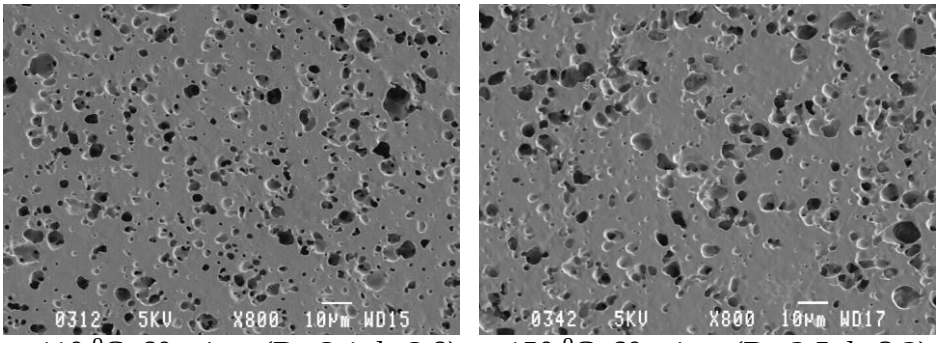

110 °C, 60 min (Dn 2.1 dv 2.8) 150 °C, 60 min (Dn 2.5 dv 3.2)

Figure 4.9 Morphology of annealed samples of PCL1/TPS36 (70/30 weight %) as a function of time of annealing at 110 and 150 °C, Samples prepared by injection molding.

4.4.5 Thermal properties of blends

DMTA results for TPS, PCL and their blends are presented in Figure 4.12. For 100% TPS, the storage modulus falls in two steps, the first between -60 and -20 °C, and the second between -10 and 45 °C. This corresponds to the tan δ peaks for 100% TPS at -38.3 and 28.0 °C, respectively. The high temperature relaxation (T_α) is attributed to the glass transition of the starch-rich phase, whereas the low temperature (T_β) arises from the glycerol-rich phase owing to the phase separation of starch and glycerol at high glycerol concentration as reported previously [Averous et al. 2000; Taguet et al. in press]. The T_g of PCL from the tan δ peak is -38.5 °C which overlaps with the T_β of TPS.

The storage moduli of PCL/TPS blends demonstrate two main tendancies which can also be used to determine the boundary of the co-continuity interval [Tischer et al. 2006]. At TPS concentrations less than and equal to 50 wt%, the moduli drop down at the melting point of PCL (not shown here) indicating PCL is the continuous phase. On the other hand, the 80 and 90 wt% TPS blends with PCL demonstrate a moduli which decreases dramatically following the starch-rich phase transition at 0 °C indicating TPS is the continuous phase. This effectively corresponds to the boundaries of phase inversion as determined by solvent gravimetry in the previous section.

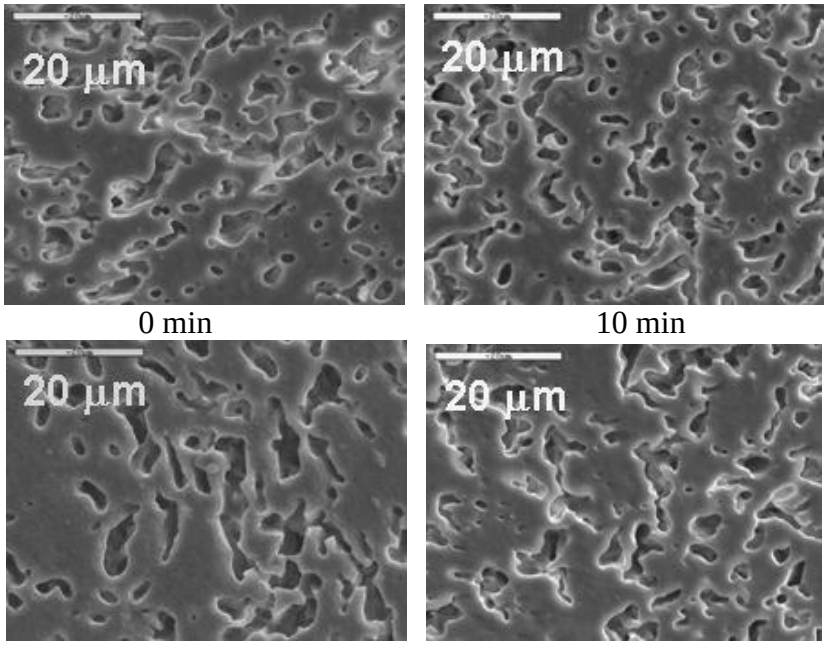

0 min 10 min

30 min 60 min

Figure 4.10 Morphology of annealed samples of PCL1/TPS36 (50/50 weight %) as a function of time of annealing at 150 ^{o}C, Samples prepared by injection molding.

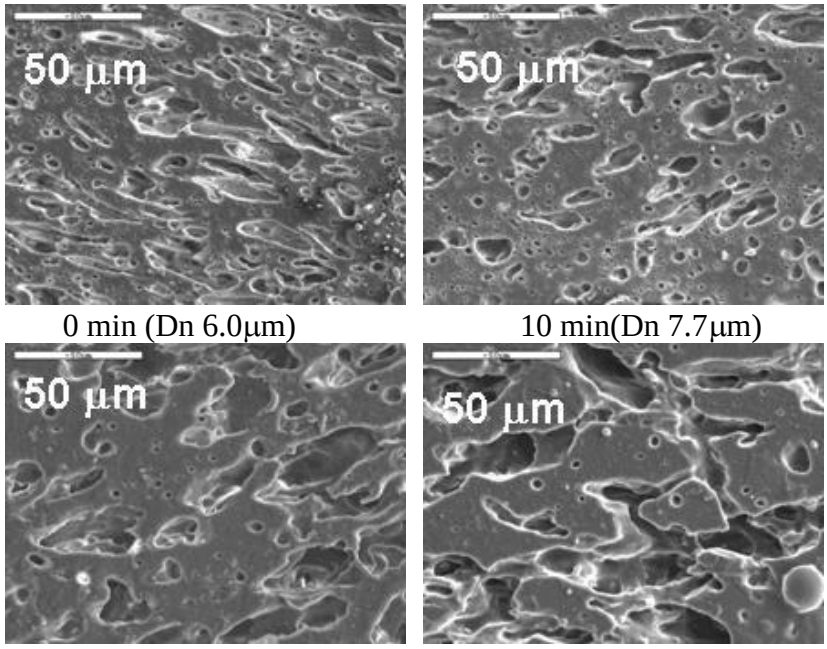

0 min (Dn 6.0μm) 10 min(Dn 7.7μm)

30 min (Dn 13.0μm) 60 min(Dn 14.9μm)

Figure 4.11 Morphology of annealed samples of 50HDPE/50TPS36 (weight %) as a function of time of annealing at 150 ^{o}C, Samples prepared by injection molding. The number in brackets indicates the average diameter of TPS.

It can be seen from Figure 4.12 that the T_β of PCL1/TPS36 blends decreases with increasing TPS36 concentration. This effect can be attributed to the further phase separation between starch and glycerol upon blending with PCL. Recent work from this laboratory, in fact, has shown that a thin glycerol-rich layer forms at the interface between TPS and polymer in TPS/polymer blends [Taguet et al. in press]. It is also interesting to note that there is a significant shift in the T_β peak to higher temperatures when the concentration is increased from 70-80 wt% TPS. This corresponds to the phase inversion of PCL and TPS as reported earlier in the paper and is related to the onset of formation of a TPS matrix phase and PCL dispersed phase.

The T_α peak for 100% TPS36 is 28.0 ^oC. However, PCL/TPS blends with 50 and 70 wt% TPS have a TPS T_α peak which only appears as a diffuse shoulder at -10 and -8 ^oC. This is a peak shift in excess of 30 C^o. At TPS contents of 30 wt% and below, the TPS T_α peak disappears entirely. These results strongly imply interactions between PCL and the starch-rich phase of TPS. The origin of this interaction will be examined in more detail below. The interaction is likely to be cause by the hydrogen bonding interactions between the carbonyl groups of PCL and hydroxyl groups on starch [Matzinos et al. 2002; Rodriguez et al. 2004].

4.4.6 FTIR

Figure 4.13 shows the FTIR spectra of PCL1, TPS36 and their blend at 50/50 wt%. PCL1 had a strong carbonyl stretching absorption at a wave number of 1720 cm^{-1}, which shifts to 1724 cm^{-1} after blending with TPS36. This shift in the stretching vibration frequency of carbonyl groups suggests a hydrogen bonding interaction between the carbonyl groups of PCL and the hydroxyl groups of TPS. Similar results have been obtained with poly(propylene carbonate)/thermoplastic starch [Ma et al. 2008] and poly(hydroxyl ether of bisphenol A)/polycaprolcatone [Coleman and Moskala 1983] blends.

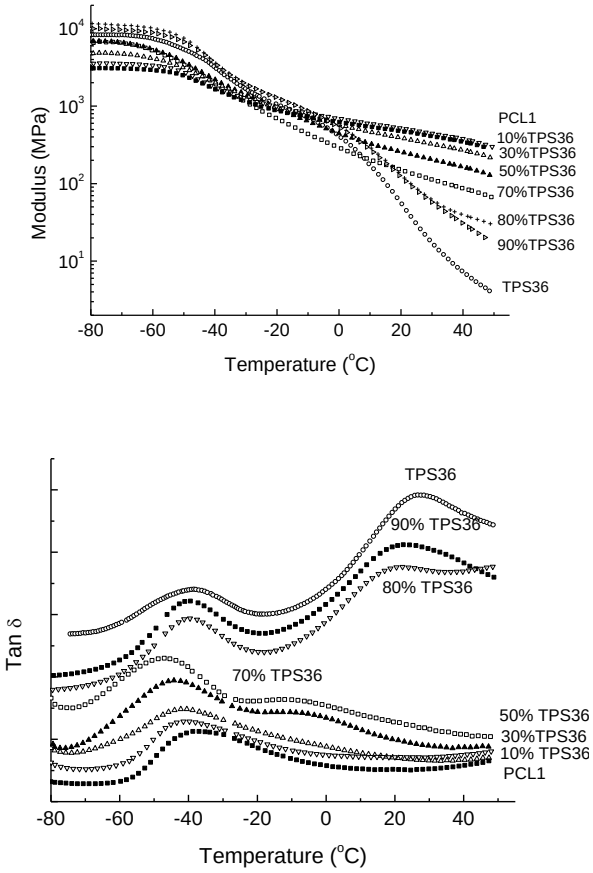

Figure 4.12 DMTA results for PCL, TPS and their blends. Concentrations are in weight %.

Figure 4.13 shows the FTIR spectra of PCL1, TPS36 and their blend at 50/50 wt%. PCL1 had a strong carbonyl stretching absorption at a wave number of 1720 cm^{-1}, which shifts to 1724 cm^{-1} after blending with TPS36. This shift in the stretching vibration frequency of carbonyl groups suggests a hydrogen bonding interaction between the carbonyl groups of PCL and the hydroxyl groups of TPS. Similar results have been obtained with poly(propylene carbonate)/thermoplastic starch [Ma et al. 2008] and poly(hydroxyl ether of bisphenol A)/polycaprolcatone [Coleman and Moskala 1983] blends.

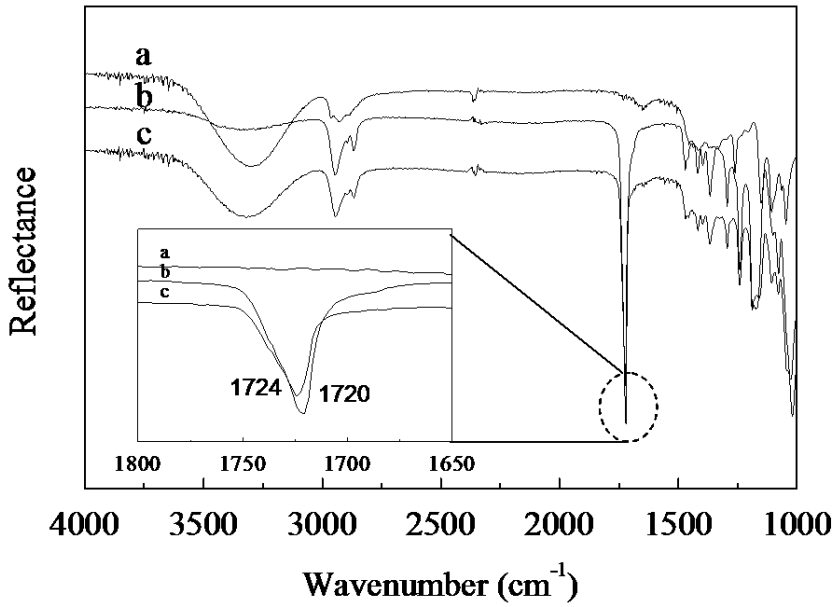

Figure 4.13 The FTIR spectra of PCL1, TPS36 and their 50/50 blend (weight %). (a)TPS36; (b)PCL1; (c) PCL1/TPS36 (50/50).

4.4.7 Mechanical properties of blends

Table 4.5 summarizes the tensile properties of PCL1, TPS36 and their blends. The stress at yield and modulus decrease continuously with increasing TPS concentrations. This behaviour is expected and follows a close to linear decrease based on the corresponding values for 100% TPS. The remarkable aspect of the results in this mechanical property data set are the elongation at break values. It is known that the elongation at break is a strong reflection of the state of the interface [Huneault and li 2007]. Low interfacial interactions between two blended ductile polymers produces a highly fragile material. However, the elongation at break of PCL/TPS36 blends over a very wide concentration range exhibit outstanding ductility. Samples with a TPS36 content of 50 wt% and less did not even break during the tensile test (max value set at 1000%). Even PCL/TPS blends with 80 and 90 wt% of TPS36 showed elongations at break of 450 and 550%, respectively. These exceptional elongational properties at high TPS concentrations are the highest ever reported in the literature to date for PCL/TPS blends. The key to these properties appears to be the high level of plasticization of the starch. It is likely that the high plasticizer

concentrations used here increase the mobility of the starch chains and thus promote a high level of specific interactions between the PCL and starch. This excellent interfacial interactions result in the exceptional ductilities observed above.

The importance of chain mobility on interfacial reactions in polymer blends through the addition of plasticizers has been shown in previous work [Bhadane et al. in press]. In that work, the addition of 5-10% plasticizer to the polyamide phase in a polyamide/brominated poly(isobutylene-*co*-*p*-methylstyrene) blend resulted in substantially finer dispersed phase morphologies, an effect that actually opposed viscosity ratio/morphology predictions. It was shown that the interfacial reaction between polyamide and brominated poly(isobutylene-*co*-*p*-methylstyrene) was substantially improved upon addition of the plasticizer due to improved polyamide chain mobility.

Virtually all the results presented in this study can be explained by a combination of two phenomena: a high elasticity of the thermoplastic starch phase and a strong compatability between TPS and PCL. The high level of compatibility in this PCL/TPS system likely results from the high mobility of the TPS chains due to the high plasticizer content and a highly effective TPS plasticization protocol. This high chain mobility facilitates hydrogen bonding interactions between TPS and PCL. In Figure 4.14 the cryogenic surface of a 40/60 PCL1/TPS 36 blend shows the characteristics of a system experiencing good adhesion with very little microvoiding or ejected particles evident. In previous work [Li et al. 2002] it has been shown that the dispersed phase in highly interacting binary blends of low interfacial tension tend to form stable fibers at very low concentrations. In such a case, termed Type I behaviour, the thread lifetime is longer than the droplet lifetime during melt mixing and the continuity development and microstructural features of the dispersed phase are dominated by thread-thread coalescence. Clearly the PCL/TPS system studied here is such a highly interacting, Type I system. However, if this were the only factor in play, Figures 4.4, 4.5 and 4.6 should show strong fiber formation and high continuity effects at low TPS concentration, which is clearly not the case. The combination of the roles of high elasticity of the TPS and a strong interaction between TPS and PCL can effectively explain this behaviour. At lower TPS volume fraction the highly elastic, gel-like TPS resists deformation, despite the strong interfacial interactions present between TPS and PCL. This leads to a droplet-like behaviour dominating the morphology of the dispersed phase at low TPS volume fraction. However, at the other end of the composition range where PCL is dispersed in TPS, the

dispersed phase is now of significantly less elasticity and the PCL transforms to fibers at very low concentrations due to the high specific interactions with TPS as expected for Type I behaviour.

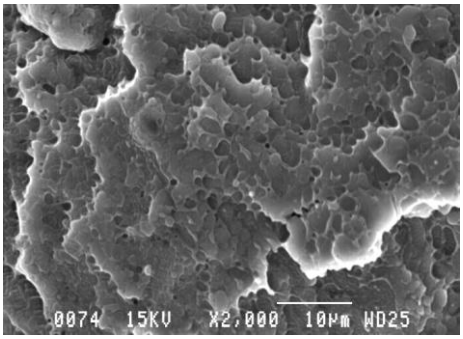

Figure 4.14 Cryogenic fracture surface of 40PCL1/60TPS36 blend (weight %).

Table 4.5 Tensile properties of PCL1/TPS36 blends

TPS36 content (wt.%)	Stress at yield (MPa)	Modulus (MPa)	Elongation at break (%)
0	19.1 ±0.30	190.4 ±0.7	>1000
10	16.7 ±0.60	162.1 ±6.4	>1000
20	14.4 ±0.61	134.0 ±5.5	>1000
30	13.1 ±0.51	118.0 ±5.1	>1000
40	11.2 ±0.30	93.5 ±2.0	>1000
50	7.0 ±0.45	73.1 ±1.0	>1000
60	5.0 ±0.30	42.5 ±1.2	836 ±27
70	3.7 ±0.40	31.7 ±4.5	790 ±47
80	2.2 ±0.69	15.1 ±2.0	455 ±100
90	2.7 ±0.30	21.0 ±1.2	558 ±130
100	0.5 ±0.40	2.1 ±1.0	181 ±20

4.5 Conclusions

In this work a detailed study of the morphology development in thermoplastic starch/polycaprolactone blends, prepared using a one-step extrusion process has been undertaken. These highly plasticized blends, without any added interfacial modifier, display remarkably low levels of coalescence and exceptional mechanical properties. The phase size of the dispersed thermoplastic starch, after twin-screw extrusion, is virtually independent of TPS composition and TPS droplets transit to stable fiber-like phases of identical phase size above 30% TPS. Although the TPS is quite insensitive to concentration-based coalescence, it displays some coalescence sensitivity to changes in processing technique (compounding vs. injection). A study of percent continuity vs TPS concentration, as determined by solvent gravimetry, indicate the region of co-continuity to be 55-65 vol% TPS. This is an asymmetric phase inversion region and indicates a strong tendency of polycaprolactone to encapsulate the thermoplastic starch, a behaviour similar to polymer blends containing partially crosslinked rubbers. The preferential encapsulation of PCL about TPS is especially evident in the continuity development region at high TPS concentration where 10 wt% of PCL1 (the lower viscosity PCL) displays 40% continuity and 20 wt% PCL1 displays 80% continuity, a remarkable result. It is interesting to note that the midpoint value of phase inversion is identical irrespective of the viscosity of PCL used. The coalescence, as observed by static annealing experiments; show that the TPS phase at both 30 and 50 wt% TPS in PCL displays no coalescence after 60 minutes of annealing. A comparative study of static annealing of TPS/polyethylene on the other hand shows significant coalescence. These results strongly point to the likely presence of specific interactions between the TPS and the PCL. Dynamic mechanical analysis confirms the region of dual-phase continuity and also strongly indicates a specific interaction between PCL and TPS. FTIR results show the presence of a hydrogen bonding interaction between the carbonyl groups of PCL and the hydroxyl groups on starch. It is likely that the high plasticizer concentrations used here increase the mobility of the starch chains and thus promote a high level of specific interactions between the PCL and starch. Mechanical properties display extremely high elongations at break, even at high TPS concentrations, typical of those observed for highly compatibilized immiscible polymer blends.

4.6 Acknowledgements

The authors would like to express their appreciation to Dr. Pierre Sarazin of Cerestech Inc. for helpful discussions and to Mr. Jacques Beausoleil for technical support.

4.7 References

F. H. Otey, R. P. Westhoff, W. M. Doane, *Ind. Eng. Chem. Prod. Res. Dev.*, **1980,** 19, 592.

L. Averous, N. Fauconnier, L. Moro, C. Fringant, *J. Appl. Polym. Sci.*, **2000**, 76, 1117.

G. Li, P. Sarazin, B. D. Favis, *Macro. Chem. Phys.* **2008**, 209, 991.

B. D. Favis.. (**2000**), Factors Influensing the Morphology of Immiscible Polymer Blends in Melt Processing. In D. R. Paul & C. B. Bucknall (Eds.), Polymer Blends Volume 1. Formulation (Vol. 1, pp. 501-538). New York: John Wiley & Sons.

J. Reignier, B. D. Favis, *Macromolecules,* **2000**, 33, 6998.

J. L.Willett, *J. Appl. Polym. Sci.* **1994,** 54, 1685.

R. L. Evangelista, W. Sung, J. L. Jane, R. L. Gelina, Z. L. Nikolov, I*nd. Eng. Chem. Res.*, **1991**, 30, 1841.

R. R. N. Sailaja, M. Chanda, *J. Appl. Polym. Sci.*, **2001**, 80, 863.

N. St-Pierre, B. D. Favis, B. A. Ramsay, L. A. Ramsay, H. Verhoogt, *Polymer* **1997**, 38, 647.

B. D. Favis, F. Rodriguez, B. A. Ramsay, *US Patent*, 6,605,657, **2003**.

F. J. Rodriguez-Gonzalez, B. A. Ramsay, B. D. Favis, *Polymer*, **2003**, 44, 1517.

F. J. Rodriguez-Gonzalez, N. Virgilio, B. A. Ramsay, B. D. Favis, *Adv. Polym. Techn.* **2003**, 22, 297.

B. D. Favis, F. J. Rodriguez Gonzalez, B. A. Ramsay, *US Patent*, 6,844,380, 2005.

F. J. Rodriguez Gonzalez. PhD Thesis, **2002**, pp. 181.

B. D. Favis, Z. H. Yuan, D. Riscanu, PCT/CA2006/000695.

Z. H. Yuan, B. D. Favis, *AIChE J.*, **2005**, 51, 271.

R. C. Willemse, E. J. J. Ramaker, J. Van Dam, A. Posthuma de Boer, P*olym. Eng. Sci*. **1999,** 39, 1717.

H. Venstra, J. Van Dam, A. Posthuma de Boer, *Polymer*, **2000,** 41, 3037.

A. Pyun, J. R. Bell, K. H. Won, B. M. Weon, S. K. Seol, J. H. Je, *Macromolecules*, **2007**, 40, 2029.

C. G. Pitt, T. A. Maeks, A. Schindler, *In Controlled Release of Bioactive Materials*, ed, R. Baker. Academic Press, NY, **1980**, p9.

B. Y. Shin, S. Lee, Y. S. Shin, S. Balakrishnan, R. Narayan, *Polym. Eng. Sci*., **2004**, 44, 1429.

P. Matzinos, V. Tserki, A. Kontoyiannis, C. Pannayioyou, *Polym. Degrad. Stab.,* **200**2, 77, 17.

L. Averous, L. Moro, P. Dole, C. Fringant, *Polymer*, **200**0, 41, 4157.

P. Sarazin, G. Li, W. J. Orts, B. D. Favis, *Polymer*, **2008**, 49, 599.

B. Y. Shin, R. Narayan, S. I. Lee, T. J. Lee, *Polym. Eng. Sci.*, **200**8, 48, 2126.

S. A. Saltikov, Proceedings of the second international congress for stereology. Springer-Verlag,Berlin, 1967.

G. Della Valle, A. Buleon, P. J. Carreau, P. A. Lavoie, B. Vergnes, *J. Rheol.* **199**8, 42, 507.

F. J. Rodriguez-Gonzalez, B. A. Ramsay, B. D. Favis, *Carbohydrate Polymers*, **2004**, 58, 139.

H. M. Wilhelm, M. R. Sierakowski, F. Reicher, F. Wypych, G. Souza, *Polymer International,* **2005**, 54, 814.

A. L. M. Smits, P. H. Kruiskamp, J. J. G. van Soest, J. F. G. Vlieganthart, *Carbohydrate Polymers,* **2003**, 53, 409.

H. Veenstra, B. Van Lent, J. Van Dam, A. Posthuma de Boer, *Polymer,* **1999**, 40, 1119.

H. Veenstra, B. Norder, J. Van Dam, A. Posthuma de Boer, *Polymer*, **1999**, 40, 5223.

P. C. S. F. Tischer, M. D. Noseda, R. A. de Freitas, M. R. Soerakowski, M. E. R. Duarte, *Carbohydrate Polymers,* **2006,** 65, 49.

A. Sopade, P. J. Halley, L. L. Junming. *J. Food Eng.,* **2004,** 61, 439.

Y. Dongryel, Y. Byoungseung, *Starch/stärke*, **2005**, 57, 254.

B. D. Favis, J. P. Chalfoux, *Polym. Eng. Sci.,* **1987**, 27, 1591.

B. D. Favis, J. M. Willis, *J. of Polym. Sci. Part B: Polym. Phys.*, **1990**, 28, 2259.

B. D. Favis, D. Therrien, *Polymer,* **1991**, 32, 1474.

G. I. Taylor, *Proceedings of the Royal Society of London,* **1934**, 146(A), 501.

P. S. Walia, J. W. Lawton, R. L. Shogren, F. C. Felker, *Polymer*, **2000**, 41, 8083.

P. L. Ma, B. D. Favis, M. F. Champagne, M. A. Huneault, F. Tofan, *Polym. Eng. Sci*., **2002**, 42, 1976.

G. M. Jordhamo, J. A. Mason, L. H. Sperling, *Polym, Eng. Sci.,* **1986**, 26, 517.

Z. H. Yuan, B. D. Favis, J. *of Polym. Sci. Part B: Polym Phys,* **2006**, 44, 711.

A. Taguet, M. A. Huneault, B. D. Favis, *Polymer*, (in press).

X. Ma, P. Chang, J. Yu, N. Wang, *Carbohydrate Polymers,* **2008**, 71, 229.

M. M. Coleman, E. J. Moskala, *Polymer*, **1983**, 24, 663.

M. A. Huneault, H. B. Li, *Polymer,* **2007**, 48, 270.

P. A. Bhadane, A. H. Tsou, J. Cheng, B. D. Favis, *in preparation for Polymer.*

J. Li, P. L. Ma, B. D. Favis, *Macromolecules,* **20**02, 35, 2005.

CHAPTER 5

BIODEGRADATION OF THERMOPLASTIC STARCH AND ITS BLENDS WITH POLY(LACTIC ACID) AND POLYETHYLENE: INFLUENCE OF MORPHOLOGY

5.1 Presentation of the article of biodegradation of thermoplastic starch and its blends with poly(lactic acid) and polyethylene: influence of morphology

5.2 Abstract

The room temperature mineralization of thermoplastic starch (TPS) with a high glycerol content and its blends with low-density polyethylene (LDPE) and poly(lactic acid) (PLA) were examined under controlled degradation conditions. The biodegradation of native granular starch was also carried out as a reference. These results are correlated with the respective morphologies and continuity behavior of the various blend systems. CO_2 evolution was measured to evaluate biodegradation properties during the test and it is shown that the mineralization per-cent of TPS36 is 57% after 14 weeks as compared to 51% for native starch. Thermoplastic starch clearly degrades more rapidly than native starch under these conditions. X-ray diffraction patterns show a completely amorphous structure for TPS36. It is also shown that lowering the glycerol content in the thermoplastic starch has virtually no effect on its biodegradation behavior in the range of glycerol studied. The morphology and the continuity diagrams of the blends of TPS with LDPE or PLA were studied and it can be seen that co-continuity is achieved at 40% TPS for the TPS/PE blend and at 50% for the TPS/PLA blend. The per-cent mineralization of blends of 50% TPS with 50% LDPE or 50% PLA, as a function of time, indicate a virtually identical behavior under the conditions studied. The only contribution to biodegradation in those blends comes from the TPS component, under these room temperature conditions, and 86% and 82% of the TPS component in LDPE/TPS36 and PLA/TPS36 respectively is accessible to biodegradation. The blending of TPS with LDPE and PLA in a co-continuous morphology at a 50/50 composition provides a significant increase in surface area for the TPS which increases the biodegradation rate for the blends as compared to pure TPS. The biodegradation of the TPS component in those blend systems was completed within 6 weeks. The biodegradation profile of the 30/70 TPS36/LDPE blend indicates that approximately 50% of the TPS biodegrades in that sample. As a whole, these

results indicate a good relationship between morphology, phase continuity and biodegradation behaviour.

5.3 Introduction

Biodegradation is an environmentally compatible pathway for the complete elimination of plastics and fragments from the environment [1]. Biodegradable plastics are synthetic polymers that have certain degrees of biodegradability such as polycaprolactone, polyhydroxybutyrate and poly (vinyl alcohol) [2]. Biopolymers are naturally occurring polymers such as cellulose, polysaccharides and proteins. Most biopolymers are biodegradable, and hence, they can be degraded by bacterial activity into natural metabolic products. Most commercially available biodegradable materials are based on natural materials, e.g. polysaccharides (starch), cellulose and polypeptides of natural origin [3].

Starch is considered as one of the most important renewable and naturally biodegradable polymers and has potential as a material to replace large quantities of petroleum-derived plastics. However, the application of starch as a material has been greatly restricted by its defects, such as processability and water absorption. These defects can be overcome by the conversion of granular starch into thermoplastic starch, followed by its subsequent blending with other polymer materials. Both partially and fully degradable materials can be obtained. It has been reported that blends of synthetic polymers with TPS containing high concentrations of glycerol plasticizer can result in materials with excellent mechanical properties [4-7]. The approach used a one-step extrusion system that is composed of a twin-screw extruder (TSE) with a single-screw extruder (SSE) connected midway onto the TSE. It allows for starch plasticization, water devolatilization, melt-melt mixing and the control of the morphology of the TPS phase within the synthetic polymer matrix. The morphology, rheology, mechanical properties and thermal properties of TPS based blends have been extensively investigated [8]. However, the biodegradability of thermoplastic starch with high glycerol contents and the influence of the morphology and continuity of the blend components on that biodegradation have not been extensively studied

Total carbon balances can be estimated during a biodegradation test. The carbon content of a polymer is typically converted into biomass carbon by microorganisms, carbon dioxide by mineralization, dissolved organic carbon and residual insoluble material. The final mineralization percentage is usually between 60 to 70% and the percentage of biodegradation including

microbial bioassimilation and mineralization of carbon is usually between 82 and 90% for most biodegradable materials, the remaining part is dissolved organic carbon. [9] Biodegradability can be assessed mainly through gravimetry, molecular weight changes, morphological changes, mechanical characteristics and emission of CO_2. These tests give an indication of the biodegradation and disintegration of the materials under real-life conditions [10].

The biodegradation of native starch and its blends with either degradable or nondegradable polymer have been well studied in the literature [11-13]. For instance, Imam [13] studied the biodegradability of enzyme treated starch granules. The results suggested that the crystallinity type of the starches has a great effect on the rates of biodegradation. Further, X-ray diffraction and FTIR results indicated that the enzyme preferentially catalyzes the anhydroglucose units in the amorphous regions of the starch granule as opposed to the crystalline domains. Another well known biodegradable polymer, polylactic acid (PLA), is initially degraded by hydrolyzing into low molecular weight oligomers and is then mineralized into CO_2 and H_2O by the microorganisms present in the environment [14]. The rate of degradation is dependent on the size and shape of the article, the isomer ratio, and temperature of hydrolysis [15]. The biodegradability of thermoplastic starch (74% of starch, 10% of glycerol and 16% of water) and PLA films by microorganisms in a liquid medium were also compared [16]. It was found that biodegradation occurs readily for thermoplastic starch whereas it is much slower for PLA. Bikiaris et al. evaluated the biodegradation of LDPE/thermoplastic starch blends using thermogravimetric analysis [17]. The biodegradation of starch depends on the starch content in the blends. In the blends with higher starch content, a greater portion of it is consumed by microbes [17,18]. Tena-Salcido et al studied the effect of morphology on the biodegradation of thermoplastic starch (TPS)/LDPE blends [19]. The results by weight loss experiments show that about 39% of TPS degrades when TPS is dispersed as spherical domains in LDPE, however, when TPS is dispersed as fiber-like particles, degradation of TPS increases to 92%.

Morphology, after enzymatic degradation of polycaprolactone/TPS blends, was observed by Vikman et al. [12]. The enzymatic hydrolysis of the blends proceeds from the surface of the material into the center indicating that microbial degradation is a surface phenomenon, as expected. Since the starch degradation rate is more rapid than most synthetic biodegradable polymers, the biodegradation of these starch blends was dominated by the starch biodegradation behavior. A non-biodegradable synthetic polymer can provide a physical protection to the starch.

The lifetime of starch in an aerobic environment may be hours, but when placed in a non-degradable matrix, its lifetime increases from days to years, depending on the concentration of starch and the connectivity between particles. Effective degradation occurs only when the starch concentration exceeds the percolation threshold and significant pathways for moisture penetration and microbial invasion were generated [20]. The conversion of starch granules into thermoplastic starch provides a potential route toward morphology control of starch blends that subsequently affects its material degradation properties.

In the present work, the biodegradation of native starch granules, thermoplastic starch with a high concentration of glycerol plasticizer and its blends with biodegradable PLA and nondegradable polyethylene will be studied. The effect of the glycerol content in TPS, the morphology of the blends and continuity of the phases on biodegradation properties will be examined.

5.4 Experimental

5.4.1 Materials

Wheat starch was obtained from ADM/Ogilvie and is composed of 25% amylose and 75% amylopectin. TGA measurements showed that the water content in the starch granules was around 10%. The plasticizers used were water and pure glycerol (provided by MAT Laboratories. 99.5%). Polylactic acid was supplied by Cargill LLC (non-commercial grade 5729B). LDPE 640I was obtained from the Dow Chemical Company.

5.4.2 Processing

Starch granules were gelatinized, plasticized with glycerol and water, and blended with the various polymers in a one-step extrusion process. The processing of the polymer/thermoplastic-starch blends was based on a process developed previously in this laboratory [4-6]. The extrusion system was composed of a single-screw extruder (SSE) connected midway to a corotating twin-screw extruder (TSE). A starch/glycerol/water suspension was fed into the first zone of the TSE. The weight compositions of the slurry suspensions are 48.5 wt.% of starch, 28.1 wt.% of glycerol and 23.4 wt.% of water for TPS36, and 48.5 wt.% of starch, 15.6 wt.% of glycerol and 35.9 wt.% of water for TPS24. Note that TPS36 and TPS24 actually contain 38% and 26% glycerol respectively [21] by weight. The native starch was gelatinized and plasticized and any volatiles were extracted in the first part of the TSE. Molten polyethylene or

PLA was fed from the SSE to midway on the TSE and the processing temperatures were set at 150 ^{o}C. The TPS and molten polymer were then mixed in the latter part of the TSE. The TSE screw speed was 150 rpm for all of the blends. The draw ratio of the strands exiting the die was held at 1. Cylindrical extruded PCL/TPS strands were cooled and pelletized. The various compositions were extruded under the same conditions. More details concerning the extrusion process are reported elsewhere [5, 6].

5.4.3 Blend morphology and continuous phase

The extruded blend strands were cut into a flat surface using a microtome equipped with a glass knife. Extraction of the TPS phase was performed using 6N HCl at room temperature. After coating with a gold-palladium alloy, the morphologies of the samples were examined by a Jeol JSM 840 scanning electron microscopy at 10 to 15 kV.

A gravimetric method was used to calculate the extent of continuity of the TPS phase. Three segments of extruded strands were cut into around 10mm length and immersed in 6N HCl at ambient temperature for 24 h. Weight loss measurements were carried out to calculate the percentage of continuity using the simple equation:

$$\%continuity = \left(\frac{W_{init.} - W_{Fin.}}{W_{init.}} \right) \times 100\% \qquad (1)$$

Where, $W_{init.}$ corresponds to the weight in the blend before the solvent extraction step, and $W_{fin.}$ corresponds to weight remaining after extraction.

5.4.4 Biodegradation studied

About 2% of pulverized sample (mesh #10, on weight basis) was mixed with 5 g of compost (Garden Basics Swiss Farm Products, Las Vegas, NV) under appropriate conditions in a 250-mL sample chamber of a fully computerized, closed-circuit Micro-Oxymax Respirometer Sysproduction system (Columbus Instruments, Inc., Columbus, OH) equipped with an expansion interface, a condenser, and a water bath. The sample chamber was placed in a water bath controlled at 25 ^{o}C and connected to the Micro-Oxydevelopment max Respirometer. Experiments were carried out over a period of 14 weeks. CO_2 evolution from each sample was measured every 6 hr. The CO_2 measurements of duplicate samples were averaged, and had <2% variability. Samples were always accompanied by duplicate blanks (compost alone) to correct for

background CO_2. Experimental conditions with a temperature of 25 ^oC, pH 7.0, moisture content between 50% and 55%, and a 12-hr day/night light cycle were the optimal conditions under which materials were evaluated for biodegradability.

The percentage of substrate carbon mineralized as CO_2 was calculated as follows:

$$\%\text{mineralization} = \frac{\text{nCO}_2 c}{\text{nCO}_2 th} \times 100 \qquad (2)$$

where nCO_2c is the total accumulated amount of CO_2 product in the assay and nCO_2th is the theoretical amount of CO_2 potentially available from the initial substrate. If all the carbon of substrate were converted into CO_2, the mineralization percentage would be 100%.

5.4.5 Wide Angle X-ray

Wide angle X-ray diffraction experiments were carried out with a Philips diffractometer (Philips Electronic Instrument Co., Houston, TX). The wheat starch granule and pulverized TPS were packed tightly in the sample holder. The generator of the diffractometer was operated at 50kV and 40mA. Nickel-filtered Cu Kα radiation (λ=1.542Å) was used. The scanning regions of the diffraction angle 2θ were 5-35^o, at a scanning rate of 2^o/min, which covers all the significant diffraction peaks of crystalline wheat starch. It has been reported that TPS has a tendency to retrogradation [22], therefore, the entire X-ray test was conducted within 24 h after preparation.

5.4.6 Rheology

A dual-bore capillary rheometer (single barrel Rosand RH-7) was used to measure the viscosities of the pure materials at high shear rate. The test temperature was 165 ^oC. The same die was used during the test (diameter of 1mm. with an entrance angle of 180^o). Simultaneous measurements were carried out on both long and short dies (0.25 and 20 mm) to determine the inlet pressure drop at the die, and thus the absolute viscosity, using the Bagley correction method. The Rabinowitch correction was also applied to calculate the true shear rate.

5.5 Results and discussion

5.5.1 Morphology and phase continuity of PLA/TPS and LDPE/TPS blends

The morphology of a highly biodegradable phase in a mixture with a significantly

less-biodegradable component would be expected to be an important factor affecting its biodegradation properties. Since biodegradation is a surface phenomenon [10], the particle size and phase continuity of given phase in a heterophase polymer mixture are critical variables affecting its biodegradability. When immiscible polymers are blended, various morphologies can be obtained, such as: droplet/matrix, fibrillar/matrix, lamellar/matrix. co-continuous morphologies and even droplet in droplet structures may occur through a judicious combination of concentration control and processing conditions [^{2}3].

The SEM micrographs of PLA/TPA36 and LDPE/TPS36 blends are shown in Figures 5.1 and 5.2. Note that the TPS phase has been extracted by 6N HCl in order to improve the contrast. It can be clearly seen that the TPS phase exists as droplets distributed in either PLA or an LDPE matrix when its concentration is 20%. At concentrations of 30, 40 and 50% one observes progressively more elongated phases. The micrographs alone for both blend systems would tend to indicate a percolation threshold of just above 20% TPS. Very high levels of continuity of the TPS phase are observed for the LDPE/TPS phase at 40% TPS whereas less a continuous structure is observed for the PLA/TPS36 blend at the same concentration. In addition to these highly elongated phases, Figures 5.2c, d also show the presence of sub-included droplets of TPS within the LDPE phase.

The quantitative measure of the continuity of the TPS phase, as a function of TPS content, was measured using a solvent extraction/gravimetric method and the results are presented in Figure 5.3. A percolation threshold for the TPS phase of about 20% is confirmed for both systems. The continuity of the TPS phase increases dramatically when the TPS content increases from 30 to 50% for both blend systems. However, it is also clear that the continuity development for LDPE/TPS is more accentuated than that for PLA/TPS. Note that at 40% TPS the continuity for LDPE/TPS is 92% hand that for PLA/TPS is 66%. These results confirm the morphological observations from Figures 5.1 and 5.2. At 50% TPS both systems can be adequately described as co-continuous and the phase continuity is 97% and 91% for the LDPE and PLA blends, respectively. Such a highly continuous TPS phase should provide a significant pathway for moisture penetration and microbial invasion, and hence a high biodegradation rate.

The viscosity of PLA, LDPE and TPS36 measured via capillary rheometer is shown in Figure 5.4. It can be seen from that the viscosity of TPS36 is significantly lower than that of PLA and LDPE. Apparently, the viscosity ratio of TPS36/PLA is lower than that of TPS36/LDPE. In

typical thermoplastic blends, a blend with a lower viscosity ratio results in a more-readily deformed dispersed phase and thus displays a low percolation threshold. However, the co-continuity results from Fig 5.3. show an opposite behavior. Similar observations were also obtained for polycaprolactone/TPS36 blends and this phenomenon was studied in more detail in a previous paper [8]. These results further confirm the conclusion that blends with TPS do not respect the classical empirical description of viscosity ratio and co-continuity composition [24]. It likely an indication of the fact that both the elastic nature and internal hydrogen bonding in TPS give it the character of a pseudo partially-crosslinked material which demonstrates asymmetric continuity diagrams [8, 25].

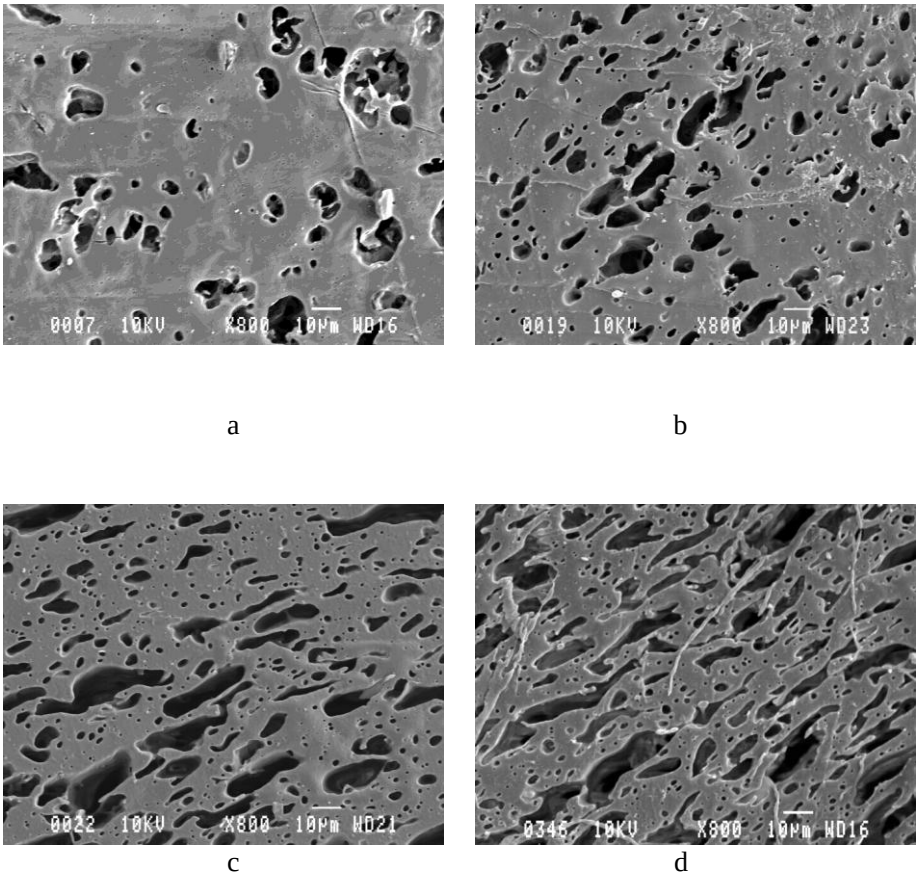

Figure 5.1 SEM micrographs for PLA/TPS36 blends: a) 80/20, b) 70/30, c) 60/40 and d) 50/50.

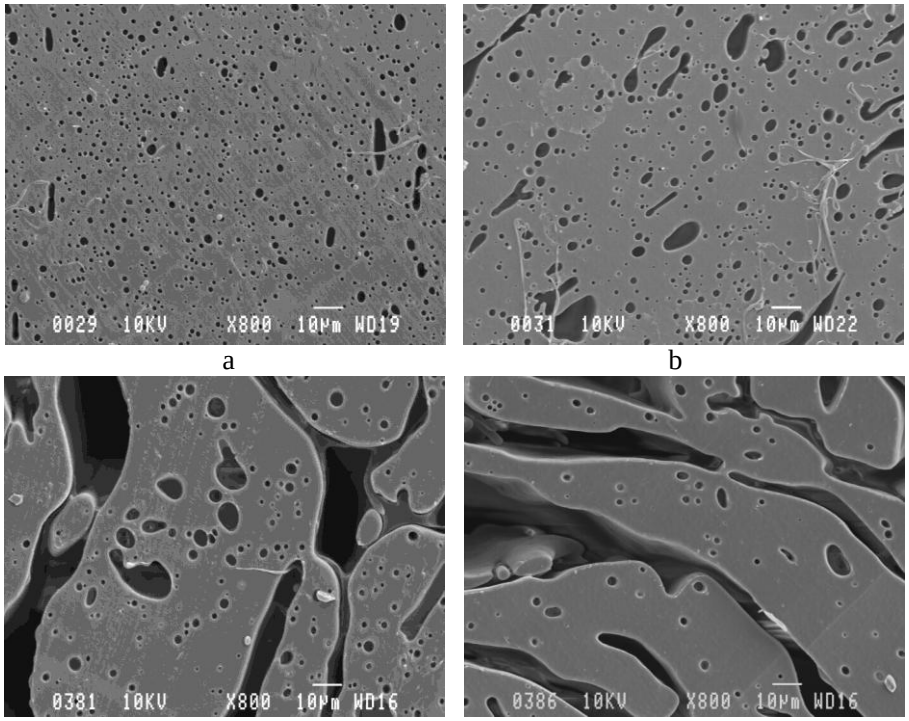

Figure 5.2 SEM micrographs for LDPE/TPS36 blends: a) 90/20, b) 70/30, c) 60/40 and d) 50/50.

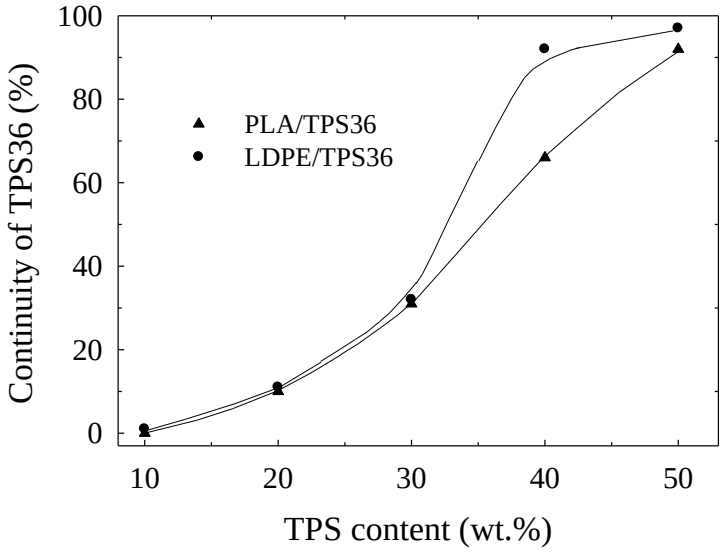

Figure 5.3 The per-cent continuity of TPS 36, as determined by solvent/gravimetry, as a function of its composition in the blend.

5.5.2 Biodegradation of TPS36, TPS24 and granular starch

The percentage mineralization was utilized to evaluate the biodegradation of the various materials. Figure 5.5 demonstrates the overall percentage mineralization of granular starch, TPS36 and TPS24. TPS36 and TPS24 appear to reach a plateau value at 10 weeks whereas granular starch is still showing increasing mineralization right up to the 14 weeks of these experiments. Examination of the mineralization% at two and four weeks time in Figure 5.5 indicates that the biodegradation rate of TPS is close to double that of granular starch. It is interesting to note that both TPS24 and TPS36 show similar biodegradation behavior with identical plateau values of 57% of mineralization achieved after 10 weeks. Hence, glycerol content does not appear to influence the biodegradation behavior of the thermoplastic starch. The granular starch, has a mineralization value of 51% after the 14 weeks of this experiment. Although granular starch has not yet reached its plateau after 14 weeks, it appears to be tending towards a similar plateau value as TPS24 and TPS36. All three samples in Figure 5.5 thus tend to converge towards a similar maximum mineralization value. Note that CO_2 generation as measured by the mineralization % is only one source of the carbon content during biodegradation. Microbial bioassimilation and dissolved organic carbon also account for a significant quantity of the carbon content of a degraded species [9].

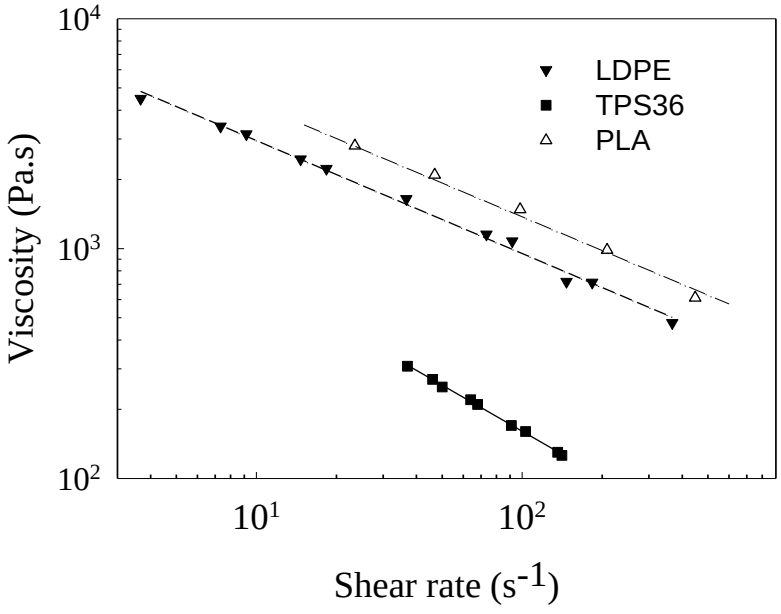

Figure 5.4 Melt viscosity for PLA, LDPE and TPS36 as a function of the shear rate at 165 ^{o}C

It is generally considered that the hydrolysis of starch occurs preferentially in the amorphous regions, at branch points and proceeds less effectively in ordered semi-crystalline domains [13, 26]. Figure 5.6 shows the X-ray diffraction pattern for native starch, TPS 24 and TPS36. It can clearly be seen that the crystalline domains within the native starch have been destroyed and a completely amorphous structure has been achieved in TPS 36. TPS 24 shows some residual crystallization peaks, but this does not appear to affect its biodegradation behavior.

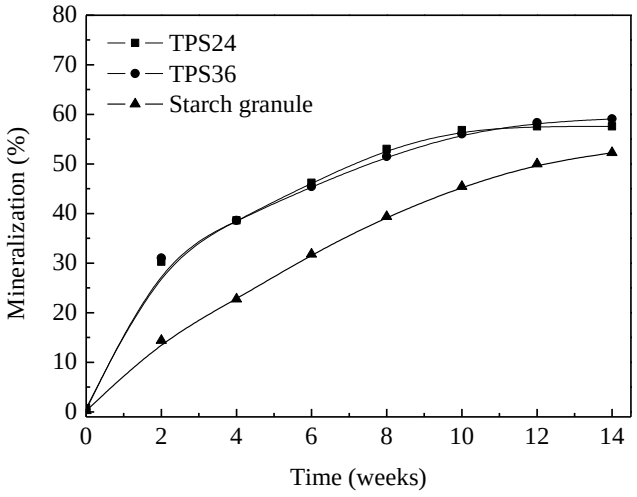

Figure 5.5 Percentage mineralization of TPS 36, TPS 24 and native starch granules under compost conditions at room temperature.

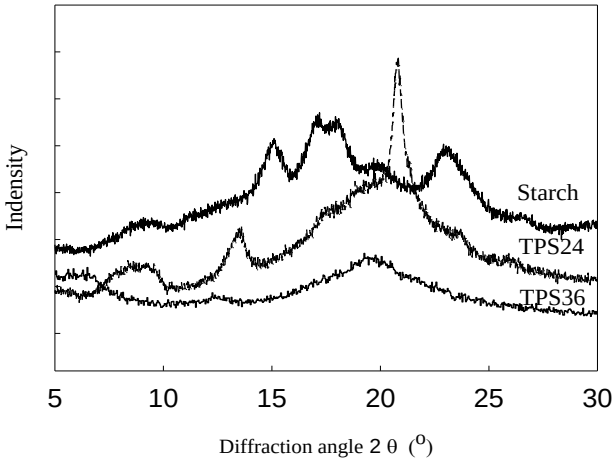

Figure 5.6 X-ray diffraction pattern for native starch, TPS24 andTPS36

5.5.3 Biodegradation of LDPE, PLA and their blends with TPS

Figure 5.7 shows the mineralization % of LDPE, PLA and their blends with TPS36. TPS36 is included as a reference in that figure. The neat LDPE and PLA samples show no mineralization of carbon whatsoever under the room temperature conditions of this test, as expected. However, the blends of LDPE/TPS36 (50/50) and PLA/TPS36 (50/50) show a significant and very similar level of biodegradation. If the plateau value of TPS36 is taken as the maximum possible mineralization of pure TPS under these conditions, then, this would indicate that approximately 86% and 82% of the TPS component in LDPE/TPS36 and PLA/TPS36 respectively is accessible to biodegradation. This indicates the virtually complete interconnectivity of the TPS domains in those blends and correlates perfectly with both the morphology and continuity data which indicated co-continuity. The small portion of non-degraded TPS can be related to the TPS droplet-like subinclusions in LDPE and PLA shown in Figure 5.1d and 5.2d. These sub-inclusions are surrounded by PLA or LDPE and would not be accessible for biodegradation. Furthermore, it should also be noted that all biodegradation of the TPS component in the blends was achieved within six weeks whereas pure TPS required 10 weeks to reach plateau behavior. This latter result can be related to the significantly increased surface area of TPS achieved after blending. In combination, the increased TPS surface area and its highly interconnected nature allow biodegradation to proceed very effectively.

Nondegradable polymer can provide a physical protection to the biodegradable component. In such a case effective degradation occurs only when the biodegradable component fraction exceeds the percolation threshold [20]. In this work, we also examined a blend of 30% TPS in LDPE in order to study the effect of partial phase continuity on the biodegradability of the blends. Figure 5.3 indicates that the TPS in 30% TPS36/70% LDPE has a continuity level of 30% whereas the TPS in 50% TPS36/50% LDPE has a continuity of 97%. The biodegradation % of the TPS component in those two blends was approximately 50% and 86% respectively. It is interesting to note that the continuity value of 30% and the mineralization value of 50% are quite different. Figure 5.3 indicates that 30% TPS is in the concentration range where continuity is increasing dramatically with TPS content. Hence, a small variation in concentration could have a significant effect on continuity. On the whole the trends in this work clearly show a reasonable relationship between morphology, continuity data and mineralization results.

In studies on native granular starch, scalar percolation theory has been applied to analyze

the static degradation of LDPE/starch mixtures [27]. The degradation is determined by the total granular starch concentration. Computer simulations have shown that native starch accessibility generally increases with increasing concentration of starch. A percolation threshold of 31.17% by volume (about 40% by weight) was obtained in those studies. Below this percolation threshold of starch, only a small amount of it can be degraded. Above that threshold, starch could be removed very effectively. In that work, for the blends of LDPE/granular starch with 30% starch, only 17.3% of the initial starch degraded [18]. In this work the ability of thermoplastic starch to form interconnected domains and even co-continuous structures clearly opens up a completely different biodegradation pattern.

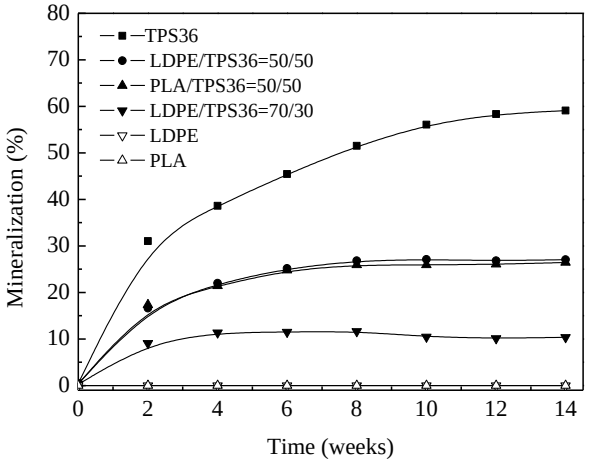

Figure 5.7 Percentage mineralization of PLA, LDPE and their blends with TPS 36 under compost conditions at room temperature.

5.6 Conclusion

In this paper, the biodegradation of thermoplastic starch and its blends with polylactic acid and low-density polyethylene were studied under compost conditions. Emissions of CO_2 from biodegradation were cumulated to evaluate the mineralization per-cent of the sample. The degradation rate of TPS is significantly higher than that of native starch due to its amorphous structure. After the first two weeks, the degradation rate of TPS is twice that of granular starch. These results and the x-ray data support the notion that the biodegradation of starch occurs

preferentially in the amorphous regions. Lowering the glycerol content in the TPS has no effect on its biodegradation behavior. The per-cent mineralization of blends of 50% TPS with 50% LDPE or 50% PLA, as a function of time, indicate a virtually identical behavior under the conditions studied. The only contribution to biodegradation in those blends comes from the TPS component under these room temperature conditions, and 86% and 82% of the TPS component in LDPE/TPS36 and PLA/TPS36 respectively is accessible to biodegradation. The blending of TPS with LDPE or PLA in a co-continuous morphology at a 50/50 composition provides a significant increase in surface area for TPS, which increases the biodegradation rate of the TPS component with plateau behavior achieved within 6 weeks as compared to 10 weeks for the pure thermoplastic starch. The biodegradation profile of the 30/70 TPS36/LDPE blend indicates that approximately 50% of the TPS biodegrades in that sample. In this work, a reasonable relationship between the morphology, continuity data and mineralization results is observed.

5.7Acknowledgements

The authors would like to thank Drs. Syed H. Imam and William J. Orts of the United States Department of Agriculture, Albany California for the use of the respirometer. The authors also thank Dr. Zhenhua Yuan for assistance with the rheological data.

5.8 References

1 G. Swift, Expectations for biodegradation testing methods in *Biodegradable Plastics and Polymers;* eds. Y. Doi and K. Fukuda, Elsevier, Amsterdam, **1994**, p. 228-236.

2 A.L. Brody and K.S. Marsh, (Eds.), **1997**. Encyclopedia of Packaging Technology, 2nd Edition. Wiley, New York.

3 L. Avérous, *J. Macromol. Sci., Part C—Polymer Reviews,* **2004**, 44, 231.

4 F. J. Rodriguez-Gonzalez, B. A. Ramsay, B. D. Favis, *Polymer,* **2003**, 44: 1517.

5 US 6,605,657 (2003), B. D. Favis, F. J. Rodriguez-Gonzalez, B. A. Ramsay.

6 US 6,844,380 (2005), B. D. Favis, F. J. Rodriguez-Gonzalez, B. A. Ramsay.

7 PCT/CA2006/000695, U.S. patent application 11/912, 045: B. D. Favis, Z. Yuan, D. Riscanu.

8 G. Li, B. D. Favis, *Macromol. Chem. Phys*., **2010**, 211, 321.

9 R. Gatttin, A. Copinet, C. Bertrand, Y. Countuier, *J. Appl. Polym. Sci.,* **2003**, 88, 825.

10 J. Mergaert, K. Ruffieux, C. Bourban, V. Storms, W. Wagemans, E. Wintermante and J. Swings, *J. Polym. Envir,* **2000**, 8, 17.

11 B. Y. Shin, S. Lee, Y. S. Shin, S. Balakrishan and R. Narayan, *Polym. Eng. Sci.,* **2004**, 44, 1429.

12 M. Vikman, S. H. D. Hulleman, D. Z. M. Van, P. M. Rinen, H. Feil, *J. Appl. Polym. Sci.*; **1999**, 74, 2594.

13 S. H. Imam, S. H. Gordon, A. Mohamed, R. Harry-O'kuru, B. S.Chiou, G. M. Glenn, W. J. Orts, *Polym. Degrad. Stab.* **2006**, 91, 2894.

14 J. Lunt, *Polym. Degrad. Stab.,* **1998**, 59, 145.

15 M. H. Hartmann in D.L. Kaplan (Ed.), Biopolymers from Renewable Resources, Spinger-Verlag, Berlin, pp. 367.

16 R. Gattin, A. Coppinet, C. Bertrand, *J. Polym. Environ*., **2002**, 9, 11.

17 D. Bikiaris, J. Prinos, C. Panayiotou, C. *Polym. Degrad. Stab*., **1997**, 58, 215.

18 I. M. Thakore, S. Desai, B. D. Sarawade, S. Devi, *Eueop. Polym. J.,* **2001**, 37, 151.

19 C. S. TenaA-Salcido, F. J. Rodriguez-Gonzalez, M. L. Mendez-Hernandez, J. C. Contreras-Esquivel, *Polymer bulletin*, **2008**, 60, 677.

20 R. P. Wool, D. Raghavan, G. C. Wagner, S. Billieux,.*J. Appl. Polym. Sci.*, **2000**, 77, 1643.

21 A. Taguet, M. A. Huneault, B. D. Favis, *Polymer*, **2009**, 50, 5733.

22 C. L. Hsu, D. R. Heldman, *J. Food Process. Eng.,* **2005**, 28,506.

23 D. Bourry, B. D. Favis, *J. Polym. Sci., Part B: Polym. Phys.,* **1998,** 36, 1889.

24 G. M. Jordhamo, J. A. Mason, L. H. Sperling, *Polym. Eng. Sci.,* **1986**, 26, 517.

25 P. L. Ma, B. D. Favis, F. Champagne, M. A. Huneault, F. Tofan, *Polym. Eng. Sci.,* **2004**, 42, 1976.

26 Y. Zhou, R. Hoover, Q. *Carbohydrate Polymers,* **2004**, 57, 299.

27 J. Peanasky, J. Long, R. P. Wool, *J. Polym. Sci. Polym. Phys,* **1991**, 29, 565.

CHAPTER 6

SCIENTIFIC CONTRIBUTIONS

It is essential research work in the field of polymer blends to study the morphology since most properties, e.g. mechanical properties, of the final product are strongly dependent on morphology. In order to apply morphology control strategies to polymer blends containing thermoplastic starch, the conversion of native starch into fully plasticized starch is a primary requirement in melt processing. However, one-step melt processing of polymer blends with thermoplastic starch is a complex operation, which involves starch plasticization, water devolatilization, melt-melt mixing and morphology control. All these must be achieved within two minutes maximum total residence time in an extruder. Therefore, the main challenge in the one-step extrusion process is the efficiency of plasticization. One of the most important scientific contributions of the present work is the production of polymer blends based on fully plasticized starch via one-step extrusion system. The role of the starch suspension component on starch gelatinization, the processing temperature, the moment water is removed and the opportunities of polymer blends have been investigated extensively.

Time/temperature boundaries ultimately required for the successful plasticization of starch in polymer melt processing were determined and these results were related to the morphology of melt-blended thermoplastic starch (TPS) in polycaprolactone (PCL). The efficacy of plasticization is demonstrated by a dramatic six-fold reduction in the dispersed TPS phase size and a unimodal phase size distribution of dispersed TPS particles, with a d_v of 3.2 μm and a d_n of 2.1 μm, was obtained. The relationship between morphology and rheology and the influence of morphology on biodegradation properties have been established. Mechanical properties tested displayed very good ductility in the blends of PCL/TPS36 even at high TPS36 concentration and in the absence of any interfacial modifier.

The demonstration of starch gelatinization has been carried out using various experimental methods. The influence of water and glycerol on gelatinization temperature and gelatinization enthalpy have been established. It is clear that the gelatinization temperature greatly depends on

the ratio of water and glycerol. Set-up of the temperature profile in the extrusion process can be easily varied according to this behaviour. Dynamic studies of wheat starch gelatinization provide more detailed information about starch gelatinization. The results indicate that if the temperature is sufficiently high, gelatinization takes place quickly for the excess water/glycerol/wheat starch mixture, and that only a partial degree of plasticization is achieved even after long treatment times at temperatures lower than the gelatinization temperature. However, the gelatinization process is significantly slower if only glycerol is applied as a plasticizer, and gelatinization then requires approximately 3 minutes. The study on morphology of extruded PCL/TPS36 blends indicated glycerol alone was unable to effectively plasticize the starch under normal extrusion conditions due to the limitation of residence time in the extruder. The effect of water in the excess water/glycerol plasticization protocol evidently serves to improve ingress rates into the starch granules.

Another scientific contribution of the present work is the study of rheology and morphology. Fully plasticized starch (TPS) is a free-flowing fluid that can be processed using conventional processing equipment like other thermoplastics. However, TPS is different in rheology from conventional plastics. The rheology of TPS demonstrates gel behaviour and no Newtonian plateau in viscosity is observed. This indicates strong interactions within the TPS due to the existence of hydrogen bonding. The presence of physical crosslinking in the melt state leads to highly elastic properties and melt yield stress, which have a stabilizing effect on the elongated structure. Thus, elongated dispersed structures are observed in TPS blends.

Finally, biodegradation of TPS and its blends with PLA and LDPE were estimated under composting conditions. The mineralization rate of pure TPS is considerably higher than that of native starch. Glycerol content has less effect on TPS degradation. The studies on biodegradability of blends of TPS with LDPE and PLA indicated that neither material has any influence on TPS biodegradation. The biodegradation of the blends can be determined by TPS only. However, the surface area of TPS was significantly increased by blending of TPS with LDPE and PLA the increase in surface will decrease the percolation threshold of TPS. Subsequently, more pathways for moisture penetration and microbial invasion were generated for the same concentration of native starch. Therefore, an increase in the biodegradation rate was achieved.

CHAPTER 7

GENERAL DISCUSSION

The one-step melt processing of polymer blends with TPS is a complex operation, which involves starch plasticization, water devolatilization and melt-melt mixing. All these must be achieved within two minutes in an extruder. In order to apply morphology control strategies to TPS-based polymer blends, high plasticizer content and a high degree of gelatinization are required. The key step of processing is the conversion of native starch into a free-flowing fluid material similar to other conventional thermoplastics. Native starch is a mixture of amylose and amylopectin. The ratio of amylose to amylopectin varies with plant resource. Gelatinizations of starch have been well demonstrated in the food industry. The effects of starch composition, water, honey and sugar on starch gelatinization have been studied extensively. These results were useful for the food industry. However, for material applications, glycerol and water are the most widely applied plasticizers, and homogeneous TPS is difficult to achieve within the time constraint of typical processing conditions. Matzinos et al. (Matzinos et al., 2002) reported that completely plasticized starch can only be achieved by being processed three times in an extruder. Most studies on TPS blends were carried out by simply mixing starch with plasticizer, or by multi-step extrusion. It is easy to conclude that incomplete plasticization of starch was obtained from morphology studies reported in the literature.

A one-step blending approach on previous work by Favis and co-workers (Favis et al., 2005 and Rodriguez-Gonzalez et al., 2003) was used for preparing LDPE/TPS blends. The starch suspension (starch/glycerol/water) was introduced into the preparation of TPS. Excellent mechanical properties were achieved even at high TPS concentration without any interfacial modifier. However, the effects of water and glycerol on starch plasticization in extrusion processing were unclear. With the present work, a series of experiments were designed to study the influence of plasticizers on starch gelatinization.

1. Change water and glycerol content in the suspension. Water content in starch suspension was varied between 25% and 54% (water/water+starch) and glycerol content was varied from 24% to 40% (glycerol/glycerol+starch). Processing conditions used were the same as in extrusion 2

experiment described in Chapter 3. Similar results were obtained in these cases. A bimodal particle distribution, with the large particles having a volume average diameter (d_v) of 10.2 μm and a d_n of 2.5 μm, was obtained. The bimodal TPS phase size distribution clearly indicated that the starch plasticization process was incomplete. It is easy to conclude that the water or glycerol content in the starch suspension have less effect on starch gelatinization in the range studied.

2. In extrusion 3 experiment, the same processing conditions and starch suspension as in extrusion 2 were used and no vacuum was applied to remove water; the vent was just left open to the atmosphere. This results in a less efficient removal of water and has the effect of increasing the residence time of water in the twin-screw extrusion process. In this case, the morphology of the TPS particles becomes unimodal with a d_v of 4.4 μm and a d_n of 3.0 μm. The influence of glycerol content on morphology of PCL/TPS (70/30) blends extruded without vacuum were studied. It is can be seen that the TPS particle size is much smaller and the distribution of the particles is uniform even at low glycerol content (24% by weight). The result clearly indicated that starch could be completely plasticized even at low glycerol content in the presence of water. The water contents in TPS obtained by TGA are about 2% and 4% in the TPS36 sample with and without applied vacuum, respectively.

3. In order to maintain a sufficiently long residence time of water and ultimately devolatilize from the system, the twin-screw was extended from 8 zones to 12 zones. The same excess water/glycerol/starch mixture as in extrusion experiments 2 and 3 and the same processing conditions were used. A unimodal phase size distribution of dispersed TPS particles with a d_v of 3.2 μm and a d_n of 2.1 μm was obtained. All above results support the conclusions of the previous section and underline the importance of not only adding excess water at the outset of the extrusion process, but also assuring a minimum residence time of water prior to removal and devolatilization.

4. For mixtures of plasticizers containing both water and glycerol, it is interesting to note that the gelatinization temperature only depends upon the glycerol concentration within the range studied. The gelatinization temperature increases with increasing concentration of glycerol. A master curve relating the gelatinization temperature and glycerol/water content was obtained

(Figure 6 of Appendix C), and it can be used to estimate the gelatinization temperature of starch/glycerol/water systems.

CONCLUSIONS AND RECOMMENDATIONS

This study examines critical aspects of starch plasticization in glycerol/excess water mixtures in order to determine the time/temperature boundaries ultimately required for the complete plasticization of starch in a polymer melt processing environment, and then relates these findings to the morphology of melt-blended thermoplastic starch (TPS) in polycaprolactone (PCL). The onset and conclusion temperatures for wheat starch gelatinization in the presence of excess water were obtained via differential scanning calorimetry (DSC), optical microscopy and wide angle X-ray diffraction (WAXS). Dynamic studies indicate that the starch granule size has very little effect on gelatinization kinetics. If the temperature is sufficiently high, gelatinization takes place within 60 seconds for the excess water/glycerol/wheat starch mixture and within 3 minutes for the glycerol/wheat starch case. However, even if the kinetics are rapid, below the conclusion temperature only a partial degree of plasticization is achieved even after long treatment time. Considering the above time/temperature constraints for starch plasticization, a series of one-step melt extrusion experiments for PCL/TPS blends were designed and the dispersed TPS morphology was examined. The TPS particle size (d_v) in a PCL matrix is 13.9 microns when only glycerol is used to plasticize native starch (contains only ambient water). This is very similar to the native starch granule size of 13.6 microns and clearly indicates the inability of glycerol alone to plasticize native starch within the time constraints of melt extrusion. When a glycerol-excess water mixture is used and a sufficient residence time is allowed prior to water devolatilization, a completely plasticized starch is obtained. The efficacy of plasticization is demonstrated by a dramatic six-fold reduction in the dispersed TPS phase size, a unimodal TPS phase size distribution in the blend system and by a completely amorphous WAXS diffraction pattern.

TPS demonstrates a gel behaviour and a non-Newtonian plateau in viscosity. This implies strong interactions within the TPS due to the existence of hydrogen bonding. The study of morphology of PCL/TPS36 blends reveals the dispersed phase of TPS is independent of compositions and the formation of stable fiber-like structures during extrusion processing. This can be explained by physical crosslinking in melt state, which leads to highly elastic properties and melt yield stress, and consequently has a stabilizing effect on elongated structures. A TPS continuous phase forms by interconnecting of elongated TPS phases. DMTA results also showed

certain interfacial reactions between plasticized starch-rich phase and PCL. These results strongly indicated partial miscibility between PCL and completely plasticized starch. Mechanical properties tested displayed very good ductility even in high TPS36 concentration in the absence of any added interfacial modifier.

Biodegradability of granular starch, thermoplastic starch and its blends with degradable poly(lactic acid) and non-degradable low-density polyethylene were demonstrated under compost conditions. Emission of CO_2 from biodegradation was cumulated to evaluate the biodegradability of material. Degradation rate of TPS is considerably higher than that of native starch due to its amorphous structure, especially in the first two weeks, where the degradation rate of TPS is twice that of the granular starch. This result is in good agreement with most of the literature, which shows that the biodegradation of starch occurs preferably in amorphous regions. However, the concentration of glycerol as a plasticizer used in TPS has no influence on TPS degradation. The surface area of TPS was increased significantly by blending TPS with LDPE and PLA, the increase in surface decreasing the percolation threshold of TPS. The value of the percolation threshold obtained varies between 20% and 30% by weight. More pathways for moisture penetration and microbial invasion were generated in the same concentration as native starch. Subsequently, an increase in biodegradation rate was achieved. Therefore, blending TPS with other polymers will provide a potential route towards environmentally compatible materials.

The critical aspects of starch plasticization in glycerol/excess water mixtures have been demonstrated extensively and these findings have been successfully applied to determine the time/temperature boundaries of prepared PCL/TPS blends used in extrusion systems. However, in the present work, the processing temperature of PCL/TPS blends is only around 110°C and the temperature set-up for starch gelatinization is between 70°C and 110°C. In some cases, for instance, high mixing temperature and high output quantity requirement, the processing conditions should be varied. The following future work should be considered:

1. According to the time/temperature boundary conditions, the thermal conductivity in the extruder must be considered in the case of high extrusion output. Extrusion temperature, water evaporation and total water residence time have more interdependent relationships, because the ratio of thermal conductivity time to total residence time will increase in these cases. The

increase in temperature is necessary in order to achieve completely plasticized starch. As a result, water evaporation increases with temperature, and thus starch gelatinization time was prolonged due to the lower water content in the systems. The detailed relationship needs to be studied in the future.

2. Glycerol can be completely removed from TPS by water extraction (first presented by Pierre Sarazin) and retrogradation (recrystallization) of starch. Re-gelatinization of the extracted TPS sample by water was demonstrated via DSC. This result indicated that starch gelatinization is a reversible process, which is contrary to what is reported in literature. Generally, starch gelatinization was regarded as an irreversible process. The re-gelatinization of starch will provide strong evidence to clarify the mechanisms of starch gelatinization and retrogradatoion (recrystallization) in further investigations.

3. DMA indicated that phase separation occurred between starch and glycerol. However, it is difficult to measure the migration of glycerol. More evidence is needed to clarify the glycerol transfer to the TPS surface.

4. The studies of biodegradability on PLA/TPS and LDPE/TPS blends are original. The morphology and mechanical properties must be studied in detail during biodegradation.

LIST OF REFERENCES

Ablazova T.I.; Tsebrenko M.B.; Yudin A.B.V.; Vinogradov G. and. Yarlykov B.V; Rheological properties of molten mixtures of polyoxymethylene and copolyamide. Their fibrillation and microstructure; *J.Appl. Polym. Sci.* 1975, 19: 1781–1798.

Avella M.; Errico H.E.; Laurienzo P.; Manolova N.; Raimo M.; Rimedio R.; Preparation and characterization of compatibilized polycaprolactone/starch composites; *Polymer* 2000, 41: 3875-3881.

Averous L, Fauconnier N, Moro L, Fringant C. Blends of thermoplastic starch and polyesteramide: processing and properties; *J. Appl. Polym. Sci.* 2000, 76: 1117-1128.

Averous L, Moro L, Dole P, Fringant C. Properties of thermoplastic blends: starch-polycaprolatone; Polymer 2000; 41:4157-4167.

Avérous L.; Biodegradable multiphase systems based on plasticized starch: a review; *J. Macromol. Sci., Part C—Polymer Reviews* 2004, 44, 231-274.

Avgeropoulos G.N.; Weissert F.C.; Biddison P.H.; Bohm G.G.A.; Heterogenous blends of polymers Rheology and morphology; *Rubber Chem. Techn.* 1976, 49: 93-104

Bastioli C.; Biodegradable materials—present situation and future perspectives. *Macromol. Symp.* 1998, 135, 193–204.

Bastioli C.; Properties and application of Mater-Bi starch-based materials, *Polym. Degrad. Stab.* 1998, 59: 263-272.

Benndict C.V.; Cameron J.A.; Huang S.J.; Polycaprolactone Degradation by Mixed and Pure Cultures of Bacteria and a Yeast*; J. Appl. Polym. Sci.* 1983, 28: 335-342.

Bhadane P.A, Tsou A.H, Cheng J, Favis B.D.; in preparation for Polymer.

Bikiaris D.; Prinos J.; Panayiotou C.; Effect of methyl methacrylate-butadiene- styrene compolymer on the thermooxidation and biodegradation of LDPE/plasticized starch blends; *Polym. Degrad. Stab*. 1997, 58: 215-228.

Biliaderis C.G.; Structures and phase transitions of starch in food systems*; Food Technol.* 1992, 6: 98-100.

Biresaw G. and Carriere C.J.; Compatibility and mechanical properties of blends of polystyrene with biodegradable polyester; *Composite*s: *Part A* 2004, 35: 313-320.

Bourry D. and Favis B.D.; Cocontinuity and phase inversion in HDPE/PS Blends: influence of interfacial modification and elasticity; *J. Polym. Sci., Part B: Polym. Phys.* 1998, 36: 1889-1899.

Bourry D. and Favis B.D; Morphology Development in a Polyethylene/Polystyrene Binary Blend During Twin-Screw Extrusion; *Polymer* 1998, 39: 1851-1856.

Brody A.L. and Marsh K.S.; (Eds.), 1997. The Wiley Encyclopedia of Packaging Technology, 2nd Edition. Wiley, New York.

Broz M.E.; VanderHart D.L.; Washburn N.R.; Structure and mechanical properties of poly(d,l-lactic acid)/poly(e-caprolactone) blends; *Biomaterials* 2003, 24: 4181-4190.

Bul éon A; Bizot H; Delage MM.; Multon JL.*;* Evolution of crystallinity and specificity gravity of potato starch versus water ad- and desorption; *Starch/Staerke* 1982, 32: 361-366.

Cagiao M.E.; Rueda D.R.; Bayer R.K.; Calleja F.J.B.; Structural Changes of Injection Molded Starch during Heat Treatment in Water Atmosphere: Simultaneous Wide and Small-Angle X-Ray Scattering Study*; J. Appl. Polym. Sci.* 2004, 93: 301-309.

Calzetta Resio A. and Suarez C.; Gelatinization kinetics of amaranth starch. *International Journal of Food Science and Technology* 2001, 36: 441-448.

Carvalho A.J.F.; Curcelo A.A.S.; Gandini A.; Surface chemical modification of thermoplastic starch: reaction with isocyanates, epoxy functions and stearoyl chloride; *Industrial Corps. Prod.* 2005, 21: 331-336.

Chandra R. and Rustgi R.; Biodegradable polymers ; *Prog. Polym. Sci.* 1998, 23: 1273-1335.

Chen X.; Xu J.; Guo B.H.; Development of Dispersed Phase Size and Its Dependence on Processing Parameters; *J. Appl. Polym. Sci.* 2006, 102: 3201-3211.

Chiotelli E.; Pilosio G.; Le Meste M.; Effect of Sodium Chloride on the Gelatinization of Starch: A Multimeasurement Study; *Biopolymers* 2002, 63: 41-58.

Chuang G.C.C. and Yeh A.I.; Effect of screw profile on residence time distribution and starch gelatinization of rice flour during single screw extrusion cooking; *J. Food Eng.* 2004, 63: 21-31.

Coleman M.M, Moskala EJ. Mechanical and microstructural properties of pectin/starch films; Polymer 1983, 24: 663-670.

Collsion R. and Mcdonald M.P.; Broadening of water proton line in high resolution nuclear magnetic resonance spectra of starch gels.; *Nature* 1960, 186:548-549

Colonna P.; Buleon A.; Mercier C.; Lemaguer M. Pisum Sativum and Vicia Faba carbohydrates – Part IV granular structure of wrinkled pea starch, *Carbohydr. Polym.* 1982, 2: 43-51.

Cook J.K.; Cameron J.A.; Bell J.P. and Huang S.J.; Scanning Electron Microscopy Visualization of Biodegradation of Polycaprolactone by Fungi; *J. Polym. Sci., Polym. Lett.*, 1981, 19: 159-164.

Cunha M.T.; Costa M.J.L.; Calado C.R.C.; Fonseca L.P.; Aires-Barros M.R. and Cabral J.M.S.; Integration of production and aqueous two-phase systems extraction of extracellular Fusarium solani pisi cutinase fusion proteins. *J. Biotech.* 2003, 100: 55-64.

Curvelo A.A.S.; Carvalho A.J.F.; Agnelli J.A.M.; Thermoplastic starch- cellulosic fibers composites: Preliminary results. *Carbohydrate Polymers* 2001, 45: 183-188.

Da Róz A.L.; Carvalho A.J.F.; Gandini A.; Curvelo A.A.S.; The effect of plasticizers on thermoplastic starch compositions obtained by melt processing; *Carbohydrate Polymers* 2006, 63: 417-424.

Davis G. and Song J.H; Biodegradable packaging based on raw materials from crops and their impact on waste management. *Industrial Crops and Products* 2006, 23: 147-161.

Della Valle G. ; Buleon A.; Carreau P.J.; Lavoie P.A. and Vergnes B.; Relationship between structure and viscoelastic behavior of plasticized starch; *J. Rheo.* 1998, 42: 507-525.

Derycke V.; Vandeputte G.E.; Vermeylen R.; De Man W.; Goderis B.; Koch M.H.J.; Delcour J.A.; Starch gelatinization and amylose-lipid interactions during rice parboiling investigated by temperature resolved wide angle X-ray scattering and differential scanning calorimetry; *J. Cereal. Sci.* 2005, 42: 334-343.

Di Paola R.D.; Asis R.; J Aldao M.A.; Evaluation of the degree of starch gelatinization by a new enzymatic method; *Starch/Stärke* 2003, 55: 403-409.

Donald A.M.; Lisa Kato K.; Perry P.A.; Waigh T.A.; Scattering studies of the internal structure of starch granules; *Starch/Stärk*, 2001, *53*: 504-512.

Dongryel Y, Byoungseung Y. Rheology of rice starch-sucrose composites; Starch/stärke 2005,.57: 254-261

Drumright R.E.; Gruber P.R. and Henton D.; Polylactic Acid Technology; *Advanced Materials* 2000, 12: 1841-1846.

Dubois Ph. ; Jacobs C. ; Jerome R.; Teyssie Ph.; Macromolecular engineering of polylactones and polylactides. 4. Mechanism and kinetics of lactide homopolymerization by aluminum isopropoxide; *Macromolecules* 1991, 24: 2266-2270.

Elmedorp J.J. and De Vos. G.; Measurement of Interfacial Tensions of Molten Polymer Systems by Means of the Spinning Drop Method, *Polym. Eng. Sci.* 1986, *26*: 415−417

Elmendorp J.J.; Van der Vegt A.K.; A study on polymer blending microrheology. Part IV. The influence of coalescence on blend microrheology origination. *Polym. Eng. Sci.* 1986, 26: 1332-1338.

Evangelista R.L, Sung W, Jane J.L, Gelina RJ, Nikolov ZL. Effect of compounding and starch modification on properties of starch-filled low-density polyethylene; *Ind. Eng. Chem. Res.* 1991, 30: 1841-46.

Fan C-Y.; and Köller W.; Diversity of cutinases from plant patogenic fungi: differential and sequential expression of cutinolytic esterases by Alternaria brassicicola; *FEMS Microbio. Lett.* 1998, 158: 33-38.

Favis B.D. and Chalfoux J.P. Influence of Composition on the Morphology of Polypropylene/Polycarbonate Blends; 1988, 29: 1761-1767.

Favis B.D. and Chalfoux J.P.; The effect of viscosity ratio on the morphology of polypropylene/polycarbonate blends, *Polym. Eng. Sci.* 1987, 27: 1591-1600.

Favis B.D, Rodriguez F, Ramsay BA. US Patent 6,605,657(2003).

Favis B.D, Rodriguez Gonzalez FJ, Ramsay BA. US Patent 6,844,380(2005).

Favis B.D, Therrien D. Factors influencing structure formation and phase size in an immiscible polymer blend of polycarbonate and polypropylene prepared by twin-screw extrusion; *Polymer* 1991, 32: 1474-1481.

Favis B.D, Willis JM. Phase Size/Composition Dependence in Immiscible Blends: Experimental and Theoretical Considerations; *J of Polym. Sci. Part B: Polym. Phys.* 1990, 28: 2259-2269.

Favis B.D, Yuan Z, Riscanu D. PCT/CA2006/000695.

Favis B.D. (2000). Factors Influensing the Morphology of Immiscible Polymer Blends in Melt Processing. In D. R. Paul & C. B. Bucknall (Eds.), Polymer Blends Volume 1. Formulation (Vol. 1, pp. 501-538). New York: John Wiley & Sons.

Fenouillot F. and Perier-Camby H.; Formation of a fibrilar morphology of crosslinked epoxy in a polystyrene continuous phase by reactive extrusion, *Polym. Eng. Sci.*, 2004, 44: 625-637.

Fields R.D., Rondriquez F.and Finn R. K., Microbial degradation of polyesters: Polycaprolactone degraded by P. pullulans*; J. Appl. Polym. Sci.* 1974, 18: 3571-3579

French D., In: Whistler R.L, Bemiller JN, Parschall EF, editors. *Starch, Chemistry and Technology.* New York: Academic Press, 1984:183–247.

French D., Fine structure of starch and its relation to the organization of starch granules; *J Jpn. Soc. Starch Sci.* 1972, 19: 8-25.

Fukuoka, M.; Ohta, K.I.; Watanabe, H.; Determination of the terminal extent of starch gelatinization in a limited water system by DSC; *J. Food Eng* 2002, 53: 39-??.

Gattin R.; Copinet A.; Bertrand C.; Couturier Y. Biodegradation study of a coextruded starch and poly(lactic acid) material in various media; *J. Appl. Polym. Sci.* 2003, 88: 825-831.

Gattin R.; Coppinet A.; Bertrand C.; Couturier Y.; Comparative biodegradation study of starch and polylactic acid- based materials; *J. Polym. Environ*. 2002, 9: 11-17.

Gernat C.; Radosta S.; Anger H.; Damashun G.; Crystalline Parts of Three Different Conformations Detected in Native and Enzymatically Degraded Starches; *Starch/Staerke* 1993, 45: 309-314.

Godet M.C; Bizot H; Bul éon A.; Crystallization of amylose—fatty acid complexes prepared with different amylose chain lengths; *Carbohydr. Polym.* 1995, 27: 47-52.

Gomi Y.I.; Fukuoka M.; Mihori T.; The rate of starch gelatinization as observed by PFG-NMR measurement of water diffusivity in rice starch/water mixtures*; J. Food Eng*. 1998, *36*: 359-369.

Han C. D., Multiphase Flow in Polymer Processing, London, 1981.

Hartmann M.H. (1998) in D. L. Kaplan (Ed.), Biopolymers from Renewable Resources, Springer-Verlag, Berlin, pp. 367–411.

Hsu C.L.; Heldman D.R.; Influence of glass transition temperature on rate of the rice starch retrogradation during low-temperature storage; *J. Food Proc. Eng.* 2005, 28: 506-525.

Hulleman S. H.; Janssen F. H. P.; Feil H.; The role of water during plasticization of native starches; *Polyme*r 1998, 39: 2043–2048.

Huneault M.A. and Li H.; Morphology and properties of compatibilized polylactide/thermoplastic starch blends, *Polymer* 2007, 48: 270-280.

Imam S.H.; Gordon S.H.; Mohamed A.; Harry-O'kuru R.; Chiou B.-S.; Glenn G.M.; Orts W.J.; Enzyme catalysis of insoluble cornstarch granules: Impact on surface morphology, properties and biodegradability; *Polym. Degrad. Stab.* 2006, 91: 2894-2900.

Imberty A; Buleon A; Tran V; Perez S.; Recent advances in knowledge of starch structure*; Starch:Staerke* 1991, 43: 375-384.

Imberty A; Chanzy H; Perez S; Buleon A; Tran V.; The Double Helical Nature of the Crystalline Part of A-Starch; *J. Mol. Biol.* 1988, 201: 365-378.

Jenkins P.J., Donald A.M.; Gelatinisation of starch: a combined WAXS/DSC and SANS study; *Carbohydrate Research* 1998, 308:133-147.

Jeroen J.G.; van Soest S.H.D.; Hulleman D.; de Wit J.F.G.; Vliegenthartbt; Crystallinity in starch bioplastics; *Industrial Crops. and Produc.* 1996, 5: 1l-22.

Jordhamo G.M.; Mason J.A.; Sperling L.H.; Phase continuity and inversion in polymer blends and simultaneous interpenetrating networks; *Polym. Eng. Sci.* 1986, 26: 517-524.

Kamal M.R.; Lai-Fook R. and Demarquette N.R.; Interfacial tension in polymer melts. Part II: Effects of temperature and molecular weight on interfacial tension; *Polym. Eng. Sci.* 1994, 34: 1834-1839.

Ke T. and Sun X..; Starch, poly(lactic acid) and poly(vinyl alcohol) composite. *Abstract submitted for AACC Annual Meeting* 2000, Nov. 5-9, Kansas City, Missouri.

Kesela C.De.; Lefevrea C.; Nagyb J.B.; Davida C.; Blends of polycaprolactone with polyvinylalcohol: a DSC, optical microscopy and solid state NMR study; *Polymer* 1999, 40: 1969–1978.

Kim C.H.; Jung K.M.; Kim J.S.; Park. J;K; Modification of aliphatic polyesters and their reactive blends with starch; *J. Polym.Envir.* 2004, 12: 179-187.

Kim C.H.; Young K.C.; Park J.K.; Reactive blends of gelatinized starch and polycarprolactone-g-glycidyl methacrylate; *J. Appl. Polym. Sci.* 2001, 6: 1507-1516.

Kim E.K.; Kim B.S.; Kim D.S.; Physical properties and morphology of polycaprolactone/ starch/pine-leaf composites; *J. Appl. Polym. Sic.* 2007, 103: 928-934.

Koo H.J.; Park S.H.; Jo J.S.; Kim B.Y. and Bail M.Y.; Gelatinization and retrogradation of 6-year-old Korean ginseng starches studied by DSC; *Lebensm.-Wiss.u.-Technol.* 2005, 38: 59-65.

Kulp K. And Lorenz K.; Heat-moisture treatment of starches. I. Physicochemical properties; *Cereal Chem.* 1981, 58: 46-48.

Kurdikar D.; Fournet L.; Slater S.C.; Paster M.; Gruys K.J.; Gerngross T. U. and Coulon R.; Greenhouse gas profile of a plastic material derived from a genetically modified plant; *J. Industr. Ecology* 2000, 4, 107-122.

Kweon D.K.; Kawasaki N.; Nakayama A.; Aiba S.; Preparation and characterization of starch/polycaprolactone blend; J. *Appl. Polym. Sci.* 2004, 92: 1716-1723.

Levine H.; Slade L.; A Polymer Physico-Chemical Approach to the Study of Commercial Starch Hydrolysis Products, *Carbohydr. Polym.* 1986, 6: 213-244.

Li Fa-De; Li Li-Te; Li Z.; Tatsumi, E.; Determination of starch gelatinization temperature by ohmic heating; *Journal of Food Engineering* 2004, 62: 113-120.

Li G, Sarazin P, Favis B.D. The Relationship between Starch Gelatinization and Morphology Control in Melt-Processed Polymer Blends with Thermoplastic Starch; *Macro. Chem. Phys.* 2008, 209: 991-1002.

Li J, Ma PL, Favis B.D. The Role of the Blend Interface Type on Morphology in Cocontinuous Polymer Blends; Macromolecules 2002, 35: 2005-2016.

Lillie M.A. and Gosline J.M.; The effects of hydration on the dynamic mechanical properties of elastin. *Biopolymers* 1990, 29: 1147-1160.

Lim K.Y.; Kim B. C.; Yoon K. J.; Structural and Physical Properties of Biodegradable Copolyesters from Poly(ethylene terephthalate) and Polycaprolactone Blends; *J. Appl. Polym. Sci.* 2003, 88: 131-138

Liu Q.; Charlet L.G.; Yelle S.; Arul J.; Phase transition in potato starch-water system I. Starch gelatinization at high moisture level*; Food Research International* 2002, 35: 397-408.

Lourdin D.; Coignard L.; Bizot H.; Colonna P.; Influence of equilibrium relative humidity and plasticizer concentration on the water content and glass transition of starch materials; *Polymer* 1997, 38: 5401-5406.

Lunt J; Large-scale production, properties and commercial applications of polylactic acid polymers. *Polym. Degrad. Stab.* 1998, 59: 145-152.

Ma PL, Favis B.D, Champagne MF, Huneault MA, Tofan F. Effect of Dynamic Vulcanization on the Microstructure and Performance of Polyethylene Terephthalate/Elastomer Blends.; *Polym. Eng. Sci.* 2002, 42: 1976-89.

Ma X, Chang P, Yu J, Wang N. Preparation and properties of biodegradable poly(propylene carbonate)/thermoplastic dried starch composites; *Carbohydrate Polymers* 2008, 71: 229-234.

Ma X. and Yu J.; The plasticizers containing amide groups for thermoplastic starch; *Carbohydr. Polym.* 2004, 57: 197-203

Ma X.F. and Yu J.G.; Formamide as the plasticizer for thermoplastic starch; *J. Appl. Polym. Sci.* 2004, 93:1769-1773.

Maaruf A.G.; Man Y.B.C; Asbi B.A.; Junainah A.H. and Kennedy J.F.; Effect of water content on the gelatinisation temperature of sago starch; *Carbohydrate Polymers* 2001, 46: 331–337.

Mariani P.; Neto A.; Silva J.;Cardoso E.; Esposito E.; Innocentini-Mei L.; Mineralization of poly(-caprolactone)/adipate mdified starch blend in agricultural soil; *J. Polym. Environ.* 2007, 15: 19-24.

Mathew A. P.; and Dufresne A.; Plasticized waxy maize starch: Effect of polyols and relative humidity on material properties. *Biomacromolecules* 2002, 3: 1101-1108.

Matzinos P, Tserki V, Kontoyiannis A, Pannayioyou C. Process and characterization of starch/ polycaprolactone products; Polym Degrad Stab 2002,77: 17-24.

Mekhilef N.; Favis B.D.; Carreau P.; Morphological stability, interfacial tension, and dual-phase continuity in polystyrene-polyethylene blends; *J. Polym. Sci., Part B: Polym. Phys.* 1997, 35: 293-308.

Mergaert J.; Ruffieux K.; Bourban C.; Storms V.; Wagemans W., Wintermante E. and Swings J.; In vitro biodegradation of polyester-based plastic materials by selected bacterial cultures; *J. Polym. Envir.* 2000, 8: 17-27.

Miles I.S. and Zurek A.; *Polym. Egn. Sci.* 1988, 28: 796-805.

Mondragón M.; Bello-Pérez L.A.; Agama-Acevedo E.; Betancur-Ancona D.; Peña J.L.; Effect of Cooking Time, Steeping and Lime Concentration on Starch Gelatinization of Corn During Nixtamalization; *Starch/Stärke*, 2004, 56: 248-253.

Morikawa K. and Nishinari K.; Effects of concentration dependence of retrogradation behaviour of dispersions for native and chemically modified potato starch; *Food Hydrocolloids* 2000, 14: 395-401.

Myllärinen P.; Buleon A.; Lahtinen R.; Forssell P. The crystallinity of amylose and amylopectin films; *Carbohydrate Polymers* 2002, 48: 41-48

Myllärinen P.; Buleon A.; Lahtinen R.; Forssell, P. Effect of glycerol on behaviour of amylase and amylopectin films; *Carbohydrate Polymers* 2002, 50: 355-361

Nayak P.L. Biodegradable polymers: Opportunities and challenges; *Journal of Macromolecular Science-Reviews in Macromolecular Chemistry and Physics,* 1999, 39: 481-505.

Ndife M.; Sumnu G.; Bayındırli L.; Differential Scanning Calorimetry Determination of Gelatinization Rates in Different Starches due to Microwave Heating; *Lebensm.-Wiss. u.-Technol.* 1998, 31: 484-488.

Nielsen L.E.; and Landel R.F.; In: *Mechanical Properties of Polymers and Composites,* Marcel Dekker, New York (1994) Chapter 7.

Normand F.; Granier A.; Leprince P.; Marec J.; Shi, M.K.; Clouet, F.; Polymer treatment in the flowing afterglow of an oxygen microwave discharge: Active species profile concentrations and kinetics of the functionalization; *Plasma chem. Plasma Process* 1995, 15: 173-198.

Otey F.H, Westhoff R.P, Doane W.M.; Starch Based Blown Films; *Ind. Eng. Chem. Prod. Res. Dev.* 1980, 19: 592–595.

Palav T.; Seetharaman K.; Mechanism of starch gelatinization and polymer leaching during microwave heating*; Carbohydrate Polymers,* 2006, 65: 364-370.

Parvinder S.; Walia; John W.; Lawton; Randal L.; Shogren; Mechanical properties of thermoplastic starch/poly(hydroxy ester ether) blends: Effect of moisture during and after processing ; *J Appl. Polym. Sci.*2002, 84: 121-131

Patel M., Bastioli C., Marini L and Würdinger E. (2003). Life-Cycle assessment of bio-based polymers and natural fiber composites. In *Biopolymers,* Volume 10, General Aspects and Special Applications Ed. Alexander Steinbüchel, John Wiley & Sons Inc.

Paula Cristina Sousa F. Tischer, Miguel D. Noseda, Rilton Alves de Freitas, Maria Rita Soerakowski, Maris Eugenia R. Duarte; Effects of iota-carrageenan on the rheological properties of starches; *Carbohydrate polymers* 2006, 65: 49-57.

Peanasky J.; Long J.; Wool R.P.; Percolation Effects in Degradable Polyethylene- Starch Blends; *J. Polym. Sci. Polym. Polym. Phys.* 1991, 26: 565-579.

Perry P.A. and Donald A.M.; The effect of sugures on the gelatinization of starch; *Carbohydrate Polymers* 2002, 49: 155-165.

Perry P.A. and Donald A.M.; The role of plasticization in starch granule assembly; *Biomacromolecules* 2000, 1: 424-432.

Pitt C.G., Chasaldo F.J., Hibionada J.M., Klina D.M. and Schindler A.; *Appl. Polym. Sci.* 1981, 28: 3779-3787.

Pitt C.G., Maeks T.A. and Schindler A., In Controller Release of Bioactive Materials, ed, R. Baker. Academic Press, NY, 1980, P9

Potts J.E., In aspect degradation and stabilization of polymers; Jelinek, H.H.G.; Elsevier: Amsterdam, 1978; P 617

Potts J.E., in Kirk-Othmer Encyclopeida of chemical Technology, Suppl. Vol., ed. M. Graysong. Wiley-Interscience, NY, 1984, P626

Pyun A, Bell JR, Won KH, Weon BM, Seol SK, Je JH. Synchrotron X-ray Microtomography for 3D Imaging of Polymer Blends; M*acromolecules* 2007, 40: 2029-2035.

Reignier J, Favis B.D. Measuring the Interfacial Tension of Polyamide/Polyethylene and Polycarbonate/Polypropylene Blends: Effect of Temperature; *Macromolecules* 2000, 33: 6998-7008.

Rodriguez Gonzalez FJ. PhD Thesis 2002, pp. 181.

Rodriguez-Gonzalez FJ, Ramsay B.A, Favis B.D.; Rheological and Thermal Properties of Thermoplastic Starch With High Glycerol Conten; *Carbohydrate Polymers* 2004;58:139-147.

Rodriguez-Gonzalez FJ, Ramsay B.A, Favis B.D.; High Performance LDPE/Thermoplastic Starch Blends: A Sustainable Alternative to Pure Polyethylene; Polymer 2003, 44: 1517-26.

Rodriguez-Gonzalez FJ, Virgilio N, Ramsay B.A, Favis B.D.; Influence of Melt Drawing on the Morphology of One- and Two-Step Processed Ldpe/Thermoplastic Starch Blends; *Adv Polym Techn* 2003, 22: 297-305.

Rodriguez-Gonzalez, F.J.; Ramsay, B.A.; Favis B.D.; Rheological and thermal properties of thermoplastic starch with high glycerol content; *Carbohydrade Polymer* 2004, 58: 139-147.

Rodriguez-Gonzalez1 F.J., Ramsay B.A., Favis B.D.; High performance LDPE/ thermoplastic starch blends: a sustainable alternative to pure polyethylene; *Polymer* 2003, 44: 1517–1526.

Roper H. and Koch H.; The role of starch in biodegradable thermoplastic materials; *Starch*, 1990, 42: 123-130.

Roulet Ph.; Raemy A. and Wuersch P.; Retrogradation kinetics of concentrated gelatinized wheat starch in gels or powders; a comparative study by rigidity modulus, differential scanning calorimetry (DSC) and x-ray diffraction; *Food Hydrocolloids* 1987, 1: 575-578.

Sailaja RRN, Chanda M.Use of maleic anhydride-grafted polyethylene as compatibilizer for HDPE-tapioca starch blends: Effects on mechanical properties; *J Appl Polym Sci;* 2001, 80: 863-72.

Saltikov S.A. Proceedings of the second international congress for stereology. Springer-Verlag,Berlin, 1967.

Sarazin P, Li G, Orts WJ, Favis B.D.; Binary and Ternary Blends of Polylactide, Polycaprolactone and Thermoplastic Starch; *Polymer* 2008, 49: 599-609.

Shi R.; Liu Q.; Ding T.; Han Y.; Zhang L.; Chen D.; Tian W.; Ageing of soft thermoplastic starch with high glycerol content; *J. Appl. Polym. Sci.* 2007, 103: 574-586.

Shin B.Y., Lee S., Shin Y.S., Balakrishan S. and Narayan R.; Rheological, mechanical and biodegradation studies on blends of thermoplastic starch and polycaprolactone; *Polym. Eng. Sci.* 2004, 44: 1429-1438.

Shin BY, Narayan R, Lee SI, Lee TJ. Morphology and rheological properties of blends of chemically modified thermoplastic starch and polycaprolactone; *Polym. Eng. Sci.* 2008, 48: 2126-2133.

Shogren H.L.; Effect of moisture content on the melting and subsequent physical aging of corn starch; *Carbohydr. Polym.* 1992, 19: 83-90.

Singh R.P.; Pandey J.K.; Rutot D.; Degee Ph.; Doubois Ph.; Biodegradation of poly(e-caprolactone)/starch blends and composites in composting and culture environments: the effect of compatibilization on the inherent biodergradability of the host polymer; *Carbohydrate research* 2003, 338: 1759-1769.

Smits A.L.M.; Kruiskamp P.H.; van Soest J.J. Vlieganthart G.; Interaction between dry starch and plasticizers glycerol or ethylene glycol, measured by differential scanning calorimetry and solid state NMR spectroscopy; *Carbohydrate Polymer* 2003, 53: 409-416.

Sopade A.; Halley P.J. and Junming L.L.; Gelatinisation of starch in mixture of sugars. I. Dynamic rheological properties and behaviours of starch-honey systems; *J. Food Eng.* 2004, 61: 439-448.

Souza Rosa R.C.R.; Andrade C.T.; Effect of chitin addition on injection-molded thermoplastic corn starch; *J. Appl. Polym. Sci.* 2004, 92: 2706-2713.

Souza Rosa R.C.R.; Andrade C.T.; Investigation of the gelatinization and extrusion processes of corn starch; *Adv. Polym. Techn*. 2002, 21: 17-24.

Spigno G.; De Faveri D.M.; Gelatinization kinetics of rice starch studied by non-isothermal calorimetric technique: influence of extraction method, water concentration and heating rate; *J. of Food Eng.* 2004, 62: 337-344.

St Lawrence S.; Walia P.; Felker F.C.; Willett J.L.; Starch Filled Ternary Polymer Composites Ii: Room Temperature Tensile Properties; *J. Polym. Eng. Sci.* 2004, 44: 1839-1847.

Stading M; Rindlav-Westling A.; Gatenholm P. Humidity-induced structural transitions in amylase and amylopectin films; *Carbohydrate Polymers* 2001, 45: 209-217.

St-Pierre N, Favis B.D, Ramsay B.A, Ramsay J.A, Verhoogt H.; Processing and Characterization of Thermoplastic Starch/Polyethylene Blends; Polymer 1997, 38: 647-55.

Swift G.; Expectations for biodegradation testing methods; *Biodegradable Plastics and Polymer;* Ed. Y. Doi and K. Fukuda, Elsevier, Amsterdam, 1993, p. 228-236.

Taguet A, Huneault M.A, Favis B.D.; Interface/morphology relationships in polymer blends with thermoplastic starch; *Polymer*, 2009, 50: 5733-5743.

Takacs E.S. and Vlachopoulos J. Biobased, biodegradable polymers for biomedical applications: properties and process; *Plast. Eng.* 2008, 10: 28-33.

Talja R.A.; Hehen H.,; Roos Y.H.; Jouppila K.; Effect of various polyols and polyol contents on the physical and mechanical properties of potato starch based films; *Carbohydrate polymers* 2007, 67: 288-295.

Tan I.; Wee C.C.; Sopade P.A.; Halley P.J.; Investigation of the starch gelatinisation phenomena in water–glycerol systems: application of modulated temperature differential scanning calorimetry ; *Carbohydrate Polymers* 2004, *58*: 191-204.

Tananuwong K. and Reid D.S.; Differential scanning calorimetry study of glass transition in frozen starch gels; *J. Agric. Food Chem.* 2004, 52: 4308-4317.

Tang M.C. and Copeland L; Analysis of complexes between lipids and wheat starch, *Carbohydrate Polymers* 2007, 67: 80–85.

Tang M.C. and Les Copeland; Investigation of starch retrogradation using atomic force microscopy, *Carbohydr. Polym.* 2007, 70: 1-7.

Taylor GI. Proceedings of the Royal Society of London 1934, 146(A):501-523

Temsiripong T.; Pongsawatmanit R.; Ikeda S.; Nishinarib K.; Influence of xyloglucan on gelatinization and retrogradation of tapioca starch; *Food Hydrocolloids* 2005, 19: 1054-1063.

Tester R.F.; Karkalas J. and Qi X.; Starch-composition, fine structure and architecture; *J. Cereal Sci.* 2004, 39: 151-165.

Thakore I.M.; Desai S.; Sarawade B.D.; Devi S.; Study on biodegradability, morphology and thermomechanical properties of LDPE/modified starch blends; *Eueop. Polym. J.* 2001, 37: 151-160.

Thomas S. and George A.; Dynamic mechanical properties of thermoplastic elastomers from blends of polypropylene with copolymers of ethylene with vinyl acetate; *Eur. Polym. J.* 1992, 28: 1451-1458.

Tischer PCSF, Noseda MD, de Freitas RA, Soerakowski MR, Duarte MER. Effects of iota-carrageenan on the rheological properties of starches
; Carbohydrate Polymers 2006, 65: 49-57.

Tomotika S.; On the Instability of a Cylindrical Thread of a Viscous Liquid Surrounded by Another Viscous Fluid; *Proc. R. Soc. London (A)* 1935, 150: 322-337.

Tsuji H., Ishizaka T.; Blends of aliphatic polyesters. VI. Lipase-catalyzed hydrolysis and visualized phase structure of biodegradable blends from poly(e-caprolactone) and poly(L-lactide); *Inte. J. Bio. Macro.* 2001, 29: 83–89.

Van Soest, J.J.G. and Knooren, N.; Influence of glycerol and water content on the structure and properties of extruded starch plastic sheets during aging; *J. Appl. Polym. Sci.* 1997, 64: 1411-1422.

Van Soest,J.J.G.; Hulleman,S.H.D.; Wit D. and Vlienthart, J.F.G.; Crystallinity in starch bioplastics; *Industrial Crops and Products* 1996, 5**:** 11–12.

Veenstra H, Norder B, van Dam J, Posthuma de Boer A. Stability of co-continuous apolystyrene / poly(ether-ester) blends in shear flow; *Polymer* 1999, 40: 5223-5226.

Veenstra H, Van Lent B, Van Dam J, Posthuma de Boer A. Formation and stability of co-continuous blends with a poly(ether-ester) block copolymer around its order-disorder temperature ; *Polymer* 1999, 40: 1119-1130.

Venstra H, Van Dam J, Posthuma de Boer A. On the coarsening of co-continuous morphologies in polymer blends : effect of interfacial tension, viscosity and physical cross-links; Polymer 2000, 41: 3037-3045.

Vikman M., Hulleman S.H.D., Van D. Z. M., Rinen P.M., Feil H.; Morphology and enzymatic degradation of thermoplastic starch–polycaprolactone blends; *J. Appl. Polym. Sci.* 1999, 74: 2594–2604

Walia P.S., Lawton J.W., Shogern R.L.; Mechanical properties of thermoplastic starch/poly(hydroxy ester ether) blends: effect of moisture during and after processing; *J. Appl. Polym. Sci.* 2002, 84: 121-131.

Walia P.S.; Lawton J.W.; Shogren R.L.; Felker F.C.; Effect of moisture level on the morphology and mely flow behavior of thermoplactic starch/poly(hydroxyl ester ether) blends, *Polymer* 2000, 41: 8083-8093.

Wilhelm H.M.; Sierakowski M.R.; Reicher F.; Wypych F. Souza G.; Dynamic rheological properties of Yam starch/hectorite composite gels, *Polymer Interbational* 2005, 54: 814-822.

Willemse R.C.; Co-continuous morphologies in polymer blends: stability; *Polymer* 1999, 40: 2175-2178.

Willemse R.C.; Ramaker E.J.J, Van Dam J, Posthuma de Boer A. Coarsening in molten quiescent polymer blends: The role of the initial morphology; *Polym. Eng. Sci*. 1999, 39: 1717-1725.

Willett J.L.; Jasberg B.K.; Swanson C.L.; Rheology of thermoplastic starch: Effects of temperature, moisture content, and additives on melt viscosity; *Polym. Eng. Sci.* 1995, 5: 202-210

Willett J.L.Mechanical properties of LDPE/granular starch composites; *J Appl. Polym. Sci.* 1994, 54: 1685-95.

Wool R.P.; Raghavan D.; Wagner G.C.; Billieux S.; Biodegradation dynamics of polymer-starch composites; *J. Appl. Polym. Sci.* 2000, 77: 1643-1657.

Wu C.S.; Performance of an Acrylic acid grafted polycaprolactone/starch composite: characterization and mechanical properties; *J. Appl. Polym. Sci*. 2003, 80: 2888-2895

Wu C.S.; Physical properties and biodegradability of maleated-polycaprolactone/ starch composite; *Polym. Degrad. Stab.* 2003, 80: 127-134

Wu S.; Brzozowski, K.; Surface free energy and polarity of organic pigments, *J. Colloid Interface Sci.* 1971, 37: 686-690.

Wu S.; Formation of dispersed phase in incompatible polymer blends: Interfacial and rheological effects; *Polym. Eng. Sci.* 1987, 27: 335-343.

Yu L. and Christie G.; Measurement of starch thermal transitions using differential scanning calorimetry, *Carbohydr. Polym.*2001, 46: 179-184.

Yuan Z, Favis B.D.; Coarsening of immiscible co-continuous blends during quiescent annealing; *AIChE J* 2005, 51: 271-280.

Yuan ZH, Favis B.D.; Influence of the efficacy of interfacial modification on the coarsening of cocontinuous PS/HDPE blends during quiescent annealing; *J of Polym Sci. Part B: Polym Phys* 2006, 44: 711-721.

Zanoni, B.; Schiraldi, A.; Simonetta, R.; A native model of starch gelatinization kinetics; *J. Food Eng*. 1995, 24: 25-33.

Zhou Y., Hoover R., Liu Q.; Relationship between a-amylase degradation and the structure and physicochemical properties of legume starches; *Carbohydr. Polym.* 2004, 57: 299-317.

Zobel H.F.; Molecules to granules: a comprehensive starch review; *Starch* 1988, 40: 44-50.

APPENDICES

APPENDIX A: BINARY AND TERARY BLENDS OF POLYLACTIDE, POLYCAPROLACTONE AND THERMOPLASTIC STARCH

Pierre Sarazin [a], Gang Li [a], William J. Orts [b], Basil D. Favis [a,*]

[a] *CREPEC, Department of Chemical Engineering, Ecole Polytechnique de Montréal, P.O. Box 6079, Station Centre-Ville, Montréal, Quebec, Canada H3C 3A7*
[b] *USDA, ARS, Western Regional Research Center, 800 Buchanan Street, Albany, CA 94710, USA*

Received 18 July 2007; received in revised form 6 November 2007; accepted 10 November 2007
Available online 19 November 2007

Abstract

In this study binary and ternary blends of polylactide (PLA), polycaprolactone (PCL) and thermoplastic starch (TPS) are prepared using a one-step extrusion process and the morphology, rheology and physical properties are examined. The morphology and quantitative image analysis of the 50/50 PLA/TPS blend transverse phase size demonstrate a bimodal distribution and the addition of PCL to form a ternary blend results in a substantial number of fine dispersed particles present in the system. Focused ion beam irradiation, followed by atomic force microscopy (AFM) shows that dispersed PCL forms particles with a size of 370 nm in PLA. The TPS phase in the ternary blends shows some low level coalescence after a subsequent shaping operation. Dynamic mechanical analysis indicates that the temperature of the tan δ peak for the PLA is independent of TPS blend composition and that the addition of PCL in the ternary blend has little influence on the blend transitions. Both the α and β transitions for the thermoplastic starch are highly sensitive to glycerol content. When TPS of high glycerol content is blended with PLA, an increase in the ductility of the samples is achieved and this effect increases with increasing volume fraction of TPS. The ternary blend results in an even greater ductility with an elongation at break of 55% as compared to 5% for the pure PLA. A substantial increase in the notched Izod impact energy is also observed with some blends demonstrating three times the impact energy of pure PLA. The mechanical properties for the ternary blend clearly indicate a synergistic effect that exceeds the results obtained for any of the binary pairs. Overall, the ternary blend approach with PLA/TPS/PCL is an interesting technique to expand the property range of PLA materials.

Keywords: Thermoplastic starch; Polylactide; Polycaprolactone

1. Introduction

Environmental concern over the use of traditional petroleum-based polymers has stimulated the development of polymers from renewable resources as an alternative. Starch, as the main reserve polysaccharide of higher plants, is a naturally occurring biopolymer and is of low cost. Starch consists of two main polysaccharides, amylose and amylopectin, based on chains of 1 → 4 linked α-D-glucose [1]. Amylose is essentially linear, amylopectin, often the major part (about 72% in wheat and maize starches), is highly branched containing on average one branch point which is 1 → 4 → 6 linked for every 20–25 straight chain residues [1]. The starch granule is partially crystalline, and various crystalline forms are reported, depending on the proportion of the two main polysaccharides and the regions in the starch granules. Since the melting temperature (T_m) of pure dry starch is close to 220–240 °C and the onset temperature of starch degradation is around 220 °C [2], native starch has to be modified in order to be melt-processed as a thermoplastic.

The addition of water to starch is known to have a strong plasticizing effect, causing a large decrease in the glass transition temperature (T_g) [3]. When starch is usually heated in the presence of water the native crystalline structure is disrupted, a phenomenon known as gelatinization. In an excess of water, above the gelatinization temperature, the starch granule loses

* Corresponding author. Tel.: +1 514 340 4711x4527; fax: +1 514 340 4159.
E-mail address: basil.favis@polymtl.ca (B.D. Favis).

0032-3861/$ - see front matter © 2007 Elsevier Ltd. All rights reserved.
doi:10.1016/j.polymer.2007.11.029

its native crystalline order and swells irreversibly to many times its original size [1]. In native wheat starch the granule size distribution is bimodal [4] and the different sizes display somewhat different gelatinization behavior [5,6]. Although water is a ubiquitous plasticizer of starch, it is volatile, and cannot be used to produce utilizable plastic-like materials. For this reason, the use of other, non-volatile, plasticizers, such as glycerol, are often used in combination with water. Glycerol appears to be a less effective plasticizer than water [7]. However, Perry and Donald [8] have shown that gelatinization proceeds even when no water is present: there is no chemical requirement for water, the only requirement being mobility, induced by some low molecular weight plasticizer. However, without water the temperature for the onset of gelatinization by glycerol increased [9,10]. Upon heating, starch granules become solvated, with the amorphous regions of the plasticized starch granule. This transformation of granular starch into a thermoplastic-like material allows it to be processed in a similar fashion to conventional polymers. At glycerol contents in the TPS lower than 10–15%, the plasticization leads to reduced mechanical properties [11]. A more effective plasticization can be obtained at higher glycerol contents, in a range where glycerol demixing can occur in the thermoplastic starch. Thermoplastic starch itself is characterized by moisture sensitivity and weak mechanical properties as compared with other thermoplastic polymers. Blends of other polymers with thermoplastic starch represent an important route to overcome these limitations.

Crop-based polylactide (PLA) is an example of a promising biopolymer prepared through a combination of biotechnology and chemistry. Polylactide is prepared from 100% renewable resources such as corn, sugar beets or rice [12]. Blending thermoplastic starch with PLA is a route to reduce raw material costs, energy consumption and also to increase its rate of biodegradation. Avérous and Martin [13] and also Park et al. [14] were the first to study TPS/polylactide blends. The gelatinized starch was prepared with various water/glycerol ratios and was then dried. After that, the dry blend was mixed using a batch mixer or extruded with a single-screw extruder. Martin and Avérous [13] observed that the modulus decreased when the TPS fraction increased. In comparison to the pure TPS and PLA materials, all the blends showed a marked decrease in the elongation at break, tensile strength and impact resistance. They explained the poor mechanical properties by the lack of affinity between the two phases. The morphology of their TPS/PLA 75/25 (wt.%) blends was characterized by a TPS continuous phase with large and non-uniform PLA domains exhibiting phase sizes in the 10–100 μm range.

Poly(ε-caprolactone) (PCL) is a well-known synthetic, biodegradable, semi-crystalline polyester, characterized by a high elongation at break. Its low melting point of around 60 °C is often perceived as an impediment for use as a common thermoplastic. However, since PCL and PLA have complementary strengths and weaknesses as polymer materials, PCL could be an interesting candidate to moderate the brittle behavior of PLA.

Previous work from this laboratory has shown that a one-step extrusion process can be used to prepare polyethylene/TPS blends with excellent properties [15]. In that process, the plasticization of starch (from a suspension of starch, glycerol and water), devolatilization of water and blending of TPS with the carrier polymer were all achieved in one single extrusion operation. The PE/TPS blends prepared in this fashion demonstrate levels of ductility and modulus similar to the virgin polyethylene even at very high loadings of TPS. This blend preparation approach is particularly effective at achieving high loadings of the glycerol plasticizer in starch and it has been shown [15–17] that loadings in excess of 28% glycerol are necessary in order to achieve a TPS phase that is sufficiently deformable to carry out morphology control protocols in blend systems.

The objectives of this research are to examine the morphology and properties of PLA/PCL/TPS binary and ternary blends prepared via a one-step melt processing operation.

2. Experimental

2.1. Materials

The wheat starch was obtained from ADM, while the glycerol was provided by MAT Laboratories. Polylactide was supplied by Cargill LLC (non-commercial grade 5729B) and polycaprolactone by Solvay-Interox ($M_w = 80{,}000$ g/mol, MFI = 3 g/10 min at 160 °C). Throughout this paper the designations TPS36 and TPS24 refer to 36% and 24% glycerol in the thermoplastic starch respectively.

2.2. Processing

The extrusion system was composed of a single-screw extruder connected to a co-rotating twin-screw extruder. The starch/excess water/glycerol suspension was fed in the first zone of the twin-screw extruder set at 150 rpm, while polylactide was fed in the single-screw extruder. After gelatinization and plasticization of the starch followed by extraction of the volatiles, TPS was mixed with the molten polylactide on the twin-screw extruder. The temperature in the zones crossed by polylactide was set at 150 °C. The draw ratio of the strands exiting the die was held at 1. All the blend compositions are given in weight fractions. More details concerning the extrusion process are reported elsewhere [15,18].

The starch suspensions destined to be fed to the twin-screw extruder were prepared in the following proportions: 48.5 wt.% of starch, 28.15 wt.% of glycerol and 23.35 wt.% of excess water for TPS36, and 48.5 wt.% of starch, 15.65 wt.% of glycerol and 35.85 wt.% of excess water for TPS24. The starch is used as-received, without drying. The water used for gelatinization was subsequently removed through venting in the zone just before the connection with the single screw. TPS36 and TPS24 contained about 36 and 24 wt.% glycerol after extrusion, respectively.

The various compositions were extruded under the same conditions, and granulated after air cooling. Pure PLA was also re-extruded. The feeding rate of the starch slurry was approximately the same for all the compositions and was held to

obtain 40–45 g/min of TPS. The feeding rate of PLA + PCL was adjusted for each blend composition. For terblends and also for PLA/PCL blends, binary dry blends of PLA and PCL were prepared by initially dry blending the corresponding pellets. True compositions were measured from the thermal decomposition of the pellets using thermal gravimetric analysis (TGA) as reported previously [19].

The compounded pellets were then used to prepare ASTM D638 Type I standard tensile dog-bone specimens and Izod type test specimens by injection molding on a Sumitomo SE50S machine. The temperature profile was 150/150/155/160 °C from the feeder to the mold. The nominal width and thickness of the tensile bars were 10 and 3 mm, respectively. The dimensions of the Izod impact bar were 63 × 12.6 × 4.7 mm. The cross-section surface at the 3 mm-depth notch was around 47 mm^2. No demolding agent was used in injection molding.

2.3. Blend morphology and image analysis

The specimens were microtomed to create a perfect plane face using a cryogenic Leica microtome with a glass knife. To increase the contrast between the polymer phases, selective solvent extractions were performed at room temperature. The TPS was extracted for 3 h in 3N HCl. The specimens were soaked in water and then dried in a vacuum oven. After coating with a gold–palladium alloy, the microtomed specimens were observed under a Jeol JSM 840 scanning electron microscope. Morphologies in the center of the microtomed cross section of the strands after extrusion and Izod impact bars are presented. Image analysis was carried out using a digitizing table from Wacom to evaluate the volume and number average diameters, d_v and d_n respectively. SEM micrographs of ×500 and ×1000 magnification were used.

2.4. Atomic force microscopy (AFM)

After the preparation of the surface by microtomy at room temperature, morphological observations of specimens PLA/PCL/TPS36 50/0/50 and 40/10/50 were carried out in tapping mode using a Multimode AFM from Veeco equipped with a Nanoscope IV controller. Silicon tips, from Pacific Nanotechnology, with spring constant of 42 N/m and resonant frequency of 320 kHz were used. Also, a binary blend of PLA/PCL was cryogenically cut, plasma-coated and then prepared using a focused ion beam (FIB) following the procedure developed by Virgilio et al. [20] to reveal the size of PCL domains in a PLA matrix.

2.5. Rheology

A dual-bore capillary rheometer (single barrel Rosand RH-7) was used to measure the viscosities of pure PLA and blends at high shear rates at 165 °C. For the rheological experiments, it should be mentioned that the pure PLA used was the original as-received. Using dies of the same diameter (1 mm, with an entrance angle of 180°), simultaneous measurements were carried out on both long and short dies (0.25 and 20 mm) to determine the inlet pressure drop at the die, and therefore the absolute viscosity, using the Bagley correction method. The Rabinowitch correction was also applied to calculate the true shear rate.

2.6. Thermal properties of blends by dynamic mechanical thermal analysis

DMTA experiments, performed on a 2980 DMA from TA Instruments, were conducted on Izod specimens for TPS/PLA, TPS/PLA + PCL blends and also on bars for PLA/PCL binary blends (molded by compression, 63 × 12.5 × 2 mm). The specimens were tested in the single cantilever bending mode at a frequency of 1 Hz with a target amplitude of 40 μm. The scanning rate was set at 2°/min in the range of −100 to 90 °C. The thermal transitions were determined from the maxima of the tan δ peaks, analyzed using the TA Instruments Universal Analysis 2000 software.

2.7. Mechanical properties

All the mechanical property measurements were performed at room temperature on injection molded blends. Tensile strength, elastic modulus and elongation at break were measured on a mechanical tensile tester (Instron 4400R) equipped with a 5kN cell, according to the ASTM D638 method. A crosshead speed of 5 mm/min was used. Ten specimens were used for each blend condition.

Izod impact tests were performed on notched samples on a Custom Scientific Instruments impact tester, equipped with a 5.42 J pendulum, according to ASTM D256 method. The units of energy are typically reported in J/m since the ASTM standard defines a constant thickness of samples. Ten specimens were used for each blend condition. Complete break and some hinge break modes were obtained. Only the complete breaks, as according to ASTM, are reported.

3. Results and discussion

3.1. Morphology and rheology

Fig. 1 presents the morphology of the native wheat starch granules and the typical morphology of the PLA/TPS blends. Wheat starch granules are characterized by a bimodal size distribution: large A-type, lenticular granules with a diameter of 10–35 μm as well as small B-type, spherical granules with a diameter of 1–10 μm are present [4,21]. Choi and Kerr [22] estimated the average diameters as 20.4 μm for the A-type and 2.3 μm for the B-type. In this study, the volume and number average diameters d_v and d_n for the starch granules are found to be 15.8 and 8.9 μm, respectively (Table 1). The morphology of the blends also reveals a bimodality for the size of dispersed TPS phase (Fig. 1b). Large deformed domains and small particles of plasticized starch coexist. It is known that the granule types can have significant differences in chemical composition and functional properties. The amylose/amylopectin ratio, for example, can have an

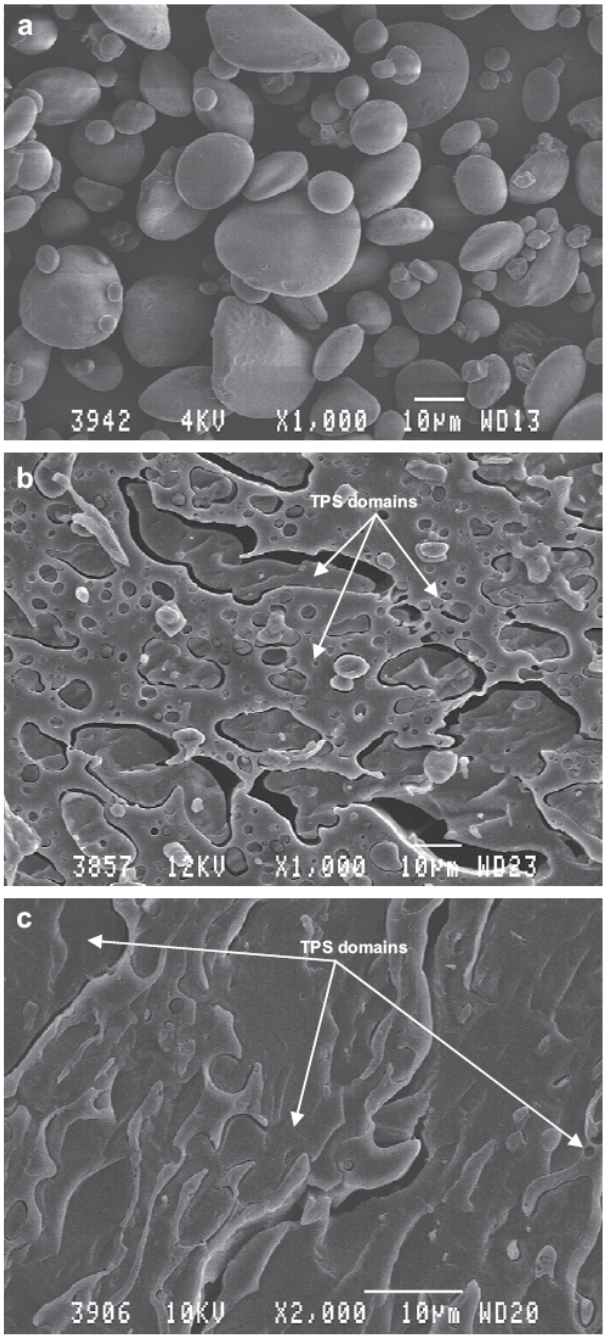

Fig. 1. Scanning electron micrographs of (a) pure wheat starch, (b) PLA/TPS36 50/50 blend and (c) PLA/TPS36 30/70 blend. The white bar indicates 10 µm.

effect on gelatinization characteristics. Van Hung and Morita [23] measured the amylose content for the two types of granules: 30% for the A-type and 23% for the B-type. Large starch granules swell more easily than small granules and the more amylose that a starch contains, the more swelling it requires for gelatinization. Peng et al. [24] showed that A-type starch granules contain higher amylose concentrations and had higher gelatinization enthalpies than did B-type starch granules. Although A- and B-type starch granules start to gelatinize at a similar temperature, B-type starch granules had a higher gelatinization peak and completion temperatures than did A-type starch granules. Large TPS domain sizes, around 20 µm, can be found even at low TPS concentration, as shown in Fig. 2a and b. This indicates that some of the large starch granules have not fragmented. Eventually, the production of blends which separates out the two types of granules could be an approach to truly study the origin of the bimodal size distribution of the TPS phase in these blends. At 50% TPS, the TPS phase is not completely continuous while at 70% TPS, the blend appears to be virtually co-continuous (Figs. 1c and 2d).

Table 1
Native starch particle size and TPS phase sizes obtained by image analysis on SEM micrographs

Materials	d_n (µm)	d_v (µm)
Wheat starch	8.9	15.8
PLA/PCL/TPS36		
50/0/50 extruded	2.9	12.9
50/0/50 molded	3.9	16.3
40/10/50 extruded	1.4	12.1
40/10/50 molded	3.3	12.1

Fig. 2c and e shows that 10% of PCL in the 50% TPS blends improves the dispersion of the well-plasticized TPS phase in the PLA matrix (the plasticization step is unchanged) and the number of the smaller TPS phase domains is visibly increased. The number average diameter of the TPS domains is halved after addition of 10% of PCL to a PLA/TPS blend, while the d_v remains the same (Table 1).

In order to further understand the morphology adopted by PCL in PLA, a FIB/AFM micrograph of the PCL/PLA blend was prepared and is shown in Fig. 3. The particle sizes are extremely small with a d_v of 510 nm and a d_n of 370 nm. Such small phase sizes in polymer blends are often an indication of some partial miscibility. However, DMTA experiments carried out on PLA/PCL binary blends (shown in Table 2) indicate no shifts in the T_g of PCL (-47.3 ± 1.0 °C) or PLA (about 63 °C) with PLA/PCL blend composition as measured using the tan δ peak. The PCL/PLA binary blend is clearly fully immiscible.

Polymer blends generally demonstrate a significant coarsening of the dispersed phase after injection molding. Fig. 2 indicates that the gross morphology for the blends in this study is preserved after the injection molding process. However, detailed image analysis in Table 1 demonstrates some low level coarsening of the dispersed phase for both binary PLA/TPS and PLA/PCL/TPS ternary blends. In the latter case the coarsening effect is more pronounced for the smaller particles in the system. For blends with TPS24, large phase domains are found (not shown here) and the addition of PCL does not influence the morphology. For this plasticizer level under the experimental conditions used, the TPS phase is formed from agglomerated starch granules, is partially plasticized, and cannot totally flow as a thermoplastic.

The viscosity of the binary PLA/TPS blends as a function of shear rate is shown in Fig. 4. In the typical range of

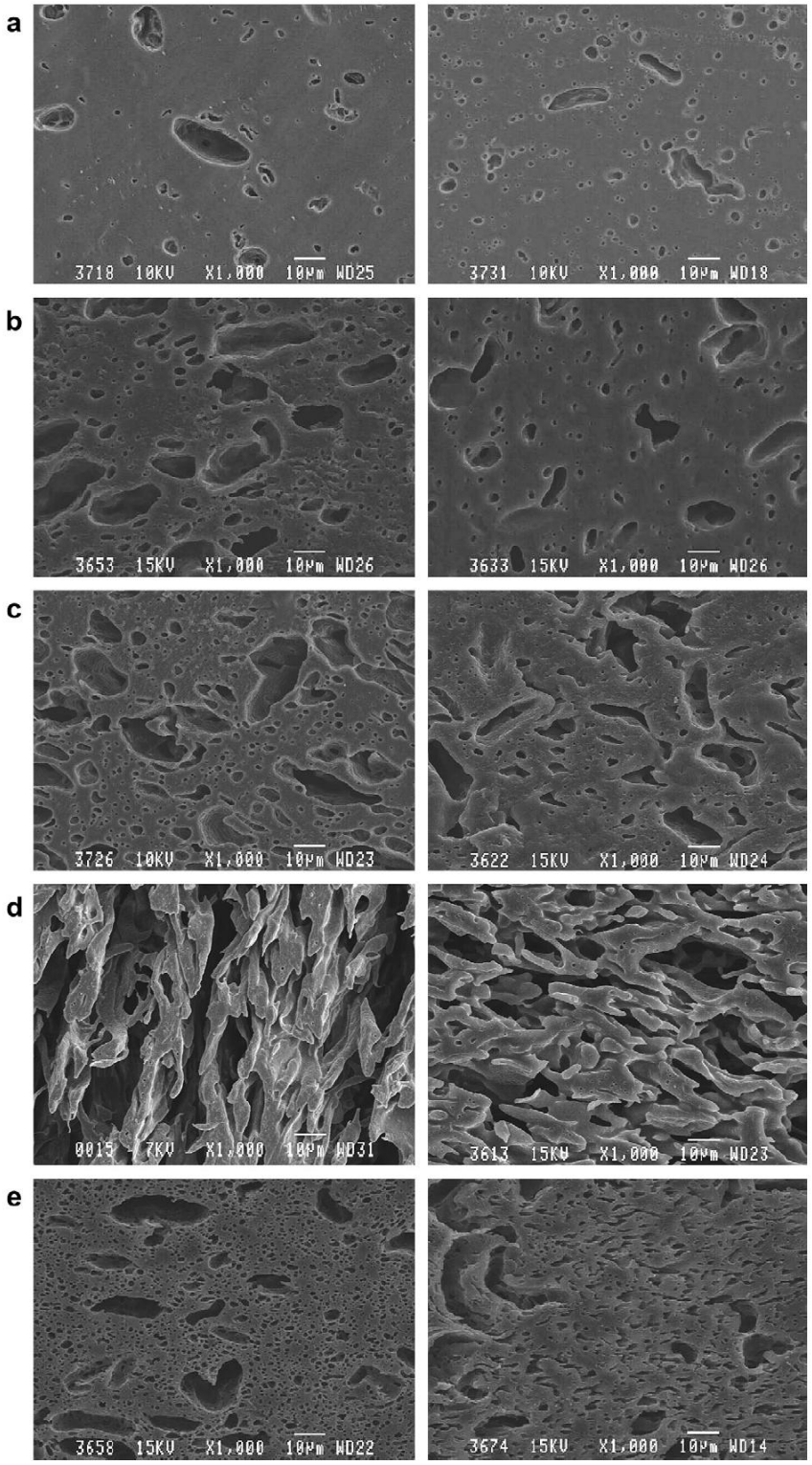

Fig. 2. SEM micrographs after TPS extraction for PLA/PCL/TPS36 blends in the transverse direction after one-step extrusion (first column) and injection molding (second column): (a) 90/0/10; (b) 70/0/30; (c) 50/0/50; (d) 30/0/70; (e) 40/10/50. The white bar indicates 10 μm.

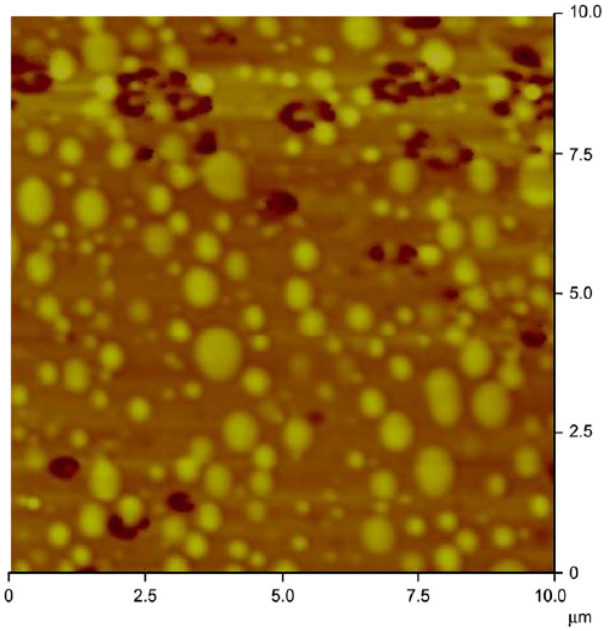

Fig. 3. Morphology obtained by FIB/AFM on PLA/PCL 75/25 blend.

processing shear rates (100–1000 s^{-1}), it can be clearly seen that the TPS containing 36% glycerol significantly reduces the blend viscosity as compared to pure PLA. This effect becomes more and more pronounced as TPS concentration increases. This viscosity reduction phenomenon is due to the presence of glycerol since TPS with 24% glycerol (Fig. 4b) shows much less of the effect. These results are important since they indicate that the optimal processing conditions for shaping operations of TPS blends could be quite different as compared to those for pure PLA. These results are also important since they indicate an increased benefit of TPS as a processing aid during melt processing. It should thus be possible to significantly reduce processing temperatures in shaping operations and hence lead to important energy reductions resulting from the use of TPS blends.

Table 2
Transition temperatures measured from tan δ (DMTA)

PLA/PCL	T_g PCL (°C)		T_g PLA (°C)
0/100	−47.2		–
25/75	−46.1		Not measured
50/50	−47.4		63.3
75/25	−48.5		63.9
100/0	–		62.8
PLA + PCL/TPS36	T_β (°C)	T_α (°C)	T_g PLA (°C)
70 + 0/30	−57.8	−5.9	62.8
50 + 0/50	−55.7	−8.6	63.1
30 + 0/70	−57.2	−7.6	62.1
47.5 + 2.5/50	−57.7	−8.6	61.9
40 + 10/50	−57.4	−9.2	62.5
PLA + PCL/TPS24	T_β (°C)	T_α (°C)	T_g PLA (°C)
70 + 0/30	−45.6	14.0	62.5
50 + 0/50	−46.7	24.5	61.2
30 + 0/70	−49.9	19.0	61.7
45 + 5/50	−46.3	20.6	62.7

3.2. Transition temperatures in the blends, measured by DMTA

The transition temperatures for TPS/PLA and TPS/PLA + PCL blends were measured by DMTA. Fig. 5a indicates that at temperatures lower than approximately −57 °C, the TPS36 phase has the higher storage modulus. At higher temperatures, the PLA phase becomes the more rigid component. The evolution of tan δ versus temperature shows three transitions (Fig. 5b and c). The higher temperature, at about 62–63 °C, corresponds to the glass transition for PLA (Table 2). The T_g of PLA measured here does not depend on the TPS composition in the blend and this finding contradicts previous results in the literature [13]. For the ternary blends, this temperature also remains unchanged. The two other transitions at lower temperature in Fig. 5 are due to the TPS phase. For glycerol contents higher than 10–15%, as described by Lourdin et al. [11,25], a relaxation peak can be found at low temperature, close to the glass transition of glycerol, suggesting that a phase separation

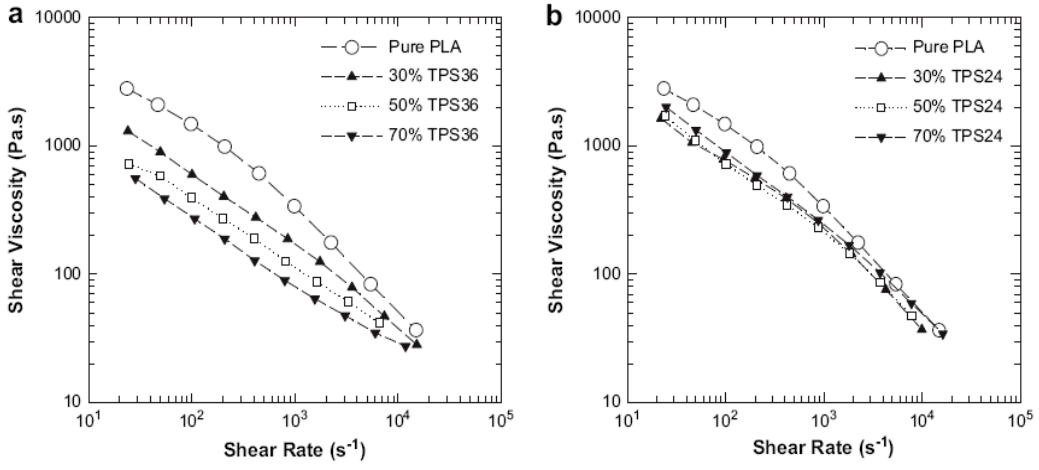

Fig. 4. Melt viscosity for pure PLA and PLA/TPS as a function of the shear rate, at 165 °C: (a) PLA/TPS36; (b) PLA/TPS24.

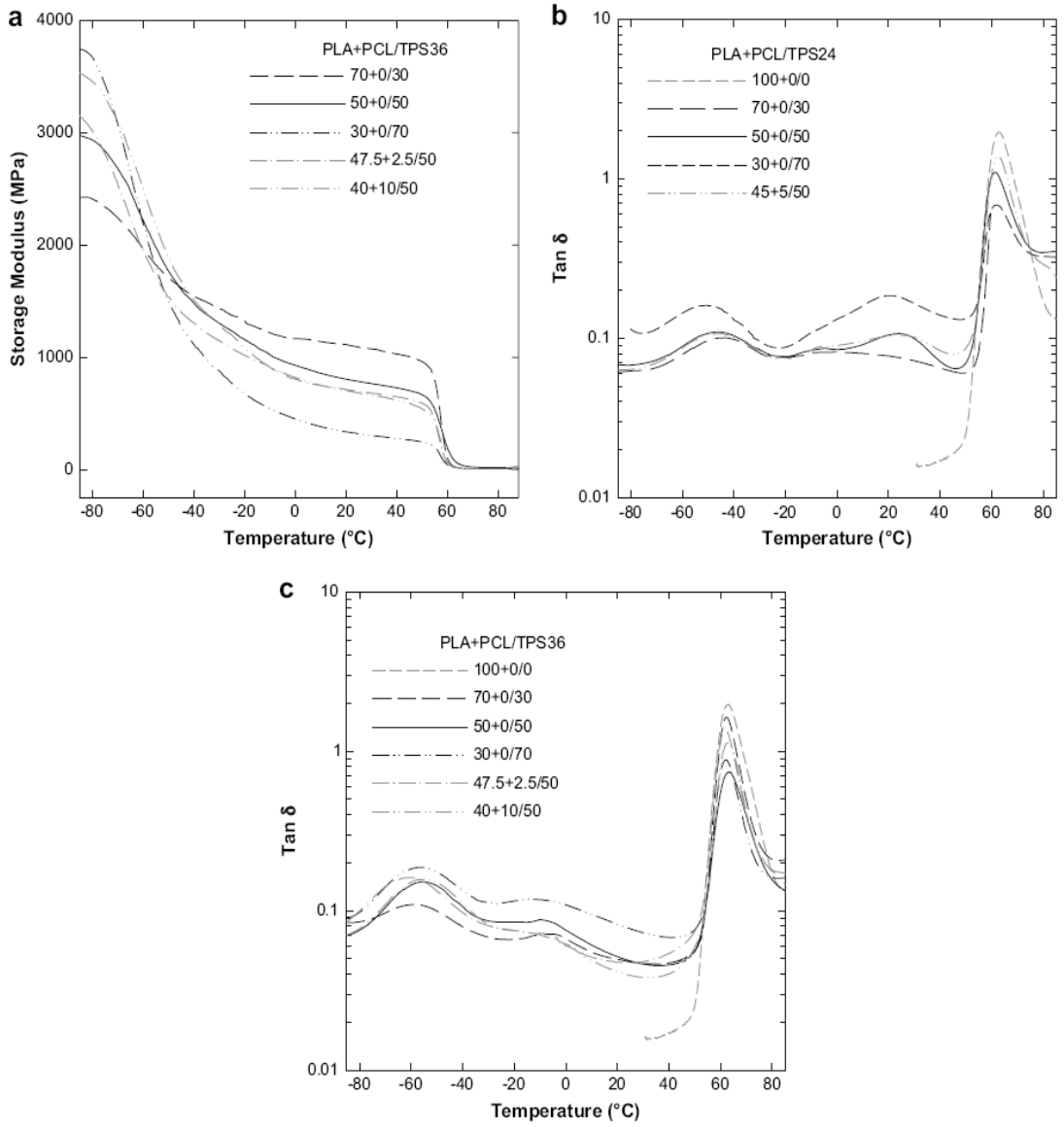

Fig. 5. (a) Storage modulus for PLA/TPS36 and tan δ as a function of the temperature for (b) PLA/TPS24 blends and for (c) PLA/TPS36 blends.

(glycerol demixing) occurs in thermoplastic starch. This peak corresponds to a glycerol rich phase transition, β [11].

For all the TPS36 blends, a tan δ peak located around −57 °C is observed (Table 2, Fig. 5c). For the terblends, this peak represents the overlapping of two transitions, relaxation β for the plasticized starch and the glass transition for PCL. Lourdin et al. [26] and Avérous et al. [27] observed that the magnitude of the tan δ peak for the β transition was strongly dependent on the glycerol content. Those results are confirmed here and TPS36 blends have a lower Tβ than TPS24 blends (more than 10 °C less) indicating that the glycerol content in these blends is superior as expected.

The other transition, α relaxation, can be related to the glass transition of the starch rich phase and the T_g shift between TPS36 and TPS24 blends (Table 2) can be attributed clearly to various amounts of plasticizer. T_α values are found to be around −8 and 20 °C, for TPS36 and TPS24, respectively. Thus the starch is, as expected, more plasticized when the concentration of glycerol in the blend increases. The TPS concentration in the blend and the presence of PCL have no effect on the starch plasticization. At room temperature, the TPS phase in the blends should demonstrate a rubbery behavior for TPS36 blends in a glass PLA matrix and a more glassy behavior for TPS24 blends due to the α relaxation of the starch rich-phase.

3.3. Mechanical properties

For TPS36 blends, increasing the concentration of TPS in PLA results in a continuously increasing strain at break as

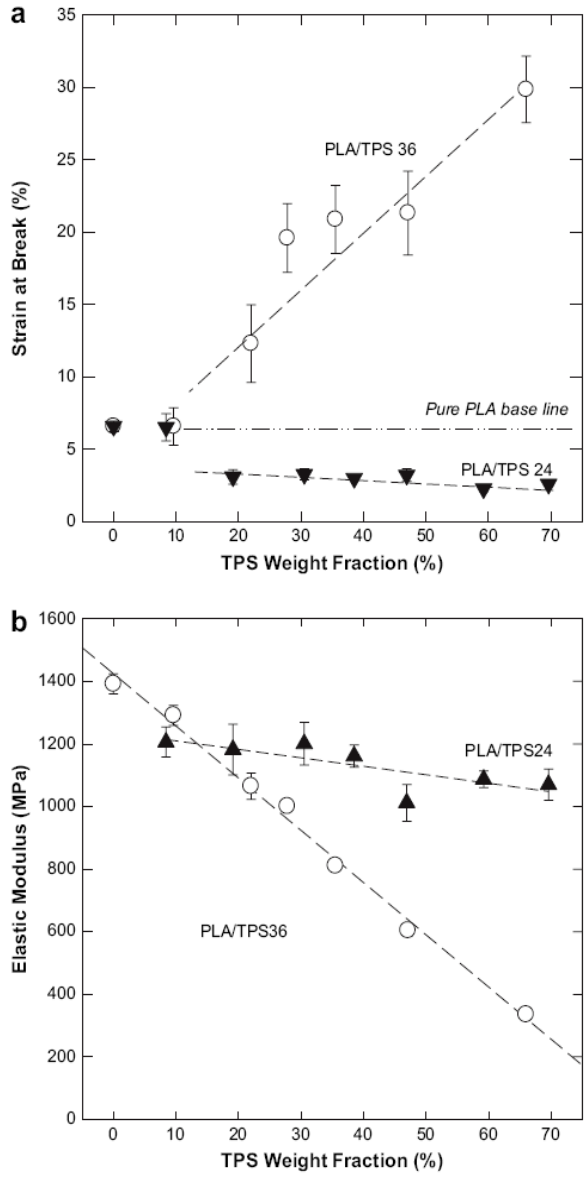

Fig. 6. (a) Strain at break and (b) elastic modulus for PLA/TPS blends, as a function of TPS weight fraction and glycerol content.

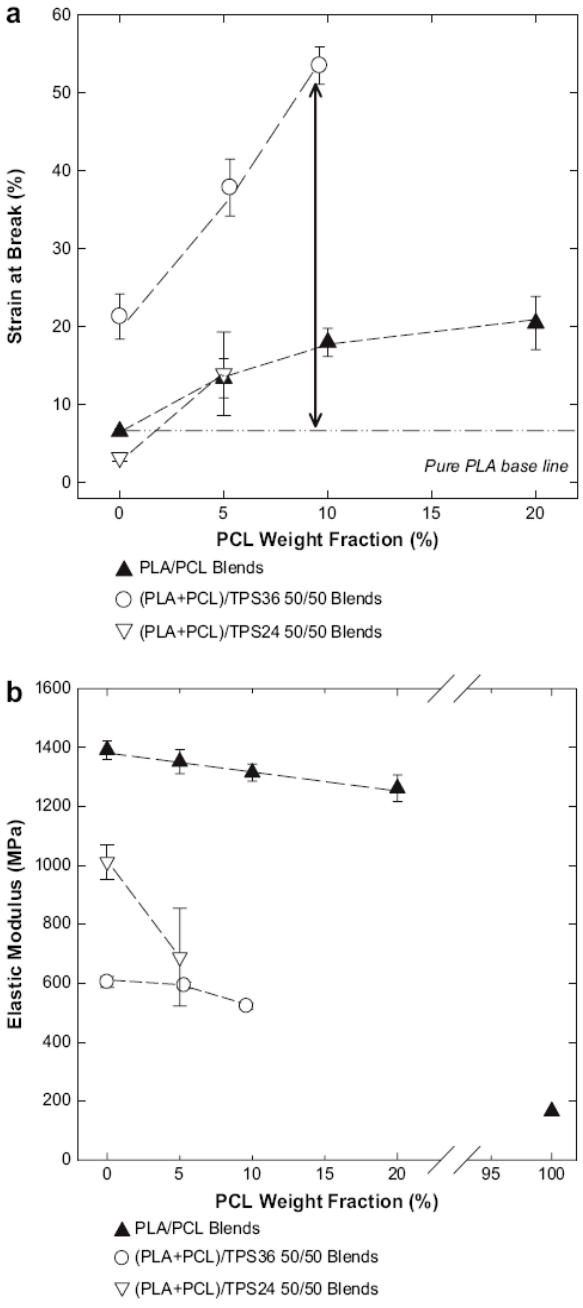

Fig. 7. (a) Strain at break and (b) elastic modulus for PLA/PCL and (PLA + PCL)/TPS 50/50 blends, as a function of PCL weight fraction.

shown in Fig. 6a. This increased strain at break of the blends is accompanied by a decrease in the elastic modulus (Fig. 6b) and maximum strength (not shown here) with TPS weight fraction. The TPS24 blends present a more brittle behavior than pure PLA, with a somewhat lower elastic modulus. Table 2 shows that TPS24 has an α relaxation temperature that is close to room temperature, while TPS36 is well below. Since PLA also has a glass transition temperature above room temperature, TPS24/PLA represents a totally glassy material.

The addition of 5% PCL in the PLA/TPS24 blends results in an increase in the strain at break, higher than for pure PLA, and is accompanied by a large decrease in the modulus (Fig. 7). The addition of 10% PCL to the PLA/TPS36 blend results in a much more evident and significant increase in the strain at break as shown in Fig. 7a with an elongation at break of 55% as compared to 5% for pure PLA. It is also accompanied by a small reduction of the elastic modulus (Fig. 7b). This increase in ductility also results in a substantial increase in the notched Izod impact energy as shown in Fig. 8. The impact energy for the ternary blends significantly exceeds that obtained for the binary PLA/TPS36 or PLA/TPS24 blends. Under these test conditions, the results indicate that

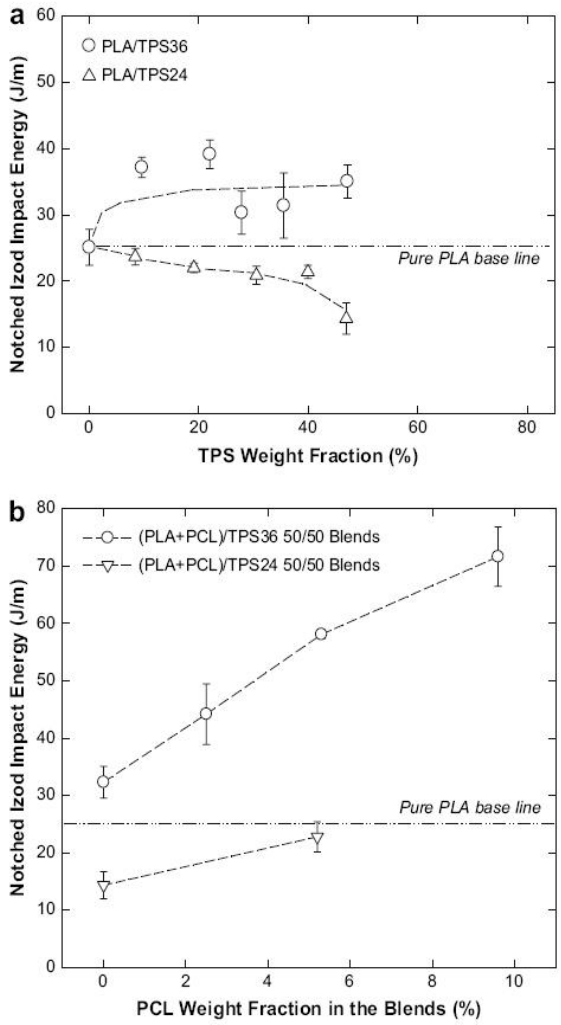

Fig. 8. (a) Impact energy as a function of TPS weight fraction; (b) impact energy as a function of the PCL fraction in (PLA + PCL)/TPS 50/50.

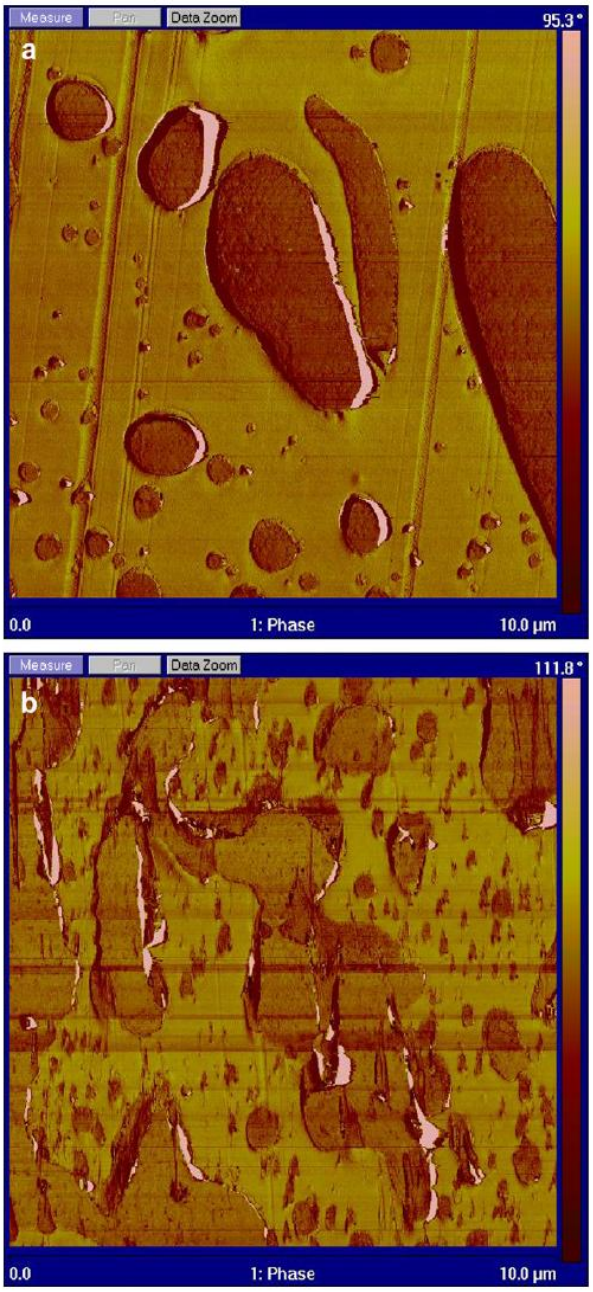

Fig. 9. Morphologies obtained by AFM after microtoming at room temperature; (a) PLA/TPS36 50/50; (b) PLA/PCL/TPS36 40/10/50.

a PLA/PCL/TPS36 40/10/50 blend possesses an impact energy that is three times greater than that for pure PLA. These results are highly dependent on the glycerol content in the starch and blends with TPS24 do not demonstrate the higher impact strength of the TPS36 samples (Fig. 8a).

The significantly improved elongation and impact strength properties observed after addition of TPS to PLA and then also after addition of PCL into a PLA/TPS blend are important. Since PLA is a fragile material, any efforts to improve its ductility are highly relevant. In a previous work from this laboratory [15], we showed that at high glycerol contents in the TPS, it was possible to prepare high loadings of hydrophilic TPS in hydrophobic polyethylene that demonstrated elongations at break very similar to the virgin PE. These results were obtained without the addition of interfacial modifier. The most important property improvements were obtained at the same high glycerol contents in the TPS as used in this work. We postulate in that paper, based on Harkins spreading coefficient theory, that a glycerol rich layer forms at the surface of the thermoplastic starch. The same highly optimal processing conditions are used here and hence it is not surprising to observe an improved ductility of PLA with addition of TPS. However, in this study the ability of TPS to improve the ductility of PLA is limited by the fragile nature of the PLA itself. In Fig. 7a we clearly show that the PCL improves the ductility of the PLA. The improved ductility obtained by the addition of PCL to PLA then allows for the additional

synergistic interactions with the ductile TPS (TPS36) to come into play. In our study, none of the SEM or AFM micrographs show any evidence of the PCL being located at the PLA/TPS interface.

In order to visualize this increased ductility, AFM micrographs of PLA/TPS36 and PLA/PCL/TPS36 specimens microtomed at room temperature are shown in Fig. 9. In Fig. 9a for the PLA/TPS blend, the effect of the microtome knife is barely evident (apart from some minor plowing). However, in Fig. 9b, 10% PCL in the blend leads to the presence of massive deformation and tearing at the interfaces between PCL and PLA. The results shown here strongly support the notion that a minimum level of ductility is necessary in the matrix phase in order to obtain significantly improved properties. When high glycerol contents are present in the TPS phase and PCL is added to modify the ductility of the PLA, synergies come into play which allow the ternary PLA/PCL/TPS blend properties to exceed that observed with any of the binary pairs.

Overall, the mechanical properties indicate that the ternary blend approach with PCL is a useful technique to expand the property range of PLA materials.

4. Conclusion

This paper reports on significant improvements in the impact and elongation at break properties of PLA through the addition of thermoplastic starch as well as PCL. A fragile to ductile transition is achieved for PLA. The work demonstrates that ternary blend preparation of polylactide, polycaprolactone and thermoplastic starch is a viable technique to expand the property range of PLA materials. Although DMA results indicate that the three components are mutually immiscible, it is shown that small quantities of a very finely dispersed PCL phase ($d_n = 370$ nm) dispersed in PLA can significantly improve the ductility of PLA/TPS blends. An elongation at break for PLA/PCL/TPS 40/10/50 of 55% was achieved, as compared to 5% for the pure PLA. A substantial increase in the notched Izod impact energy is also observed with some blends demonstrating three times the impact energy of pure PLA. The results shown here strongly support the notion that a minimum level of ductility is necessary in both the TPS and PLA phases in order to obtain significantly improved properties. When high glycerol contents are present in the TPS phase and PCL is added to modify the ductility of the PLA, synergies come into play which allow the ternary PLA/PCL/TPS blend properties to exceed that observed with any of the binary pairs.

Acknowledgements

The authors are grateful to the Natural Science and Engineering Research Council of Canada (NSERC) for sponsoring this research through a strategic grant. The authors express appreciation to Florence Perrin-Sarazin of the Industrial Materials Institute (NRCC) for assistance with AFM imaging and Nick Virgilio and Jacques Beausoleil of the Ecole Polytechnique de Montréal for assistance with the FIB/AFM measurement and injection molding, respectively.

References

[1] Parker R, Ring SG. The physical chemistry of starch [chapter 24] p. 591–604. In: Dumitriu Severian, editor. Polysaccharides, structural diversity and functional versatility. 2nd ed. New York: Marcel Dekker Inc.; 2005. 1204 p.
[2] Avérous L. Biodegradable multiphase systems based on plasticized starch: a review. J Macromol Sci Part C 2005;C44(3):231–74.
[3] Zeleznak KJ, Hoseney RC. The glass transition in starch. Cereal Chem 1987;64(2):121–4.
[4] Evers AD. The size distribution among starch granules in wheat endosperm. Starch/Stärke 1973;25(9):303–4.
[5] Soulaka AB, Morrison WR. The amylose and lipid contents, dimensions, and gelatinisation characteristics of some wheat starches and their A- and B-granule fractions. J Sci Food Agric 1985;36(8):709–18.
[6] Lindeboom N, Chang PR, Tyler RT. Analytical, biochemical and physicochemical aspects of starch granule size, with emphasis on small granule starches: a review. Starch/Stärke 2004;56(3–4):89–99.
[7] Forssell PM, Mikkilä JM, Moates GK, Parker R. Phase and glass transition behavior of concentrated barley starch–glycerol–water mixtures, a model for thermoplastic starch. Carbohydr Polym 1997;34:275–82.
[8] Perry PA, Donald AM. The role of plasticization in starch granule assembly. Biomacromolecules 2000;1:424–32.
[9] Nashed G, Rutgers RPG, Sopade PA. The plasticisation effect of glycerol and water on the gelatinisation of wheat starch. Starch/Stärke 2003;55(3–4):131–7.
[10] Tan I, Wee CC, Sopade PA, Halley PJ. Investigation of the starch gelatinisation phenomena in water–glycerol systems: Application of modulated temperature differential scanning calorimetry. Carbohydr Polym 2004;58(2):191–204.
[11] Lourdin D, Bizot H, Colonna P. 'Antiplasticization' in starch-glycerol films? J Appl Polym Sci 1997;63:1047–53.
[12] Vink ETH, Rábago KR, Glassner DA, Gruber PR. Polym Degrad Stab 2003;80:403–19.
[13] Martin O, Avérous L. Poly(lactic acid): plasticization and properties of biodegradable multiphase systems. Polymer 2001;42:6209–19.
[14] Park JW, Im SS, Kim SH, Kim YH. Biodegradable polymer blends of poly(L-lactic acid) and gelatinized starch. Polym Eng Sci 2000;40:2539–50.
[15] Rodriguez-Gonzalez FJ, Ramsay BA, Favis BD. High performance LDPE/thermoplastic starch blends: a sustainable alternative to pure polyethylene. Polymer 2003;44:1517–26.
[16] Rodriguez-Gonzalez FJ, Ramsay BA, Favis BD. Rheological and thermal properties of thermoplastic starch with high glycerol content. Carbohydr Polym 2004;58:139–47.
[17] Rodriguez-Gonzalez FJ, Virgilio N, Ramsay BA, Favis BD. Influence of melt drawing on the morphology of one- and two-step processed LDPE/thermoplastic starch blends. Adv Polym Technol 2003;22:297–305.
[18] Favis BD, Rodriguez F, Ramsay BA. Polymer compositions containing thermoplastic starch. US Patent 6,605,657 B1; 2003;
Favis BD, Rodriguez F, Ramsay BA. Method of making polymer compositions containing thermoplastic starch. US Patent 6,844,380 B2; 2005.
[19] Sarazin P, Huneault MA, Orts W, Favis BD. Blends of polylactide with thermoplastic starch. Annu Technol Conf Soc Plast Eng, Boston MA; 2005.
[20] Virgilio N, Favis BD, Pépin MF, Desjardins P, L'Espérance G. High contrast imaging of interphases in ternary polymer blends using focused ion beam preparation and atomic force microscopy. Macromolecules 2005;38:2368–75.
[21] Evers AD. Scanning electron microscopy of wheat starch. Starch/Stärke 1971;23:157–62.

[22] Choi SG, Kerr WL. Swelling characteristics of native and chemically modified wheat starches as a function of heating temperature and time. Starch/Stärke 2004;56:181–9.

[23] Van Hung P, Morita N. Physicochemical properties of hydroxypropylated and cross-linked starches from A-type and B-type wheat starch granules. Carbohydr Polym 2005;59:239–46.

[24] Peng M, Gao M, Abdel-Aal ESM, Hucl P, Chibbar RN. Separation and characterization of A- and B-type starch granules in wheat endosperm. Cereal Chem 1999;76(3):375–9.

[25] Lourdin D, Coignard L, Bizot H, Colonna P. Influence of equilibrium relative humidity and plasticizer concentration on the water content and glass transition of starch materials. Polymer 1997;38(21): 5401–6.

[26] Lourdin D, Bizot H, Colonna P. Correlation between static mechanical properties of starch–glycerol materials and low-temperature relaxation. Macromol Symp 1997;114:179–85.

[27] Avérous L, Moro L, Dole P, Fringant C. Properties of thermoplastic blends: starch–polycaprolactone. Polymer 2000;41:4157–67.

APPENDIX B: MORPHOLOGY AND RHEOLOGY OF POLYCAPROLACTONE/THERMOPLASTIC STARCH BLENDS

Conference paper- ANTEC 2005

Gang Li, Pierre Sarazin, Zhenhua Yuan and Basil D. Favis

CRASP, Department of Chemical Engineering, Ecole Polytechnique de Montreal, CP 6079, Succ. Centre Ville, Montreal, Quebec, Canada, H3C 3A7

Abstract

Polycaprolactone (PCL)/thermoplastic starch (TPS) biodegradable blends were prepared via a one-step extrusion system over the entire range of composition at different viscosity ratios. A detailed morphology analysis of the PCL/TPS blends was investigated by electron microscopy after selective extraction. Through a judicious combination of concentration control and processing conditions, the volume average diameter of TPS droplets can be closely controlled from 0.5 to 16μm. The rheological behavior of these blends is also examined in depth.

Introduction

Polycaprolactone (PCL) is a synthetic polyester obtained by the self-condensation of the cyclic ester ε-caprolactone. PCL has unique properties that make it attractive for biomaterials applications. Like most synthetic polymers, it has excellent water-resistant properties. At the same time, like most natural polymers, it has excellent biodegradability and biocompatibility properties. These properties have made it possible for PCL to be used in variety of biomaterial applications including drug release, medical devices, cell cultivation/cell culture, and biodegradable packaging material. However its cost is significantly greater than that of typical commodity plastics. Blends of polycaprolactone with thermoplastic starch represent an important potential route towards more economically viable, fully biodegradable and sustainable plastics.

PCL has been blended with natural polymers, such as starch, to improve its water-resistance properties without impairing the biodegradability/biocompatibility properties (1-3). However, the properties of polymer blends depend greatly upon their morphology and on thenterfacial

interactions between components (4) and this aspect has not been considered in detail. As the final morphology has a controlling influence on the blend properties and hence on the application, the knowledge of the mechanisms involved in the blending stage is required. As polymers are often immiscible, various morphologies may be observed during melt mixing. Droplet, fibrillar, lamellar and co-continuous morphologies have been observed. Each of them depends on several factors such as composition, processing condition (mixing time, temperature, shear and elongation rate) as well as the nature of the polymers (interfacial tension, viscosity, elasticity) (5).

Polycaprolactone blends containing both native starch and thermoplastic starch have been studied by several authors (6-9). Avella and coworkers have studied the biodegradability of native and compatibilized PCL-granular starch blends (6). They conclude that acceptable mechanical properties can only be obtained in the presence of a compatibilizing agent or with lower starch content. More recently, the development of thermoplastic starch from granular starch and plasticizer (7-9) allows for the transformation of starch into a free-flowing fluid like other conventional thermoplastics. In previous studies, however, the blending was carried out by two-step twin-screw extrusion and with only about 20% glycerol content in TPS. The commercial production of these blends has been limited due to the high cost and variation in mechanical properties. In this laboratory a one-step twin-screw extrusion approach has been developed which allows for the preparation of blends with TPS at high glycerol contents (10).

In this paper, we study the morphology and rheology of PCL/TPS blends containing a high concentration of glycerol prepared via a one-step extrusion system over the entire range of composition.

Experimental Procedure

The PCL used in this study was CAPA® thermoplastics from Solvay. Two kinds molecular weights were used: CAPA6500 has a molar mass of 50,000gmol^{-1} and CAPA6800 has a molar mass of 80,000 gmol^{-1}. we define CAPA6500 and CAPA6800 as CAP1 and CAP2. The native wheat starch (Supergell 1203-C) obtained from ADM/Ogilvie is composed of 25% amylose and 75% amylopectin. TGA measurements show that the water content in the starch granules is 7.1%. The water content of Glycerol (SIMCO Chemical products Ins.) was determined by its refractive index to be 5.9%.

Starch suspensions were prepared using the ratios of native starch, glycerol and water listed in

Table 1.

The starch suspension was fed in the 1st zone of the TSE. Native starch was gelatinized and plasticized in zones 2 to 4 of the TSE. Volatiles were extracted in the 4th zone by venting under vacuum. Molten PCL was fed from the SSE to the 5th zone of the TSE using an adapter designed specially for this purpose. The mixing of PCL with TPS started in the same zone and continued to the 7th zone of the TSE.

Smooth surfaces of all the samples were prepared using a microtome (Leica-Jung RM2165) equipped with a glass knife. After extraction with HCl acid (6N) and coating with a gold-palladium alloy, the morphology of the samples was examined by a Jeol JSM 840 scanning electron microscope at 10 to 15 kV. A gravimetric method was used to calculate the extent of continuity of the TPS phase, using the simple equation:

$$\% \text{ continuity of } P = \left(\frac{\text{weigth } P_{\text{initial}} - \text{weigth } P_{\text{final}}}{\text{weigth } P_{\text{initial}}} \right) \times 100\% \qquad (1)$$

where P corresponds to the TPS phase. P_{initial} corresponds to the weight of P in the blend before the extraction step, and P_{final} corresponds to weight of P remaining after extraction.

Dynamic rheological measurements were carried out on a Rheometrics Scientific SR 5000 dynamic stress rheometer. Extruded ribbons were cut into small disks of about 25mm diameter. Before rheological measurements, samples were conditioned in a vacuum for one week to completely remove the moisture. These measurements were then run with 25mm parallel plate geometry and a gap of about 1.0mm. The dynamic viscoelastic properties were determined with frequencies from 0.03 to 100 rad/s. In order to keep the response in the viscoelastic linear domain, the applied stress was controlled to keep the total deformation at around 0.1, except for very low frequencies where larger stress inputs were used to increase the sensitivity. All measurements were carried out under a nitrogen atmosphere. The morphologies of samples after rheological measurements under small deformation were found to be very similar to those of samples from parallel annealing tests at the same temperature for the same amount of time.

Results and Discussion

In polymer blends, it is essential to study the morphology of the final product since most properties, especially mechanical properties, depend on it. The development of morphologies of PCL/TPS blends over the entire range of composition during the blending processing was studied.

TPS materials have been studied and it was found that 30% glycerol is required to effectively plasticize starch (10). Below that limit, the viscosity and elasticity of TPS are too high to allow LDPE to greatly deform the TPS dispersed phase in the LDPE/TPS blend system. TPS used in the study of PCL/TPS blends contained 36 and 40% glycerol. The axial direction morphologies of CAP1/TPS36 ribbons are shown in figure 1. The starch component of the PCL/TPS blend was removed with HCl acid treatment leaving cavities behind in the polymeric matrix. Blends containing up to 50% wt.% TPS exhibited a similar morphology. From Fig. 1a-c it is clear, as indicated by the presence of cavities, that the dispersed phase consists of plasticized starch, which in the form of droplet-like particles have number volume diameter range from 1.8 to 3.7 μm. Comparison of the size of the granules existing in native starch with that of the particles present in PCL/TPC blend, show that starch granules underwent significant particle size reduction during processing. Increasing the TPS concentration increases the particle size of TPS due to particle-particle coalescence. At high TPS concentration (above 60 wt.%), it was difficult to distinguish whether PCL or TPS constituted the matrix (Fig.1d). Both components appear to be fully continuous in the axial direction.

In order to quantitatively determine the extent of continuity, samples were exposed to extraction and the percent continuity was measured as a function of TPS weight loss. The percent starch continuity as a function of TPC content for both of CAP1/TPS36 and CAP2/TPS36 blends is shown in Figure 2.

As mentioned in the literature, the type of morphology formed during processing does not only depend upon the nature of the polymers (interfacial energy and viscosity ratio) and their volume but on the processing conditions as well. Processing conditions play an important role in the morphology of LDPE/TPS blends (10) and the melt draw ratio has an especially important effect on the deformation of TPS dispersed phase particles. The elongational deformation imposed by passing through the die is even more marked. Conversely, PCL/TPS blends compounded with TPS36 and TPS40 show very little deformation along the extruder direction (results not shown here). Since PCL has a lower melt viscosity than LDPE, stress transfer was insufficient to result in TPS deformation. Different TPS particles after extracting PCL matrix using THF are demonstrated in Fig. 3.

The morphology of an immiscible blend is closely related to its rheology. Therefore, the rheological properties of the CAP2 and TSP40 and their blends have been studied here at 150 ℃

(Fig. 4 and 5). Frequency sweep results show that all the pure materials studied in this work show a shear thinning Newtonian behavior in the frequency range from 0.03 to 100 rad/s. The complex viscosity of PCL reaches a plateau value at low frequencies whereas TPS does not. At sufficiently low frequencies, the storage modulus of TPS is higher than that of PCL by about four orders of magnitude and the loss modulus is higher by two orders of magnitude. TPS exhibits the rheological behavior of a typical gel as characterized by a storage modulus (G') larger than the loss modulus (G") and with both moduli largely independent of frequency over the amplitude of the experimental window (11).

The most important rheological parameters determining the morphology development of immiscible blends are the viscosity and elasticity ratio of the components, necessary to calculate their ratios. They have been derived from the dynamic moduli by applying the Cox-Merz rule for pure polymers:

$$\eta^* = \eta_s (\dot{\gamma} = \omega) \qquad (2)$$

where η^* is the complex viscosity (Pa.s), $\eta_{s,}$ steady shear viscosity (Pa.s), $\dot{\gamma}$ is the steady shear rate (s^{-1}), and ω, frequency (rad/s). The viscosity and elasticity ratios calculated from the dynamic data at 100 rad/s are 0.70 and 0.97, respectively.

The storage and loss modulus of PCL/TPS blends increases with increasing TPS concentration over the whole range of frequencies. For some multiphase blend systems, the storage modulus of the blends at low dispersed phase concentration exhibit much higher values than that of pure polymer components. This enhancement of elasticity at low frequencies has been attributed to the deformability of the dispersed phase particle. There is no such enhancement of storage modulus in the PCL/TPS blend system. A detailed study of relationship between rheological properties, interfacial tension and morphology is currently underway.

Summary

Morphological and rheological studies on PCL/TPS blends of various compositions were carried out. The results showed that the volume average diameter of TPS droplets could be closely controlled from 0.5 to 16μm through a judicious combination of concentration control and

processing conditions. The linear viscoelastic properties of molten CAP2/TPS40 blends have been determined and analyzed.

Acknowledgements

The authors gratefully acknowledge the financial support received from the Natural Sciences and Engineering Research Council of Canada through a Strategic Grant.

References

1. Tsuji H., Ishizaka T., Blends of Aliphatic Polyesters. VI. Lipase-catalyzed Hydrolysis and Visualized Phase Structure of Biodegradable Blends from Poly(ε-caprolactone) and Poly(L-lactide), *Inte. J. Bio. Macro.*, **29**, 83–89 (2001).

2. Matzinos P., Tserki V., Kontoyiannis A., Panayiotou C., Processing and Characterization of Starch/polycaprolacctone Products, *Polym. Degrad. Stab.*, **77**, 17–24 (2002).

3. Roper, H. and Koch, H., The Role of Starch in Biodegradable Thermoplastic Materials, *Starch*, **42**, 123-130 (1990).

4. Wu, S., Phase Structure and Adhesion in Polymer Blends: A Criterion for Rubber Toughening, *Polymer*, **26**, 1855-1863 (1985).

5. Cassagnau, P., Michel., A., New Morphologies in Immiscible Polymer Blends Generated by a Dynamic Quenching Process, *Polymer*, **42**, 3139-3152 (2001).

6. Avella, M., Errico, H.E., Laurienzo, P., Manolova N., Raimo, M., Rimedio, R., Preparation and Characterisation of Compatibilised Polycaprolactone/ Starch Composites, *Polymer*, **41**, 3875-3881 (2000).

7. Wu C.S., Performance of an Acrylic Acid Grafted Polycaprolactone/starch Composite: Characterization and Mechanical Properties, *J. Appl. Polym. Sci.*; **89**, 2888-2895 (2003).

8. Singh R.P., Pandey J.K., Rutot D., Degee Ph., Doubois Ph., Biodegradation of Poly(ε-caprolactone)/starch Blends and Composites in Composting and Culture Environments: The Effect of Compatibilization on The Inherent Biodergradability of The Host Polymer, *Carbohydrate research*, **338**, 1759-1769 (2003).

9. Shin B.Y., Lee, S.I., Shin, Y.S., Balakrishnan, S., Narayan, R., Rheological, Mechanical and Biodegradation Studies on Blends of Thermoplastic Starch and Polycaprolactone, *Polym. Eng. Sci.*, **44,** 1429-1438 (2004).

10. Rodriguez-Gonzalez1 F.J., Ramsay B.A., Favis B.D., High Performance LDPE/thermoplastic Starch Blends: a Sustainable Alternative to Pure Polyethylene, *Polymer*, **44,** 1517–152 (2003).

11. Ross-Murphy, S.B., Structure-property Relationship in Food Biopolymer Gels Blends Including Thermoplastic Starch, *Proceeding of Sixteenth Annual Metting of Polymer Processing Society*, Shanghai, China, 350-351 (2000)

Table 1. Composition of starch suspensions.

Samples	Starch (%)	Glycerol (%)	Water (%)	Glycerol content in TPS (%)
TPS40	48.5	32.5	19.0	40
TPS36	48.5	28.0	23.5	36

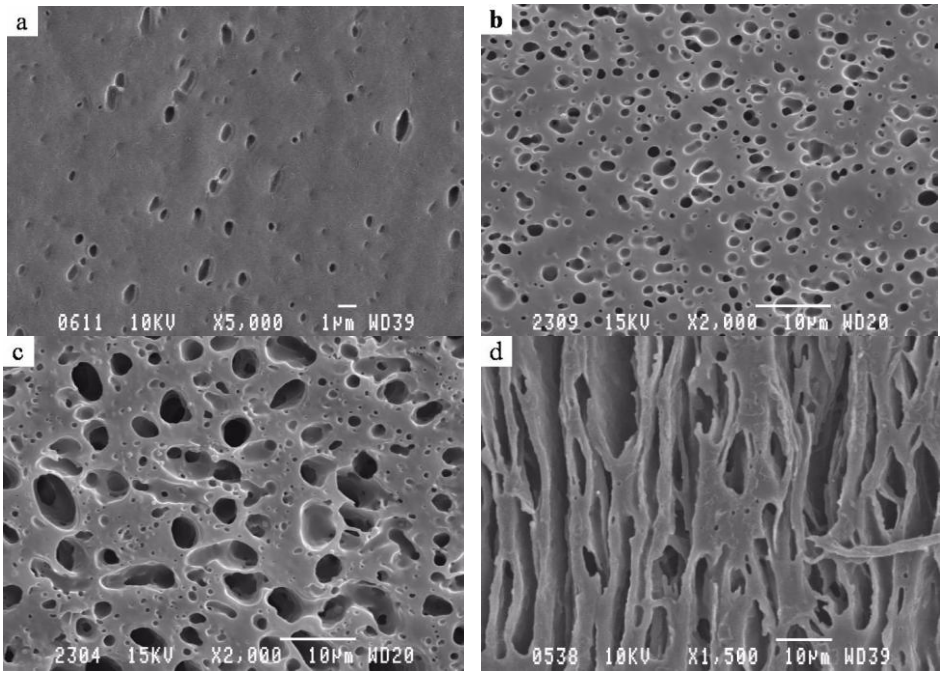

Figure 1. Morphology of CAP1/TPS36 blends. a) 90/10 b) 70/30 c) 50/50 d) 32/68.

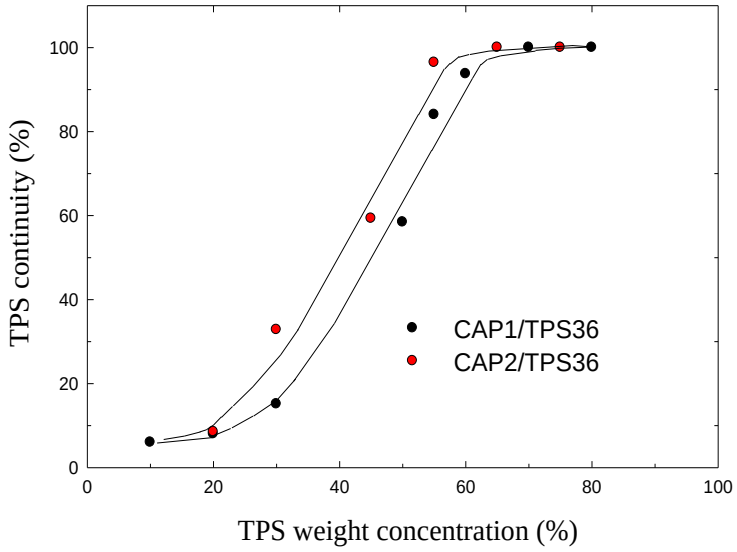

Figure 2. Effect of TPS content on the percent continuity of blends

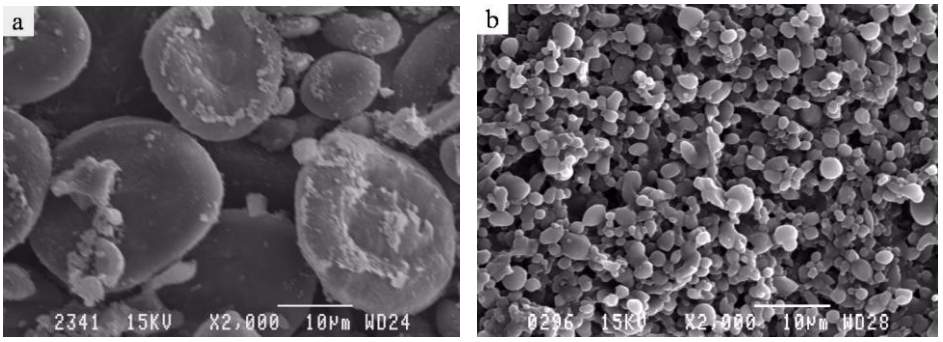

Figure 3. TPS36 particles extracted from different CAP1/TPS36 (70/30) blend.

a) Partial plasticized starch and b) fully plasticized starch

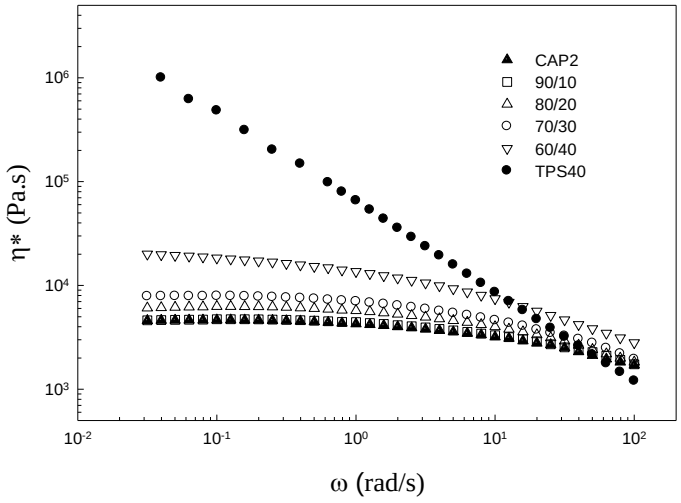

Figure 4. The Complex viscosity η* of CAP2/TPS40 blends at 150 ℃.

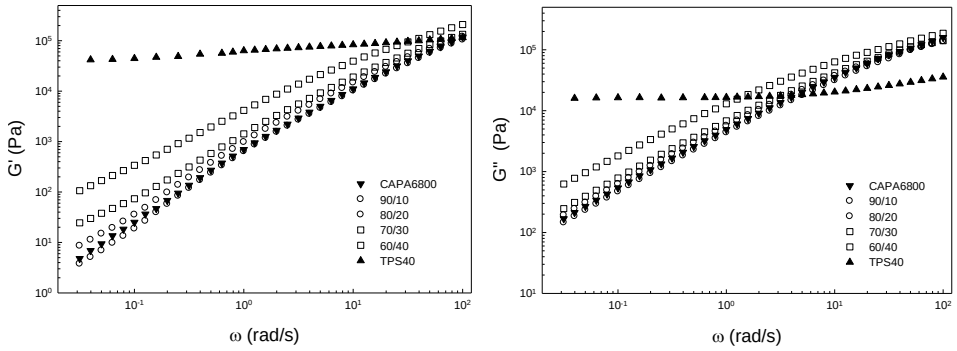

Figure 5. The storage and loss modulus of CAP2, TPS40 and their blends at temperature of 150 ℃.

APPENDIX C: MORPHOLOGY CONTROL IN POLYMER BLENDS WITH HIGHLY PLASTICIZED THERMOPLASTIC STARCH

Conference paper-Bioplastics 2006

G. Li, P. Sarazin and B. D. Favis

CREPEC, Department of Chemical Engineering, Ecole Polytechnique de Montreal
P. O. Box 6079 Station Centre-Ville, Montreal, QC, Canada H3C3AY

Abstract – Recent work has shown that thermoplastic starch can be blended with a wide range of thermoplastics and that, if the starch plasticizer content is sufficiently high, polymer blend morphology control strategies can be applied to the TPS. This morphology control can result in excellent material properties. However, such high plasticizer contents, well-dispersed within the starch, can be difficult to achieve. In this paper we examine the critical aspects of starch plasticization required for an extrusion process and relate these findings to the melt-blended TPS morphology. Wheat starch gelatinization was studied via differential scanning calorimetry (DSC), optical microscopy and wide angle X-ray diffraction(WAXS). Subsequently, the morphology of blends of polycaprolactone (PCL) and thermoplastic starch prepared via a one-step extrusion process was studied. These results indicate that the conversion of native starch to fully plasticized thermoplastic starch (TPS) is much more difficult and problematic than what is often reported in the literature. Water is a necessary ingredient for glycerol to plasticzed starch in a melt processing operation, and a sufficient residence time of water in contact with the starch is required prior to devolatilization.

Introduction

Over the last two decades, numerous papers have been published on polymers containing

native granular starch. These studies have generally shown that the physical and mechanical properties of the polymer/starch mixtures become quite poor with increasing starch content in the blend. This can be attributed to the incompatibility between the hydrophilic starch and hydrophobic polymer as well as to the poor interfacial adhesion between the components.

More recently, the development of thermoplastic starch (TPS) from granular starch and plasticizer allows for the transformation of starch into a free-flowing fluid like other conventional thermoplastics. It has been reported that blends of LDPE with TPS can achieve excellent mechanical properties without any classical interfacial modifier or having to chemically modify the starch surface(1,2). However, the conversion from native starch to highly plasticized TPS is much more difficult and problematic than what is often reported in the literature. Completely plasticized starch only can be achieved through three times extruding (3).

Starch can be converted into a thermoplastic material through the disruption of molecular interactions in the presence of plasticizer under specific conditions. Water and glycerol are the most widely used plasticizers in TPS materials. Once starch granules are gelatinized, the gelatinized starch can be processed on existing plastics fabrication equipment, i.e. extruder, compression molding and injection molding.

From the viewpoint of droplet deformation/breakup mechanisms during polymer blend morphology formation, the morphological study of blended TPS is anexcellent tool to observe starch plasticity. Since morphology modification in blends requires high levels of fluidity of the respective phase, high glycerol contents are required in order to control the TPS phase size. The objective of this work is to study the effect of various parameters influencing gelatinization on the melt processed dispersed phase morphology of TPS based blends.

Experimental

Wheat starch gelatinization was studied via differential scanning calorimetry (DSC), optical microscopy and wide angle X-ray diffraction (WAXS). A one-step blending approach was used for preparing PCL/TPS blends(1).

Results and Discussion

Starch gelatinization

The gelatinization of wheat starch was investigated using a differential scanning calorimeter. The properties of the plasticizer, such as diffusivity, viscosity, molecular size and hydrogen bonding capacity determine its effectiveness to gelatinize starch. According to the DSC results, the gelatinization temperature (Tp) increases from 99.0 ℃ to 124.0 ℃ when the glycerol concentration increases from 65 to 400 g per 100 g dry starch, whereas the Tp is constant at 64.5℃ when water is used as sole plasticizer. The enthalpy of gelatinization (△H) can be determined from the area below the DSC endotherm and increases with increasing concentration of plasticizer. By extrapolating the curves to the cross point at which the enthalpy of gelatinization is zero, the minimum requirement of plasticizer for starch can be obtained. The minimum requirement for water during starch gelatinization is somewhat lower than that of glycerol due to the highly effective plasticizing ability of water.

For mixtures containing both water and glycerol, it is interesting to note that the gelatinization temperature only depends upon the glycerol concentration in the starch/plasticizer mixture within the range of this experiment and the gelatinization temperature increases with increasing concentration of glycerol. A master curve related to the gelatinization temperature and glycerol/water content was found and it can be used to estimate the gelatinization temperature of water-glycerol-water systems can be readily adjusted through the water/glycerol concentrations according to this master curve. The gelatinization of starch was also demonstrated by optical microscopy and wide angle X-ray diffraction.

Effect of starch gelatinization on blend morphology

In order to understand the effect of starch gelatinization of the morphology of melt processed blends, PCL/TPS blends are prepared under various conditions with glycerol and/or water as plasticizers. The morphology of PC/TPS36 (70/30) blends is shown in Fig.1 (note that 36 in TPS36 refers to the per-cent glycerol content based on the total weight of thermoplastic starch). The TPS phase was removed by selective solvent extraction and can be observed as cavities in the PCLA MATRIX. As shown in Fig.la, when glycerol was added as a single plasticizer to plasticize

starch, the large droplet-like particles have a volume average diameter (dv) of 16.1 μm dispersed in the PCL matrix. The size of the TPS particles was found to be virtually identical with that of native starch. That is an indication that glycerol, by itself, is not sufficient to plasticize starch as anticipated. As water was added to glycerol-starch and, keeping all other components concentration and processing conditions unchanged a much more effective gelatinization was achieved even if the water was removed completely during processing. A bimodal size distribution of TPS particles was observed(Fig.1b). Some of the plasticized starch was completely broken-down to smaller particles. The large particles have a volume average diameter (dv) of 13.3 μm and the smaller particles of 1.0 μm. It implies that water is an important function of starch gelatinization in starch-water-glycerol systems and greatly affects the morphology of PCL/TPS blends. Smaller dispersed TPS particles of 1.7 μm in the blends and a unimodal size distribution was achieved by increasing the residence time of water during extrusion prior to devolatilization.(Fig.1c)

Conclusion

A master curve related to the gelatinization temperature and glycerol content can be used to estimate the gelatinization temperature of a water-glycerol-starch system. In the morphological investigation of melt blended PCL and TPS, the TPS particle size is the same as native starch when glycerol was used as the sole plasticizer. A bimodal particle siz distribution was observed as water was added to the glycerol-starch system. Smaller dispersed particles of completely plasticized starch and a unimodal TPS dispersed phase size distribution was achieved by increasing the residence time of water during extrusion prior to devolatilization. It can be readily concluded that water cannot be entirely replaced by glycerol in the melt processing of TPS. Water is a necessary ingredient for glycerol to gelatinize starch, and a sufficient residence time of water in contact with the starch is required prior to devolatilization.

Acknowledgements

The authors gratefully acknowledge the financial support received from the Natural Sciences and Engineering Research Council of Canada through a Strategic Grant.

References

1. Rodriguez-Gonzalez, F.J.; Ramsay, B.A.; Favis, B.D.; Polymer,2003,44,1517.
2. Favis, B.D.; et al. U.S. Patents 6 606 657 and 6 844 380.
3. Matzinos, P., Tserki, V., Kontoyiannis, A., Panayiotou, C., Polym. Degrad. Stab., 2002, 77, 17.

APPENDIX D: MORPHOLOGY, THERMAL AND MECHANICAL PROPERTIES OF BLENDS OF POLYCAPROLACTONE AND THERMOPLASTIC STARCH

Conference paper-Bioplastics 2007

G. Li and B.D. Favis*

CREPEC, Department of Chemical Engineering, Ecole Polytechnique de Montreal
P.O. Box 6079 Station Centre-Ville, Montreal, QC, Canada H3C 3A7
Gang-2.li@polymtl.ca, Basil.Favis@polymtl.ca

Abstract - In this work the morphology, thermal and mechanical properties of blends of polycaprolactone (PCL) with thermoplastic starch (TPS) of high glycerol content were investigated. The blends demonstrate remarkably low levels of coalescence. Up to 30% TPS content, the dv and dn of the dispersed TPS droplets remain constant and are less than 1.8 and 1.4 μm, respectively. Beyond 30% TPS, elongated dispersed structures are observed and the fiber diameters of those elongated phases also remain constant with TPS composition. The results of per-cent continuity via gravimetric solvent extraction indicate that the concentration range of co-continuity is wide from 50-80% TPS. This is a very highly asymmetric phase inversion region and these results indicate a very strong tendency of the polycaprolactone to preferentially encapsulate the thermoplastic starch. DMA and DSC results indicate the possibility of a glycerol-rich layer at the TPS/PCL interface. Mechanical properties display an extremely high ductility even at very high TPS concentration and in the absence of any added interfacial modifier.

APPENDIX E: MORPHOLOGY DEVELOPMENT AND INTERFACIAL INTERACTIONS IN POLYCAPROLACTONE/THERMOPLASTIC STARCH BLENDS

Conference paper- ANTEC 2010

G. Li and B. D. Favis

CREPEC，Department of Chemical Engineering，Ecole Polytechnique de Montreal,

P.O. Box 6079 Station Centre-Ville, Montreal, QC, Canada H3C 3A7

Abstract

The coalescence, continuity development, dynamic and static mechanical properties, as well as interfacial interactions, were studied for polycaprolactone/ thermoplastic starch blends. These materials, prepared by a one-step extrusion process, demonstrate the features of a highly interacting system and the tensile mechanical properties demonstrate exceptional ductility at very high levels of thermoplastic starch without any added interfacial modifier.

Introduction

Starch materials have attracted considerable attention in the bioplastics field due to their abundance, biodegradability and low cost. The mixing of conventional polymers with native unplasticized starch blends always leads to brittle materials. In that case the starch component behaves as a solid filler. St Pierre *et al.*[1] carried out an investigation on thermoplastic starch/polyethylene blends and demonstrated that dispersed phase/matrix morphology control protocols could be applied to this blend. In a later work, B. D. Favis *al*. developed an effective one-step melt processing technique and controlled the level of continuity of the TPS phase [2]. This is achieved through the application of heat and in the presence of water and/or another plasticizer for starch. The advantage of TPS is that it can be processed on typical melt-processing equipment.

It is well known in polymer blends that the morphology control of the respective phases is a

key factor to achieve desired material properties. The phases in a polymer blend can be structured in droplet, fiber, laminated, and co-continuous form. Phase coalescence is an important phenomenon affecting the final morphology of polymer blends and has been studied in some detail in recent years. Typically, coalescence can be divided into two categories: dynamic and static processes. The dynamic case is a flow-induced coalescence process during polymer blending with the final morphology being governed by a balance of particle breakup and coalescence. Static coalescence is a quiescent process whereby the phase or phases are coarsened over time at high temperature. Co-continuous systems, in particular can demonstrate very elevated levels of coalescence during static annealing [3].

PCL is a synthetic polymer having unique properties that make it attractive for biomaterials applications. It has excellent biodegradability and biocompatibility properties. However, PCL is still more expensive than conventional plastics, and the degradation rate is not completely satisfactory in some instances. The blending of PCL with TPS could provide a potential route towards more economic fully biodegradable materials. A number of studies on PCL/TPS blends have been carried out [4]. Shin et al. reported large diameters of the TPS dispersed phase in blends of PCL and thermoplastic starch plasticized with 20% glycerol. Matzinos et al. reported on the obtention of a completely plasticized thermoplastic starch and a morphology with a relatively fine and uniform dispersion of TPS phase within the PCL matrix after a three-times extrusion protocol. The mechanical and thermal properties of PCL/TPS with various moisture and glycerol contents were investigated by Averous et al.. Results indicated low compatibility between PCL and TPS according to DMA and DSC measurements. Sarazin et al. showed that the addition of small amounts of polycaprolactone to a blend of poly(lactic acid) and thermoplastic starch significantly improved the ductility and impact strength of the blends. Recently Shin et al. studied blends of polycaprolactone with thermoplastic starch and showed that the chemical modification of starch with maleic anhydride led to improvements in interfacial adhesion and processability. To date, very little work has been done on the detailed morphology development and morphology control in PCL/TPS blends.

The objective of this study is to carry out a detailed study on the morphology development in PCL/TPS blends with high plasticizer content prepared using a one-step process. This work will closely examine the coalescence and continuity development in these systems.

Materials

Two commercial grades of polycaprolactone CAPA6500 and CAPA6800, with different molecular weights were used in this work. Native starch was obtained from ADM/Ogilvie and is composed of 25% amylose and 75% amylopectin. The plasticizers used were water and pure glycerol (SIMCO Chemical products Inc. 99.5%).

Starch granules were gelatinized, plasticized with glycerol and water, and blended with PCL in a one-step extrusion process. For the composition study, the entire ranges of PCL/TPS36 blend composition from 100/0 to 0/100 in steps of 10 wt% were prepared. For the investigation of the effect of viscosity ratio on blend morphology, two kinds of PCL with different molecular weights and TPS with different glycerol contents were blended;

The coalescence, continuity development, dynamic and static mechanical properties, as well as interfacial interactions, were detail studied by rheological measurements, SEM, quiescent annealing test and Fourier transform infrared spectroscopy (FTIR).

Results and Discussion

The rheological properties of the neat PCL and TPS as a function of frequency are measured. The TPS with high glycerol concentration exhibits the rheological behavior of a typical gel and is characterized by a storage modulus (G') which is larger than the loss modulus (G") over the entire frequency sweep (Fig 1a). This behavior has been observed by other authors and is generally explained by the presence of an elastic network embedded in a softer matrix, i.e. the existence of a protein network; remaining crystalline structure in the samples; or strong hydrogen bonding [5]. In the present case, no crystalline structure in this highly plasticzed TPS was found as determined by X-ray diffraction and very little protein exists in the starch as well. The gel-like behavior is most likely the result of hydrogen bonding between the starch and plasticizer and could also be due to high levels of entanglement of starch molecules in the melt state creating a type of pseudo-crosslinking effect. Note that the elasticity is significantly higher than the complex viscosity over a wide range of shear rates. Also, the TPS is significantly more elastic than PCL (not shown here). The gel-like properties of TPS and its elastic nature will tend to make it more difficult to deform/disintegrate as a dispersed phase in a polymer blend.

The complex viscosity (η^*) of TPS follows a power-law behavior and there is no Newtonian plateau for the viscosity curve within the measured region of frequency range (Fig 1a), another characteristic of gel-like behavior. Thus, the zero shear viscosity of TPS cannot be obtained. The

extreme shear thinning behaviors have been associated with a melt yield stress. The complex viscosities of PCL1 and PCL2 were measured at temperatures of 110 and 130 ^{o}C, respectively. PCL1 and PCL2 demonstrate shear thinning behavior in the high frequency range from 0.5 to 500 rad/s (Figure 1b).

In the present work, two kinds of PCL with different molecular weights and two kinds of TPS with various glycerol concentrations were chosen to study the influence of viscosity ratio on the blend morphology of strands after twin-screw extrusion. Figure 2 demonstrates the SEM image of PCL/TPS (70/30 weight %) blends at various viscosity ratios. The results show that the viscosity ratio, in the range studied, has virtually no influence on dispersed phase diameter. Although previous studies have clearly shown that the viscosity ratio has an important influence on phase size for immiscible blends, compatibilized blends often show significantly less dependence on viscosity ratio. Another potential explanation for the low dependence on viscosity ratio could be related to the presence of strong elongational flow fields present during twin-screw extrusion. It is well known that elongation flow is much more effective in droplet breakup than shear flow.

The SEM images of PCL1/TSP36 blends indicate that TPS exists as dispersed droplets in a PCL matrix up to a TPS concentration of 30 wt% (not shown here). Image analysis of these droplets indicate that the *dn* and *dv* are around 1.4 and 1.8 microns, respectively (Fig. 3). Further increasing the TPS concentration to 40 wt%, the co-existance of elongated structures (fiber-like) and droplets of TPS with a similar diameter are observed. Finally, when the TPS content increases up to 50 wt%, a solely fibrillar TPS is attained and the aspect ratio increases to about 25. It is of particular interest to note that the diameter of TPS droplets and fibers are independent of composition right up to 45 vol% TPS. Further increasing the TPS36 concentration above 54 vol%, results in dramatically increased TPS fiber diameters. The region of dual-phase continuity appears to exist in the concentration range of 54 to 65 vol% TPS. TPS appears to resist deformation/disintegration, but once deformed forms stable fibers.

Veenstra et al. investigated the morphology of blends of polystyrene and poly(ether-ester) thermoplastic elastomer [6]. When the processing temperature was chosen below the block copolymer order to disorder transition, the flow curves of poly(ether ester) did not show a Newtonian plateau in viscosity. Shear thinning behaviour over the entire range of measured shear rate was found. In that case, physical crosslinks of crystalline structures are present in the melt state and a melt yield stress was estimated in the range between 500 and 3800 Pa. These structures

were found to limit and even stop the breakup and retraction behaviour of poly(ether ester) threads and formed stable elongated structures.

In the present work, the rheology of TPS demonstrates a gel behaviour and no Newtonian plateau in viscosity was obtained during melting processing (Fig. 1). It indicates the existence of strong interactions within the TPS that can be attributed to hydrogen bonding. The presence of physical crosslinks in the melt state leads to highly elastic properties and a melt yield stress, which also have a stabilizing effect on elongated structure. Thus, this highly elastic state in the TPS typically resists deformation, but once deformed forms stable fibers. It is possible that the elongated structure can also be attributed to twin-screw extrusion processing which provides a significant elongational flow component. It is well known that the deformation of a droplet to produce a fibril is more easily obtained by subjecting the fluid to an extensional flow.

As a comparison, PCL2/TPS36 blends were prepared and the morphologies are studied. As observed for the PCL1/TPS36 blends, the dispersed TPS droplet/fiber diameters are independent of concentration.

The continuity of TPS/PCL2 via gravimetric solvent extraction is also shown in Figure 4 in order to examine the influence of a more viscous PCL on continuity development. In that case it can be seen that the percolation thresholds of both dispersed PCL2 and dispersed TPS36 are shifted to higher concentration. This is an unexpected shift since in typical thermoplastic blends, a lower viscosity ratio blend typically results in a more readily deformed dispersed phase and thus typically displays a lower percolation threshold. The opposite is observed here. This result is likely a reflection of the fact that both the elastic nature and internal hydrogen bonding in TPS give it the character of a pseudo-partially-crosslinked material. In this case the dispersed TPS is quite difficult to breakup, but once deformed forms stable fibers with less of a tendency to breakup than typical thermoplastics. Crosslinked materials classically demonstrate asymmetric continuity diagrams. In the case of TPS36/PCL2, since the more viscous PCL2 has virtually no additional effect on the deformation of dispersed TPS, the only effect is that the more viscous PCL2 actually retards the coalescence required for TPS droplets to transit to stable TPS fibers. Clearly these TPS/PCL blends do not respect the classical empirical description of the relationship of viscosity ratio and co-continuity composition.

The morphologies of injection moulded samples were obtained (not shown here). The results show the small effect of concentration based coalescence. The change in processing condition did

lead to significantly different particle sizes. This indicates that changes in processing techniques, with their different balances of shear and elongation flow fields, can have an effect on TPS coalescence.

As an immiscible blend is annealed in the melt state, the phase size grows as a function of annealing time and temperature indicating that significant coarsening effects are taking place. This coarsening is strongly affected by the state of the interface with compatibilized blends showing significantly less coalescence and more stable morphologies. A 25 vol% TPS36 in PCL1 blend with droplet/matrix morphology was used to study the TPS coalescence at annealing temperatures of 110 and 150 ^{o}C. The results clearly show that the TPS particle size in the blend does not change with annealing time and temperature indicating no coalescence whatsoever. In a second quiescent annealing experiment, a 43 vol% TPS in PCL1 blend (50/50 by weight), was also studied. However even at this concentration no further coarsening was observed even after long times of annealing. As a comparison, a completely immiscible HDPE/TPS36 blend (50/50 by weight) was also subjected to quiescent annealing to study the coarsening of TPS. In this case strong coalescence effects are observed for the TPS phase with the average TPS36 phase diameter increasing from 6.0 to 14.9 μm when annealing time was increased from 0 min to 60 min. These results strongly suggest the presence of compatibilization effects between TPS and PCL.

DMTA results for TPS, PCL and their blends are presented in Figure 5. For 100% TPS, the storage modulus falls in two steps, the first between -60 and -20 ^{o}C, and the second between -10 and 45 ^{o}C. This corresponds to the tan δ peaks for 100% TPS at -38.3 and 28.0 ^{o}C, respectively. The high temperature relaxation (T_{α}) is attributed to the glass transition of the starch-rich phase, whereas the low temperature (T_{β}) arises from the glycerol-rich phase owing to the phase separation of starch and glycerol at high glycerol concentration as reported previously. The T_g of PCL from the tan δ peak is -38.5 ^{o}C which overlaps with the T_{β} of TPS.

The storage moduli of PCL/TPS blends demonstrate two main tendancies which can also be used to determine the boundary of the co-continuity interval. At TPS concentrations less than and equal to 50 wt%, the moduli drop down at the melting point of PCL indicating PCL is the continuous phase. On the other hand, the 80 and 90 wt% TPS blends with PCL demonstrate a moduli which decreases dramatically following the starch-rich phase transition at 0 ^{o}C indicating TPS is the continuous phase. This effectively corresponds to the boundaries of phase inversion as determined by solvent gravimetry in the previous section.

It can be seen from Figure 5 that the T_β of PCL1/TPS36 blends decreases with increasing TPS36 concentration. This effect can be attributed to the further phase separation between starch and glycerol upon blending with PCL. Recent work from this laboratory, in fact, has shown that a thin glycerol-rich layer forms at the interface between TPS and polymer in TPS/polymer blends [7]. It is also interesting to note that there is a significant shift in the T_β peak to higher temperatures when the concentration is increased from 70-80 wt% TPS. This corresponds to the phase inversion of PCL and TPS as reported earlier in the paper and is related to the onset of formation of a TPS matrix phase and PCL dispersed phase.

The T_α peak for 100% TPS36 is 28.0 ^oC. However, PCL/TPS blends with 50 and 70 wt% TPS have a TPS T_α peak which only appears as a diffuse shoulder at -10 and -8 ^oC. This is a peak shift in excess of 30 C^o. At TPS contents of 30 wt% and below, the TPS T_α peak disappears entirely. These results strongly imply interactions between PCL and the starch-rich phase of TPS. The interaction is likely to be cause by the hydrogen bonding interactions between the carbonyl groups of PCL and hydroxyl groups on starch.

The FTIR spectra of PCL1, TPS36 and their blend at 50/50 wt%. PCL1 had a strong carbonyl stretching absorption at a wave number of 1720 cm^{-1}, which shifts to 1724 cm^{-1} after blending with TPS36. This shift in the stretching vibration frequency of carbonyl groups suggests a hydrogen bonding interaction between the carbonyl groups of PCL and the hydroxyl groups of TPS. Similar results have been obtained with poly(propylene carbonate)/thermoplastic starch and poly(hydroxyl ether of bisphenol A)/polycaprolcatone blends.

The tensile properties of PCL1, TPS36 and their blends were studied as well. The stress at yield and modulus decrease continuously with increasing TPS concentrations. The remarkable aspect of the results in this mechanical property data set are the elongation at break values. The elongation at break of PCL/TPS36 blends over a very wide concentration range exhibit outstanding ductility. Samples with a TPS36 content of 50 wt% and less did not even break during the tensile test (max value set at 1000%). Even PCL/TPS blends with 80 and 90 wt% of TPS36 showed elongations at break of 450 and 550%, respectively. The key to these properties appears to be the high level of plasticization of the starch. It is likely that the high plasticizer concentrations used here increase the mobility of the starch chains and thus promote a high level of specific interactions between the PCL and starch. This excellent interfacial interactions result in the exceptional ductilities observed above.

Conclusions

In this work a detailed study of the morphology development in thermoplastic starch/polycaprolactone blends, prepared using a one-step extrusion process has been undertaken. These highly plasticized blends, without any added interfacial modifier, display remarkably low levels of coalescence and exceptional mechanical properties. The phase size of the dispersed thermoplastic starch, after twin-screw extrusion, is virtually independent of TPS composition and TPS droplets transit to stable fiber-like phases of identical phase size above 30% TPS. Although the TPS is quite insensitive to concentration-based coalescence, it displays some coalescence sensitivity to changes in processing technique (compounding vs. injection). A study of percent continuity vs TPS concentration, as determined by solvent gravimetry, indicate the region of co-continuity to be 55-65 vol% TPS. This is an asymmetric phase inversion region and indicates a strong tendency of polycaprolactone to encapsulate the thermoplastic starch, a behaviour similar to polymer blends containing partially crosslinked rubbers. The preferential encapsulation of PCL about TPS is especially evident in the continuity development region at high TPS concentration where 10 wt% of PCL1 (the lower viscosity PCL) displays 40% continuity and 20 wt% PCL1 displays 80% continuity, a remarkable result. It is interesting to note that the midpoint value of phase inversion is identical irrespective of the viscosity of PCL used. The coalescence, as observed by static annealing experiments, show that the TPS phase at both 30 and 50 wt% TPS in PCL displays no coalescence after 60 minutes of annealing. A comparative study of static annealing of TPS/polyethylene on the other hand shows significant coalescence. These results strongly point to the likely presence of specific interactions between the TPS and the PCL. Dynamic mechanical analysis confirms the region of dual-phase continuity and also strongly indicates a specific interaction between PCL and TPS. FTIR results show the presence of a hydrogen bonding interaction between the carbonyl groups of PCL and the hydroxyl groups on starch. It is likely that the high plasticizer concentrations used here increase the mobility of the starch chains and thus promote a high level of specific interactions between the PCL and starch. Mechanical properties display extremely high elongations at break, even at high TPS concentrations, typical of those observed for highly compatibilized immiscible polymer blends.

References

1. N. St-Pierre, B. D. Favis, B. A. Ramsay, L. A. Ramsay, H. Verhoogt, *Polymer* **1997**, 38, 647.

2. B. D. Favis, F. Rodriguez, B. A. Ramsay, *US Patent,* 6,605,657, **2003**.

3. Z. H. Yuan, B. D. Favis, *AIChE J.*, **2005**, 51, 271

4. L. Averous, L. Moro, P. Dole, C. Fringant, *Polymer*, **200**0, 41, 4157.

5. H. M. Wilhelm, M. R. Sierakowski, F. Reicher, F. Wypych, G. Souza, *Polymer International*, **2005**, 54, 814.

6. H. Veenstra, B. Norder, J. Van Dam, A. Posthuma de Boer, *Polymer*, **1999**, 40, 5223

7. A. Taguet, M. A. Huneault, B. D. Favis, *Polymer*, (in press).

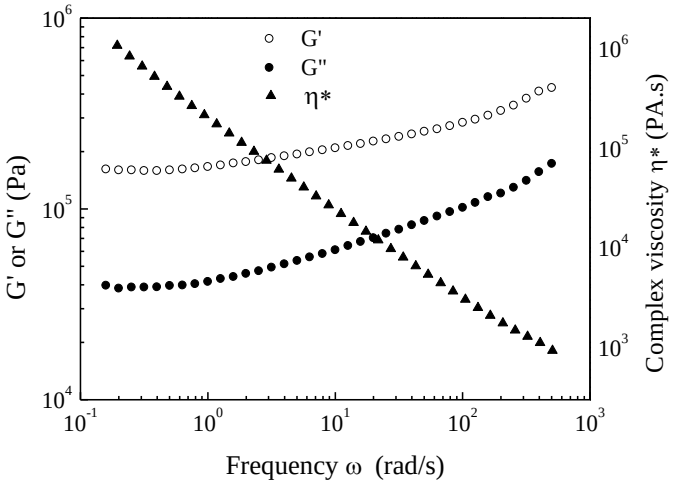

a

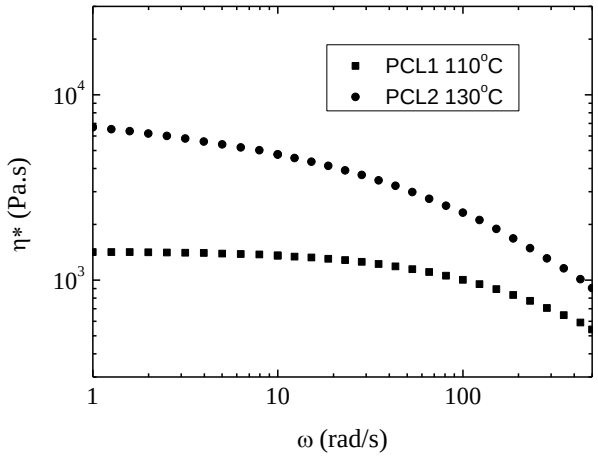

b

Figure 1 Rheological properties of a) TPS36 at 110°C and complex viscosity at 110°C and 130 °C for PCL.

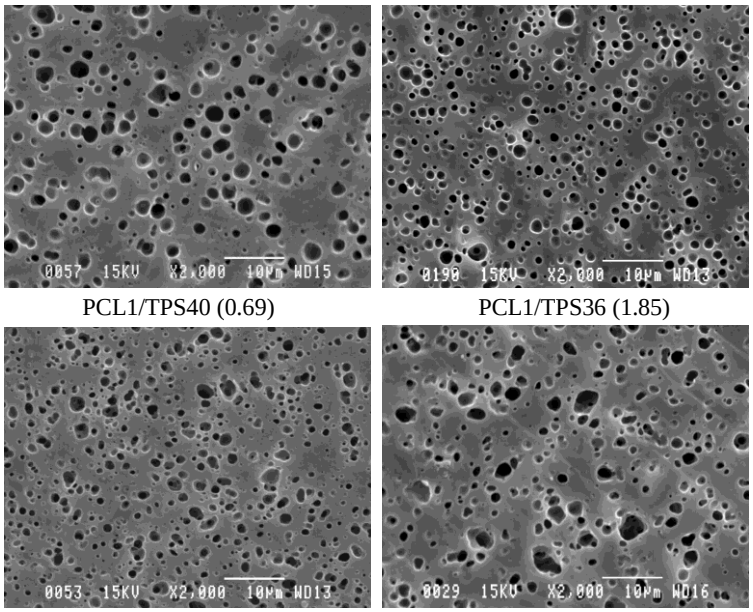

Figure 2 Effect of viscosity ratio on the morphology of PCL/TPS36 blends (70/30 weight %). The number in brackets indicates the viscosity ratio of dispersed phase to matrix.

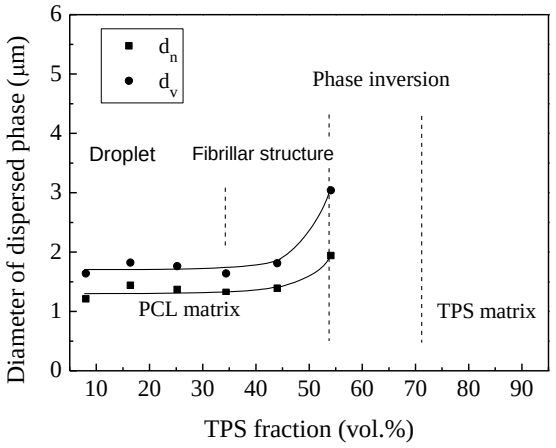

Figure 3 Diameter of phases as a function of TPS concentration obtained from the image analysis of PCL1/TPS36 extruded strands

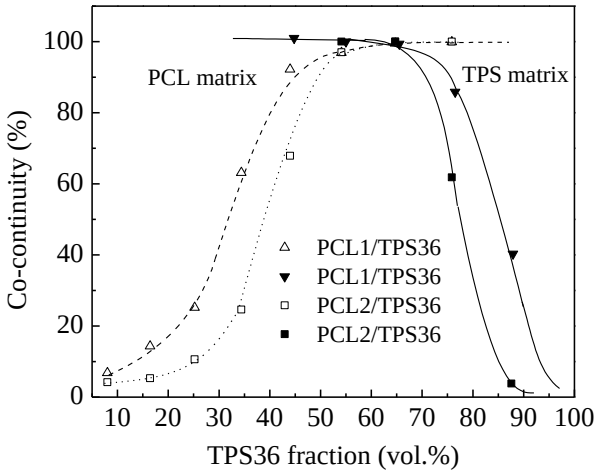

Figure 4 Phase continuity development of PCL/TPS36 blends using the gravimetric solvent extraction technique.

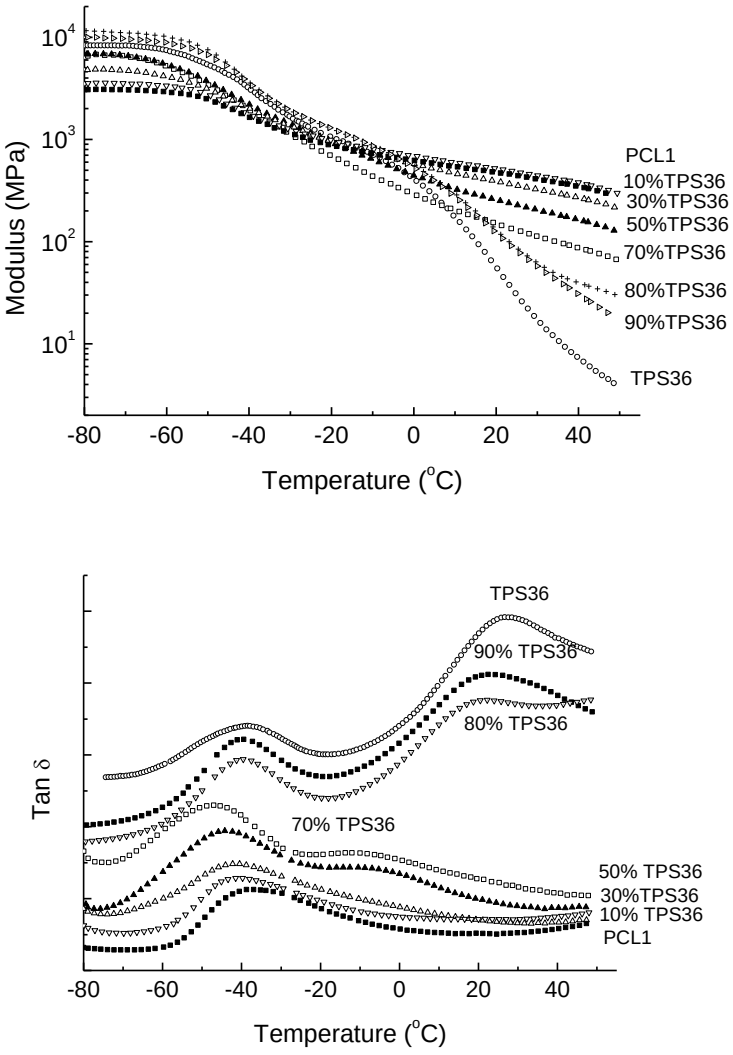

Figure 5 DMTA results for PCL, TPS and their blends. Concentrations are in weight %.